

Inhibition of HBV replication by
RIG-I stimulation with 5`-triphosphated siRNA
in vitro and *in vivo*

Inaugural-Dissertation

zur

Erlangung des Doktorgrades
der Mathematisch-Naturwissenschaftlichen Fakultät
der Universität zu Köln



vorgelegt von
Gregor Ebert
aus Buchen

Köln, September 2009

Berichterstatter: Prof. Dr. Thomas Langer
Prof. Dr. Martin Krönke

Prüfungsvorsitzender: Prof. Dr. Ansgar Büschges

Tag der Disputation: 27. Oktober 2009

Abstract

For a proportion of patients, HBV infection results in chronic disease with severe consequences like liver cirrhosis or hepatocellular carcinoma. Approved therapies of chronic hepatitis B include administration of antivirally active IFN- α and inhibitors of viral reverse transcription. These drugs control replication, but HBV cccDNA, the episomal transcription template, persists in most cases. Hence, lifelong therapy is required, accompanied by severe side effects and development of drug resistant mutants. An alternative and probably safe immunotherapeutic approach for clearance of HBV may be achieved by the stimulation of pattern-recognition receptors inducing an endogenous type-I IFN response. In this study the cytosolic helicase RIG-I was triggered by *in vitro* transcribed 5'-triphosphated (3p-) dsRNA. Stimulation induced an RIG-dependent antiviral type-I IFN response and controlled HBV replication *in vitro* in stable HBV replicating cell lines as well as in HBV infected primary human hepatocytes. *In vivo*, virus replication in HBV transgenic animals was transiently controlled when RIG I ligands were complexed and i.v. injected.

To enhance and prolong the antiviral effect, siRNAs targeting overlapping open reading frames of the HBV genome at the 3'-end of multiple HBV-RNAs were designed and investigated whether they can be *in vitro* transcribed and act as RIG-I ligands, and thus combine the immune stimulatory potential with HBV specific gene silencing. 3p-siRNAs were transfected into HBV replicating cells, induced INF-I and IFN-stimulated genes. HBV replication markers were significantly reduced and the antiviral effect of 3p-siRNA was superior to siRNA or 3p-RNA alone. Stronger effects of 3p-siRNAs on HBV replication were confirmed in HBV infected primary human hepatocytes, as well as *in vivo*. Nevertheless, the gene silencing effect of 3p-siRNA seemed to be limited in the mouse model due to insufficient targeting of hepatocytes, the HBV host cells. Application of cholesterol coupled siRNA improved hepatocyte specific targeting. Furthermore, we showed that 3p-siRNA besides a direct antiviral effect additionally induced infiltration of cytotoxic CD8⁺ T cells to the liver, potentially leading to elimination of infected hepatocytes.

The results of this study demonstrate that HBV-specific 5'-triphosphated siRNAs efficiently block HBV replication *in vitro* and *in vivo*. Combination of endogenous type-I IFN induction by stimulation of RIG-I with HBV sequence-specific gene silencing by RNAi in one single molecule could be a promising alternative to the actual standard therapeutic approaches against chronic HBV infection.

Zusammenfassung

Eine Infektion mit dem Hepatitis B Virus führt bei einem Teil der Patienten zu einem chronischen Infektionsverlauf mit schwerwiegenden Spätfolgen, wie Leberzirrhose oder hepatozellulärem Karzinom. Die gängigen Therapien einer chronischen HBV Infektion umfassen IFN- α und Reverse Transkriptase Inhibitoren als Hemmstoff der viralen Replikation. Diese Medikamente kontrollieren die Virusreplikation. In den meisten Fällen ist es aber nicht möglich, die episomal persistierende virale Transkriptionsmatrize (HBV cccDNA) zu eliminieren. Dadurch wird eine lebenslange Therapie erforderlich, die von Nebenwirkungen und dem Entstehen von arzneimittelresistenten HBV-Mutationen begleitet sein kann. Die Stimulation von RIG-I, einer cytoplasmatischen Helikase, kann zu der Freisetzung von endogenem, antiviral wirksamen Typ 1 IFN führen und stellt somit einen neuen, therapeutischen Ansatz für eine Behandlung der chronischen Hepatitis B dar. Die Stimulation von RIG-I mittels durch *in vitro* Transkription generierte 5'-triphosphorylierte (3p), doppelsträngige RNA führte in stabil HBV exprimierenden Zelllinien, in HBV infizierten primären humanen Hepatozyten und in HBV transgenen Mäusen zu einer Ausschüttung von Typ 1 IFN, und folglich zu einer Suppression der Virusreplikation. Um diesen antiviralen Effekt zu verstärken, wurden siRNAs entworfen, die die überlappenden offenen Leseraster des HBV Genoms am 3'-Ende aller viralen RNAs als Ziel haben. Es wurde untersucht, ob diese nach *in vitro* Transkription zur Stimulation von RIG-I fähig sind und es somit zu einer Kombination von Immunstimulation und Hemmung der viralen Genexpression kommt. Die ausgewählten 3p-siRNAs führten in HBV replizierenden Zellen zur Induktion von Typ 1 IFN und IFN-stimulierter Gene. Sie kontrollierten die HBV Replikation sowohl in stabil HBV exprimierenden Zellen, in HBV infizierten primären Hepatozyten, als auch in HBV transgenen Mäusen effizienter als die alleinige Applikation von siRNA oder 3p-RNA. Im Mausmodell konnte außerdem durch die Kopplung von siRNA an Cholesterin ein verbessertes Targeting von Hepatozyten, den HBV-Wirtszellen, erreicht werden. Die Injektion von 3p-siRNAs führte *in vivo* zu Einwanderung von zytotoxischen CD8⁺ T-Zellen in die Leber, die zur Elimination der HBV infizierten Zellen beitragen können. Somit kann durch HBV-spezifische 3p-siRNA die HBV Replikation *in vitro* und *in vivo* effektiv unterdrückt werden. Vereinigt in einer Substanz stellt die kombinierte Induktion von endogenem Typ 1 IFN und die spezifische Hemmung der viralen Genexpression eine vielversprechende Alternative zu den Therapien der chronischen HBV-Infektion dar.

Table of contents

Abstract.....	I
Zusammenfassung.....	II
Table of content.....	III
Table of figure.....	VIII
1 Introduction.....	1
1.1 The Immune System.....	1
1.1.1 Adaptive immunity.....	2
1.1.2 Innate immunity.....	5
1.1.3 Pathogen-associated molecular patterns: PAMPs.....	7
1.1.4 Pattern-recognition receptors: PRR.....	7
1.2 Cytosolic helicase RIG-I.....	10
1.2.1 Structure of RIG-I, the retinoic acid inducible gene-I.....	10
1.2.2 RIG-I activation.....	11
1.2.3 RIG-I signaling.....	14
1.3 Interferon class I.....	17
1.3.1 The interferon type-I system.....	17
1.4 Hepatitis B virus.....	18
1.4.1 Classification.....	18
1.4.2 HBV history and research.....	19
1.4.3 Liver structure.....	20
1.4.4 Epidemiology of HBV infection.....	21
1.4.5 Morphology and structure of HBV.....	24
1.4.6 Genomic organization and protein function of HBV.....	26
1.4.7 Replication of HBV.....	29
1.4.8 HBV specific immune response.....	35
1.5 Therapeutic approaches.....	38
1.5.1 Approved and novel inhibitors for antiviral therapy against HBV.....	38
1.5.2 Combinatorial treatment of HBV.....	41
1.5.3 Antiviral activity of IFN-I against HBV.....	42
1.5.4 Antiviral activity of HBV-sequence specific siRNA.....	46
1.6 Aims of the study: Hypothetical activity of 3p-siRNA against HBV.....	48
2 Results.....	50
2.1 Hepatocellular expression profile of RIG-I.....	50

2.2 Applicability of 3p-RNA.....	51
2.2.1 Induction of IFN- β by 3p-RNA.....	51
2.2.2 Induction of IFN- β by 3p-RNA in HuH7 cells.....	53
2.2.3 Three different HBV models.....	54
2.2.4 Cytotoxicity of 3p-RNA.....	56
2.3 Functionality of 3p-RNA as RIG-I ligand in HBV replicating liver cells.....	58
2.3.1 IFN induction by 3p-RNA and activation of interferon-stimulated genes <i>in vitro</i> and <i>in vivo</i>	58
2.3.2 RIG-I dependent IFN- β induction by 3p-RNA.....	62
2.4 Antiviral effects of 3p-RNA induced IFN-I on HBV.....	64
2.4.1 Antiviral effects of 3p-RNA treatment <i>in vitro</i>	64
2.4.2 Antiviral effects of 3p-RNA treatment <i>in vivo</i>	66
2.5 HBV sequence specific 3p-siRNA as RIG-I ligand.....	68
2.5.1 Design of HBV-sequence specific siRNAs.....	68
2.5.2 Functionality of 3p-siRNA as RIG-I ligand.....	69
2.5.3 Antiviral effects of 3p-siRNA treatment <i>in vitro</i>	71
2.5.4 Comparison of 3p-RNA and 3p-siRNA treatment <i>in vitro</i>	74
2.5.5 Long-term treatment of HBV by 3p-siRNA <i>in vitro</i>	77
2.5.6 Antiviral effects of 3p-siRNA treatment <i>in vivo</i>	80
2.5.7 Long-term treatment of HBV by 3p-siRNA <i>in vivo</i>	82
2.6 Liver directed targeting of RNA-oligonucleotides <i>in vivo</i>.....	85
2.6.1 Targeting specificity of applied RNA-oligonucleotides.....	85
2.6.2 Liver-specific targeting of RNA-oligonucleotides.....	88
2.6.3 IFN- β induction by 3p-siRNA in different liver cell populations.....	92
2.7 Initiation of an adaptive immune response against HBV.....	93
2.7.1 3p-siRNA induced expression of proinflammatory cytokine in liver cells.....	93
2.7.2 Induction of an adaptive immune response against HBV after RNA-oligonucleotide stimulation <i>in vivo</i>	94
3 Discussion.....	99
3.1 RIG-I dependent induction of IFN-I and interferon stimulated genes by 3p-RNA suppressed HBV replication <i>in vitro</i> and <i>in vivo</i>.....	100
3.1.1 3p-RNA induced IFN-I suppresses HBV replication.....	100
3.1.2 HBV escapes from antiviral activity of IFN.....	106
3.2 3p-siRNA combines RIG-I stimulation and siRNA mediated gene silencing and indicates a long lasting and superior anti-HBV effect.....	108
3.2.1 HBV-sequence specific siRNAs.....	108
3.2.2 HBV-sequence specific 3p-siRNAs efficiently suppress HBV replication.....	110
3.3 Liver targeting of modified siRNAs using different applications <i>in vivo</i>.....	113
3.4 Application of immune-stimulatory RNA-oligonucleotides initiates an adaptive T cell response against HBV.....	115

4 Material and methods	117
4.1 Biotic and abiotic material	117
4.1.1 Consumable items.....	117
4.1.2 Chemicals.....	118
4.1.3 Kits.....	119
4.1.3.1 Cell isolation.....	119
4.1.3.2 DNA labelling.....	120
4.1.3.3 ELISA.....	120
4.1.3.4 <i>In vitro</i> transcription (IVT).....	120
4.1.3.5 Luciferase detection.....	120
4.1.3.6 Nucleic acid isolation.....	120
4.1.3.7 Plasmid preparation.....	120
4.1.3.8 PCR reaction mix.....	120
4.1.3.9 Real time PCR.....	121
4.1.3.10 Transfection reagent.....	121
4.1.3.11 Nucleic acid complexation.....	121
4.1.3.12 Radioactive probes.....	121
4.1.3.13 Western blot.....	121
4.1.3.14 XTT-Test.....	121
4.1.4 Cell culture	121
4.1.4.1 Cell lines and primary cells.....	121
4.1.4.2 Consumable cell culture items.....	122
4.1.4.3 Antibiotics.....	123
4.1.4.4 Cell culture media.....	123
4.1.5 Oligonucleotides for <i>in vitro</i> transcription (IVT).....	124
4.1.6 siRNAs.....	125
4.1.7 PCR primer.....	126
4.1.8 Quantitative real time PCR primers.....	126
4.1.9 Primers for PCR amplification of purified HBV-DNA.....	127
4.1.10 Sequencing primer of purified HBV-DNA.....	127
4.1.11 Enzymes.....	127
4.1.12 Weight- and Length standards.....	128
4.1.12.1 DNA standards.....	128
4.1.12.2 Protein standards.....	128
4.1.13 Antibodies.....	128
4.1.13.1 Primary antibodies Western Blot.....	128
4.1.13.2 Secondary antibodies Western Blot.....	128
4.1.13.3 Histology.....	128
4.1.14 Radioactive [³² P] dCTP.....	128
4.1.15 Mouse strain.....	128

Table of contents

4.1.16 Technical equipment.....	129
4.1.16.1 Instruments.....	129
4.1.16.2 Centrifuges.....	130
4.1.16.3 Microscopes.....	130
4.1.16.4 Software.....	130
4.2 Methods.....	131
4.2.1 Molecular biology methods.....	131
4.2.1.1 In vitro transcription (IVT).....	131
4.2.1.2 Alexa 488 and cholesterol coupled siRNA.....	131
4.2.1.3 DNA and RNA quantification.....	132
4.2.1.4 Gelelectrophoresis.....	132
4.2.1.5 Polymerase chain reaction.....	133
4.2.1.6 DNA sequencing.....	133
4.2.1.7 cDNA synthesis.....	134
4.2.1.8 Quantitative real time polymerase chain reaction (qRT-PCR) / Light cycler [®] PCR).....	134
4.2.1.9 Isolation of progeny HBV-DNA from cell supernatant.....	136
4.2.1.10 Protein precipitation.....	136
4.2.1.11 Calculation of protein concentrations.....	136
4.2.1.12 SDS-page gel electrophoresis.....	136
4.2.1.13 Western blot analysis.....	137
4.2.1.14 ELISA assay HBsAg.....	137
4.2.1.15 ELISA assay human IFN- γ and IL-6 and mouse IFN- α	137
4.2.1.16 Preparation of total RNA with Trizol [®]	137
4.2.1.17 Separation of total liver cell RNA and Northern blot analysis.....	138
4.2.1.18 Preparation of genomic DNA.....	138
4.2.1.19 Separation of total liver cell DNA and Southern blot analysis.....	139
4.2.1.20 Radioactive HBV-genome specific probes.....	139
4.2.1.21 Hybridization with radioactive labeled probes.....	139
4.2.2 Cell biology methods.....	140
4.2.2.1 Eukaryotic cell lines.....	140
4.2.2.2 Isolation of primary human hepatocytes (PHHs).....	140
4.2.2.3 Isolation of LSECs and Kupffer cells.....	141
4.2.2.4 Transfection of cells.....	142
4.2.2.5 Production of wild type HBV.....	142
4.2.2.6 Caesium chloride density gradient.....	143
4.2.2.7 Dot blot analysis.....	144
4.2.2.8 HBV-infection of PHHs.....	144
4.2.2.9 Dual-luciferase assay.....	144
4.2.2.10 Luciferase detection.....	145
4.2.2.11 Cytotoxicity assays XTT.....	145

Table of contents

4.2.3 Mouse experiments	146
4.2.3.1 Bleeding of mice and serum preparation.....	146
4.2.3.2 Determination of ALT activity.....	146
4.2.3.3 Classical and hydrodynamic intravenous injection.....	146
4.2.3.4 Organ perfusion.....	147
4.2.3.5 Fluorescence microscopy.....	147
4.2.3.6 Histology.....	147
4.2.4 Statistical analysis	148
4.3 HBV sequence	148
5 List of abbreviations	150
6 Bibliography	153
Erklärung	170
Publication	171

Table of figures

Introduction

Fig. 1.1: Toll like receptors (TLRs), cytosolic helicases and their different ligands.....	9
Fig. 1.2: Schematic representation of RIG-I.....	11
Fig. 1.3: Model of RIG-I activation.....	13
Fig. 1.4: RIG-I-mediated signaling cascade and its regulation.....	16
Fig. 1.5: Formation of liver cells.....	21
Fig. 1.6: Clinical development of HBV infection in adults.....	23
Fig. 1.7: Hepatitis B prevalence 2005.....	24
Fig. 1.8: Structures of hepatitis B virus particles.....	26
Fig. 1.9: The HBV genome.....	28
Fig. 1.10: The replication cycle of HBV.....	31
Fig. 1.11: Schematic illustration of rc-DNA synthesis by reverse transcription.....	33
Fig. 1.12: Clinical courses and serologic profiles of acute resolving and chronic hepatitis B.....	36
Fig. 1.13: New targets of antiviral therapy.....	41
Fig. 1.14: Principles and antiviral activity of IFN-I system.....	43
Fig. 1.15: Anti-HBV functions of IFN-I inducible proteins.....	45
Fig. 1.16: RISC-model of siRNA mediated gene silencing.....	47
Fig. 1.17: Schematic model of HBV specific gene silencing and IFN-I signaling activation by RIG-I stimulation with 3p-siRNA and resulting antiviral effects on HBV replication in hepatocytes.....	49

Results

Fig. 2.1. RIG-I expression in hepatoma cell lines and primary human hepatocytes.....	51
Fig. 2.2: RIG-I expression in HEK 293 cells and induction of IFN- β by 3p-RNA prepared of different <i>in vitro</i> -transcriptions.....	52
Fig. 2.3: IFN-I induction by 5'-triphosphorylated dsRNA in HuH7 cell lines.....	53
Fig. 2.4: Potential induction of antiviral IFN-I by 3p-RNA in 3 HBV-model systems.....	55
Fig. 2.5: Cytotoxicity of 3p-RNA <i>in vitro</i> and <i>in vivo</i>	57
Fig. 2.6: IFN-I induction by 5'-triphosphorylated dsRNA <i>in vitro</i> and <i>in vivo</i>	59
Fig. 2.7: IFN-I dependent induction of 2'-5'-oligoadenylate synthetase (OAS).....	60
Fig. 2.8: IFN dependent induction of IP-10.....	61
Fig. 2.9: RIG-I dependent IFN- β induction by 3p-RNA.....	63
Fig. 2.10: Suppression of HBV replication by IFN-I induction after application of 3p-RNA in HepG2 H1.3 cells.....	64
Fig. 2.11: Stimulation of RIG-I by 3p-RNA suppressed HBV replication in primary human hepatocytes.....	65
Fig. 2.12: Stimulation of RIG-I by 3p-RNA suppressed HBV replication in HBV tg mice.....	67

Table of figures

Fig. 2.13: HBV-sequence specific siRNA targeting.....	69
Fig. 2.14: HBV sequence specific 5`-triphosphorylated siRNAs served as RIG-I ligands.....	70
Fig. 2.15: HBV-sequence specific 3p-siRNAs suppressed HBV replication <i>in vitro</i>	72
Fig. 2.16: HBV-sequence specific 3p-siRNAs suppressed genotype A HBV replication in HepG2 2.15 cells.....	73
Fig. 2.17: 3p-siRNA combined RIG-I stimulation and siRNA mediated gene silencing <i>in vitro</i>	76
Fig. 2.18: Longterm effects of 3p-siRNA on HBV replication <i>in vitro</i>	78
Fig. 2.19: Direct sequencing analysis of siRNA binding site within HBV-DNA genome of secreted virions.....	79
Fig. 2.20: 3p-siRNAs were functional as RIG-I ligands <i>in vivo</i>	81
Fig. 2.21: Combined antiviral efficiency of 3p-siRNA <i>in vivo</i>	83
Fig. 2.22: HBV-core antigen staining in liver of RNA-oligonucleotide treated HBV tg mice.....	84
Fig. 2.23: IFN- β expression in different organs of si-1.2 and 3p-1.2 treated HBV tg mice.....	86
Fig. 2.24: Targeting efficiency of fluorescently labeled and complexed si-1.2 to different organs.....	87
Fig. 2.25: Targeting efficiency of fluorescently labeled naked siRNA to different organs by intravenous injection and hydrodynamic injection.....	89
Fig. 2.26: Targeting efficiency of cholesterol coupled siRNA to different organs using different forms of applications.....	91
Fig. 2.27: IFN- β induction in different liver cell populations after uptake of complexed 3p-siRNA.....	92
Fig. 2.28: IL-6 and TNF- α induction in purified liver cell populations after uptake of complexed 3p-siRNA.....	94
Fig. 2.29: Induction of an adaptive immune response in HBV tg mice.....	96
Fig. 2.30: Liver staining (HE and PAS) of RNA-oligonucleotide treated HBV tg mice.....	97

Material and methods

Fig. 4.1. Schematic representation of triphosphated siRNA.....	125
Fig. 4.2: Schematic representation of fluorescently labeled and cholesterol coupled si-1.2.....	132

1 Introduction

1.1 The Immune System

The immune system is a multifunctional and highly adaptable defense system of mammals to protect the body from different invading pathogenic microorganisms and eliminate infective pathogens. It is able to detect a wide variety of agents like viruses, bacteria, pathogenic fungi or parasites. Beside the ability to generate a variety of cells and proteins capable to recognize and eliminate foreign invaders, the immune system is additionally able to recognize and remove disordered and damaged cells, which are prone to emerge as malignant tumors. An essential assumption of this interacting, elaborate and dynamic network is the ability to distinguish infected or degenerated cells from healthy cells and tissues to differentiate between self and non-self.

All components of the immune response are mediated by white blood cells, named leukocytes, which derive together with red blood cells (erythrocytes) from one common cell type in the bone marrow, the pluripotent hematopoietic stem cell. These lymphoid and myeloid progenitor cells differentiate in the bone marrow. The common lymphoid progenitors display the precursor of lymphocytes. There are three major types of lymphocytes: first, natural killer cells (NK cells); second, B-lymphocytes (B-cells), which differentiate in the bone marrow and third, T-lymphocytes (T-cells), which differentiate in the thymus. The emerging myeloid progenitors are the precursor of granulocytes, circulating in the blood, as well as macrophages, dendritic cells (DCs) and mast cells entering tissues (Janeway, 2007).

Immunity, the status of protection from infectious diseases, basically is divided into two phylogenetic different stages. The older and less specific component is the innate immunity, providing the first line of host defense against invading pathogens. The initial and antigen non-specific immune response is rapidly activated to eliminate or neutralize the invading organism. This effector response is primarily based upon anatomical barriers like skin and physiological barriers such as temperature or pH-value in the host. Major tasks of innate immunity are activation of NK cells and leukocytes, like mast cells, eosinophils or basophils as well as phagocytic cells, such as macrophages, neutrophils and DCs. Furthermore the recognition of pathogen

specific patterns by non-catalytic receptors, followed by the synthesis of antimicrobial mediators like interferons play an important role in innate immune response.

In contrast to the broad reactivity of the innate immune response, the phylogenetic younger and more specific component of the immune system is known as adaptive or acquired immunity. The antigen-specific adaptive immune response is activated after antigenic challenge to the organism and is established within five to six days after the initial exposure to the antigen in the late phase of infection. Repeated exposure to the specific antigen generates immunological memory. This fast occurring immune response, followed after a secondary encounter with the same specific pathogen, is stronger and more efficient and can lead to lifelong protection against the specific pathogen. Two types of adaptive immunity are involved in antigen-specific pathogen neutralization: first, the cellular immunity mediated by antigen-specific T-lymphocytes and their release of various cytokines in response to an antigen. The second component of the adaptive immune system is the humoral immunity, mediated by secreted antibodies produced by B-cells.

The rapid and non-specific innate immune response provides the first line of defense during the critical period directly after exposure to the pathogen. In addition, it plays a crucial role in stimulation of adaptive immunity. The adaptive immune response requires some time to arrange a definite and pathogen specific immune response, after repeated exposition of the host to microbial pathogens (Janeway, 2007).

1.1.1 Adaptive immunity

The adaptive immune system is able to recognize, adapt to and selectively eliminate specific foreign microorganisms. Adaptive immunity is divided into a humoral response, mediated by B-cells and a cellular response, mediated by T-cells. The humoral response of B-cells is based on antibody production and reacts on pathogenic organisms and viruses as well as on extracellular free circulating, pathogen derived and foreign antigens. Naïve B-cells, that had no previous contact with an antigen, circulate in the blood after they left the bone marrow. They express a unique antigen-binding receptor on their surface, termed membrane-standing immunoglobulin (IgM) or B-cell receptor (BCR). BCRs consist of two identical heavy and two identical light polypeptide chains. Every chain contains a constant and a

variable region. The amino-terminal variable ends of the pairs form a cleft within the specific antigen binds (Janeway, 2007).

The high diversity of BCRs is given by a mechanism called somatic recombination of gene segments, which results in the high genetic diversity in the variable regions. The number of B-cells that are able to bind to a given antigen is very small. To expand this population of B-cells, they are stimulated after antigen binding to divide rapidly into a clone with the same antigenic specificity, a process called clonal selection. During this process the progeny cells differentiate to effector B-cells. After activation the original membrane-standing BCRs are secreted as antibodies. On the one hand the antibodies neutralize pathogens or their toxic products by specific binding, and thus prevent the access of pathogens to potential target cells. On the other hand, phagocytotic cells recognize the constant region of the antibodies and ingest the antibody-covered pathogens. After the pathogenic antigen is removed from the body most of the effector B-cells undergo apoptosis (Banchereau, Briere et al. 1994). A small population of naïve B-cells develop into memory B-cells during clonal selection by an immunoglobulin-isotype change from IgM to IgG. Memory B-cells circulate in the lymphoid organs and mediate lifelong immunity against the specific pathogenic antigen (Liu, Zhang et al. 1991).

The cellular response mediated by T-cells is mainly directed against intracellular pathogens. It requires processing and presentation of pathogen-specific antigens by infected cells. After T-cells arise in the bone marrow, they migrate to the thymus gland to mature under positive and negative selection (Janeway, 2007). During maturation, T-cells express a unique antigen-binding receptor on their surface, called T-cell receptor (TCR). The TCR differs from BCR in structure, but the high diversity of TCRs is also obtained by somatic gene recombination. In contrast to BCRs, which can recognize antigens alone, TCRs can only recognize antigenic peptides that are bound to cell membrane proteins, called major-histocompatibility-complex (MHC) molecules (Klein 1986). This event is termed antigen presentation. T-lymphocytes can be differentiated into two well-defined subpopulations by the expression of membrane glycoprotein co-receptors beside the TCR, named CD4 and CD8 (CD, cluster of differentiation). These co-receptors differentiate both T-cell types in general and also determine their interaction with the MHC molecules. CD8⁺ T-cells interact with MHC I and CD4⁺ T-cells interact with MHC II (Lustgarten, Waks et al. 1991). MHC I is expressed by nearly all nucleated cells and presents processed intracellular

antigens, for example resulting from virus infection. Furthermore, MHC I and II are inherent body-identity markers. MHC II is expressed only by professional antigen-presenting cells (APCs), like macrophages and DCs, and presents phagocytosed antigens of extracellular pathogens to CD4⁺ T-cells. This phenomenon is known as MHC restriction.

As an exception, internalized extracellular antigens can be transferred to and presented by MHC I, a mechanism termed cross-presentation (Bevan 1976). After the uptake of extracellular proteins by DCs, macrophages (Brode and Macary 2004), B-cells (Hon, Oran et al. 2005) and also liver sinusoidal endothelial cells, LSECs (Limmer, Ohl et al. 2000), via receptor-mediated endo- or macropinocytosis, the proteins are transferred by an unknown mechanism into the cytoplasm where they are processed to peptides by the proteasome. Afterwards, they are transported by TAP (transporter associated with antigen processing) into the lumen of the ER, get loaded on MHC I (and MHC II) and presented on the cell surface to CD8⁺ (and CD4⁺) T cells. Thereby, professional APCs are able to present for example antigens from different viruses, which are not able to infect APCs (Sigal, Crotty et al. 1999).

CD4⁺ T-cells bind antigens presented on MHC II and differentiate upon activation into effector T cells with specific effector functions and cytokine profiles. They essentially participate to humoral and cellular immunity, as well to initiation and development of immunological memory. During the adaptive immune response against HBV infection, HBV-specific CD4⁺ T-cells induce and maintain a CD8⁺ T-cell response and activate B-cells (Rehermann 2003). CD4⁺ T-cells are separated into T-helper cells (T_H) and T-regulatory cells (T_{regs}). The population of T_H-cells is subdivided into T_H1-, T_H2-, T_H17- and T_H22-helper cells with specific roles in host defense against certain pathogens and in organ-specific autoimmunity. T_H1-cells activate macrophages, support antigen specific proliferation of CTLs and stimulate B-cells to produce opsonizing immunoglobulins, leading to phagocytosis of antibody-marked pathogens. T_H2-cells assist the humoral immune response by B-cells activation to produce neutralizing antibodies (Ridge, Di Rosa et al. 1998). Another subset of T_H-cells highly produce interleukin-17 (IL-17) and are designated T_H17-cells. Their role, together with other inflammatory cells, in induction of tissue inflammation during host defence and organ-specific autoimmunity is under discussion (Korn, Oukka et al. 2007). Recently, a previously uncharacterized IL-22-and TNF- α producing T-helper cell population has been described (Trifari, Kaplan et al. 2009). These peripheral

lymphocytes, subject to be named T_H22 -cells, are primarily found in epithelial tissue and are involved in inflammatory and wound healing processes. A supposed contribution to HBV infection has to be elucidated.

A small subpopulation of $CD4^+$ T-cells, named regulatory T cells (T_{regs}) provide regulatory functions in adaptive immunity. T_{regs} additionally express surface markers such as CD25, CD45 or FoxP3. It was shown, that they regulate immune-inflammatory aspects during viral infections (Suvas, Azkur et al. 2004) and may play a regulatory role in viral resistance during chronic HBV infection (Peng, Li et al. 2008). $CD8^+$ T-cells recognize intracellular or phagocytosed (by cross-presentation) antigens presented on MHC I complex and differentiate under the influence of T_H cell-derived cytokines to cytotoxic T lymphocytes (CTLs). CTLs kill infected or malignantly transformed cells. During an HBV infection CTLs specific for different HBV epitopes remove infected hepatocytes from the liver by lysis. Additionally, they may control an infection also on a non-cytolytic level by secreting antiviral cytokines (Guidotti, Ishikawa et al. 1996).

Nevertheless, most of the microorganisms, which entered a healthy individual are already cleared within a few days by distinct defense mechanisms of the innate immunity. Before the adaptive immune response eradicates foreign pathogens, the innate immune system is able to repress a pathogenic invasion by distinct features.

1.1.2 Innate immunity

The less specific and initial acting part of the immune response is the innate immune system, which often leads to the destruction of pathogens during the first days of infection without the help of the adaptive immune response. This complex system unifies different types of defensive barriers during a first contact of the host with a nonspecific microbial pathogen (Kuby, 2000).

First, the skin and mucosal membranes, as well as low pH-value in the stomach and digestive enzymes provide a protective anatomic, mechanical and chemical barrier between the internal and the external milieu. Once a pathogen passed this first barrier through a breached or wounded skin, the internal epithelial surface or body fluid exchange, the body possesses further physiological barriers. Normal body temperature or fever response inhibits the growth of some pathogens. Moreover,

chemical barriers, for example antiviral acting interferons, are produced by virus-infected cells. Bactericidal peptides like defensins are produced or released by phagocytes after the ingestion of microorganisms, which represent the endocytotic barrier of the innate immune system.

After a pathogenic microorganism crossed the anatomic barrier of epithelial cells and escaped all physiological barriers, the pathogen is able to start replication in the affected tissue of the host. Normally, the site of infection is immediately recognized and invaded by various cells that internalize (endocytose) and dissolve the foreign macromolecules. Circulating phagocytes, such as monocyte derived macrophages or neutrophils, phagocytose, kill and digest microorganism during beginning and acute phase of inflammation. Macrophages and neutrophils recognize pathogens via pattern recognition receptors (PRRs) on their cell surface and are able to discriminate between pathogen-associated molecular patterns (PAMPs) and those of the host.

Once bound, microorganisms are engulfed and degraded in endosomes and lysosomes. The generated peptides can be presented by MHC class II to CD4⁺ T-cells, a process connecting innate and adaptive immune response. Macrophages are localized especially in connective tissues, in the mucosa of the gastrointestinal tract, in the lung, in the spleen and also in the liver. In the liver the specialized macrophages are called Kupffer cells, where they remove large numbers of dying cells from the blood. Contact to the pathogen initiates the activation of macrophages to release chemical mediators, cytokines and chemokines (chemoattractant), which indicate an inflammation in the tissue. Neutrophils circulate in the blood stream and migrate, attracted by macrophage-derived cytokines, a process called chemotaxis, to the site of infection (Janeway, 2007).

DCs are the key players of antigen presentation to T-cells. Immature phagocytotic DCs migrate to peripheral tissues, where they continuously and unspecifically take up extracellular material via macropinocytosis. Additionally they selectively recognize and ingest pathogens through receptor-mediated endocytosis (Banchereau, Briere et al. 2000). After uptake and degradation of a microorganism, the expression and presentation of MHC and co-stimulatory molecules on the cell surface is up-regulated. DCs are now able to effectively present antigens on their surface, activate T-cells and stimulate the innate and adaptive immune response via secretion of cytokines like IL-6, IL-12, IL-18, IFN- α and IFN- γ (Banchereau, Briere et al. 2000). The DCs, now called mature, migrate to the local lymphoid tissue, where they

activate naïve T-cells. Thereby, following T-cell development can be driven in different directions. IL-12 and IFN- γ expressed by DCs lead to the differentiation of CD4⁺ T-cells into T_H1-helper cells. (Lanzavecchia and Sallusto 2001). Uptake of extracellular pathogens by DCs and presentation via MHC II mediates development of CD4⁺ T-cells into T_H2-helper cells (Moser and Murphy 2000). DCs also present phagocytosed and cross-primed antigens from viruses, bacteria and also tumors to CD8⁺ T-cells via MHC I, which thereupon become CTLs (Janssen, Lemmens et al. 2003).

The main pathway by which DCs get activated, mature and present antigens to naïve T-cells, is the recognition of PAMPs by PRRs. DCs display the key cell type coupling PRR-mediated innate immune recognition and initiation of adaptive immune response. Consequently, the innate immune response is not completely non-specific. The system is able to discriminate between self and broad variety of foreign pathogens (Janeway and Medzhitov 2002).

1.1.3 Pathogen-associated molecular patterns: PAMPs

The variety of pathogens that can be recognized is given through highly conserved structures, a broad spectrum of microbial components, and known as pathogen-associated molecular patterns (PAMPs) or microbe-associated molecular patterns (MAMPs). PAMPs are essential for the survival of the microorganism and therefore difficult for the microorganism to alter. A prototypical PAMP is bacterial lipopolysaccharide (LPS) of gram-negative bacteria, a component of their outer bacterial cell wall. Other PAMPs are for example bacterial flagellin, peptidoglycan, unmethylated bacterial CpG-DNA, or nucleic acid variants of viruses, such as double-stranded RNA (dsRNA) or double-stranded DNA (dsDNA) (**Fig. 1**).

1.1.4 Pattern-recognition receptors: PRR

Pattern-recognition receptors (PRR) are the key players in innate immune host defense. They are tagged by the PAMPs, which leads to induction and activation of

inflammatory and antimicrobial innate immune responses (Medzhitov 2001). Different PRRs react with specific PAMPs (**Fig. 1**). The binding activates specific signaling pathways, which lead to altered gene expression and to distinct antipathogenic responses. PRRs can be subdivided into four different families: a) Toll-like receptors (TLR) b) RIG-I-like receptors (RLR) c) C-type lectin receptors (CLR) and d) NOD (nucleotide binding and oligomerization domain) -like receptors (NLR) (Palsson-McDermott and O'Neill 2007).

Toll-like receptors are probably the most important family of PRRs. Their name originates from Toll, a receptor that was primarily identified in *Drosophila* (Hashimoto, Hudson et al. 1988). Subsequent studies revealed that Toll also play an essential role in insect innate immunity (Lemaitre, Nicolas et al. 1996). In the following, homologues of Toll were identified in mammals. To date 10 members of the human TLR family have been identified. TLRs, which are type I transmembrane glycoproteins are expressed by various immune cells including macrophages, DCs, B cells and specific types of T-cells, but also by non-immune cells such as fibroblasts and epithelial cells (Akira, Uematsu et al. 2006). The receptors are able to detect PAMPs derived from fungi, parasites, bacteria or viruses via an extracellular leucine-rich repeat (LRR) sequences and transmit signals through the cytoplasmic Toll-interleukin (IL)-1 receptor (TIR) domain. They can be divided in several subfamilies by different aspects and characteristics. One characteristic is that each subfamily of TLRs recognizes related PAMPs: TLR1, 2 and 6 predominantly recognize lipids, TLR5 flagellin and TLR9 bacterial and viral CpG-DNA. TLR3, 7 and 8 are triggered by viral nucleic acids (Barton 2007). TLR4 recognizes a collection of different ligands with totally different structures, such as lipopolysaccharide (LPS), viral proteins, fibronectin or heat-shock proteins. Another aspect for discrimination is that certain TLRs are expressed on the cell surface (TLR1,2,4,5 and 6), others are found in intracellular compartments such as endosomes (TLR3,7,8 and 9). Initially, TLRs were described to be involved in bacterial pathogen recognition (TLR1,2,4,5,6 and 9), but they also play a crucial role in the host response to viruses. Endosomal TLR3, 7 and 8 recognize viral nucleic acids, which requires internalization to the endosome, before induction of an antiviral response is possible. In contrast viral glycoproteins interact with TLR 2 and 4 on the cell surface before or during viral entry (Akira and Takeda 2004; Akira, Uematsu et al. 2006; Thompson and Locarnini 2007).

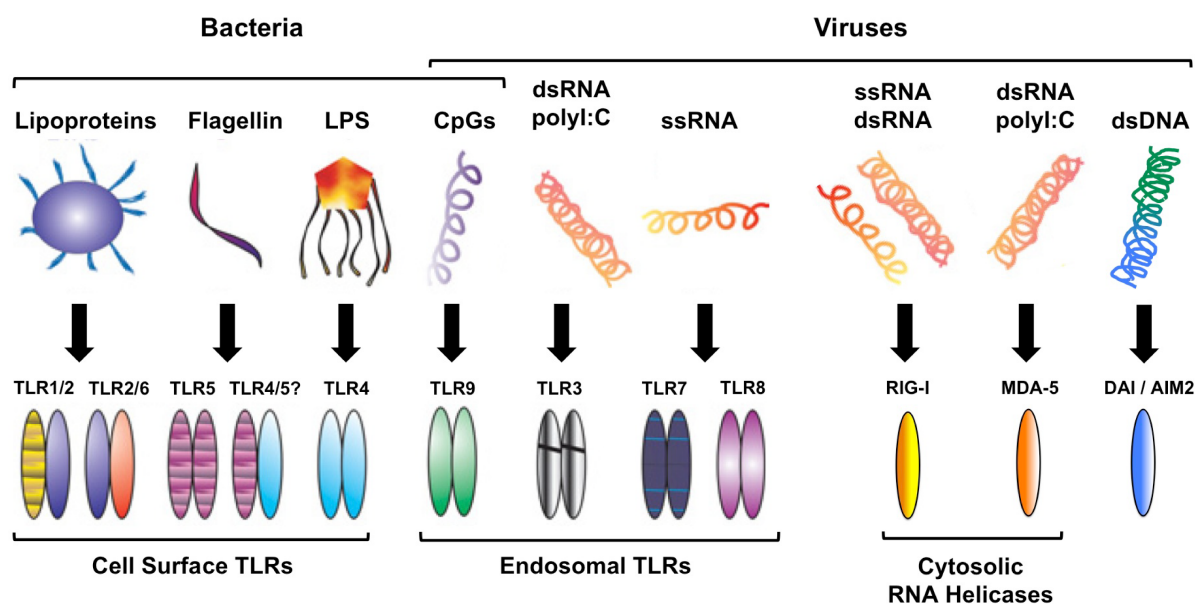


Fig. 1.1: Toll like receptors (TLRs), cytosolic helicases and their different ligands. Illustration modified after (Chaudhuri, Dower et al. 2005)

The second family of PRR identified to be involved in the recognition of viral nucleic acids beside TLRs are the retinoic acid-inducible gene-1 (RIG-I)-like receptors (RLR). RLR comprise RIG-I (retinoic acid inducible gene-1), MDA-5 (melanoma differentiation associated gene 5) and LGP-2 (laboratory of genetics and physiology 2) (Yoneyama, Kikuchi et al. 2004; Rothenfusser, Goutagny et al. 2005; Yoneyama, Kikuchi et al. 2005; Gitlin, Barchet et al. 2006). All RLRs are ubiquitously expressed cytosolic helicases. RIG-I and MDA-5 survey the cytoplasm for viral RNA and recognize different RNA viruses. Additionally, MDA-5, as well as TLR3 are preferentially triggered by poly(I:C) (polyinosinic:polycytidylic acid), a synthetic analogue of short double-stranded RNA (Alexopoulou, Holt et al. 2001; Gitlin, Barchet et al. 2006; Kato, Takeuchi et al. 2006). RLR binding of viral nucleic acids lead to the induction of an antiviral interferon type-I response, as further described in chapter 1.2.2 and 1.2.3. Although LGP-2 is able to recognize dsRNA, it lacks a downstream signaling domain and functions as negative regulator of RIG-I (Saito, Hirai et al. 2007).

Another antimicrobial defense line of PRRs beside TLRs and RNA helicases are cytoplasmic DNA sensors that recognize viral or bacterial (B-form) DNA and induce IFN type-I (Ishii, Coban et al. 2006). DAI (DNA-dependent activator of IFN-regulatory

factors) was identified as a possible DNA receptor (Takaoka, Wang et al. 2007), but DAI knockout mice showed no abnormal DNA induced IFN production (Ishii, Kawagoe et al. 2008). Recently AIM2 (absent in melanoma 2), a PYHIN (pyrin and HIN domain-containing protein) family member, was identified as a receptor for cytosolic dsDNA recognition, which potently activates innate immunity via the inflammasome (Takaoka, Wang et al. 2007; Fernandes-Alnemri, Yu et al. 2009; Hornung, Ablasser et al. 2009).

Membrane-bound C-type lectin receptors detect extracellular fungal PAMPs (Willment and Brown 2008). The cytosolic NOD-like receptors exhibit a characteristic C-terminal LRR and an internal nucleotide-binding domain (NBD). NLRs are known to detect cytoplasmic bacterial PAMPs. This leads to the activation of cytokine expression including IL-1 β (Inohara, Chamillard et al. 2005; Martinon, Gaide et al. 2007).

1.2 Cytosolic helicase RIG-I

1.2.1 Structure of RIG-I, the retinoic acid inducible gene-I

RIG-I, the retinoic acid inducible gene-I (also known as DDX58), was originally identified and named by the ability to be induced by retinoic-acid during differentiation of acute promyelocytic leukemia cells (Sun, 1997). Subsequently, RIG-I was described to be stimulated after transfection of synthetic dsRNA poly(I:C) and thereby activate IRF-regulated reporter gene expression (Yoneyama, Kikuchi et al. 2004). Expression of RIG-I can be enhanced by retinoic acid, interferon and viral infection. RIG-I is a member of the DExD/H box RNA helicase (dsRNA unwinding) family (Yoneyama, Kikuchi et al. 2005). The human RIG-I gene encodes for a protein of 925 amino acids and 115 kDa that comprises two characteristic caspase recruitment domain (CARD)-like motifs at its N-terminus, and a C-terminal RNA binding domain (**Fig. 2**) (Cui, Eisenacher et al. 2008). CARD as the signaling domain is responsible for activation of a downstream signaling cascade, the C-terminal region containing several conserved helicase motifs and a repression domain (RD) (Yoneyama, Kikuchi et al. 2005), is responsible for RIG-I function. The C-terminal repressor

domain is involved in inhibition of RIG-I activation in the absence of stimulating viral RNAs (Saito, Hirai et al. 2007). The C-terminal domain (CTD), aa792-925, which is part of the RD-domain, is responsible for the recognition of specific viral RNAs (Cui, Eisenacher et al. 2008; Takahasi, Yoneyama et al. 2008). The helicase domain comprises an adenosine-triphosphate (ATP)-binding lysine residue. Substitution of lysine to alanin renders RIG-I into a dominant negative inhibitor form, which indicates that RIG-I requires ATP to activate signaling (Yoneyama, Kikuchi et al. 2004).

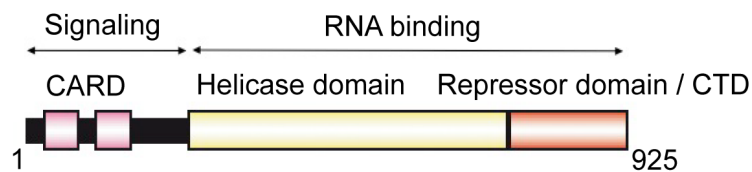


Fig. 1.2: Schematic representation of RIG-I. N-terminal CARD (caspase recruitment domain) motifs are responsible for downstream signaling after binding of RNA to helicase domain and C-terminal domain (CTD), including the repressor domain. Modified after (Yoneyama and Fujita 2009)

1.2.2 RIG-I activation

RIG-I recognizes a specific set of RNA viruses, such as Flaviviridae, Paramyxoviridae, Orthomyxovirida and Rhabdoviridae (Kato, Takeuchi et al. 2006). All this viruses affiliate a common feature, an RNA genome modified by phosphorylation. Recent studies showed that RIG-I distinguishes viral RNA from the broad amount and variety of cellular RNAs by the recognition of 5`-triphosphates (Hornung, Ellegast et al. 2006; Pichlmair, Schulz et al. 2006). This oligonucleotide modification arises from RNA synthesis by various viruses already mentioned above. The variation of 5`-triphosphorylation is not found on cellular RNA due to several modifications. Although cellular primary transcripts contain 5`-triphosphate, just like the viral transcripts, they undergo several various modifications. The mRNA acquires a 7-methylguanosine CAP structure at its 5`-end; tRNA undergoes 5`-cleavage and series of nucleotide base modifications. Primary transcripts of ribosomal RNA are directly complexed with ribosomal proteins to form ribonucleoproteins, and are therefore masked. Modification of 5`-triphosphated RNA like artificial capping or base modifications abolished detection by RIG-I (Hornung, Ellegast et al. 2006).

Thus, RIG-I is the key sensor of negative strand RNA viruses in the cytosol of cells. RNA containing a triphosphate at the 5'-end activates RIG-I, but the exact structure of RNA supporting 5'-triphosphate recognition, the requirement of 5'-triphosphate group and the existence of RNA stimulating RIG-I in the absence of a 5'-triphosphate group remain controversial. Until now, there are six proposed RIG-I ligands, capable for the induction of an IFN type-I (IFN-I, IFN- α and - β) response (Schlee, Hartmann et al. 2009). Beside single-stranded (ss) and double-stranded (ds) RNA with 5'-triphosphate groups, short (23 - 30 bp) dsRNA with 5'-monophosphate and triphosphorylated ssRNA with A- and U-rich sequence at the 3'-end, as well as intermediate (300 – 2000 bp) and short (23 - 30 bp) dsRNAs without 5'-triphosphate efficiently stimulate RIG-I. Nevertheless, sequence unspecific dsRNAs, prepared by a technique called *in vitro* transcription (IVT), preferentially activate RIG-I (Kato, Takeuchi et al. 2006), a characteristic that is utilized in this work. For this purpose, an ssDNA template is transcribed by a T7 RNA polymerase into dsRNA. During this procedure the 5'-ends of the RNA-oligonucleotide become triphosphorylated.

A model of possible RIG-I activation by Yoneyama and Fujita (Yoneyama and Fujita 2008) proposes, that RIG-I is inactivated in the absence of stimulating RNA by intramolecular interaction between C-terminal repressor domain (RD) and caspase recruitment domain (CARD) (**Fig. 3**). After the transfer of 5'-triphosphorylated dsRNA (5'ppp-dsRNA or shortly 3p-RNA) or the appearance of viral RNA as a result of viral infection in the cytoplasm of the cell, RIG-I detects the RNA motifs via basic cleft like structure of the C-terminal domain (CTD). Stable complex of RNA and RIG-I via CTD activates intrinsic ATPase, which leads to an ATP-dependent conformational change of RIG-I, rather than ATP-dependent RNA unwinding by the helicase function of RIG-I (Takahashi, Yoneyama et al. 2008). Due to the conformational change of RIG-I the N-terminal CARD domain is exposed for interaction with downstream adaptor molecules. Alternatively, it was shown that RIG-I primarily could form a dimer or oligomer via RD (**Fig. 3**) in response to 3p-RNA interaction (Cui, Eisenacher et al. 2008). The consequently activated RIG-I is predicted to directly interact with interferon beta promoter stimulator-1 (IPS-1), located in the outer membrane of mitochondria and also known as mitochondrial antiviral signaling (MAVS), CARD adaptor inducing interferon beta (CARDIF) or virus-induced signaling adaptor (VISA) (Kumar, Kawai et al. 2006). IPS-1 consists of two domains characterized as an N-terminal CARD-like domain sharing homology with those of RIG-I, and a C-terminal

effector domain. IPS-1 associates with RIG-I via the CARD domain and provides a link between RIG-I and downstream signaling molecules (**Fig. 3 and 4**).

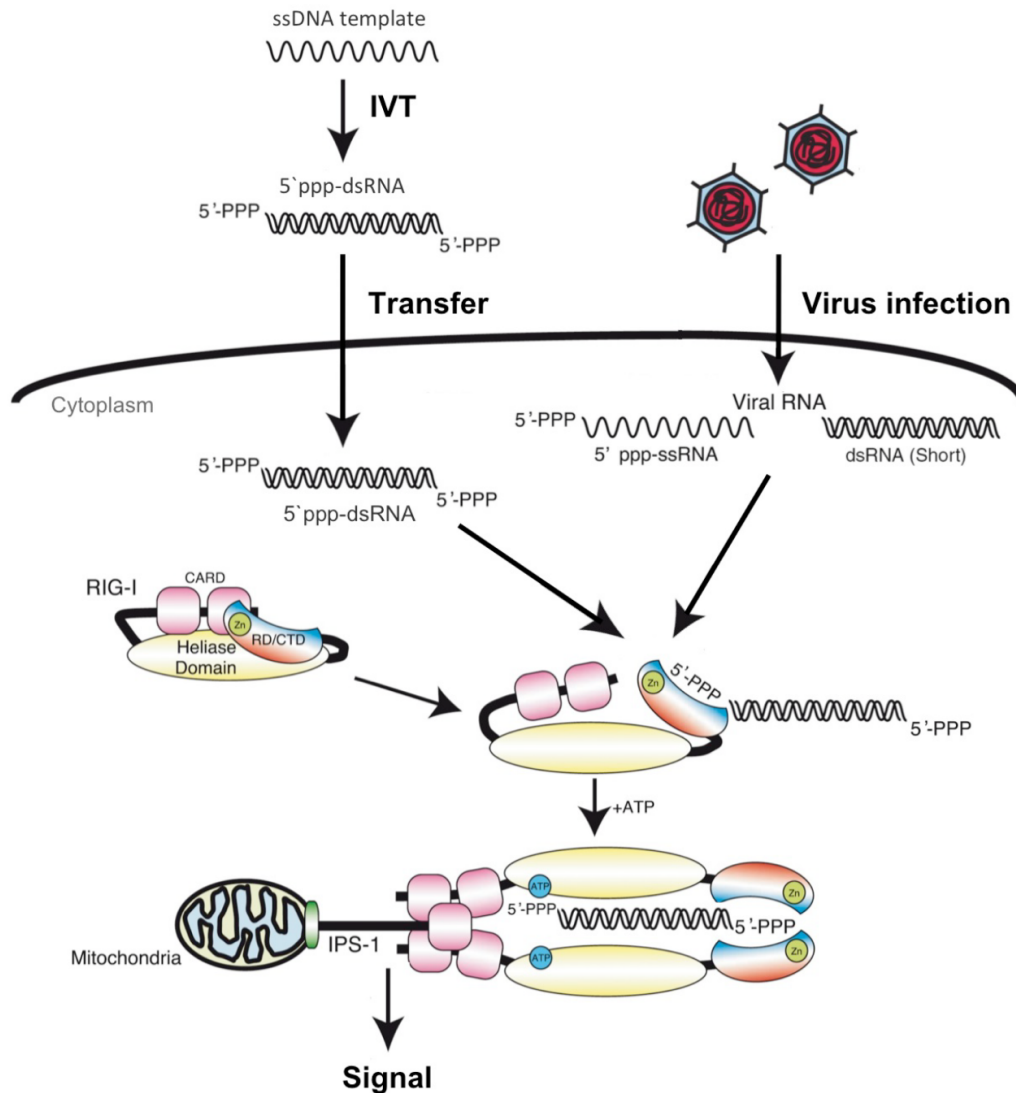


Fig. 1.3: Model of RIG-I activation. In the absence of stimulating RNA, RIG-I is present in an inactivated form by intramolecular interaction between C-terminal repressor domain (Inohara, Chamailard et al.) and caspase recruitment domain (CARD) or a linker region of the helicase domain. In the presence of stimulating RNA in the cytoplasm, such as transferred 5'-triphosphorylated dsRNA (3p-RNA) or viral RNA, RIG-I detects this non-self RNA via basic cleft-like structures of the C-terminal domain (CTD). The detection of RNA induces an ATP-dependent conformational change and forming of a dimer, which allows CARD to interact with the mitochondrial downstream adaptor protein interferon beta promotor stimulator-1 (IPS-1), which itself include a CARD domain and links downstream signaling. Modified after (Yoneyama and Fujita 2009).

1.2.3 RIG-I signaling

The RIG-I signaling cascade converges at the expression of activating transcription factors such as nuclear factor kappa-light-chain-enhancer of activated B-cells (NF- κ B) and Interferon regulatory factors (IRFs). These factors are translocated to the nucleus, where they bind to the promoter region of IFN-I and other proinflammatory cytokines, in order to activate their transcription. Besides NF κ B especially IRF-3 and IRF-7 are phosphorylated due to a viral induced signal and activate antiviral immunity (Sato, Suemori et al. 2000) (**Fig. 4**).

More precisely, binding of activated RIG-I to IPS-1 via CARD-CARD interaction induces a complex downstream signaling cascade. First, IPS-1 is essential for RIG-I specific induction of IFN-I, demonstrated in IPS-1 KO cells, which show an impaired IFN-I induction after RIG-I specific stimulation (Kumar, Kawai et al. 2006; Sun, Sun et al. 2006). IPS-1 encodes beside an N-terminal CARD domain additionally a transmembrane domain at its C-terminal effector side and a proline-rich region (PRR) in the middle of the protein. The expression in the outer mitochondrial membrane suggests an essential role of mitochondria in RIG-I mediated signaling. It has been shown that tumor necrosis factor (TNF) receptor-associated factors (TRAF) 3, an E3 ligase for Lys63-linked polyubiquitination, directly interacts with the PRR of IPS-1 (Oganesyan, Saha et al. 2006), as well as TRAF 2 and TRAF 6 (Xu, Wang et al. 2005). The signaling cascade proceeds on one hand via the recruited TRAF family member associated NF- κ B activator (TANK), which transmits the signal to downstream protein kinases, inhibitor of NF- κ B (I κ B) kinase (IKK) family members. The canonical IKK complex, consisting of IKK- α , IKK- β and the regulatory subunit of NF- κ B essential modulator (NEMO), also termed IKK- γ , phosphorylates I κ B. Subsequently, proteasome-dependent degradation of I κ B allows functional NF- κ B to translocate to the nucleus (Karin and Ben-Neriah 2000) and induces the transcription of proinflammatory cytokines like IL-1, IL-6 and TNF- α (Dinarello 2000) (**Fig. 4**, left part of cascade). In contrast, TANK recruits binding of non-canonical IKKs, TANK-binding kinase 1 (TBK1) and IKK- ι (also termed IKK- ϵ), which themselves activate the signal-dependent phosphorylation of IRF-3 and IRF-7 to form a functional homodimer or heterodimer (Fitzgerald, McWhirter et al. 2003; Sharma, tenOever et al. 2003). Following translocation of IRFs into the nucleus allows transcription factor activity and the induction of IFN-I (**Fig. 4**, right part of cascade). The interaction between the PRR

region of IPS-1 and TRAF-3 is essential for the activation of both, canonical and non-canonical IKK complexes, whereas TRAF-2 / -6 is responsible for NF- κ B activation (Xu, Wang et al. 2005).

As a regulatory element NAK-associated protein 1 (NAP1) is involved in the non-canonical IKK activation of IRFs (Sasai, Shingai et al. 2006). NEMO, which is known to be a regulatory subunit of the canonical IKK complex, also plays a role in the non-canonical IKK complex formation and activation of IRFs (Zhao, Yang et al. 2007), pointing to a crosstalk between both IKK complexes during RIG-I signaling. Already upstream in the signaling cascade, Fas-associated death domain (FADD) and receptor interacting protein 1 (RIP1), which are both death domain-containing proteins, are involved in the IPS-1 signaling complex (Kawai, Takahashi et al. 2005). They interact with the C-terminal part of IPS-1 and activate the NF- κ B inducing pathway via the activation of caspase-8 and caspase-10 (Takahashi, Kawai et al. 2006). Additionally, tumor necrosis factor receptor (TNFR) -associated DD (TRADD) complexes with IPS-1, TRAF-3, TANK, RIP1 and FADD, which leads to the activation of NF- κ B and IRF-3 (Michallet, Meylan et al. 2008).

It remains unclear why IRF-3 is activated via IPS-1 containing signaling, but not via TNFR-mediated signaling. Possibly, mediator of IRF-3 activation (MITA), localized like IPS-1 on the outer mitochondrial membrane, is a critical scaffold protein for IRF-3 activation. MITA interacts directly with IPS-1 and regulates the recruitment of TBK1 to the IPS-1 complex on mitochondria (Zhong, Yang et al. 2008). Other molecules are responsible for post-translational modifications of RIG-I signaling. The tripartite motif protein 25 (TRIM25), an E3 ubiquitin ligase, specifically interacts with the CARD-domain of RIG-I and conjugates ubiquitin to RIG-I CARD, which results in a marked increase in RIG-I downstream signaling activity (Gack, Shin et al. 2007). The modification of RIG-I is essential for the interaction with IPS-1 and subsequent signaling. A negative regulator of RIG-I mediated signaling is NLRX1, a member of the NLR family. NLRX1 is also expressed on the outer membrane of mitochondria and negatively regulate IPS-1 activity by direct interaction between the IPS-1 CARD domain and NLRX1 (Moore, Bergstralh et al. 2008). This negative regulation is necessary, because prolonged and unwanted activation of antiviral signaling via RIG-I and IPS-1 might be harmful for host survival.

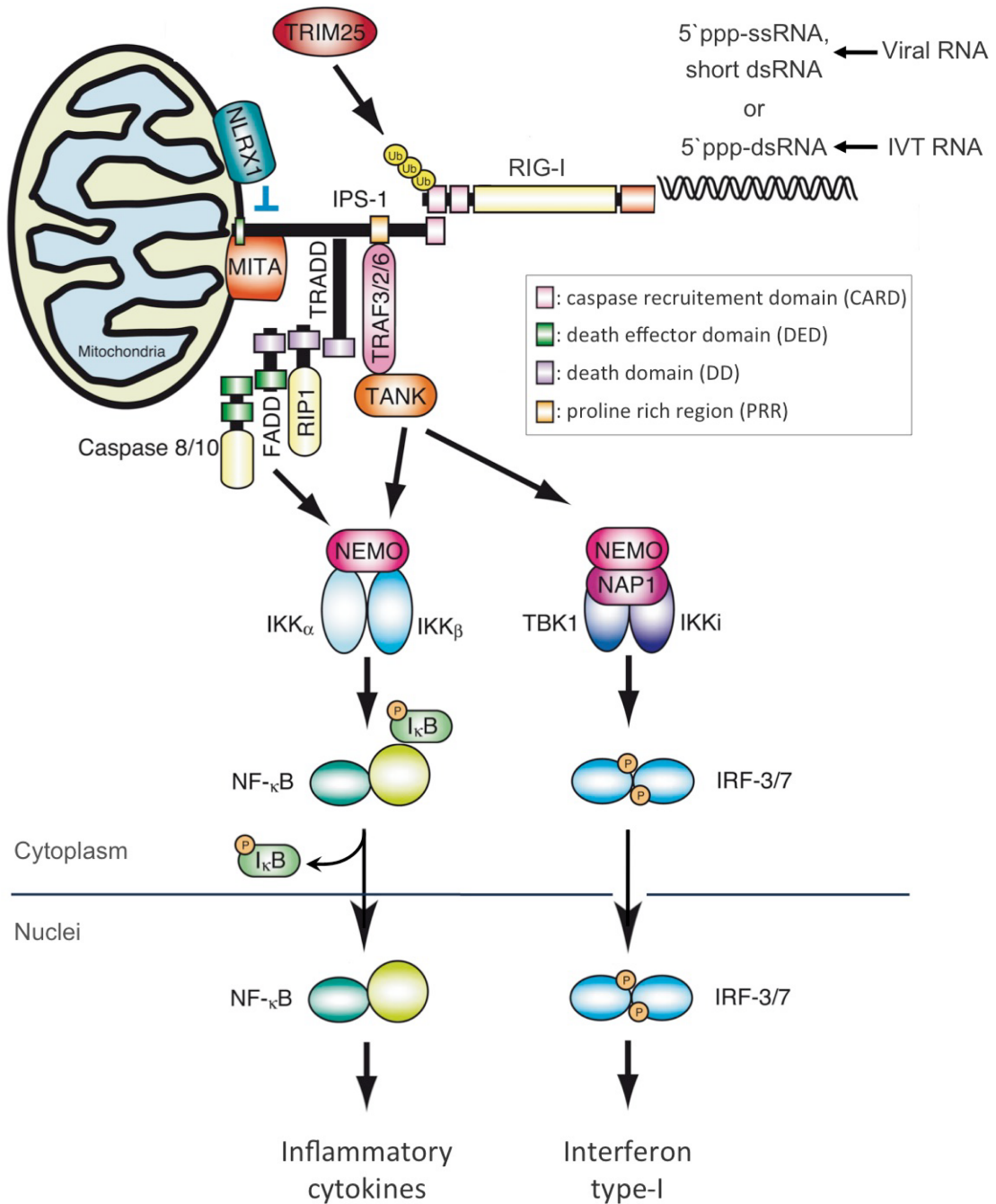


Fig. 1.4: RIG-I-mediated signaling cascade and its regulation. Activated RIG-I interacts directly with mitochondrial IPS-1 and transmits the signal through the indicated signaling molecules, resulting in the activation of the transcription factors NF- κ B and interferon-response factors (IRF) 3 and 7 (detailed described in the text). Translocation to the nucleus allows transcription factor activity and the induction of proinflammatory cytokines and interferon type-I. Black arrows and blue lines indicate positive or negative regulation of the signal, respectively, by cellular proteins. Modified after (Yoneyama and Fujita 2009).

1.3 Interferon class I

1.3.1 The interferon type-I system

The detection of determined PAMPs by PRRs initiates effective antimicrobial machinery. The recognition of pathogenic nucleic acids by TLR3, 7, 8 and 9, RIG-I and MDA-5, as well as bacterial LPS by TLR4, induce an inflammatory response and the production of different cytokines. The antimicrobial key cytokine produced after stimulation of RIG-I is interferon type-I (IFN-I). IFN was initially identified as a soluble factor secreted by virus-infected cells, acting as an inhibitor of viral replication (Isaacs and Lindenmann 1957). Beside its antiviral activity, other major biological activities include antitumor and immunomodulatory effects.

The IFN-I family comprises of one IFN- β and 13 IFN- α subtypes in humans (plus IFN κ , IFN ϵ , IFN ω , IFN τ and IFN δ) (Roberts, Liu et al. 1998). The IFN-I system includes two different signaling cascades. First, an IFN-I producing signal, which is induced by PRR dependent recognition of specific oligonucleotides and second, an IFN α/β receptor (IFNAR) mediated signal, which is activated by released IFN-I itself (Randall and Goodbourn 2008). When IFN-I is released out of the cell, IFN α/β is bound autocrine and paracrine by the heterodimeric transmembrane receptor IFNAR, which is broadly expressed by nearly every cell type, and consists of two subunits, IFNAR-1 and IFNAR-2 (Gaboriaud, Uze et al. 1990). Interaction of IFN-I with IFNAR on the cell surface leads to the activation of the Janus-Kinase (Jak)-signal transducer activator of transcription (STAT) pathway (Darnell, Kerr et al. 1994). The intracellular domains of the IFNAR subunits are associated with Janus protein tyrosine kinases (Jak PTKs or JAK), namely Tyk2 and Jak1. Binding of IFN-I to IFNAR results in cross-activation of these Jak kinases through a conformational change, bringing the two JAKs close enough to phosphorylate each other. After autophosphorylation the JAKs phosphorylate their downstream substrates, which are two members of the family of signal transducers and activators of transcription (STATs), named STAT1 and STAT2 (Darnell, Kerr et al. 1994). The tyrosine-phosphorylated and activated STAT1 and STAT2 dissociate from the IFNAR receptor and form together with another transcription factor member, IRF-9, the heterotrimeric complex ISGF3. The complex translocates to the cell nucleus and subsequently

binds to its specific DNA sequence, the IFN-stimulated regulatory element, ISRE (Kessler, Veals et al. 1990). The IFN-stimulated activation of the promoter results in the transcriptional induction of more than 300 target genes, so called IFN-stimulated genes, ISGs (Der, Zhou et al. 1998). A few of these ISGs implicate antiviral effects, also against HBV (detailed explained in chapter 1.5.4), encoding for example for PRRs, transcription factors or candidates with immediate antiviral activity, which include proteins that regulate post-transcriptional and post-translational events.

1.4 Hepatitis B virus

1.4.1 Classification

The Hepatitis B virus (HBV) is a small and enveloped deoxyribonucleic acid (DNA) virus, which is highly species- and liver specific. HBV replicates only in hepatocytes and belongs to the family of *hepadnaviridae* (hepatotrop associated DNA viruses) (Gust, Burrell et al. 1986). The replication of the DNA genome occurs via a ribonucleic acid (RNA) intermediate by reverse transcription in the cytoplasm of host liver cells. Therefore the virus also belongs to *pararetroviruses*. HBV is divided into four major serotypes (adr, adw, ayr, ayw) to distinguish between different variations in between subspecies of HBV (Magnius and Norder 1995). The differentiation is based on antigenic epitopes presented by the envelope proteins. Furthermore, HBV is divided into eight genotypes (A-H), according to diverse overall nucleotide sequence variations of the HBV genome (Kramvis, Kew et al. 2005). The genotypes differ by at least 8% of their sequence, which has been associated with anthropological history and exhibit distinct geographical distributions (Norder, Courouce et al. 1992). For example, type A is prevalent in Europe, North America and Africa (Norder, Hammas et al. 1993), genotype D has a worldwide distribution but predominates in the Mediterranean area (Lindh, Andersson et al. 1997). Type A and D are also predominant in Germany (Vieth, Manegold et al. 2002). The differences in between the genotypes A-H significantly affect the disease severity, the response to distinct treatment therapies and possible vaccination strategies against the virus.

1.4.2 HBV history and research

Lürmann made the earliest record of an epidemic caused by HBV in 1885 in Bremen, Germany (Lürmann A., 1885). Almost a century later Blumberg discovered in 1965 the 'Australian antigen', afterwards known to be the Hepatitis surface antigen, HBsAg, in the blood of Australian aboriginal people (Blumberg, Melartin et al. 1966). Subsequently, he identified the antigen as the infectious agents of viral hepatitis (Blumberg, Sutnick et al. 1969), a discovery made him receive the Nobel prize of Medicine in 1977. Finally, Dane discovered the virus particle in 1970 by electron microscopy (Dane, Cameron et al. 1970). In 1979, the genome of the virus has been sequenced (Galibert, Mandart et al. 1979). A vaccine against human hepatitis B is available since 1981. After completion of 3 required vaccinations, 95% to 100% of recipients achieve adequate protection in preventing HBV infection.

Human HBV infects only humans and humanoid primates, such as Chimpanzees (Vaudin, Wolstenholme et al. 1988), Gibbons (Norder, Ebert et al. 1996) and Gorillas (Grethe, Heckel et al. 2000). Close relatives of human HBV, which also belong to the genus of *orthohepadnaviridae* and specifically infect different animal populations, are the Woodchuck hepatitis B virus (Summers, Smolec et al. 1978), the Beechey Ground squirrel hepatitis B virus (Marion, Oshiro et al. 1980) and the New World Woolly Monkey hepatitis B virus (Lanford, Chavez et al. 1998). Another genus of *hepadnaviridae* is called *avihepadnaviridae*, hepatitis B viruses that infect birds, including snow goose hepatitis B virus (Schettler 1971), Peking duck hepatitis B virus (Mason, Seal et al. 1980) and heron hepatitis B virus (Sprengel, Kaleta et al. 1988).

There is a lack of appropriate animal models for investigations of interaction between virus and host in HBV research due to the high species specificity of HBV. The animal models already mentioned above are little characterized, difficult to keep and rather expensive. For this reason, up to date, HBV-transgenic mice serve as a model for chronic HBV infection (Chisari, Pinkert et al. 1985; Guidotti, Matzke et al. 1995). Additionally, the transduction of mice with adenoviral vectors for hepatocyte-specific expression of a complete HBV-genome reflects some characteristics of an acute HBV infection accompanied by liver inflammation and followed by elimination of HBV replication (Ren and Nassal 2001; Sprinzl, Oberwinkler et al. 2001; Isogawa, Kakimi et al. 2005). Surprisingly, hepatocytes of *tupaia belangeri*, a tree shrew, which is not related with primates, are infectable with human HBV (Walter, Keist et al. 1996; Yan,

Su et al. 1996). The *tupaia* hepatocytes can repopulated a mouse liver in immune deficient mice, whose endogenous hepatocytes were destroyed by a liverspecific urokinase treatment (Dandri, Burda et al. 2005). But this infection model is inefficient and self-limiting.

The repertoires of cells, which can be infected with human HBV, and therefore are suitable as cell-culture model, are limited by the viral hepatotropism. Human hepatoma cell lines, such as HuH7 (Nakabayashi, Taketa et al. 1982) and HepG2 (Hirayama, Kohgo et al. 1993), are not infectable with HBV apart from some rare clones for example HepG2-BV cell line (Bchini, Capel et al. 1990), but are a useful tool to investigate intracellular aspects of viral replication. For this purpose the HBV genome is transferred into the cells by transient transfection or adenoviral vectors. Nevertheless, HepaRG cells, a cell line that exhibits hepatocyte-like morphology and express specific hepatocyte functions, is susceptible to HBV infection. Differentiation and infectability are maintained only when these cells are cultured in the presence of corticoids and dimethyl sulfoxide (Gripon, Rumin et al. 2002). Stably HBV transfected hepatoma cell lines, such as HepG2 2.15 expressing genotype A HBV (Sells, Zelent et al. 1988) and HepG2 H1.3 expressing genotype D HBV (Jost, Turelli et al. 2007; Protzer, Seyfried et al. 2007), replicate from several copies of integrated HBV overlenght genomes. These cells additionally allow the production of high titers of HBV, suitable for infection of HepaRG cells and primary human hepatocytes (PHH) (Schulze-Bergkamen, Untergasser et al. 2003). PHHs are isolated from surgical liver resections and are a useful tool to investigate early steps of HBV replication after acute infection with HBV. Interestingly, HepG2 H1.3 cells and HBV infected PHH additionally express covalently closed circular HBV-DNA (cccDNA). This supercoiled HBV-DNA form accumulates and persists as an episome in the nucleus of hepatocytes, serving as the viral transcription template during natural infection.

1.4.3 Liver structure

The liver (greek *hēpar*) is the central organ of metabolism in the human body. It can be divided into two lobes or 8 segments and has a wide range of functions, such as plasma protein synthesis (e.g. coagulation factors), utilization of nutritional components (e.g. glycogen and fat storage), cholesterin and bilic acid synthesis, as

well as detoxification. Nutrients, absorbed from the intestine into blood, catabolism products of the spleen and pancreatic hormones reach the liver by the portal vein. The liver predominantly consists of mostly multinucleated parenchymal cells, the hepatocytes (**Fig. 2.27**). Extended capillaries, so called liver sinusoids, are blood vessels located between hepatocytes that provide liver cells with oxygen-rich blood from the hepatic arteries and with nutrient-rich blood from the portal vein. The blood is then taken up by central veins, which join the liver vein, and finally delivered back to the circulation. Sinusoids are flanked by liver endothelial cells (LSECs) and contain specialized macrophages of the liver, so called Kupffer cells. The room between LSECs and hepatocytes, the space of *Disse* (named after Joseph Disse), contains a third type of non-parenchymal cells; vitamin A containing and fat-storing stellate cells named *Ito* cells. Nevertheless, HBV replication only takes place in the the hepatocytes.

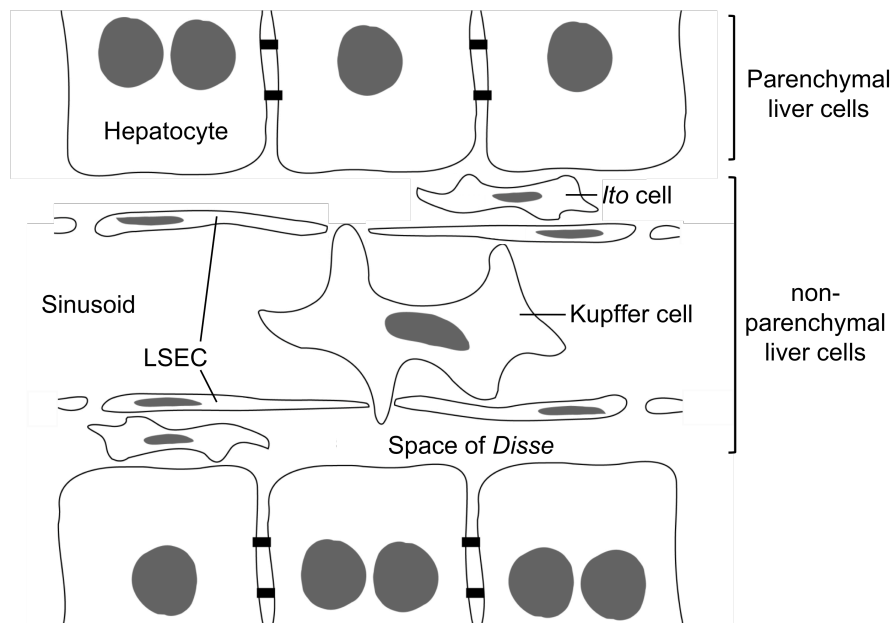


Fig. 1.5: Formation of liver cells. Modified after K. Esser.

1.4.4 Epidemiology of HBV infection

Despite the availability of an HBV vaccine, infection rates of HBV increase constantly worldwide, especially in developing countries. The WHO estimate worldwide two billion infected people and more than 360 million chronic carriers, with high risk to develop liver cirrhosis and HCC. Approximately 700 000 people die each year due to the acute or chronic consequences of hepatitis B (WHO, 2008). Infection with HBV occurs by exchange of body fluids through blood or sexual contacts with an infected person and proceeds in between adults by horizontal transmission or from an infected mother to a newborn by vertical transmission (Ganem 1982). People with high risk of HBV infection therefore include parental drug users, people with multiple sex partners and infants born to HBV-infected mothers. After an acute phase of infection with HBV, some patients develop a chronic state with a lifelong infection. The two primary adverse outcomes of chronic HBV infection are liver cirrhosis and primary hepatocellular carcinoma (HCC); either of both can lead to a liver related death (Beasley, Hwang et al. 1981).

HBV infection, acute or chronic, holds variable manifestations (**Fig. 5**). During the acute state, HBV infection can manifest as a subclinical or icteric hepatitis and rarely in 0.1% to 0.5% of patients, as acute fulminant hepatitis with acute liver failure. Chronic HBV infection can be asymptomatic or can be manifested by symptoms and signs of cirrhosis or hepatocellular carcinoma or both. Subsequent course of disease after primary HBV infection is individual and depends on age and general immune status of the patient. After primary infection with HBV the acute phase of infection starts with an incubation period without any symptoms (asymptotic) that ranges from four to six weeks. During the acute phase of infection approximately one third of all patients proceed asymptotic and develop neutralizing immunity. Thus, the majority of patients show after an asymptomatic incubation time symptoms like fatigue, malaise, anorexia or flu-like symptoms until jaundice may become apparent. Afterwards, the patients develop an acute liver inflammation (hepatitis). In 95% of infected adults the virus is cleared after an acute infection, only 5% of infected adults, but 20-50% of infants in early childhood (one to five years) and even 90% of infected perinatals develop a chronic state of infection (McMahon, Alward et al. 1985).

Dependent on different phases of chronic infection, the annual rate of progression to cirrhosis in untreated patients has been estimated to be 2 – 9 % (Yim and Lok 2006).

HBV is a non-cytopathic virus, but strongly carcinogen. Severe liver damage is due to a strong inflammatory response against the virus (Chisari and Ferrari 1995 a; Chisari and Ferrari 1995 b) and the risk of hepatocellular carcinoma is 100 times higher in patients with HBV infection than in uninfected ones (Pungpapong, Kim et al. 2007).

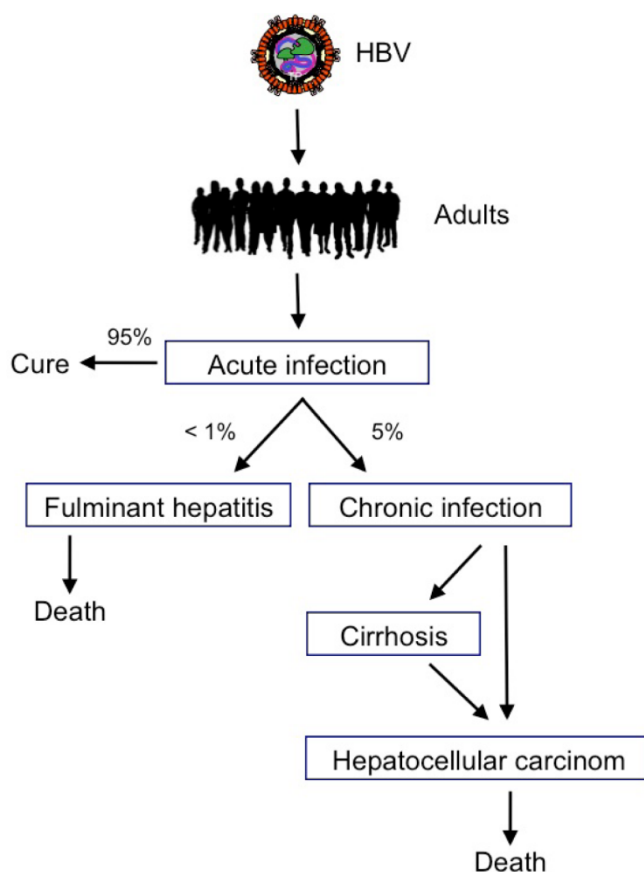


Fig. 1.6: Clinical development of HBV infection in adults.

About half of the world's population has had contact with HBV, but HBV prevalence varies drastically worldwide (**Fig. 6**). Regions with low prevalence, where less than 2% of the population is chronic HBsAg carrier, are developed countries in Central Europe, in North America, in southern parts of South America, as well as Australia. Decreasing numbers of between 0.4% and 0.7% (~500.000) of the population in Germany live with chronic hepatitis B (Robert Koch Institut, Epidemiologisches Bulletin 2004). Intermediate infection rates (2 -7% HBsAg positive) are found in East Europe, Middle East, Russia, India, North Africa and in southern parts of Brazil. High prevalence is given in developing countries like in Africa south of the equator, in

Southeast Asia, or in China, where hepatitis B is endemic and about 10% of the population is HBV positive (WHO, 2008).

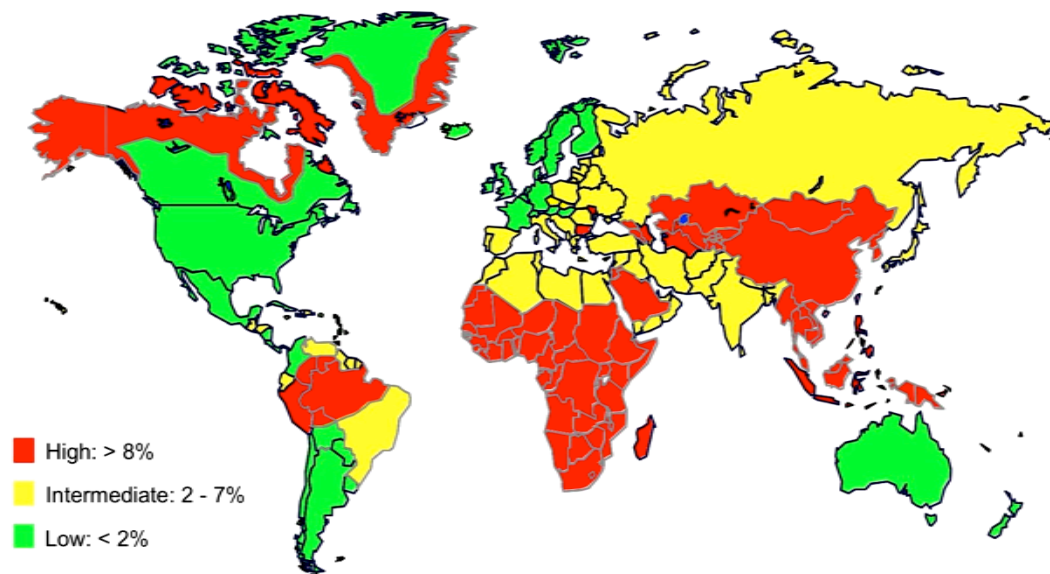


Fig. 1.7: Hepatitis B prevalence 2005. Worldwide distribution of chronic HBsAg carriers

1.4.5 Morphology and structure of HBV

Electron microscopy (EM) imaging of purified preparations of HBV from serum of patients shows that infected hepatocytes secrete three different types of particles (**Fig. 7**). First, infectious virions with a diameter of 42 - 47 nm, known as *Dane* particles and second two different types of subviral particles, which are not infectious (Dane, Cameron et al. 1970). Infectious virions contain a single copy of a partially double-stranded DNA genome of ~3.2 kilo base (kb) pairs, which is covalently linked via a terminal protein (TP) domain at the 5'-end of the negative strand to the viral polymerase (P) (Bartenschlager and Schaller 1992). The viral genome is packaged into a icosahedral nucleocapsid of about 27 nm diameter, composed of 180 or 240 homodimeric subunits of the viral *core* protein, which is arranged with triangulation numbers of $T = 3$ or $T = 4$ (Crowther, Kiselev et al. 1994). There are evidences, that cellular proteins, including chaperones and protein kinases are also packaged inside of nucleocapsids (Hu, Toft et al. 1997). The capsid itself is surrounded by a host derived lipid bilayer. Integrated into the lipid membrane are three different viral

surface proteins, expressed by the viral genome, the large (L-), the middle (M-) and the small (S-) protein (Neurath, Kent et al. 1985). All three surface proteins are anchored in the lipid membrane by a hydrophobic C-terminus with four transmembrane α -helices (Berting, Hahnen et al. 1995). The L-protein is expressed at levels of about 5 – 15 % compared to S-protein on the surface of Dane particles, the M-protein at levels of about 1 – 2 % compared to S-protein (Robinson, 1995).

The secreted non-infectious subviral particles (SVP) are divided into spherical SVP (or spheres) and filamentous SVP (or filaments) with a diameter between 15 and 22 nm and consist exclusively of surface proteins (Ganem and Prince 2004). Spheres represent, for a protein complexed particle uncommon, octahedral symmetry with a diameter of approximately 20 nm and comprise basically of S-protein and marginal M-protein. The enclosed lipids of spherical SVPs appear not to be located in a typical semifluid lipid bilayer, but rather in an immobilized form on the surface (Satoh, Imai et al. 2000; Gilbert, Beales et al. 2005). Filaments consist of all three surface proteins, L-, M- and S-protein, and are variable in size (**Fig. 7**). The SVPs contain neither viral capsids nor viral DNA and are therefore not infectious. Nevertheless they are highly immunogenic. The pathological role of SVPs is still unclear. Titers of Dane particles in the blood of patients can range from less than 10^4 / ml to more than 10^9 / ml. In contrast, filamentous SVP can be present in 100 fold excess, spherical SVPs even in 10 000 fold excess (Ganem and Schneider 2001). For this reason, SVPs might be responsible for capturing anti-HBV antibodies, produced naturally in the body, which are preferentially directed against the S-protein. Through the neutralization of the antibodies the virions might be protected against an immune response of the host (Rehermann and Nascimbeni 2005). The HBV surface antigen HBsAg, predominantly exposed on SVPs and used as a serological marker, reaches concentrations of 500 mg / ml in the blood of HBV patients (Hoofnagle 1981).

All three surface proteins of HBV are translated from one open reading frame. They differ by distinct in-frame starting codons of initiation; the carboxyterminal ends are identical

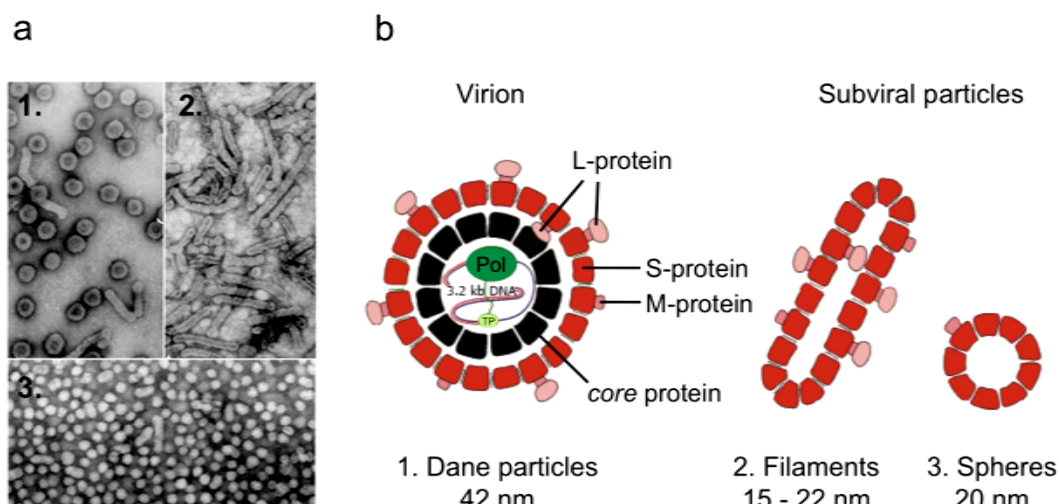


Fig. 1.8: Structures of hepatitis B virus particles. **a)** Electron microscopy (EM) from HBV carrier plasma and **b)** schematic presentation of human HBV particles structures. The infectious Dane particles (1.) with a diameter of ~42 nm are composed of a host derived lipid bilayer with integrated HBV surface proteins (L-, M- and S-protein). This envelope covers the nucleocapsid, composed of viral core proteins. The nucleocapsid harbors the 3.2kb HBV DNA genome, covalently linked via the terminal protein (TP) to the viral polymerase (Dandri, Burda et al.). The non-infectious subviral particles (SVP), filaments (2.) and spheres (3.), differ in structure, size and HBV surface-protein composition. SVPs contain neither viral capsids nor viral DNA. Images modified after a) (Gerlich and Kann) and 2005 b) (Glebe and Urban 2007)

1.4.6 Genomic organization and protein function of HBV

The HBV genome present in virions is a 3.2 kb partially double-stranded relaxed, circular DNA (rcDNA) molecule and the smallest known full replicative mammalian viral genome (**Fig. 8**). Therefore, the genome has a very complex organization with multiple overlapping open reading frames (ORFs). Every nucleotide in the HBV-genome encodes for one of the HBV-proteins.

The viral polymerase is covalently attached via the terminal protein (TP) to the 5'-end of the full-length antisense minus-strand, which is complementary to the viral mRNA. The 3'-end of the sense plus-strand is of variable length, hence a part of the viral genome is single stranded (ss). After infection of the cell the viral DNA translocates into the nucleus, where plus-strand of the rcDNA molecule is repaired, resulting in circularized cccDNA. The cccDNA serves as a template for the viral pre- (pg-) and

subgenomic (sg) messenger RNAs (mRNAs). The small and compactly organized HBV genome consists of four overlapping ORF on the (-)-antisense DNA-strand (Schlicht and Schaller 1989). The ORF preC/Core encodes for the precore protein (HBeAg) and the *core* protein (C), ORF preS1/preS2/S encodes for the surface proteins (L, M and S), ORF polymerase encodes for the viral polymerase (Pol) and the ORF X encodes for the viral X protein (X). The transcription of viral mRNAs is regulated by four promoters, the preC/C-, preS1 (L)-, preS2 (S)- and the X-promotor. Starting at these different promoter sites, transcription in all cases ends at one common polyadenylation (polyA) signal, resulting in one pregenomic and three subgenomic viral mRNAs (Cattaneo, Will et al. 1984). Two internal enhancer elements (Enh1/Enh2) differently influence the promoters. Enh1 increases transcription of all four promoters, whereas the liver-specific Enh2 (Hu and Siddiqui 1991) only upregulates the transcription-rate of preS2/S (Ganem and Schneider 2001).

Once formed, the cccDNA in the nucleus serves as a template for the transcription of four groups of viral RNA. First these are the 3.5 kb pre-core mRNA (pre-C) and pregenomic (pg) RNAs. PreC mRNA (also named e mRNA in **Fig. 8**) is translated to produce a precore protein that is further proteolytically cleaved into e antigen (HBeAg). HBeAg is not a component of viral and subviral particles, but is secreted from infected liver cells. The function of HBeAg is widely undefined, but it has been implicated as an immune tolerogen, whose function is to promote a persistent infection (Milich and Liang 2003). Viral replication levels correlate with HBeAg levels in the serum of patients and HBeAg level is therefore used as serological marker. The 3.5 kb pgRNA transcript is bi-functional. On the one hand it serves as mRNA for the translation of viral capsid protein and the DNA polymerase, initiated at different startcodons. On the other hand pgRNA serves as a template for reverse transcriptional synthesis of the viral genome and is afterwards packaged together with the complex of viral polymerase and terminal protein into the nucleocapsid. The *core* protein has the intrinsic property to self-assemble into capsid structure (Zhou and Standing 1992) and contains a cluster of aminoacids at the C-terminus with RNA-binding activity to get in contact with the pgRNA (Hatton, Zhou et al. 1992).

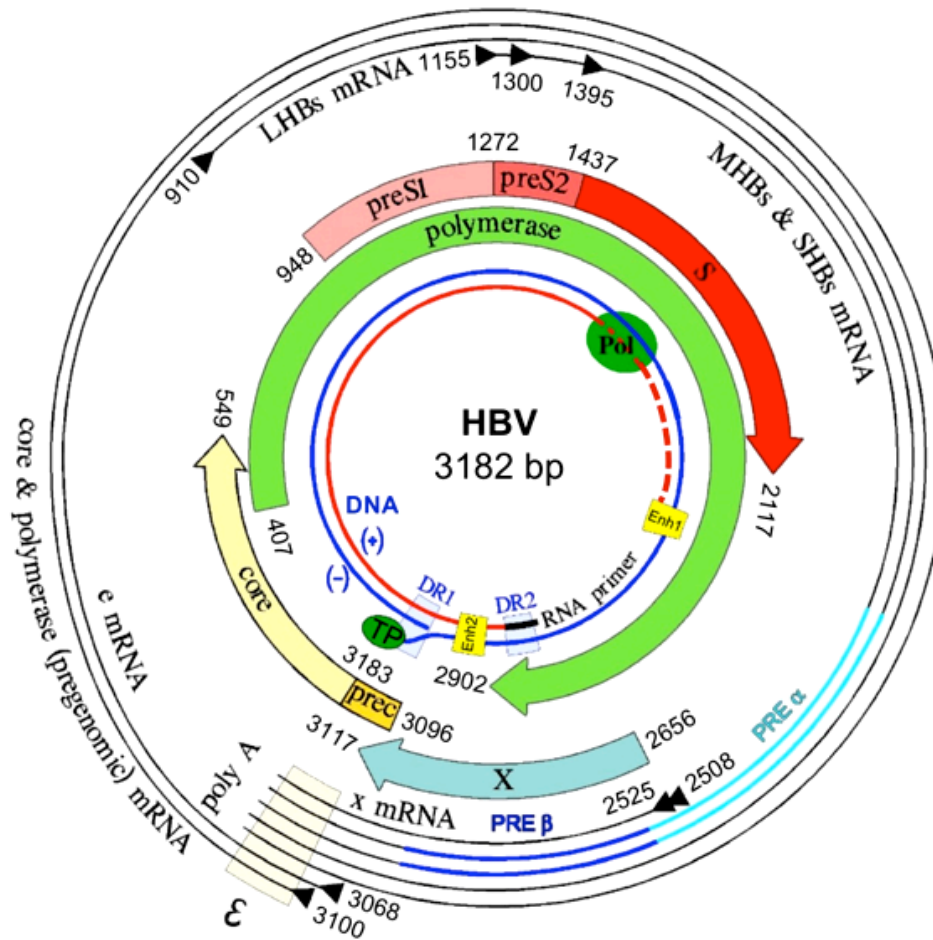


Fig. 1.9: The HBV genome. a) Schematic organization of the HBV genome: The inner red and blue circles represent the partially double-stranded HBV genome, which displays the viral relaxed circular (rc) HBV DNA form, with polymerase (pol) and terminal protein (TP) as green circles, enhancer (Enh1/Enh2) and direct repeat (DR1/DR2) elements as boxes. PreC- (e-), Pre- and subgenomic mRNA transcripts are illustrated in black outer circles. PreC mRNA encodes for the precore protein (HBeAg), the pregenomic mRNA encodes for core protein and polymerase, subgenomic L-, M- and SHBs (large, medium and small hepatitis B surface) mRNAs for the envelope proteins. Triangles indicate transcription starts, the yellow square symbol the encapsidation signal (ϵ) and blue lined areas the post-translational regulatory element (PRE). The colored arrows inside the scheme depict the four open reading frames (ORFs) and the translated viral products: prec/core (HbeAg), core (capsid-protein), polymerase, preS2, preS1 and S (surface proteins L, M and S), and X (X-protein). Modified after (Gerlich and Kann 2005).

The viral polymerase is functional divided into three domains. The terminal protein domain, which is involved in encapsidation and initiation of minus-strand synthesis; the reverse transcriptase (RT) domain, which catalyzes viral genome synthesis; and

the ribonuclease H (RNaseH) domain, which degrades pgRNA and facilitates replication. The three subgenomic RNAs include exclusively mRNA functions. The sgRNAs of 2.4 kb and 2.1 kb are the transcripts for translation of all three viral surface envelope proteins L, M and S, and HBsAg, respectively. The mRNA of all surface proteins is transcribed from one ORF with different internal start-codons and all proteins share the S- protein sequence leading to identical C-termini. The M-protein is extended by the preS2 domain at the N-terminus, the L-protein is extended by the preS2- plus the pres1 domain (**Fig. 8**). The surface proteins are synthesized at the endoplasmic reticulum (ER), where they get integrated into the ER-membrane and thus build up the viral envelope. The sgRNA of 0.7 kb encodes for the X protein (HBx). HBx is indispensable for viral infection *in vivo* and influences multiple cellular gene functions necessary for virus survival, including signal transduction, transcriptional activation and inhibition of protein degradation (Bouchard and Schneider 2004). Moreover, HBx is controversially discussed to be involved in the mediation of HBV associated cancer. On the level of transcribed mRNA additional regulatory elements are found. Present on all mRNA is the post-transcriptional regulatory element (PRE), which suppresses splicing of the transcribed RNAs (Huang and Liang 1993). Additional posttranscriptional regulation elements within the HBV genome are the two direct repeats (DR1 and DR2) at the 5'-end of the plus-strand, which are required for plus-strand specific DNA synthesis during replication (Seeger, Ganem et al. 1986).

1.4.7 Replication of HBV

The replication of *hepadnaviridae* occurs similar to *retroviruses* via a RNA-intermediate that is packaged into the viral capsid in the cytoplasm of the host cell and afterwards reversely transcribed into viral DNA (**Fig. 9**). Therefore, HBV is also known as a *pararetrovirus* (Ganem and Schneider 2001). The replication of HBV is strongly restricted to hepatocytes of the host organism due to the liver tropism. Early steps of HBV infection, such as the attachment of the viral particle on the cell surface, the entry and release of the capsid into the cytoplasm and the transport of the viral genome into the nucleus of the host cell are not completely clarified. Nevertheless, actual data suggest that the N-terminal region of the L-protein is responsible for

attachment to the cell surface, followed by receptor-mediated endocytosis via still unknown receptor(s) (Tai, Suk et al. 2002). The binding of HBV to specific cellular receptor(s) is thought to trigger the actin-independent and microtubule-dependent entry of the virion into hepatocytes by endocytosis (Schmitt, Glebe et al. 1999; Funk, Mhamdi et al. 2004). These findings support the idea of endocytosis since endosomes are transported via microtubules towards the perinuclear region. Presumably, the viral capsid is released into the cytoplasm from endosome upon fusion of the viral envelope and endosomal membranes, a process that might be induced by low pH and proteolytic cleavage of envelope proteins (Lu, Block et al. 1996). After this uncoating event near the cell surface the intra-cytosolic translocation of the nucleocapsid to the nucleus is facilitated by the interaction with microtubules. Delivery of the rcDNA into nucleus is mediated by close contact of the viral capsid and the nuclear-pore complex (NPC) via interaction of a nuclear localization signal (NLS) at the C-terminus of the *core* protein and nuclear import receptors importin α and β . (Kann, Sodeik et al. 1999). Exposure of the NLS is regulated and depends on phosphorylation of the capsid protein (Kann, Schmitz et al. 2007). Size restrictions indicate that the complete disassembly of the capsid and the release of the viral genome into the nucleus occur in the nuclear basket of NPC (Andreyev, Norman et al. 2001). After entry of the viral genome into the nucleus the gap in the plus-strand of the partially double-stranded rcDNA molecule is repaired and completed by cellular enzymes, resulting in a supercoiled HBV genome with cccDNA form. Mechanisms and enzymes involved in this process are intensively investigated. The cellular RNA-polymerase II promotes transcription from the cccDNA template to synthesize pre- and subgenomic RNAs. Afterwards, the RNA transcripts are transported into the cytoplasm without any splicing events (Kock and Schlicht 1993), where translation into viral surface proteins L, M and S as well as the X-protein based on subgenomic RNAs takes place. The translation of the surface proteins is mediated by ribosomes of the ER. The surface proteins get integrated into the ER membrane and obtain modifications like glycosylation and myristoylation, indispensable for proper protein folding (Helenius 1994) and infectivity of the virion (Glebe and Urban 2007). Free ribosomes promote the translation from preC-RNA to “pre-C protein” that is further proteolytically processed into HBeAg (Ganem and Schneider 2001). They also mediate the translation from the pgRNA to obtain viral polymerase and the capsid-protein *core*.

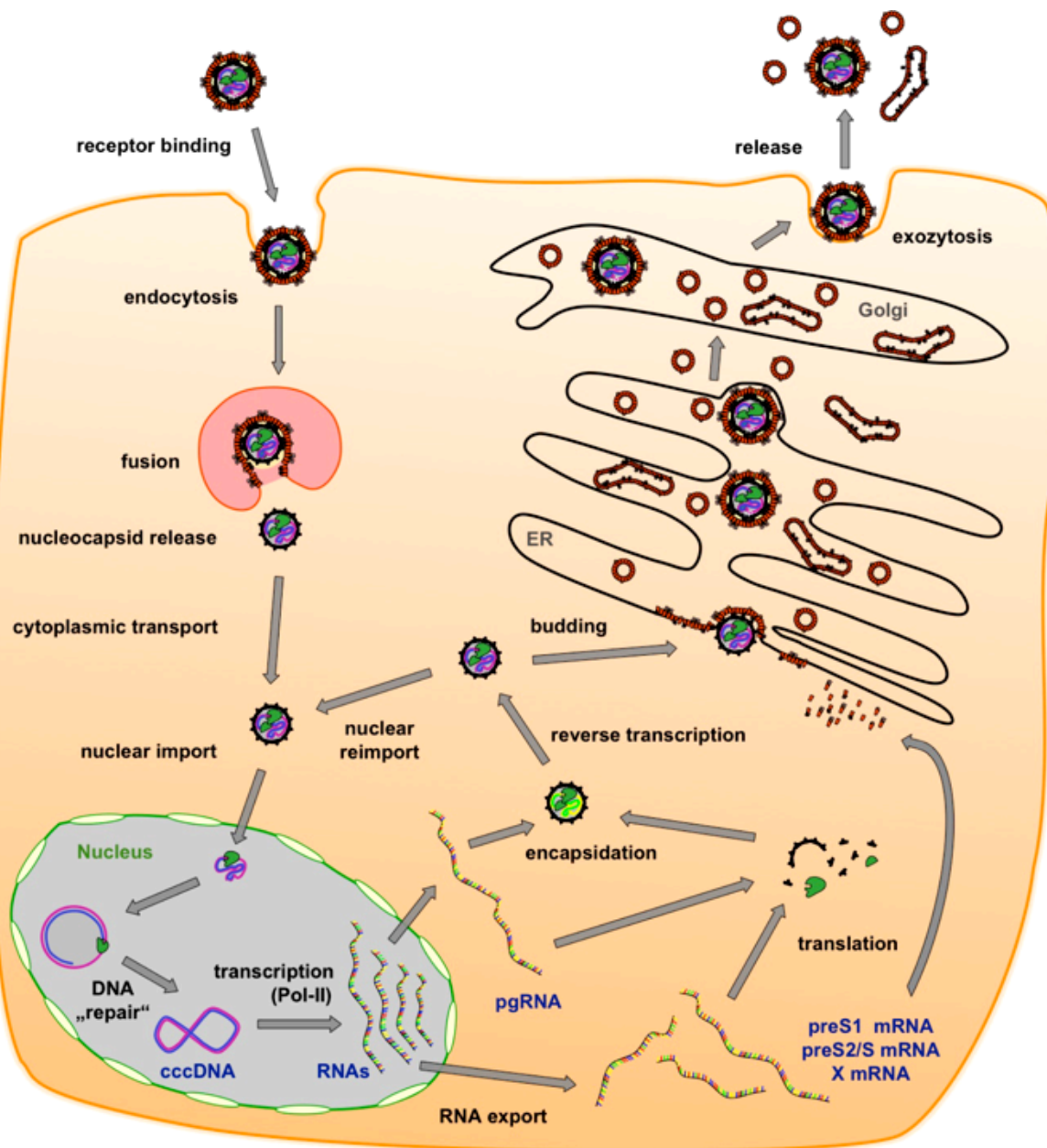


Fig. 1.10: The replication cycle of HBV. HBV virions attach to the cell surface of the hepatocyte via an unknown receptor. During the entry step the nucleocapsid gets uncoated and is released into cytoplasm of the cell. The partially double-stranded DNA genome is imported into the nucleus, where cellular enzymes repair the plus-strand gap, leading to the formation of cccDNA. The episomal viral cccDNA genome is transcribed into viral pre- and subgenomic RNAs. After the export of the RNAs into the cytoplasm, translation into viral proteins takes place. The pregenomic RNA gets encapsidated and reverse transcribed into the HBV DNA genome. The viral genome of mature nucleocapsids is either re-imported into the nucleus or the capsid buds into the ER, where it receives its envelope containing the HBV surface proteins. Virions and subviral particles are transported through the ER/Golgi network to the cell surface and get secreted.

Additionally, the pgRNA represent the viral genome and is packaged in the viral capsid in the cytoplasm of the HBV-infected cell (Beck and Nassal 2007). Therefore, the complex of viral polymerase and terminal protein initially interacts with a stem-loop structure (encapsidation-signal ϵ) at the 5'-end of the pgRNA and gets covalently linked to the pgRNA (Bartenschlager and Schaller 1992). The encapsidation of the pgRNA-protein-complex is initiated by the attachment of core-protein-dimers to ϵ (Pollack and Ganem 1994), followed by self-assembling of the capsid. After completion of the newly synthesized capsid, the viral polymerase promotes reverse transcription of the pgRNA (**Fig. 10**). Binding of the DNA polymerase protein complex to ϵ at the 5'-end of pgRNA additionally initiates reverse transcription. A tyrosin residue of the terminal protein primes viral DNA minus-strand synthesis for extension of three nucleotides (Wang and Seeger 1992). Subsequently, polymerase and covalently attached nascent DNA is translocated to the 3'-end copy of DR1 and minus strand DNA synthesis continues by copying pgRNA. Simultaneously, the positive orientated RNA of the RNA/DNA-hybrid is eliminated by the RNaseH activity of the reverse transcriptase, (**Fig. 10 a**) (Walton, Wu et al. 2001). When the polymerase reaches the 5'-end of pgRNA, an RNA oligomer that contains DR1 sequence is left uncleaved and subsequently translocated and annealed to DR2 (**Fig. 10 b, left**). This short RNA-oligonucleotide at the 5'-end serves as a primer (Lien, Aldrich et al. 1986) for plus-strand synthesis, initiated at DR2 (Beck and Nassal 2007). Several cis-elements appear to promote close proximity of the DR regions (**Fig. 10 b, right**). After the copy of the 5'-end of DNA minus-strand during synthesis the growing 3'-end of the DNA plus-strand switches to the 3'-end on the DNA minus-strand, which leads to circularization of the HBV genome and enables further elongation (**Fig. 10 c**) (Lien, Petcu et al. 1987). Extension of the DNA plus-strand on the DNA minus strand template creates the partially double-stranded relaxed, circular DNA (rcDNA) genome (**Fig. 10 d**).

development of hepatocellular carcinoma.

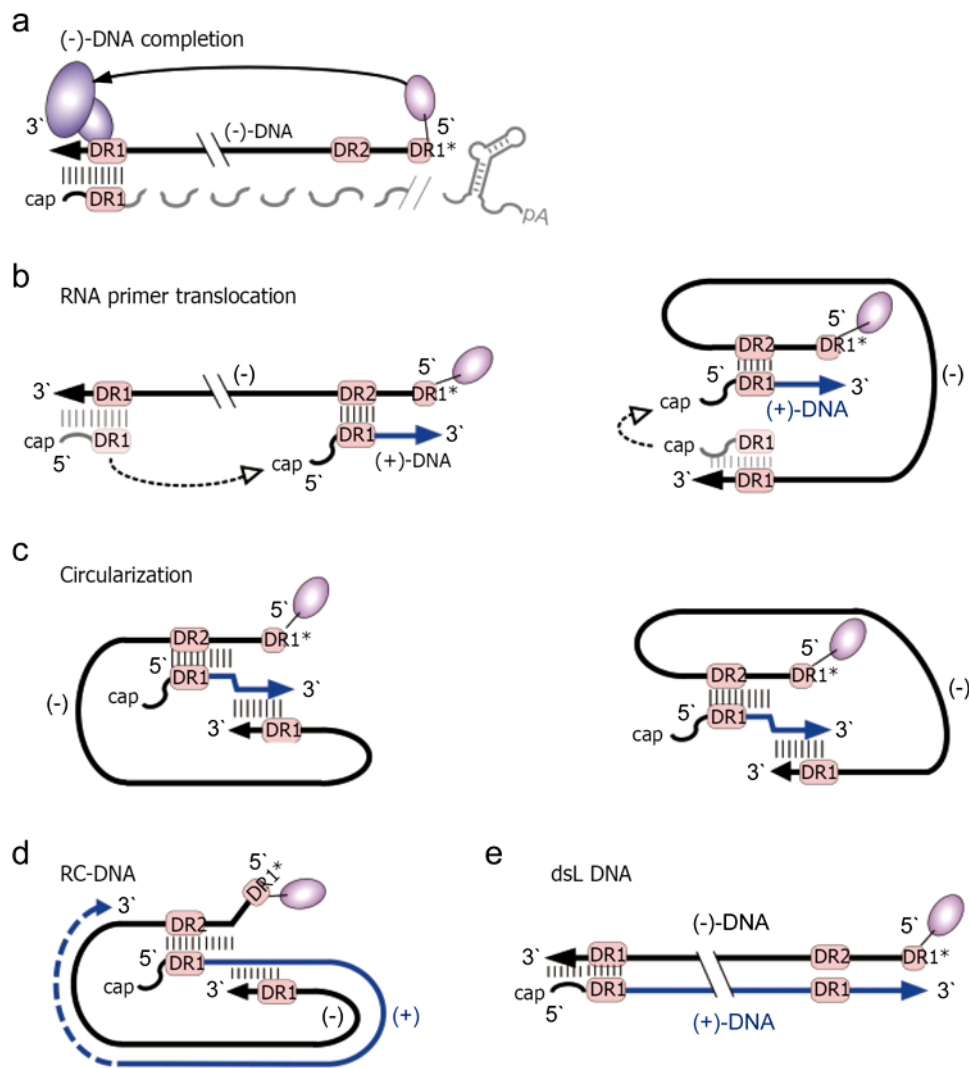


Fig. 1.11: Schematic illustration of rc-DNA synthesis by reverse transcription. **a)** During (-)-DNA synthesis and completion, the DNA primer, still linked to TP, is extended from DR1* to the 5'-end of pgRNA. The pgRNA is simultaneously degraded by the RH domain, except for its capped 5' terminal region including 5' DR1 **b)** The RNA primer translocates to DR2, and is extended to the 5'-end of (-)-DNA. **c)** The growing 3'-end of the (+)-DNA switches to 3' -end (-)-DNA, enabling further elongation and circularization. **d)** Elongation on the (-)-DNA template creates rcDNA genome **e)** Double-stranded linear (dsL) DNA synthesis due to failed primer translocation to DR2, called "in situ priming". Modified after (Block, Guo et al. 2007).

A minor DNA form of double-stranded linear (dsl) DNA originates when the RNA primer failed to translocate from DR1 to DR2 (**Fig. 10 e**). This process is called “*in situ*” priming and occurs in around 1 - 5% of naive human HBV replication (Nassal 1992). Dsl-DNA arises by *in situ* priming or by non-homologous recombination (Yang and Summers 1995) can be integrated directly into the host DNA. It is assumed, that presence of foreign viral DNA in the host genome, together with expression of viral proteins such as X protein may trigger the subsequent

When rcDNA is formed, the mature viral capsids can follow to different pathways. Some of them translocate through the cytoplasm back to the nucleus. The rcDNA is re-imported into the nucleus (Tuttleman, Pourcel et al. 1986) and converted into more cccDNA molecules (Wu, Coates et al. 1990), a way to increase cccDNA levels in the absence of re-infection of cell. This viral strategy operates very efficiently in the early stages of infection to build up and amplify the cccDNA pool, which is essential for HBV-transcription and replication (Werle-Lapostolle, Bowden et al. 2004). In stably infected hepatocytes of chronic HBV carriers, the nucleus may contain between 30 and 50 copies of cccDNA. The number of cccDNA molecules *in vitro* varies drastically. Stably HBV expressing HepG2 H1.3 cells contain approximately between 4 - 10 copies of cccDNA per cell. (Illing, IMMIH, Cologne, Diploma thesis). Other mature viral capsids bud to the ER-lumen, by which they get enveloped with a lipid bilayer that contains the modified viral surface proteins integrated into the ER membrane (Huovila, Eder et al. 1992). Afterwards virions and SVPS pass the Golgi and the trans-golgi-network (TGN) and are then further transported to the plasma membrane in microtubule independent endosomal vesicles, distinct from the transcytotic pathway, to bud out of the cell by exocytosis and efficiently infect neighboring cells and new hosts. It is likely that sphingolipids (lipid rafts) are utilized for this transport, similar to other enveloped viruses like influenza (Scheiffele, Rietveld et al. 1999).

1.4.8 HBV specific immune response

Analysis and determination of early events in human HBV specific immune responses are difficult, because HBV infected patients are screened for the first time after the onset of clinical symptoms, which means four to six weeks after primary infection. However, the following clinical courses and serologic profiles of acute and chronic hepatitis B differ in several aspects (**Fig. 11**). The typical course of acute and self-limiting hepatitis B (**Fig. 11a**) is initiated with detectable HBV-DNA in the serum four weeks after primary infection, with low concentrations about 10^2 to 10^4 genome equivalents per ml blood (Rehermann and Nascimbeni 2005). HBsAg arises four weeks after primary exposure to the virus, followed by HBeAg and antibody responses against the viral core protein (anti HBc) two weeks later, which primarily disclose an IgM-isotype during early progress (Hoofnagle 1981). Viremia is established with high viral titers of about 10^9 to 10^{10} viral particles per ml (Ribeiro, Lo et al. 2002) and studies with chimpanzees revealed that 75 – 100% of hepatocytes are infected at this time point (Kajino, Jilbert et al. 1994). Additionally, after 5 to 15 weeks after primary infection, alanine aminotransferase (ALT) levels in the serum rise during the acute phase and jaundice may appear, indicating a cytotoxic liver-inflammation and the begin of an adaptive immune response. ALT is secreted by apoptotic hepatocytes and is used as a clinical marker for the degree of liver damage. HBeAg is usually cleared early at the peak of clinical illness, whereas HBV DNA and HBsAg persists in the serum for the duration of symptoms and are cleared with recovery. In 95% of infected adults the virus is cleared after an acute infection, accompanied by the formation of HBe-, HBs- and HBeAg specific IgG antibodies, providing protective immunity (Rehermann and Nascimbeni 2005).

Patients who develop chronic hepatitis B show similar initial patterns of serological markers with appearance of HBV DNA, HBs- and HBeAg, as well as anti HBc (**Fig. 11b**). The subsequent course and severity of chronic hepatitis B is quite variable (Ganem and Prince 2004). In contrast to acute infection, the chronic progression is characterized by lack of anti HBsAg specific IgG antibodies and a late and weak HBeAg specific antibody response. Also typical for chronic hepatitis B are variably high but persistent HBV DNA and ALT levels and a persisting production of HBsAg, which remains detectable for years, if not for life after primary exposure to HBV (Ganem and Schneider 2001).

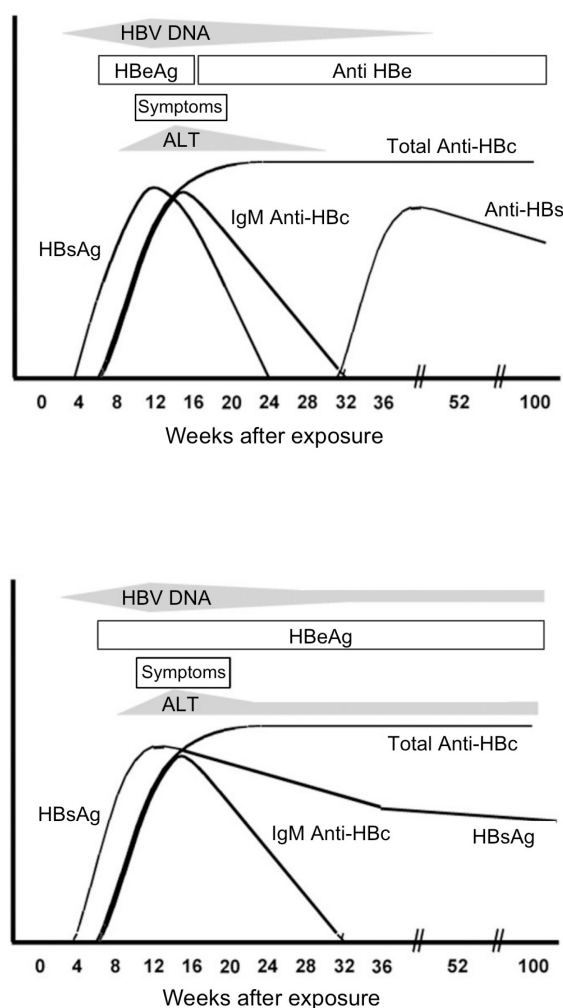


Fig. 1.12: Clinical courses and serologic profiles of a) acute resolving and b) chronic hepatitis B. Relative amounts and appearance of viral replication (HBV DNA), HBV proteins (HBs- and HBeAg), HBV specific antibodies (anti-HBc, - Hbs, -HBe), liver injury (alanine aminotransferase, ALT) and symptoms during time-courses of a) acute, self-limiting and b) chronic hepatitis B infection. Modified after (Liang 2009).

The course of HBV infection strongly depends on the adaptive T-cell immune response of the host (Wieland, Thimme et al. 2004). Cytotoxic T-cells are responsible on the one hand for elimination of the virus during acute and self-limiting hepatitis B and on the other hand for liver injury during chronic HBV-infection (Thimme, Wieland et al. 2003). Patients with acute but resolving hepatitis B develop a strong, polyclonal and virus specific T-cell response (Bertoletti, Ferrari et al. 1991). The T-cell response in patients with a chronic course in contrary is weak, monoclonal and virus non-specific (Penna, Chisari et al. 1991; Webster, Reignat et al. 2004). Cell lysis and turnover repopulate the

liver with new and uninfected cells. However, a chronic liver inflammation and following massive regenerative processes may also lead to mutagenesis that could promote development of DNA damage and consequently HCC formation (Chisari and Ferrari 1995). Additionally, it has been shown that an HBV-specific T-helper cells response is absent during chronic HBV infection (Ferrari, Penna et al. 1990), but regulatory T-cells (Tregs) have a suppressive impact on T-cell response, supporting persistence of HBV (Stoop, van der Molen et al. 2005). Other *in vivo* studies suggested that HBV core-antigen specific B-cells respond in a T-cell independent fashion along with production of neutralizing antibodies to prevent infection of new hepatocytes (Cao, Lazdina et al. 2001).

To prevent elimination HBV was thought to widely circumvent innate immune response and is therefore considered as a “stealth” virus. For instance, a study of experimental HBV infection of chimpanzees suggested that infection, *per se*, might induce no or little innate response in hepatocytes (Wieland, Thimme et al. 2004). However, several studies over three decades of research indicate that HBV is able to counteract the innate immune response by inhibition of several actors of the IFN-signaling pathway or down-regulation of functional TLR expression (Twu, Lee et al. 1988; Foster, Goldin et al. 1993; Visvanathan, Skinner et al. 2007; Wu, Xu et al. 2007; Xie, Shen et al. 2009). In contrast, recent analysis of patients revealed early development of NK and CD56+ natural T (NT) cell response during early stages of HBV infection (Fiscaro, Valdatta et al. 2009). Furthermore, it has been shown that HBV induces IL-6 production in primary human liver cells and that IL-6 inhibits transcription of HBV (Hösel et al., 2009, in press). These controversial results indicate that HBV is not a stealth virus at all and that the innate immune system is able to sense HBV and allow timely induction of adaptive immune response.

Nevertheless, HBV developed like other viruses different escape mechanisms to evade elimination by the immune system of the host. An important role in chronic course is proposed for the high quantity of produced SVPs. They contain high amounts of strongly immunogenic HBsAg-monomers and are produced in 10^4 - 10^6 fold excess over virions. Therefore they might be responsible for capture of HBsAg specific antibodies, thus mask infectious particles and prevent them from neutralization (Mangold and Streeck 1993; Rehmann and Nascimbeni 2005). Moreover high amounts of secreted HBeAg seem to participate to tolerating effects of HBV-specific T-cell (Milich and Liang 2003). HBV also seems to attenuate the expression of MHC I on hepatocytes, required for effective

presentation of HBV specific antigens on the cell surface to stimulate cytotoxic T-cell response (Chen, Tabaczewski et al. 2005). Another escape mechanism of HBV to evade an immune response is the outgrowth of mutated viruses. But this phenomenon occurs very rarely during acute and chronic HBV infection (Rehermann, Pasquinelli et al. 1995; Whalley, Brown et al. 2004). “Escape” variants of HBV, such as the G145R mutant with alterations in the S-protein, are frequently found in vaccinated individuals with breakthrough infections (Kalinina, Iwanski et al. 2003) or in graft infected liver transplant recipients under passive immunoprophylaxis with polyclonal hepatitis B hyperimmune globulin (HBIG) (Protzer-Knolle, Naumann et al. 1998).

1.5 Therapeutic approaches

1.5.1 Approved and novel inhibitors for antiviral therapy against HBV

Prophylactic vaccination against hepatitis B, available since 1981, provides efficient protection from HBV infection and its consequences. Acute hepatitis B infection does not usually require treatment, because 95% of adults clear the infection spontaneously. Early antiviral treatment is required in less than 1% of patients, whose infection develop into a fulminant hepatitis or who are immuno-compromised. Therapy of patients chronically infected with HBV mirrors the main effort for development of antivirals, which made significant improvements during the last decade. Approved and novel inhibitors potentially target all steps of viral replication (**Fig. 12**). Chronic hepatitis B hallmarks of candidates for therapy are active viral replication in the hepatocytes, positive HBV surface antigen levels for more than six months (Ganem and Prince 2004) and variable, but persistent HBV titers in the blood for more than twenty weeks (Robinson, 1996).

Approved treatments (**Fig. 12**, in red) include orally administered nucleos(t)ide reverse transcriptase inhibitors (NRTIs), also called nucleos(t)ide analogues. Their application inhibits viral replication and improves clinical outcome, including reduction of hepatocellular carcinoma (Liaw, Sung et al. 2004). There are currently licensed four NRTIs; *Lamivudine* (or *Epivir*), *Telbivudine* (*Tyzeka*), *Entecavir* (*Baraclude*) and *Adefovir* (*Hepsera*). Additionally, *Emtricitabine* and *Tenofovir* are approved in patients

co-infected with the human immunodeficiency virus (HIV) and HBV. Treatment of chronic HBV patients with NRTIs is well tolerated and strongly suppresses HBV replication, but require long-term application, which is limited by the increasing risk for the development of drug-resistant mutants. Due to spontaneous viral genome variability, pharmacological pressure may select for the viral species that exhibit the best replication capacity in this new treatment environment. Mutations that might lead to NRTI resistance are located in the viral polymerase gene.

Alternative to a monotherapy with one of the RT-inhibitors, IFN- α is used for antiviral therapy alone or in combination with *lamivudine* and enables in 10 - 15% an elimination of HBV (Marcellin, Lau et al. 2004). IFN- α treatment relies on distinct antiviral effects with anti-proliferative and immunoregulatory properties, including the stimulation of the immune system by T-cell response activation (Guan 2000). Previously, treatment of chronic HBV patients with standard IFN- α required an injection every second day. To date, stabilized pegylated (PEG) IFN- α (*Pegasys*) is approved and has to be injected only once weekly (Barnard 2001). The treatment efficacy is limited, also dependent on the individual and on the genotype of the virus (Kao, Wu et al. 2000). Only in 30% of chronically infected patients, treated for one year with PEG IFN- α , the therapy is associated with a sustained antiviral effect (Marcellin, Lau et al. 2004; Lau, Piratvisuth et al. 2005). Moreover, treatment with IFN- α is attended by occurrence of severe side effects, such as anemia, thrombocytopenia, neutropenia and depression. In addition, the available drugs rarely clear the infection, but they potentially stop viral replication and minimize liver damage.

Nevertheless, the single HBV replication cycle steps (**Fig. 12**, in blue) implicate and encourage the development of novel inhibitors (**Fig. 12**, in orange). First, viral entry represents a target for antiviral compounds. It was shown that myristoylated peptides, identical to the pre-S1 domain of the large viral envelope protein, which interacts with the cellular receptor, are able to inhibit viral entry *in vitro* (Glebe, Urban et al. 2005). The next possible target step in viral replication, the cccDNA formation, is the most ambitious aspect in the development of new antivirals. The major reason for needful life-long treatment of chronic patients with approved drugs is that these not necessarily eliminate cccDNA. The cccDNA may persist over decades, even after serological clearance of viral infection. The discovery of compounds specifically inhibiting cccDNA formation remains a major goal of HBV research.

There were several approaches to target HBV genome transcription or the viral transcripts themselves, using small interfering RNAs (siRNAs), antisense oligonucleotides or ribozymes, often limited by the delivery of such nucleic acids to hepatocytes *in vivo* (von Weizsacker, Wieland et al. 1997; Klein, Bock et al. 2003; Shlomai and Shaul 2003). Phenylpropenamide derivatives were shown to inhibit nucleocapsid formation by inhibition of pgRNA packaging *in vitro*, also in *lamivudine* resistant HBV strains (Delaney, Edwards et al. 2002). Heteroaryldihydropyrimidines are able to inhibit viral capsid formation and increase degradation of the core protein (Deres, Schroder et al. 2003). Furthermore, IFN- α also affects stability of the viral nucleocapsid (Schultz, Summers et al. 1999; Wieland, Guidotti et al. 2000). The next step, viral reverse transcription can be efficiently inhibited, as already mentioned, by nucleos(t)ide analogues (Zoulim 2004) or antisense oligonucleotides (Robaczewska, Narayan et al. 2005). Moreover, several studies showed that iminosugars interfere in the correct folding of viral envelope proteins and therefore disturb proper virion packaging morphogenesis (Block and Jordan 2001). Strategies to support defective immune responses against HBV include treatment with IFN- α or PEG-IFN- α to stimulate and activate an HBV specific T-cell response, as mentioned above, as well as the development of DNA or recombinant protein vaccines (Zhang, Jiang et al. 2008; Rapicetta, D'Ugo et al. 2009). Furthermore, it was shown that modified primary human T-cells, which express chimeric TCRs directed against HBV surface proteins, efficiently lyse HBV replicating and cccDNA-positive cells (Bohne, Chmielewski et al. 2008). Additionally, several studies revealed that modulations of TLR-signaling and response efficiently inhibit HBV replication *in vitro* and *in vivo* (Isogawa, Robek et al. 2005; Wu, Lu et al. 2007).

Finally, as ultimate salvation for patients, who already developed liver failure by HBV-related cirrhosis, HCC or both, often only orthotopic liver transplantation remains (Todo, Demetris et al. 1991), accompanied with high risk for graft re-infection or graft rejection.



Fig. 1.13: New targets of antiviral therapy. Approved inhibitors (red) and novel inhibitors in development (orange) of hepatitis B life cycle (blue). All steps of HBV replication are potential targets of antiviral therapy, except the inhibition of cccDNA formation. Modified after (Zoulim and Lucifora, 2006).

1.5.2 Combinatorial treatment of HBV

Nevertheless, the variety and efficacy of already approved monotherapies, such as nucleos(t)ide analogues and IFN- α are strongly limited. Their application along with severe side effects and treatment of patients is time-consuming and associated with high costs. For that reasons, the development and improvement of novel antiviral therapies are indispensable. More efficient therapies with combined antiviral activity

acting simultaneously on several steps of the HBV life cycle are preferentially required. Immunotherapeutic strategies that combine HBV-specific and HBV-nonspecific treatments are a promising approach, which additively and advantageously act along with avoidance of HBV resistance during treatment. It has been demonstrated that induction of antiviral cytokines by stimulation of TLR-9 with CpG-oligonucleotides (HBV-nonspecific) paired with the application of polymerase inhibitor *lamivudine* (HBV-specific) represents a promising combination to suppress HBV replication *in vitro* (Vincent, Lucifora et al. 2009).

The immunotherapeutic and combinatorial antiviral approach aspired in this study is to affiliate induction of antiviral innate immunity by stimulation of RIG-I (HBV-nonspecific) with siRNA mediated gene silencing, targeting free cytosolic HBV pgRNA (HBV-specific). Lately, it has been shown, even though in another context, that 5'-triphosphorylated siRNA (3p-siRNA) efficiently turns gene silencing and RIG-I activation against melanoma (Poeck, Besch et al. 2008). Potential induction of antiviral IFN-I via RIG-I stimulation in combination with HBV-sequence specific siRNA silencing by 3p-siRNA appears to be a powerful tool for combinatorial treatment of chronic hepatitis B.

1.5.3 Antiviral activity of IFN-I against HBV

IFNs and interferon-stimulated genes (ISGs) are key components of the innate immune response, and therefore are the first line of defense against virus infection, as well as potent inhibitors of viral replication (**Fig. 13**). We hypothesized that IFN-I induction by 3p-(si)RNA stimulation of RIG-I exhibits antiviral activities against HBV replication. First, IFN- α/β (and IFN- γ) inhibit HBV-replication in a proteasom dependent way by an unknown mechanism (Robek, Wieland et al. 2002; Zhang, Protzer et al. 2004). An IFN-induced increase in ubiquitination of proteins required for viral particle assembly or maturation could lead to their degradation by the proteasome, thus limiting viral replication. Second it was shown, that IFN-I inhibits the formation and/or promotes the destabilization of immature HBV RNA-containing capsids in HBV transgenic (tg) mice (Wieland, Guidotti et al. 2000).

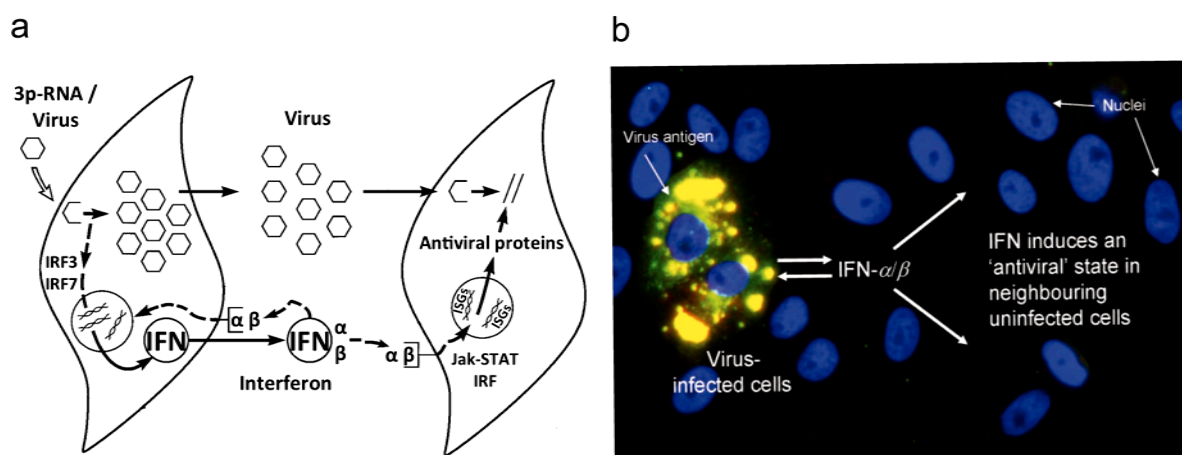


Fig. 1.14: Principles and antiviral activity of IFN-I system. a) Schematic summary of the antiviral IFN-I system and b) fluorescence microscopy of IFN-I activity. The image shows cells infected with parainfluenza virus (PIV5) and 24h later stained with antibodies to the viral nucleocapsid protein (virus antigen, yellow) and to the cell nuclei, (DAPI, blue). Virus infection (and also 3p-RNA stimulation) induces a cell (a+b, left) to synthesize IFN-I, which acts autocrine or paracrine via the Jak-STAT pathway on the induction of interferon stimulated genes (ISGs). These ISGs code for antiviral acting proteins responsible for the inhibition of virus multiplication in neighboring cells (a+b, right). IFN may also act in an autocrine manner on the IFN producer cell. Modified after a) (Samuel 2001) and b) (Randall and Goodbourn 2008)

Furthermore, IFN-I stimulates the expression of distinct ISGs, which efficiently suppress HBV replication. For example, induced IFN-I directly enhances the expression of PRRs, such as RIG-I, in turn resulting in increased pattern (3p-(si)RNA) recognition. But ISGs also code for other antiviral effector proteins believed to affect virus multiplication within single cells (**Fig. 14**). 2'-5' oligoadenylate synthetase (2'-5' OAS) activates the endoribonuclease RNase L leading to RNA degradation. IFN-I, induced via activation of RIG-I or TLR3, activates the latent form of 2'-5' OAS that synthesizes 2'-5'-linked phosphodiester bonds to polymerize ATP into oligomers of adenosine (Rebouillat and Hovanessian 1999). These unique 2'-5' oligomers again specifically activate the latent form RNase L. The enzyme RNase L is constitutively expressed as an inactive monomer. Upon binding of 2'-5'- oligomers, homodimerization takes place. The active dimeric enzyme then degrades viral RNA and cellular RNAs, including cellular rRNA, by cleaving on the 3'-end of UpXp-sequences (Silverman 2007). Viral RNA degraded by RNase L is

able to activate the cytoplasmic PRRs like RIG-I itself or MDA-5, resulting in enhanced ISG induction again (Floyd-Smith, Slattery et al. 1981).

IFN-I also induces the expression of guanosine-hydrolysing GTPases, probably the best characterized and most efficient antiviral effector protein. But only the human GTPase MxA (myxovirus resistance protein A) demonstrates antiviral activity, also potentially inhibiting HBV replication at a posttranscriptional level (Gordien, Rosmorduc et al. 2001). MxA has a large N-terminal GTPase domain, a central interacting domain (CID) and a C-terminal leucine zipper (LZ). The CID and the LZ domain are required to recognize the main viral target, which are nucleocapsid-like structures. Following stimulation with IFN-I, MxA accumulates in the cytoplasm on intracellular membranes, such as the ER, as oligomers via association between CID and LZ domains. Upon virus infection, the oligomers bind viral nucleocapsids or other viral components to degrade them. Interestingly, MxA proteins do not interact with HBV nucleocapsids, but inhibit the nucleocytoplasmic export of HBV mRNA via the PRE sequence (Gordien, Rosmorduc et al. 2001).

Another validated IFN-inducible, dsRNA dependent effector is the protein kinase R (PKR), which belongs to a small family of kinases that respond to environmental stress to regulate protein synthesis. PKR is found predominantly as a monomer in the cytoplasm and associated with ribosomes (Thomis, Doohan et al. 1992). IFN-I leads to activation of PKR by dimerization through autophosphorylation. Following activation, PKR catalyzes the phosphorylation of the α -subunit of translation initiation factor eIF-2 α . This results in impairment of the limiting guanine nucleotide exchange factor eIF-2 β that catalyzes the recycling of GDP, required for translation. For this reason, the activation of PKR by IFN-I leads to the inhibition of viral and cellular mRNA translation (Samuel 2001).

Accessory IFN-I induced antiviral acting proteins are members of the APOBEC family. APOBEC3G (A3G) and APOBEC3C (A3C) are cellular cytidine deaminases with a broad spectrum of antiretroviral activity (Mangeat, Turelli et al. 2003; Harris and Liddament 2004). Both contain an N-terminal RNA-binding domain and one (A3C: C-terminal) or two, respectively (A3G: N- and C-terminal) deaminase domains (Harris and Liddament 2004). The larger A3G protein (384aa), by chance entrapped into preassembled capsids by HBV-RNA binding, is thought to inhibit subsequent steps of capsid formation and HBV DNA synthesis *in vitro* (Rosler, Kock et al. 2005). The smaller A3C protein (190aa), readily packaged into replication-competent

capsids, may deaminate newly synthesized HBV-DNA. The C-to-U editing could result in enhanced hypermutation of HBV DNA (Baumert, Rosler et al. 2007). However, it was recently suggested, that induction of APOBEC proteins is not responsible for the control of HBV by IFN-I (Turelli, Liagre-Quazzola et al. 2008).

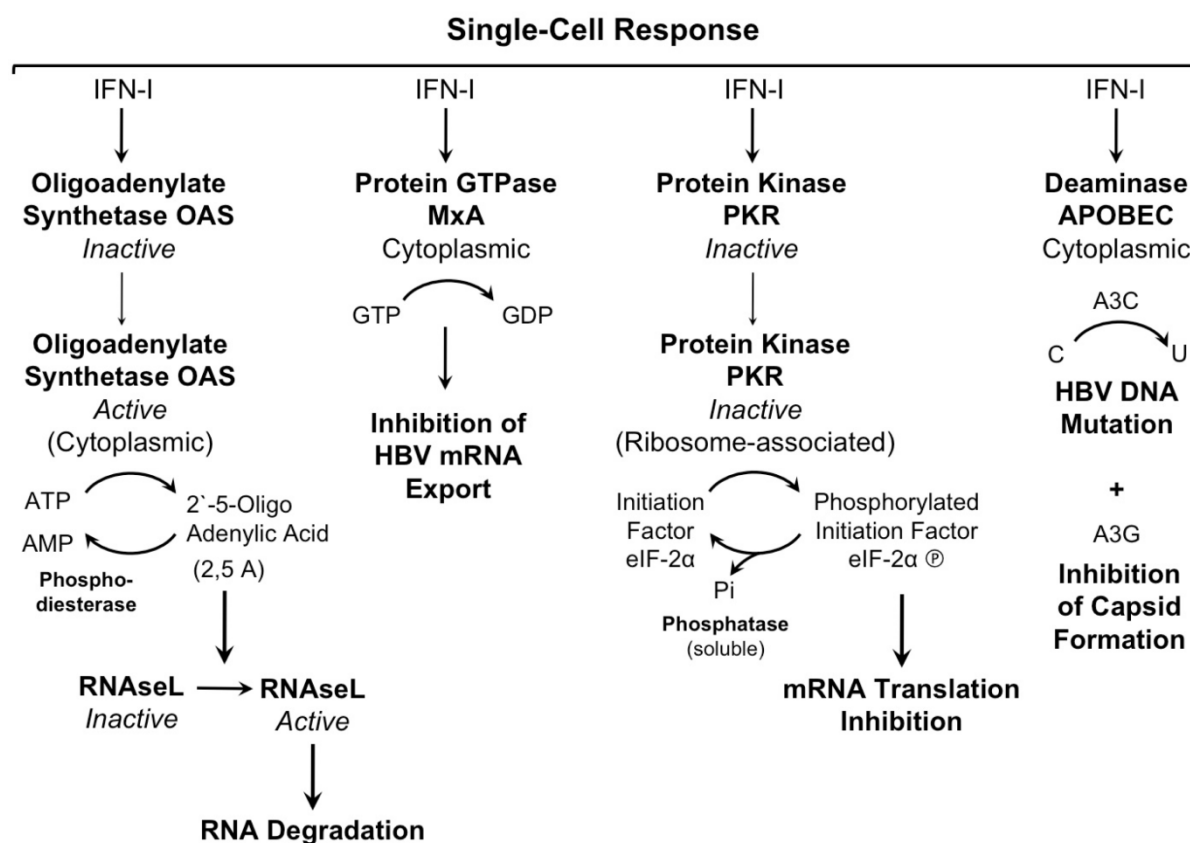


Fig. 1.15: Anti-HBV functions of IFN-I inducible proteins. Among IFN-I induced proteins thought to affect HBV replication within single cells are OAS synthetase and RNase L nuclease, which mediate RNA degradation; MxA protein GTPase, which appear to inhibit nucleocytoplasmic export of HBV mRNA; PKR kinase, which inhibits translation initiation through phosphorylation of protein synthesis initiation factor eIF-2 α ; and APOBEC A3C and A3G, which edit newly synthesized HBV-DNA and may block capsid formation, respectively. IFN-I induced expression of MHC class I antigens might contribute to the antiviral multiple-cell response. Modified after (Samuel 2001).

1.5.4 Antiviral activity of HBV-sequence specific siRNA

Application of siRNA potentially mediates HBV-sequence specific gene silencing by targeting the pgRNA. Several studies demonstrated that siRNA mediated gene silencing show potent antiviral effects against HBV (Shlomai and Shaul 2003; Morrissey, Lockridge et al. 2005; Peng, Zhao et al. 2005). The genomic organization in overlapping ORFs and multiple RNAs make the virus particularly susceptible to RNA interference (Mahato, Cheng et al. 2005).

RNA interference (RNAi) is a natural process by which canonical siRNA duplex directs sequence-specific post-transcriptional gene silencing of homologous genes (Almeida and Allshire 2005). The siRNA binds to its complementary mRNA and triggers its elimination. This evolutionary highly conserved mechanism controls gene activity in most eukaryotic cells and protects the genome against invasion by distinct viruses. Potent knockdown of a gene of interest with high sequence-specificity provided RNAi as a powerful tool for studying gene function and is already used for treatment for various diseases. RNAi takes place post-transcriptionally in the cytoplasm (Zeng and Cullen 2002) and is an ATP-dependent and translation independent process. siRNAs are 9 - 27 bp dsRNA molecules with a characteristic overhang of two nucleotides at the 3'-end on both strands. Each strand has a 5' phosphate group and a 3' hydroxyl group. In mammalian cells this structure is the result of processing by the RNase III nuclease named Dicer (Zhang, Kolb et al. 2004). Dicer converts either virus derived long dsRNA, cellular microRNA (miRNA), responsible for gene regulation or short hairpin RNAs (shRNA) used in expression vectors, into siRNAs. Therefore, dicer catalyzes the first step in the RNAi pathway and then delivers the siRNA to the RNA-induced silencing complex (RISC) (Tang 2005).

Exogenous siRNA can be directly introduced into target cells by various transfection methods (**Fig. 15**). The delivered siRNA binds independent of Dicer to RISC, which contains the splicing protein Argonaute 2 (Ago2). After the siRNA is loaded onto RISC, Ago 2 unwinds the siRNA, cleaves both strands and releases the sense or "passenger" RNA strand in an ATP dependent process (Meister, Landthaler et al. 2004). This leads to activation of RISC, loaded with the single stranded antisense or "guide" RNA molecule. Afterwards the siRNA/RISC complex associates with the

target mRNA. Target mRNA molecules complementary to the antisense siRNA strand are recognized and then cleaved by Ago2 (Tang 2005).

Chemical modifications and incorporation of siRNA into cationic liposomes are widely used to improve siRNA stability, cellular uptake and gene silencing effectivity in RNAi-based therapy (Soutschek, Akinc et al. 2004; Wolfrum, Shi et al. 2007).

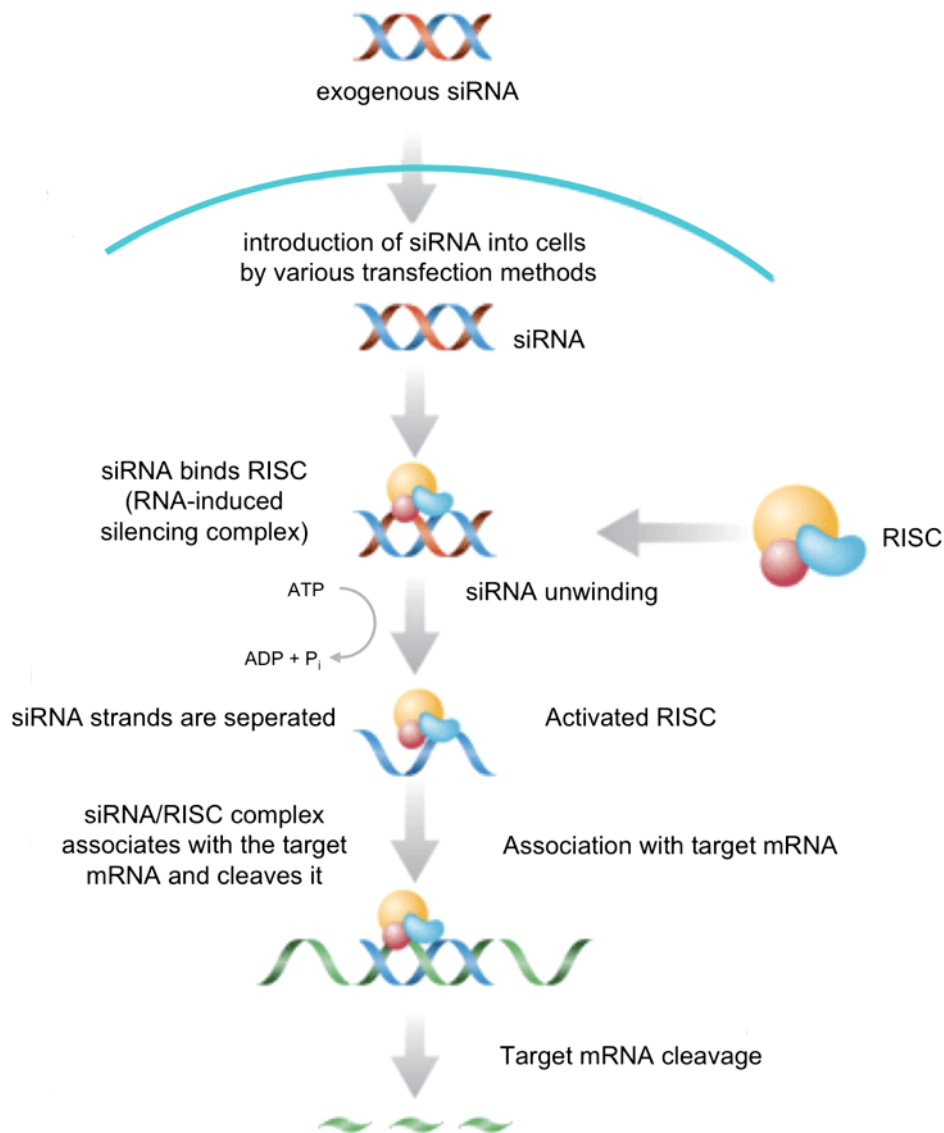


Fig. 1.16: RISC-model of siRNA mediated gene silencing. Binding of the RNA-induced silencing complex RISC follows delivery of siRNA into the cell. RISC component Ago-2 mediates ATP hydrolysis dependent siRNA unwinding, cleavage of the siRNA strands and maturation of RISC. Mature RISC loaded with the siRNA “guide” strand associates with the complementary target mRNA sequence and cleaves it. Modified after RNAi gene silencer, Santa Cruz Biotechnology, Inc..

1.6 Aims of the study: Hypothetical activity of 3p-siRNA against HBV

As said before, chronic HBV infection is the major cause of liver cirrhosis and primary liver cell carcinoma. These long-term consequences of persistent HBV infection represent a severe health problem leading to high mortality worldwide. Approved clinical therapies of chronic hepatitis B include administration of antiviral active IFN- α , as well as nucleos(t)ide analogues, which inhibit viral reverse transcription. These drugs can control replication effectively, but HBV cccDNA, the episomal replication template, persists in most cases, generating a relapse of infection after the therapy has been ceased. Hence, lifelong therapy is required, often accompanied by severe side effects and development of drug resistant mutants (Dienstag 2009). Therefore, new combinatorial treatment concepts targeting multiple steps in HBV replication cycle are urgently required for antiviral HBV therapy.

It is known that induction of IFN-I by stimulation of TLRs results in strong suppressive antiviral effects on HBV replication (Isogawa, Robek et al. 2005). Moreover, distinct hepatoma cell lines are susceptible to IFN-I induction by stimulation of the cytosolic helicase RIG-I (Preiss, Thompson et al. 2008) and thus, HBV replication can be controlled *in vitro* (Guo, Jiang et al. 2009). In addition, it was shown that RIG-I is stimulated by *in vitro* transcribed 5'-triphosphated RNA (3p-RNA), leading to a potent IFN-I expression (Hornung, Ellegast et al. 2006).

Accordingly, we wanted to analyze, whether stimulation of the cytosolic helicase RIG-I by *in vitro* transcribed 3p-RNA may induce an endogenous antiviral active type-I IFN response, suppressing HBV replication. Moreover, it was shown that 5'-triphosphorylated siRNA (3p-siRNA) efficiently combines gene silencing and RIG-I activation in treatment of melanoma (Poeck, Besch et al. 2008). Consequently, suitable HBV sequence-specific siRNAs were sought to be *in vitro* transcribed to additionally act as RIG-I ligands, combining induction of antiviral active IFN-I by RIG-I stimulation with HBV-sequence specific gene silencing. Therefore, the following study addressed the question, whether an alternative immunotherapeutic approach for successful treatment of HBV could be achieved by application of *in vitro* transcribed 3p-siRNA to efficiently suppress HBV replication. It was investigated, whether 3p-siRNA could lead on the one hand to siRNA mediated gene silencing of HBV by RNAi (Model, **Fig. 16, left side**), combined on the other hand with the activation of

the RIG-I signaling cascade, followed by the induction of antiviral acting IFN-I and ISGs (Model, Fig. 16, right side).

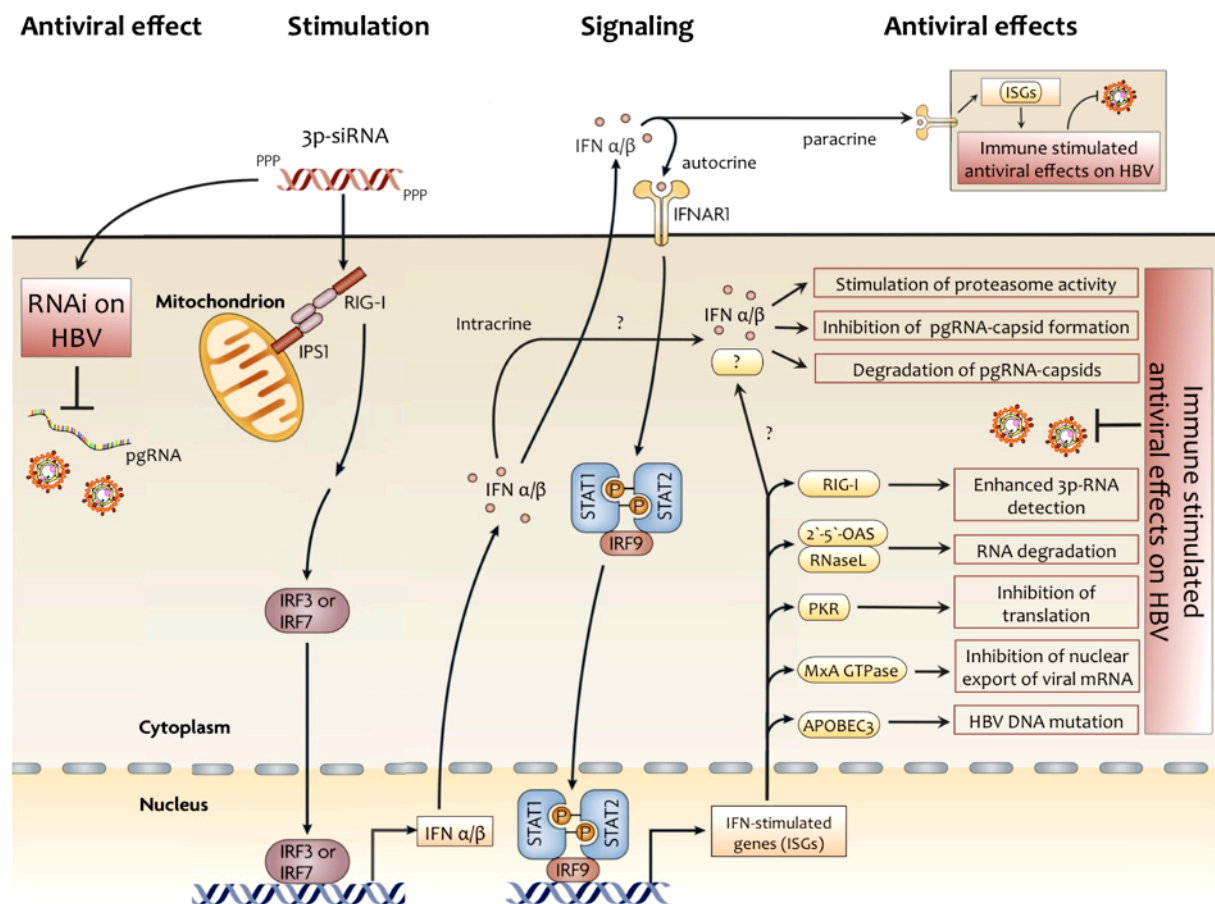


Fig. 1.17: Schematic model of HBV specific gene silencing and IFN-I signaling activation by RIG-I stimulation with 3p-siRNA and resulting antiviral effects on HBV replication in hepatocytes. Delivery of 3p-siRNA into HBV infected hepatocytes might have on the one hand a specific antiviral effect on HBV replication by RNAi (left). On the other hand cytosolic helicase RIG-I binds distinct viral RNAs, but also *in vitro* transcribed 3p-siRNA (stimulation). Binding of 3p-siRNA should lead to activation of IFN-I signaling cascade via different adaptor molecules. Transcription factors IRF3/7 induce production of IFN-I. IFN-I exhibits antiviral effects against HBV via unknown, probably intracrine acting mechanisms. Furthermore, IFN-I is secreted from the cell and binds auto- or paracrine to IFNAR1 receptor, which leads to activation of JAK-STAT pathway and therefore to the induction of IFN-stimulated genes (ISGs) (signaling). ISGs code for several antiviral active proteins, which provide immune stimulated antiviral effects against HBV replication (right). Modified after (Bowie and Unterholzner 2008).

2 Results

2.1 Hepatocellular expression profile of RIG-I

HBV replication is IFN-I sensitive. Activation of the innate immune system by stimulation of the ubiquitous cytosolic helicase RIG-I results in a strong induction of endogenous IFN-I potentially suppressing HBV replication. Liver derived cell lines are useful tools to investigate the influence of therapeutic approaches for suppression of HBV replication *in vitro*. Human hepatoma cells such as HuH7 are not permissive for HBV, but are suited to analyze HBV replication. Stably HBV expressing hepatoma cells like HepG2 2.15 and HepG2 H1.3 mimic a chronic HBV infection *in vitro*. In contrary, HBV infected primary human hepatocytes (PHHs) simulate acute HBV infection.

To find a suitable *in vitro* model for this study it was first investigated, whether the cytosolic helicase RIG-I is present in different hepatoma cell lines and primary human hepatocytes. Previous IFN-I stimulation of cells is known to increase the expression of RIG-I (Bowie and Unterholzner 2008). Therefore, presence of cytosolic RIG-I was compared by Western blot analysis, with and without previous addition of IFN-I into the supernatant of the cells.

Both, the hepatoma cell line HuH7 and its subline HuH7.5 contained comparable RIG-I levels, strongly increased after stimulation with IFN-I (**Fig. 2.1 a**). Also the stably HBV producing cell lines HepG2 H1.3 and HepG2 2.15 strongly expressed the cytosolic helicase, although at different levels (**Fig. 2.1 b**). PHHs also showed RIG-I expression, compared to HepG2 H1.3 cells even at higher levels (**Fig. 2.1 c**). In all cell types the expression of RIG-I could be enhanced by previous addition of exogenous IFN-I.

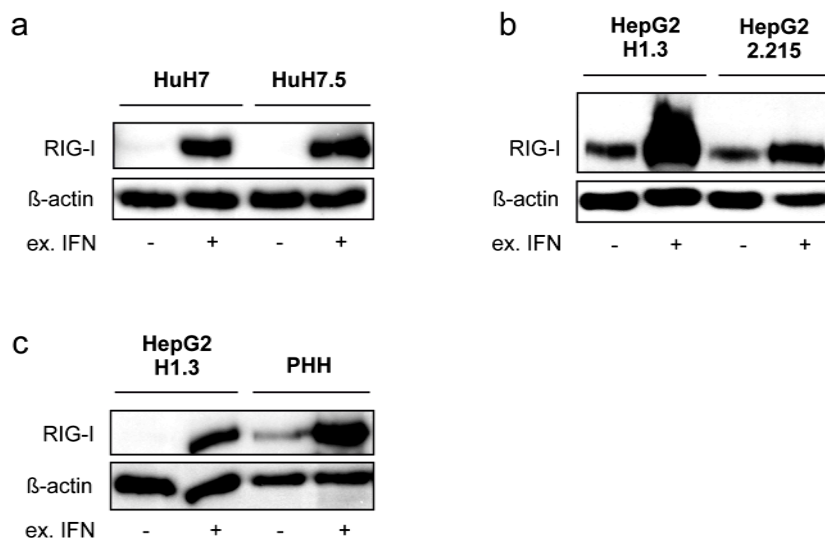


Fig. 2.1. RIG-I expression in hepatoma cell lines and primary human hepatocytes. Comparison of RIG-I expression levels in **a)** Hepatoma cells HuH7 and HuH7.5 **b)** stably HBV expressing hepatoma cells HepG2 H1.3 and HepG2 2.215 **c)** stably HBV expressing hepatoma cells HepG2 H1.3 and primary human hepatocytes (PHHs). Cells were cultured for 36 hours with and without previous addition of exogenous IFN type I (1000 U / ml). Total cell lysates were prepared and RIG-I expression was determined by Western blot analysis with β -actin as loading control. a) and c) 40 μ g b) 50 μ g total cell lysate was applied per lane.

2.2 Applicability of 3p-RNA

2.2.1 Induction of IFN- β by 3p-RNA

IFN-I production can be induced by different RNA-oligonucleotides serving as RIG-I ligands (Schlee, Hartmann et al. 2009). The exact structure of the RNA stimulating RIG-I, predominantly supported by 5'-triphosphate recognition, remains controversial. However, it was reported that short dsRNA generated by *in vitro* transcription (IVT) induces IFN-I in cell lines (Kim, Longo et al. 2004). Subsequently, it was shown that *in vitro* transcribed 3p-RNA strongly induces IFN-I by stimulation of RIG-I (Hornung, Ellegast et al. 2006). The 3p-RNA used in this study consists of a dsRNA-oligonucleotide of 23 nucleotides with an overhang of one nucleotide at the 5'-position, both 5'-ends are coupled with triphosphate groups due to *in vitro* transcription by T7 polymerase. Quantity and potency of IFN- β induction by 3p-RNA differed drastically between different 3p-RNA *in vitro* transcriptions. Therefore, a dual-

luciferase assay was used to determine the potency of each 3p-RNA to induce IFN- β . This assay was performed with human embryonic kidney cells (HEK 293), a cell line, which well compensates necessary transfections and allows high transfection efficiency (Aiello, Guilfoyle et al. 1979). Therefore, HEK 293 cells were firstly transfected with two plasmids. One construct contained a *Firefly*-luciferase cassette under control of an IFN- β promotor as a reporter gene. The second construct included a *Renilla*-luciferase cassette with a constitutive promotor and was used as an internal control to determine transfection efficiency. On the following day cells were transfected with 3p-RNA from four different *in vitro* transcriptions (#1 - 4) to be tested. It is known that IFN-I expression peaks 6 - 18 hours after treatment with 3p-RNA *in vitro* (Hornung, Ellegast et al. 2006). Therefore, HEK cells were lysed 12 hours after stimulation with 3p-RNA, *Firefly*-luciferase substrate (*Luciferin*) was added to the lysate and IFN- β dependent activity of the *Firefly*-luciferase was quantified by measuring luminescence. After quantifying the firefly luminescence the reaction was stopped and simultaneously the renilla luciferase reaction was initiated by addition of its substrate (Coelenterazien). Accordingly, the quotient of *Firefly*- and *Renilla* luciferase expression correlated with induced IFN- β expression. Cells expressing both luciferase constructs but not transfected with 3p-RNA served as mock control (**Fig. 2.2**).

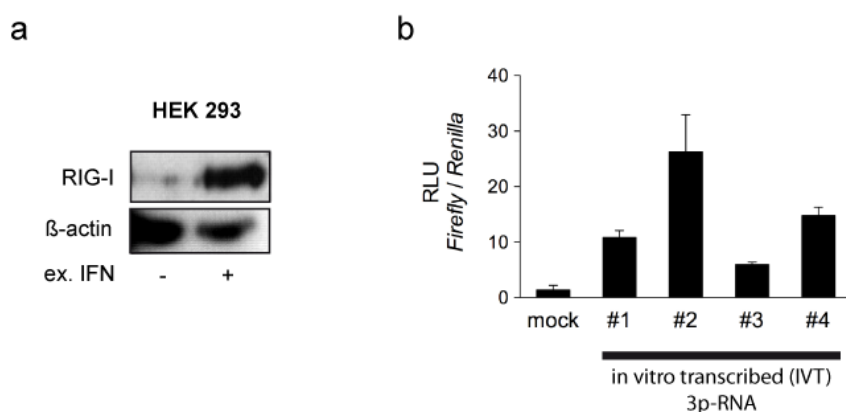


Fig. 2.2: RIG-I expression in HEK 293 cells and induction of IFN- β by 3p-RNA prepared of different *in vitro*-transcriptions. a) RIG-I expression levels in HEK 293 cells with and without previous addition of exogenous IFN type I (1000 U / ml). 50 μ g total protein lysate per lane b) HEK 293 cells were transfected with dual luciferase constructs and treated with several 3p-RNA preparations of different *in vitro* transcriptions (IVT). Luminescent signals (relative light units, RLU) of Firefly- and renilla luciferase, respectively, were determined in a luminometer. Data are shown as mean \pm SD, n=3.

The dual luciferase assay showed different levels of IFN- β induction by 3p-RNA after four different *in vitro* transcriptions. 3p-RNA of IVT #1 and #3 revealed only minor and 3p-RNA of IVT #4 medial IFN- β induction, whereas 3p-RNA generated by IVT #2 exhibited the strongest potency to induce IFN- β and was thereby favoured for further experiments. The results show the variability of IFN- β stimulation by 3p-RNA generated in several *in vitro* transcriptions, which was normalized before application of 3p-RNA in further experiments.

2.2.2 Induction of IFN- β by 3p-RNA in HuH7 cells

To determine the potency of 3p-RNA to induce IFN-I in different hepatoma cell lines, HuH7 and HuH7.5 cells were transfected with 3p-RNA (0.5 μ g / ml) and IFN- β expression levels were determined after 12h by quantitative RT-PCR (qRT-PCR) (**Fig. 2.3**). Poly(I:C) (0.05 μ g / ml) was transfected as a positive control. Poly (I:C), polyinosinic-polycytidylic acid, is a synthetic analogue of dsRNA that induces a potent IFN type I response triggering another ubiquitous cytosolic helicase, the human melanoma differentiation associated gene-5 (MDA-5) (Gitlin, Barchet et al. 2006) as well as the endosomal TLR 3 (Kulka, Alexopoulou et al. 2004). Inert (non-stimulating) polyA-RNA (polyriboadenosine) was used as negative control (Ctrl-RNA). Cells treated only with transfection reagent Hiperfect served as mock control.

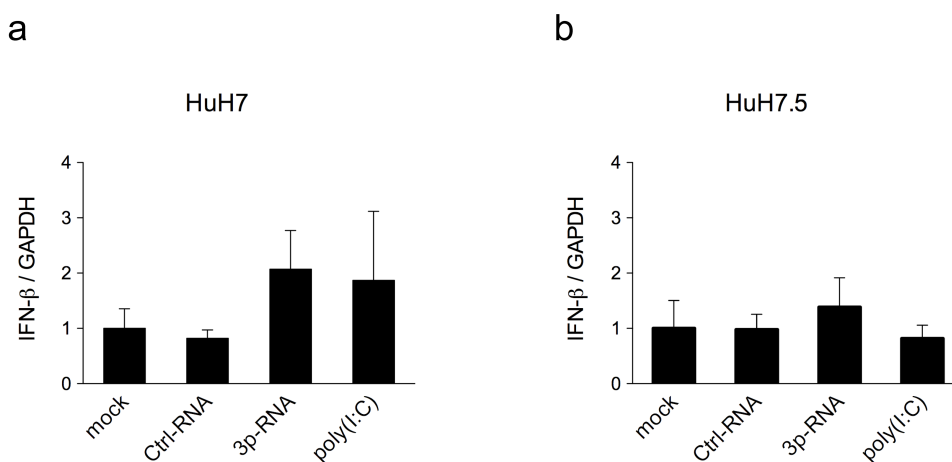


Fig. 2.3: IFN-I induction by 5'-triphosphorylated dsRNA in HuH7 cell lines. a) HuH7 cells and **b)** HuH7.5 cells were treated with 3p-RNA, Ctrl-RNA (polyA-RNA; negative control) and poly(I:C)

(polyinosinic:polycytidylic acid, a synthetic analog of double-stranded RNA; positive control). Mock cells were treated with transfection reagent Hiperfect. IFN- β levels were analyzed by quantitative RT-PCR relative to GAPDH and normalized to mock treated cells 12 hours p. tr.. Data are shown as mean \pm SD, n=3.

HuH7 cells treated with 3p-RNA or poly(I:C), respectively, showed only IFN- β induction at background levels 12 hours after transfection (**Fig. 2.3 a**). HuH7.5 cells, a subline of HuH7 cells, exhibit no measurable IFN- β expression at all after transfection of the appropriate ligands (**Fig. 2.3 b**). Other groups have already shown that Huh7 cells are inadequate for production of IFN-I caused by minor TLR 3 expression and by an defect on RIG-I receptor level (Li, Chen et al. 2005; Preiss, Thompson et al. 2008) The results show that the human hepatoma cell line HuH7 as well as its subline HuH7.5 are devoid of proper signaling after stimulation of RIG-I by 3p-RNA or intracellular TLR3 by poly(I:C) transfection, respectively, and hence were not suitable for further *in vitro* experiments.

2.2.3 Three different HBV models

Other hepatoma derived cell lines display different PRR expression patterns compared to HuH7 cells, such as HepG2 cells, which are known to be impaired in TLR3 dependent, but competent for RIG-I dependent IFN-I signaling (Preiss, Thompson et al. 2008). Additionally, a stably HBV expressing cell line was preferred for cell culture experiments. Available stably HBV expressing HepG2 cells, such as HepG2 H1.3 (Jost, Turelli et al. 2007; Protzer, Seyfried et al. 2007) and HepG2 2.15 (Sells, Chen et al. 1987) replicate HBV at higher levels than comparable HBV producing HuH7 cells (Bohne, Chmielewski et al. 2008). In order to use the optimal stably HBV expressing cell line for this work, initially HepG2 H1.3 were preferred over HepG2 2.15 cells due to their enhanced expression of RIG-I (**Fig. 2.1 b**). Moreover, HepG2 H1.3 cells also express, in comparison to HepG2 2.15 cells, episomal cccDNA as an additional and sensitive marker of HBV replication (**Fig. 2.4**, Southern blot (SB) analysis kindly provided by D.Webb).

Primary human hepatocytes (PHHs) are another useful *in vitro* system to investigate early steps of HBV replication after acute infection with HBV. Nevertheless, their

availability is restricted because they are isolated from fresh liver specimen. PHHs expressed cytosolic RIG-I at levels comparable to HepG2 H1.3 cells (**Fig. 2.1 c**) and also establish a nuclear cccDNA pool. According to that reason, the stable HBV expressing hepatoma cell line HepG2 H1.3 as well as HBV infected PHHs were considered as optimal tools for further *in vitro* investigations (**Fig. 2.4**).

To investigate the different aspects of antiviral RIG-I stimulation by 3p-RNA *in vivo*, two distinct HBV transgenic (tg) mouse strains were available. On the one hand, HBV1.3 tg mice and on the other hand HBV1.3 –xfs tg mice containing a frameshift mutation within the X-gene (Weber, Schlemmer et al. 2002). We found that HBV1.3 –xfs tg mice replicate HBV at 10 times higher levels (10^7 - 10^8 virions per ml serum) than HBV1.3 tg mice. Therefore, HBV1.3 –xfs mice were used in all following *in vivo* studies (**Fig. 2.4**).

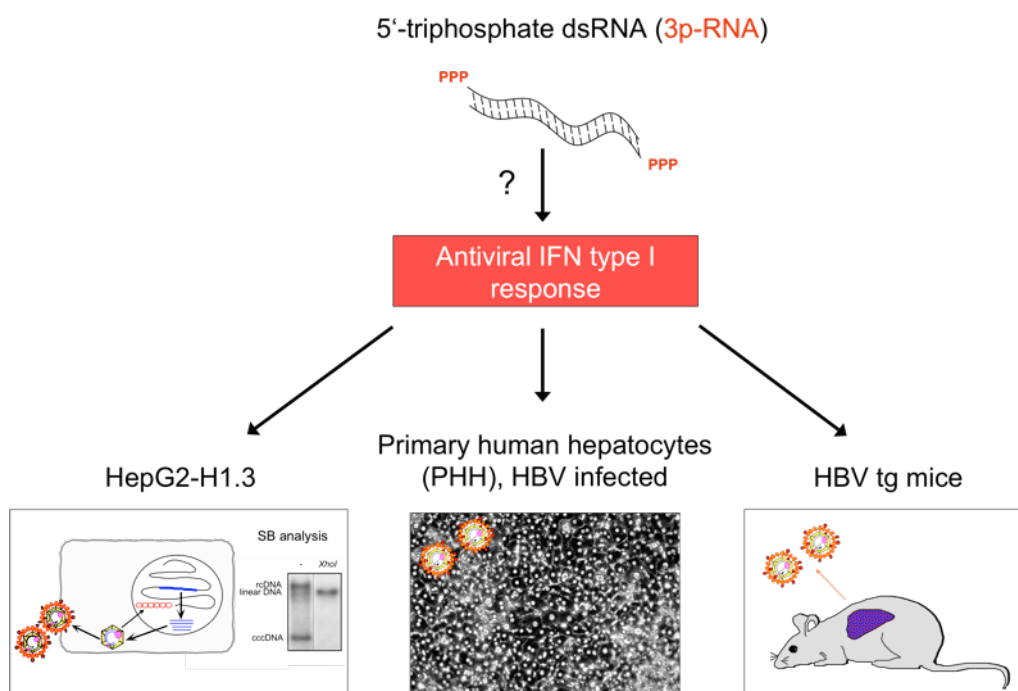


Fig. 2.4: Potential induction of antiviral IFN-I by 3p-RNA in 3 HBV-model systems. Three different HBV models were used to test 3p-RNA for potential induction of an antiviral IFN-I response against HBV. Stably HBV expressing hepatoma cell line HepG2 H1.3 and HBV infected primary human hepatocytes (PHHs) were used as *in vitro* models, HBV tg mice were used as an *in vivo* model.

2.2.4 Cytotoxicity of 3p-RNA

After the choice of the best model systems, potential toxicity of 3p-RNA was analyzed for liver cells and HBV tg mice, respectively. Therefore, different amounts of 3p-RNA were transfected into HepG2 H1.3 cells and cell viability was determined by an XTT-based assay over a period of 16 days (**Fig. 2.5 a**). No obvious toxicity at a concentration of up to 0.5 μg per ml medium was observed. Furthermore, 3p-RNA complexed with jetPEI was injected intravenously (i.v.) at day 0 and day 3 into the tail vein of HBV tg mice (Hornung, Ellegast et al. 2006). PolyA-RNA was used as negative control (Ctrl-RNA). Mice treated with the RNA delivery agent jetPEI served as mock control. Alanine aminotransferase (ALT) levels, a marker for cytotoxic liver damage, were determined in the sera of mice 6 hours after the two injections and at day 6, respectively (**Fig. 2.5 b**). 3p-RNA injected at a concentration of 25 μg per application showed no cytotoxic effects after both injections until day 6 in comparison to mock treated mice. Surprisingly, significantly elevated ALT levels were observed in a few mice treated with Ctrl-RNA over time.

According to these results, 3p-RNA was applied at 0.5 μg per ml medium in all following *in vitro* experiments. Due to its known toxicity, poly(I:C) was transfected at lower concentrations of 0.05 μg per ml medium throughout the study. 25 μg 3p-RNA per mouse and application were injected twice at day 0 and day 3 in all further *in vivo* experiments throughout the study.

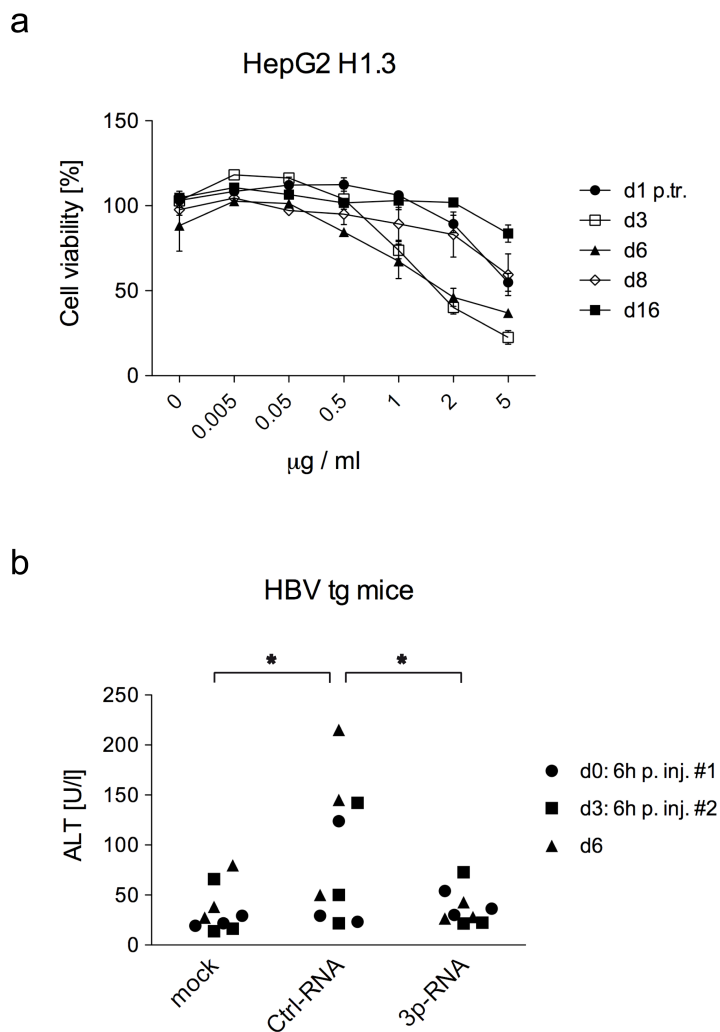


Fig. 2.5: Cytotoxicity of 3p-RNA *in vitro* and *in vivo*. **a)** HepG2 H1.3 cells were transfected with different doses of 3p-RNA and cell viability was monitored by XTT-cell-viability-test at indicated time points. Data are shown as mean \pm SD, $n=3$. **b)** HBV tg mice ($n=3$) were intravenously injected twice (at d0 and d3) with 25 μ g of 3p-RNA or Ctrl-RNA (polyA-RNA; negative control), respectively, per mouse and application. Mock (HBV tg) mice were treated with RNA delivery agent jetPEI. Serum alanine aminotransferase (ALT) levels were determined 6 hours after the first injection at day 0 and 6 hours after the second injection at day 3, respectively, as well as at day 6.

2.3 Functionality of 3p-RNA as RIG-I ligand in HBV replicating liver cells

2.3.1 IFN induction by 3p-RNA and activation of interferon-stimulated genes *in vitro* and *in vivo*

After exclusion of cytotoxic effects, 3p-RNA dependent induction of IFN- β and IFN- γ , as well as activation of interferon-stimulated genes such as 2'-5'-oligoadenylate synthetase (OAS) and IFN-inducible protein 10 (IP-10), respectively, were determined in all three models. The IFN-I induced expression of 2'-5'-OAS (Hovanessian 1991) leads to the activation of the latent endoribonuclease RNaseL, which is able to effectively degrade viral RNA (Hassel, Zhou et al. 1993). Moreover, IFN-I and IFN-II (IFN- γ) stimulate the expression of IP-10 (also named CXCL10), a chemokine that is secreted predominantly by monocytes, endothelial cells and fibroblasts. PRR stimulation with ligands such as LPS or poly(I:C) also induces expression of IP-10, which functions as a chemoattractant for the recruitment of effector T cells, macrophages, NK cells and DCs *in vivo* (Luster, Unkeless et al. 1985; Dufour, Dziejman et al. 2002).

HepG2 H1.3 cells and HBV-infected (MOI 100) PHHs were transfected with 3p-RNA, poly(I:C) as positive control and inert polyA-RNA as negative control (Ctrl-RNA). Cells treated with the transfection reagent Hiperfect were used as mock control. In addition, 3p-RNA or Ctrl-RNA, respectively, was injected intravenously into the tail vein of HBV tg mice with. Mice treated with nucleic acid delivery reagent jetPEI served as mock control. Expression of IFNs and interferon-stimulated genes 2'-5'-OAS and IP-10 were determined on mRNA level by qRT-PCR at indicated timepoints.

Transfection of both, 3p-RNA or poly(I:C), respectively, exhibited induction of IFN- β (**Fig. 2.6 a**) and IFN-I dependent 2'-5'-OAS (**Fig. 2.7 a**) in HepG2 H1.3 cells. The expression of both remained at high levels until day 3 and was still detectable until day 6 after transfection. Accordingly, HBV infected PHHs also revealed strong induction of IFN- β at day 1 after stimulation with 3p-RNA or poly(I:C), respectively (**Fig. 2.6 b**), as well as IFN-I induced expression of 2'-5'-OAS, which decreased over time (**Fig. 2.7 b**). Both cell types showed no induction of IFN- β after Ctrl-RNA or mock transfection.

Injection of 3p-RNA in HBV tg mice resulted in a very fast and potent IFN-I response, which dropped markedly until day 3 and was not detectable at day 6 after administration (**Fig. 2.6 c**). Despite high amounts of IFN- α in the sera of mice determined 6 hours after application of 3p-RNA, only residual expression of 2'-5'-OAS was found at day 6 after application (**Fig. 2.7 c**).

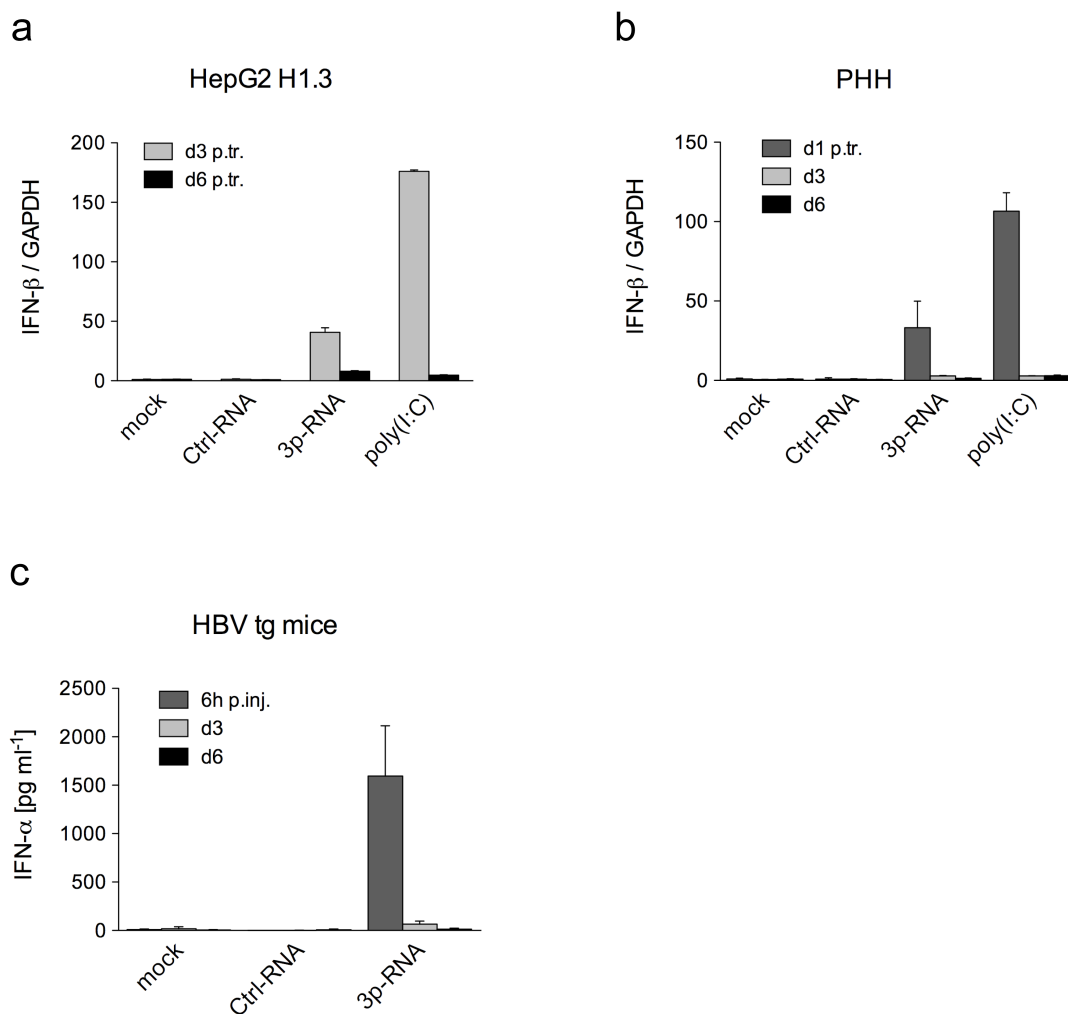


Fig. 2.6: IFN-I induction by 5'-triphosphorylated dsRNA *in vitro* and *in vivo*. a) HepG2 H1.3 cells b) HBV infected PHHs and c) HBV tg mice were treated with indicated RNA-oligonucleotides. Mock (HepG2 H1.3 and PHH) Hiperfect; mock, (HBV tg mice) jetPEI. IFN- β mRNA expression was analyzed by quantitative RT-PCR relative to GAPDH mRNA levels and normalized to mock treated cells at indicated timepoints. Serum IFN- α levels of HBV tg mice were determined by cytokine bead assay at indicated time points. Data are shown as mean \pm SD, n=3.

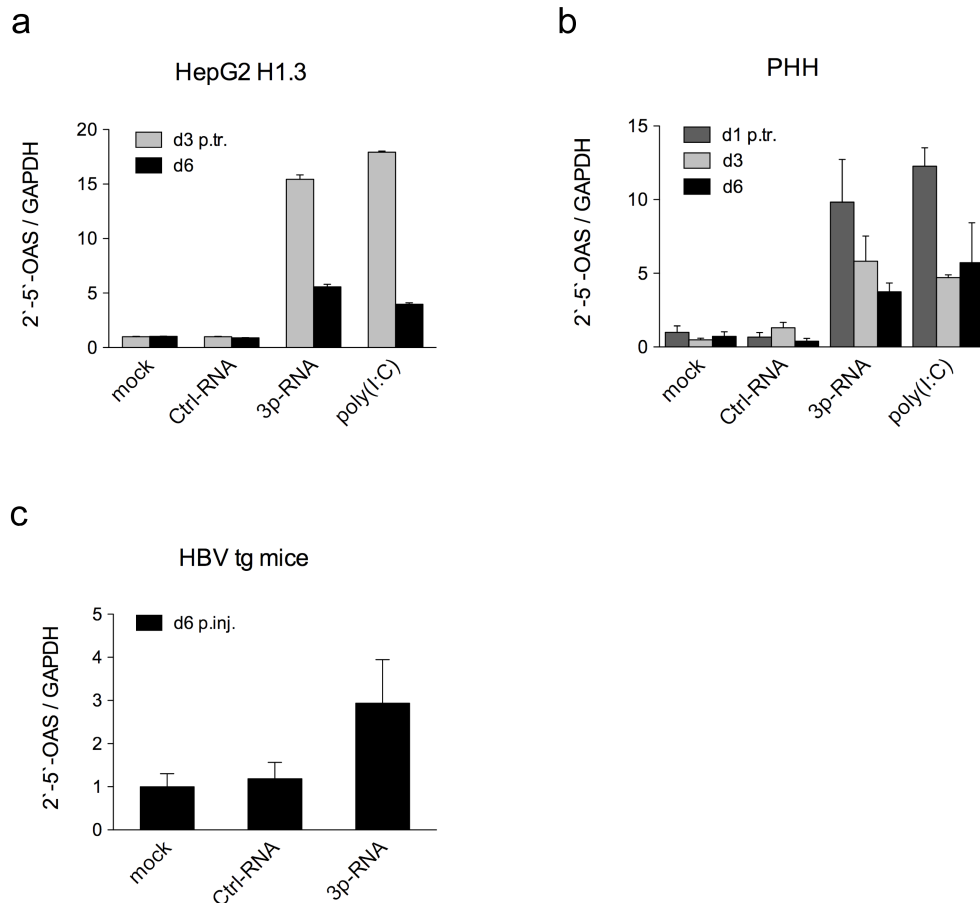


Fig. 2.7: IFN-I dependent induction of 2'-5'-oligoadenylate synthetase (OAS). **a)** HepG2 H1.3 cells **b)** PHHs and **c)** HBV tg mice were treated with indicated RNA-oligonucleotides and hepatocellular 2'-5'-OAS mRNA levels were determined at indicated timepoints by quantitative RT-PCR relative to GAPDH and normalized to mock treated cells or animals, respectively. Data are shown as mean \pm SD, n=3.

The results clearly showed that application of 3p-RNA led to a strong induction of IFN-I and is followed by expression of 2'-5'-OAS *in vitro* and *in vivo*.

In contrast, IFN- γ expression could not be detected in any model system, at any timepoint. Nevertheless, transfection of 3p-RNA or poly(I:C), respectively led to the expression of IP-10 in HepG2 H1.3 cells (**Fig. 2.8 a**) and in PHHs (**Fig. 2.8 b**). Ctrl-RNA or mock transfected cells exhibited no IP-10 expression at any timepoint. Remarkably, 3p-RNA injected HBV tg mice showed no residual IP-10 expression at day 6, independent of treatment (**Fig. 2.8 c**).

These results show that IP-10 expression was strongly induced, at least in the cell culture systems, after application of 3p-RNA and in the absence of IFN- γ . Type II interferon (IFN- γ) was not induced or, if so, to minor extends.

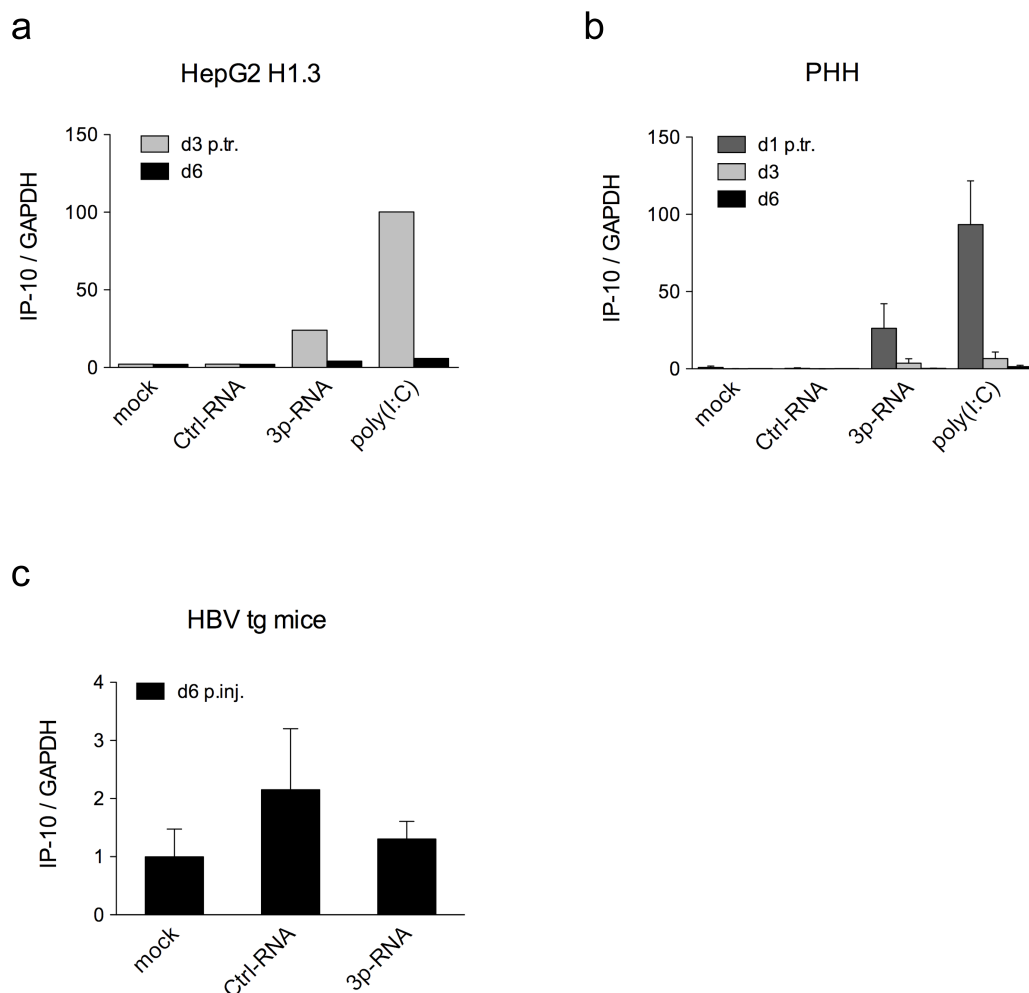


Fig. 2.8: IFN dependent induction of IP-10. a) HepG2 H1.3 cells b) PHHs and c) HBV tg mice were treated with indicated RNA-oligonucleotides and analyzed at indicated timepoints for mRNA expression of IP-10 by quantitative RT-PCR relative to GAPDH and normalized to mock treated cells or animals, respectively. Results of a) are representative of three different experiments, data of b) and c) are shown as mean \pm SD, n=3.

2.3.2 RIG-I dependent IFN- β induction by 3p-RNA

To confirm the contribution of RIG-I in 3p-RNA induced IFN-I expression, RIG-I expression was knocked down by transient transfection of a RIG-I specific siRNA in HepG2 H1.3 cells and PHHs (**Fig. 2.9**). RIG-I expression was determined on protein levels at several time points after siRNA treatment. The most prominent reduction of about 80% was observed 72 hours after siRNA transfection (**Fig. 2.9 a**). In parallel, it was investigated, whether the auto- and paracrine acting IFN-pathway via the interferon- α/β -receptor (IFNAR) was also required for the antiviral induction of IFN-I by 3p-RNA. Functional active human IFNAR consists of two subunits, IFNAR-1 and IFNAR-2 (Gaboriaud, Uze et al. 1990). Therefore, the expression of the interferon- α/β -receptor in HepG2 H1.3 cells was inhibited by using an IFNAR specific siRNA. RIG-I specific - and an HBV sequence specific siRNA (Ctrl siRNA) were used as negative controls. Knockdown-efficiency of IFNAR-I was determined on mRNA level by quantitative real-time PCR (qRT-PCR). Expression of IFNAR was significantly reduced by 70% upon RNAi knockdown after 72 hours in comparison to Ctrl siRNA treated cells (**Fig. 2.9 b**). According to these results, HepG2 H1.3 cells were stimulated 72 hours after treatment with siRNAs against RIG-I or IFNAR-1, respectively, with 3p-RNA to stimulate IFN-I signaling. Unstimulated cells transfected previously with Ctrl siRNA served as negative control. In fact, significantly reduced IFN- β levels were observed in HepG2 H1.3 cells in which RIG-I had been knocked down. However, the cells with IFNAR knockdown only showed a minor reduction on IFN- β expression (**Fig. 2.9 c**). Confirming results were obtained in PHHs (**Fig. 2.9 d**). These data indicate that RIG-I is strictly required for 3p-RNA induced IFN- β response, while a positive feedback via IFNAR-pathway seems to play a minor role.

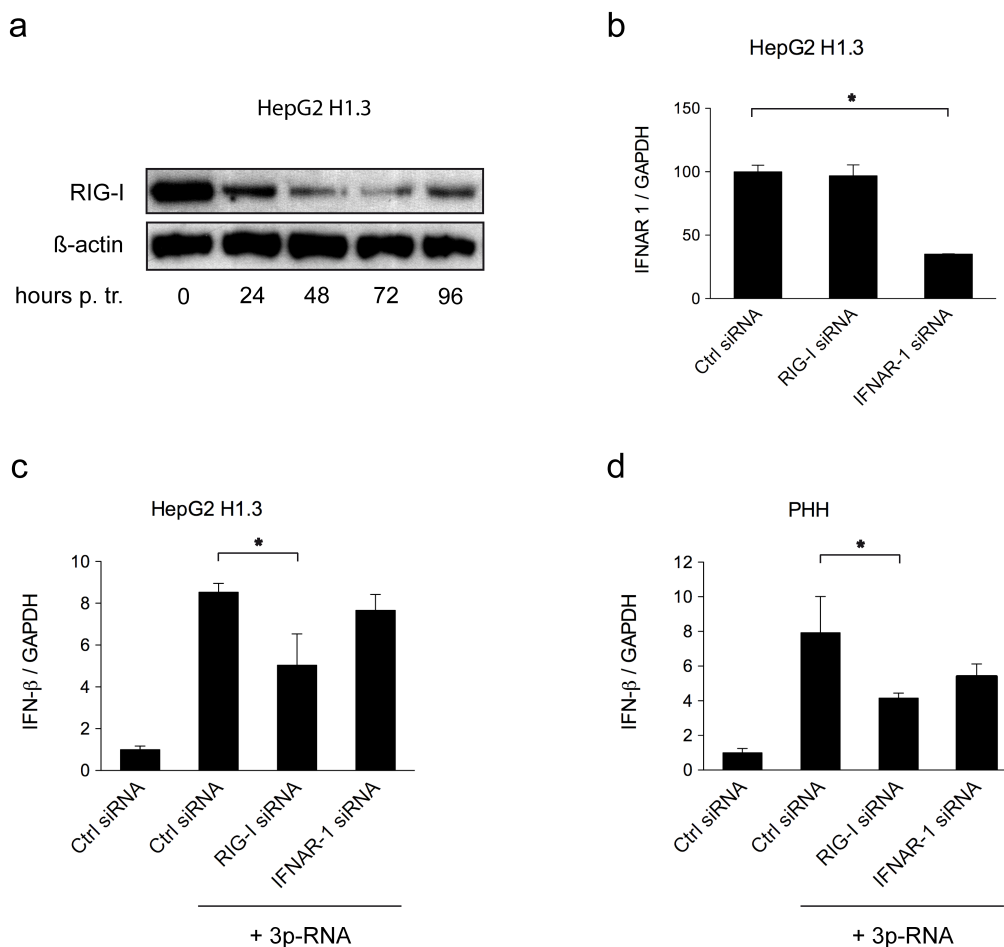


Fig. 2.9: RIG-I dependent IFN-β induction by 3p-RNA. HepG2 H1.3 cells (a-c) and PHHs (d) were transfected with siRNA against RIG-I, IFNAR-1 or with Ctrl-siRNA (HCV-sequence specific siRNA). **a)** HepG2 H1.3 cells treated with αRIG-I siRNA were lysed at indicated timepoints and analyzed for RIG-I expression by Western blot analysis with β-actin as loading control. 30 μg total cell lysate was applied per lane. **b)** HepG2 H1.3 cells treated with indicated siRNA were lysed 72 h p. tr. and IFNAR-1 expression was determined by quantitative RT-PCR **c)** HepG2 H1.3 cells and **d)** PHHs were transfected with indicated siRNAs. After 72 h indicated cells were transfected with 3p-RNA and after 12 h analyzed for IFN-β expression by quantitative RT-PCR. RT-PCRs are relative to GAPDH and normalized to Ctrl siRNA treated cells. Data are shown as mean ± SD, n=3 (*P<0.05, t-test).

2.4 Antiviral effects of 3p-RNA induced IFN-I on HBV

2.4.1 Antiviral effects of 3p-RNA treatment *in vitro*

To test the therapeutic potential of 3p-RNA on HBV replication, first the antiviral effects of transfected 3p-RNA (0.5 μg / ml) were determined in stably HBV expressing HepG2 H1.3 cells. Therefore, the cells were transfected with indicated RNA-oligonucleotides. After treatment accumulated HBV-DNA levels of progeny virus released into the supernatant of cells were measured at three different timepoints by qRT-PCR (**Fig. 2.10**). Released HBV-progeny DNA levels were comparable at day 1 after application. At day 3, HepG H1.3 cells treated with 3p-RNA secreted less virions relative to ctrl-RNA and mock controls. At day 6 after transfection the media of cells transfected with 3p-RNA contained strongly reduced (1.5 log scales) HBV-DNA levels, but not after treatment with Ctrl-RNA (polyA-RNA) (**Fig. 2.10 a**). Additionally, affected HBeAg and HBsAg secretion were determined by ELISA, HBeAg was about 50% and HBsAg about 40% reduced, compared to untreated cells (**Fig. 2.10 b**).

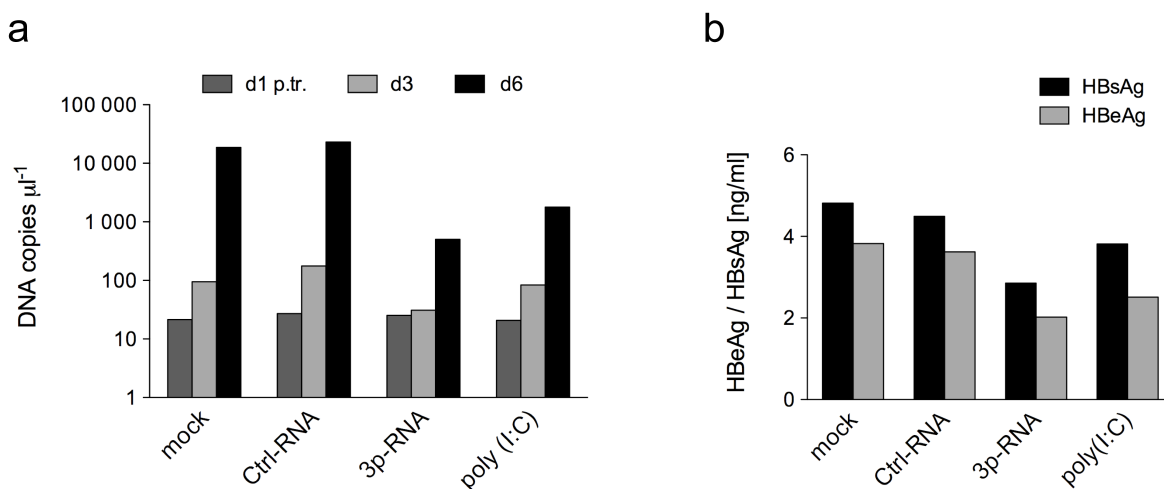


Fig. 2.10: Suppression of HBV replication by IFN-I induction after application of 3p-RNA in HepG2 H1.3 cells. HepG2 H1.3 cells were treated with 3p-RNA, Ctrl-RNA (polyA-RNA; negative control) or poly (I:C) (positive control). Mock cells were treated with transfection reagent Hiperfect. **a)** Quantitative RT-PCR analysis of HBV-DNA levels at day 1, day 3 and day 6 p. tr., respectively. **b)** Enzyme immunoassay of HBV-antigen levels (HBsAg and HBeAg) in supernatant of 3p-RNA treated HepG2 H1.3 cells at 6 days p. tr.. One representative of three different experiments is shown.

Second, the antiviral effect of 3p-RNA was examined in HBV infected PHHs. The primary cells were analyzed for HBV-replication markers at day 6 after treatment (**Fig. 2.11**). Both, 3p-RNA and poly(I:C) treated PHHs exhibited a significant 10-fold reduction of secreted virions compared to untreated cells (**Fig. 2.11 a**). Antigen levels in the supernatant were significantly reduced (**Fig. 2.11 b**). In addition, quantification of pgRNA levels by qRT-PCR disclosed a significant reduction of HBV-RNA in PHHs after application of 3p-RNA (**Fig. 2.11 c**). Antiviral effects were as strong as those of poly(I:C).

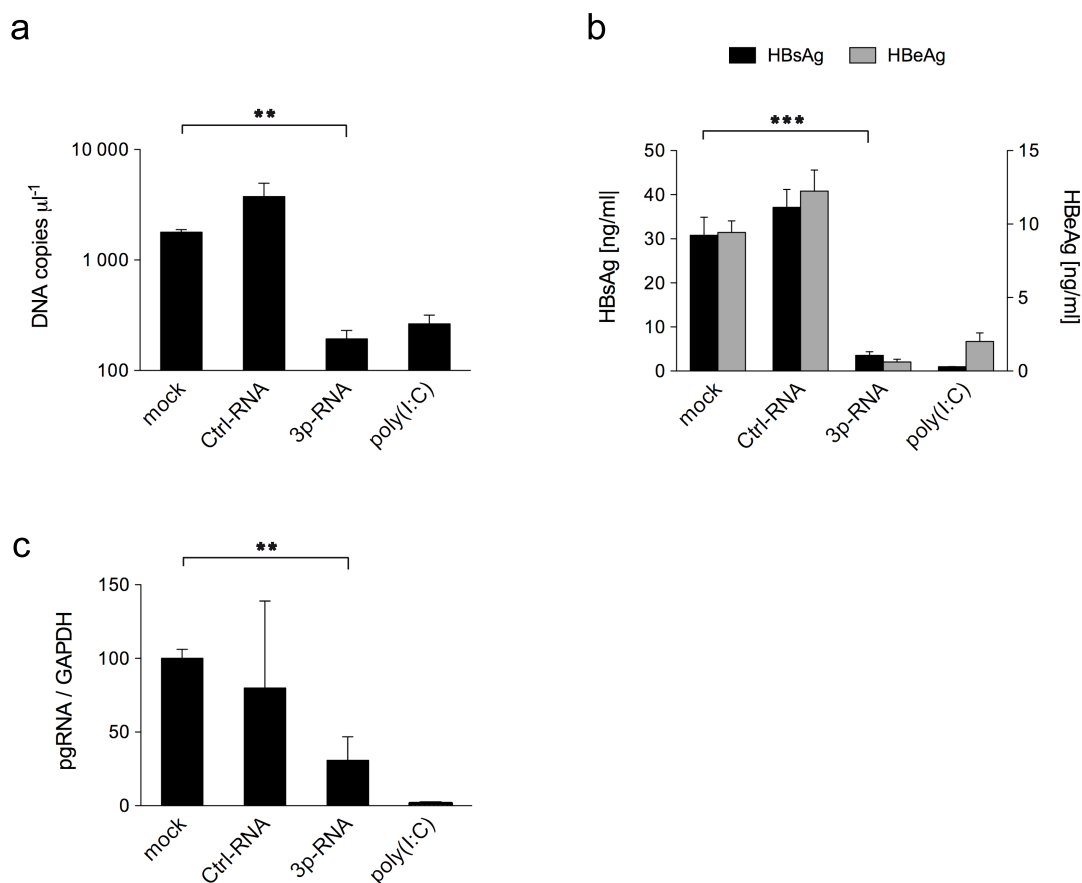


Fig. 2.11: Stimulation of RIG-I by 3p-RNA suppressed HBV replication in primary human hepatocytes. HBV infected PHHs were treated with indicated RNA-oligonucleotides. Mock cells were treated with transfection reagent Hiperfect. **a)** Quantitative PCR analysis of HBV-DNA levels and **b)** enzyme immunoassay of HBV-antigen levels (HBeAg, HBsAg) in the supernatant of PHHs at day 6 p. tr. **c)** Quantitative RT-PCR of pregenomic RNA levels at day 6 p. tr. relative to GAPDH and normalized to mock treated cells. Data are shown as mean \pm SD, $n=3$ (** $P<0.01$, *** $P<0.001$, t-test).

The results clearly demonstrate a strong immuno-stimulatory, antiviral activity of 3p-RNA against HBV by induction of IFN-I via RIG-I stimulation. Analyzed HBV-replication markers were significantly reduced in both HepG2 H1.3 cells and HBV infected PHHs.

2.4.2 Antiviral effects of 3p-RNA treatment *in vivo*

Next, the antiviral effects of 3p-RNA were examined in HBV tg mice. Ctrl-RNA and jetPEI injected mice served as negative controls. HBV replication markers such as progeny HBV-DNA and HBV-antigens levels in the sera as well as HBV-RNA levels in the livers of HBV tg mice were determined at day 6 p. inj. (**Fig. 2.12**).

HBV tg mice showed a 1.6 log reduction of HBV-DNA levels in the blood after 3p-RNA injection compared to Ctrl-RNA or mock treated mice (**Fig. 2.12 a**). Furthermore, HBsAg levels were significantly reduced (**Fig. 2.12 b**). HBeAg, at comparable levels at the day of application, was significantly reduced at day 6 compared to untreated mice or basal levels at day 0 (**Fig. 2.12 c**). 3p-RNA application also reduced pregenomic HBV-RNA (**Fig. 2.12 d**). RT-PCR results were confirmed by Northern blot analysis of pooled liver RNA within the different groups. It showed a reduction of both HBV-RNA forms, pgRNA and sgRNA after injection of 3p-RNA compared to untreated mice (**Fig. 2.12 e**). GAPDH served as loading control and indicated that loaded RNA amount of 3p-RNA treated mice was lower than of mock treated mice, suggesting even stronger differences in HBV-RNA levels.

The data confirm the potent therapeutic effectivity of 3p-RNA by induction of antiviral IFN-I leading to strong suppression of HBV replication *in vivo*.

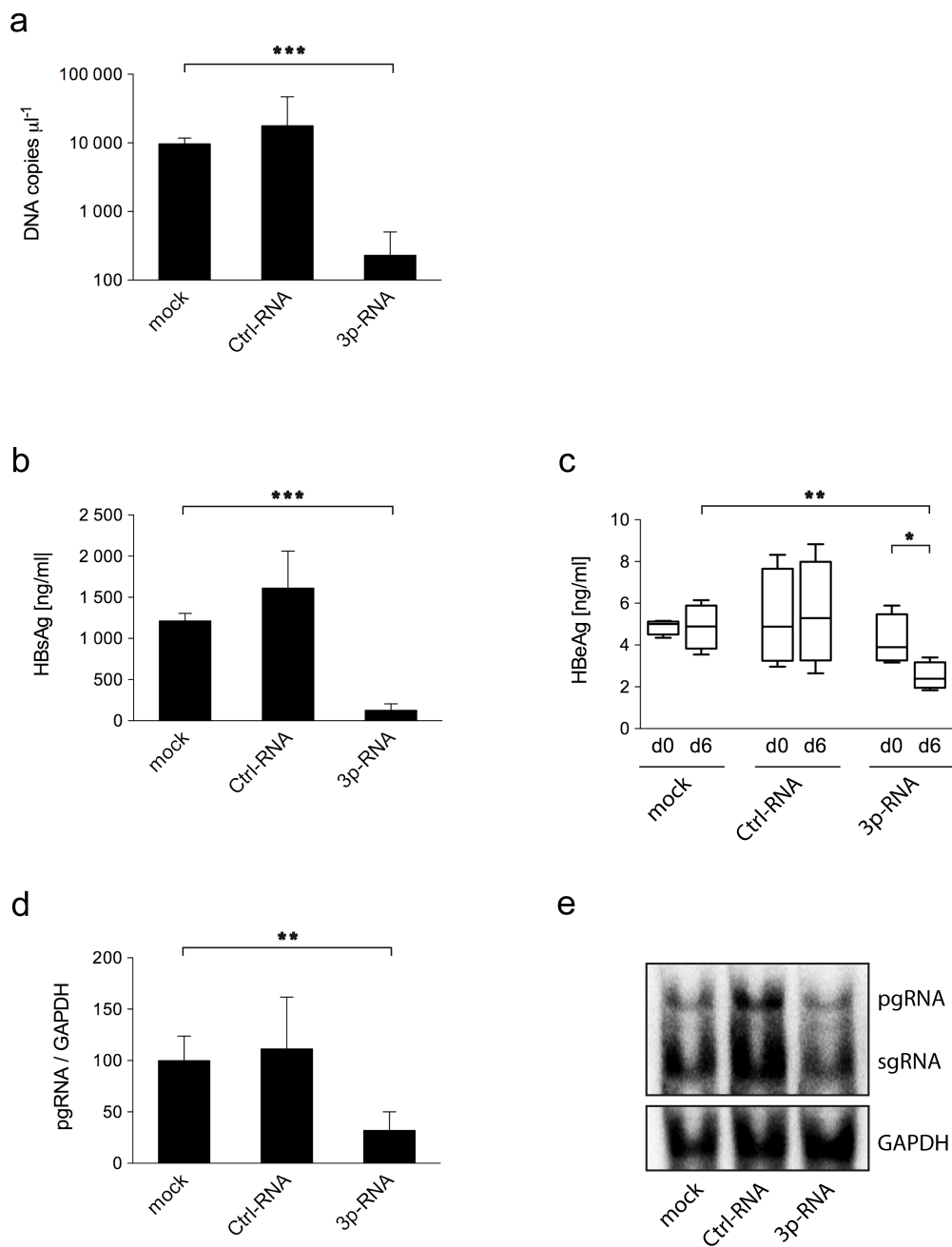


Fig. 2.12: Stimulation of RIG-I by 3p-RNA suppressed HBV replication in HBV tg mice. HBV tg mice were treated with 3p-RNA or si-Ctrl (HCV-sequence specific siRNA; negative control) or with nucleic acid delivery reagent jetPEI as mock control. **a)** Quantitative PCR analysis of HBV-DNA levels and **b)** HBsAg levels in serum of HBV tg mice at day 6 p. inj. and **c)** HBeAg levels in serum at the day of application (day 0) and day 6 p. inj. (EIA) **d)** Quantitative RT-PCR analysis of intrahepatic pregenomic RNA levels relative to GAPDH, normalized to mock treated mice and **e)** Northern blot of pooled liver RNA (n=4/group) that reflect the effect of 3p-RNA on pre- and subgenomic RNA levels at day 6 after treatment with indicated RNA-oligonucleotides. GAPDH as loading control. 25 μg pooled total RNA was applied per lane. Data are shown as mean \pm SD, n=4 (*P<0.05, **P<0.01, ***P<0.001, t-test).

2.5 HBV sequence specific 3p-siRNA as RIG-I ligand

2.5.1 Design of HBV-sequence specific siRNAs

To enhance the therapeutic efficiency against HBV it was intended to combine the antiviral immune regulatory effect of RIG-I stimulation with an RNAi mediated gene-silencing effect on cytosolic HBV-RNAs. Therefore, three different HBV-sequence specific siRNAs of 19 nt were designed, which target three different regions at the 3'-end of the HBV-RNAs within the overlapping ORFs of HBV (**Fig. 2.13**). The siRNA si-1.1 targets a region of the HBV genome within the overlapping ORFs of the X-protein and the precore protein (processed to HBeAg), and was predicted to affect all HBV-mRNAs (**Fig. 2.13**, orange arrows). The siRNA si-1.2 targets an alternative region within the X-protein ORF, but, as si-1.1, all HBV-mRNAs transcripts. Another alternative HBV-genome target region, the ORF of the polymerase, is targeted by siRNA si-1.3, which potentially affects all HBV mRNA transcripts except for the 0.7 kb transcript of the X-protein. All HBV targeting sequences are conserved among all HBV genotypes, except the rare genotype F. Genotype D HBV is present in HepG2 H1.3 cells and in the HBV tg mice used in this study. In contrast, primary hepatocytes were infected with HBV genotype A before treatment, originated and purified from stably HBV expressing hepatoma cell line HepG2 2.15.

To combine the antiviral effect of siRNA mediated HBV gene silencing and endogenous IFN-I induction via RIG-I stimulation, DNA templates for HBV-sequence specific siRNAs were reverse transcribed by *in vitro* transcription and thereby coupled to triphosphate groups at both 5'-ends. The resulting RNA-oligonucleotides were named 3p-1.1, 3p-1.2 and 3p-1.3, according to their unphosphated siRNA counterparts.

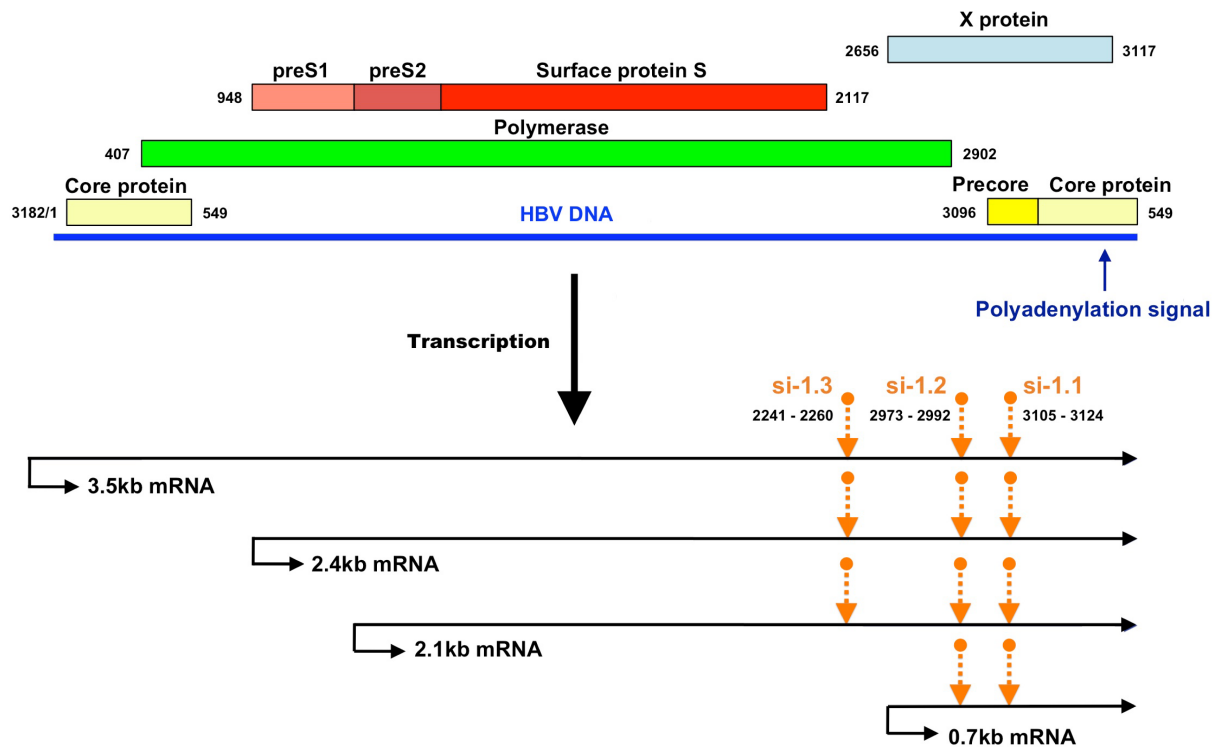


Fig. 2.13: HBV-sequence specific siRNA targeting. The HBV-sequence specific siRNAs named si-1.1, si-1.2 and si-1.3 were designed to target the ORFs of the X-protein or the polymerase within the 3'-end region of the mRNA transcripts near the polyadenylation signal, indicated by orange arrows.

2.5.2 Functionality of 3p-siRNA as RIG-I ligand

Subsequently, the ability of 3p-siRNA to induce an antiviral IFN response was tested. Therefore, HepG2 H1.3 cells were transfected exemplarily with 3p-1.2, (triphosphorylated, HBV-sequence specific siRNA), its non-phosphorylated counterpart si-1.2 (HBV-sequence specific siRNA) or si-Ctrl (inert HCV-sequence specific siRNA). Mock cells were treated with transfection reagent Hiperfect (**Fig. 2.14**). Only HepG2 H1.3 cells transfected with 3p-1.2 showed an induction of IFN- β after 12 hours determined on mRNA level by quantitative RT-PCR. Cells treated with si-1.2 or si-Ctrl, respectively, revealed no or only marginal IFN- β expression in comparison to mock treated cells (**Fig. 2.14 a**). Next, IFN-I induction levels of all three triphosphorylated siRNAs (3p-1.1, 3p-1.2 and 3p-1.3) were compared. Therefore, IFN-I stimulated 2'-5'-OAS levels were determined 8 days after

transfection of the 3p-siRNAs in HepG2 H1.3 cells (**Fig. 2.14 b**) and in HBV infected PHHs (**Fig. 2.14 c**). Cells treated with transfection reagent Hiperfect were used as mock controls. All three 3p-siRNAs induced 2'-5'-OAS in both *in vitro* models; in HepG2 H1.3 cells at comparable levels, in PHHs less pronounced and at variable strength.

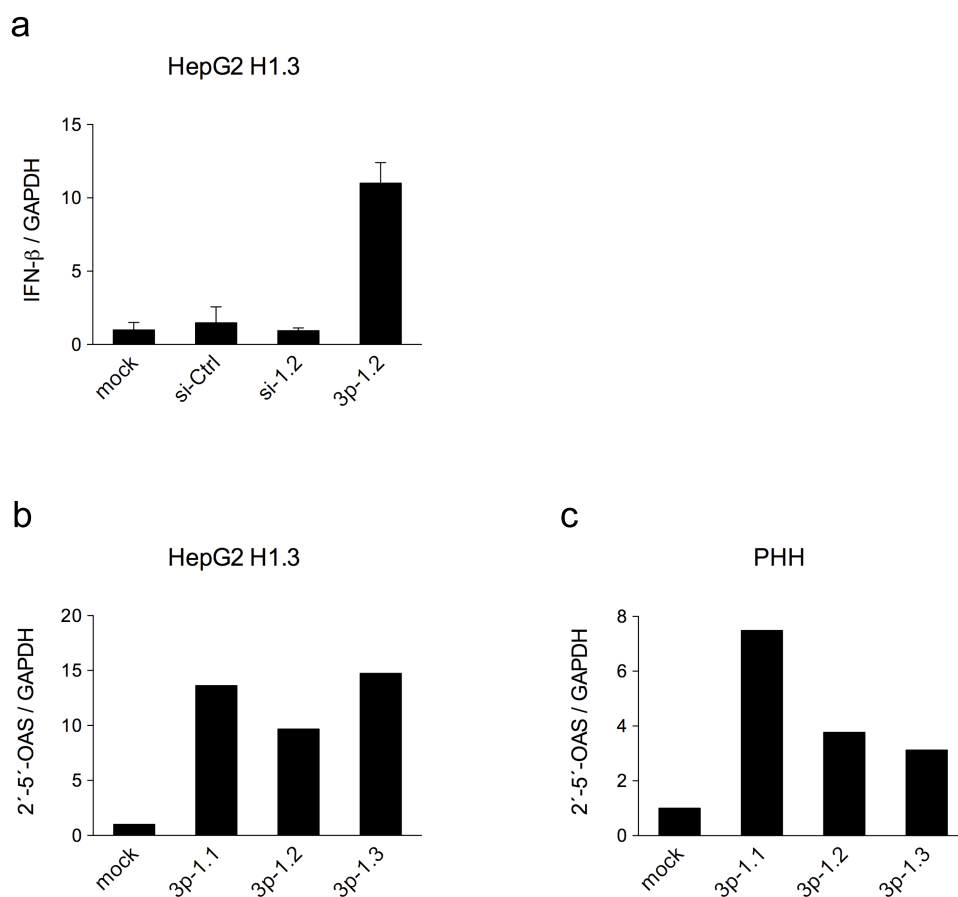


Fig. 2.14: HBV sequence specific 5'-triphosphorylated siRNAs served as RIG-I ligands. **a)** HepG2 H1.3 cells were transfected with control siRNA (HCV-sequence specific siRNA), si-1.2 (unphosphated HBV-sequence specific siRNA) or 3p-1.2 (triphosphorylated HBV-sequence specific siRNA). Mock cells were treated with transfection reagent (Hiperfect). 12h after treatment the cells were tested for IFN- β induction by quantitative RT-PCR relative to GAPDH and normalized to mock treated cells. Data are shown as mean \pm SD, n=3. **b+c)** HepG2 H1.3 cells and HBV infected PHHs were transfected with 3p-siRNAs (3p-1.1, 3p-1.2 or 3p-1.3), mock cells were treated with transfection reagent Hiperfect. Cells were analyzed by quantitative RT-PCR at day 8 p. tr. for mRNA expression of interferon-inducible 2'-5'-oligoadenylate synthetase (OAS) relative to mRNA GAPDH, normalized to mock treated cells. One representative of three different experiments is shown.

This data clearly elucidate that HBV sequence specific triphosphated siRNAs were suitable as RIG-I ligands, competent for induction of IFN-I, as determined by IFN-I induced 2'-5'-OAS expression in both *in vitro* models.

2.5.3 Antiviral effects of 3p-siRNA treatment *in vitro*

To elucidate the therapeutic efficiency of the modified RIG-I ligands, the effects of applied 3p-siRNAs on HBV-replication markers were determined at day 8 after transfection in HepG2 H1.3 cells and HBV infected PHHs (**Fig. 2.15**). All three 3p-siRNAs had a significant impact on HBV-progeny release of HepG2 H1.3 cells (**Fig.2.15, a**) and PHHs (**Fig.2.15, b**). 3p-1.2 reduced virion secretion in HepG2 H1.3 cells about 1 log (**Fig. 2.15 a**). All 3p-siRNAs reduced HBV-DNA release from HBV-infected primary cells more than 0.75 log scales (**Fig. 2.15 b**). Furthermore, the antiviral effects of 3p-siRNAs on HBV-antigen levels (HBeAg and HBsAg) were examined by ELISA assays (**Fig. 2.15 c + d**). All three 3p-siRNAs led to a clear reduction of secreted HBeAg in HepG2 H1.3 cells, on average around 50% (**Fig. 2.15 c**) and in HBV infected PHHs of approximately 35% (**Fig. 2.15 d**). HBsAg levels were also significantly reduced in HepG2 H1.3 cells by all three 3p-siRNA, but most drastically for 80% by the application of 3p-1.2 (**Fig. 2.15 c**). In HBV infected PHHs 3p-siRNAs showed a minor effect on HBsAg, with reduction of approximately 40% (**Fig. 2.15 d**).

HepG2-H1.3 cells and HBV infected PHHs additively express episomal HBV-cccDNA. This supercoiled HBV-DNA accumulates and persists in episomal form in the nucleus and serves as viral transcription template during HBV infection. Examined cccDNA levels were decreased after application of 3p-siRNAs in both, HepG2 H1.3 cells (**Fig. 2.15 e**) and in PHHs (**Fig. 2.15 f**).

Taken together, these results indicate that 3p-siRNAs efficiently suppress HBV-replication on HBV-DNA and HBV-protein level. Furthermore, nuclear HBV cccDNA levels were reduced by 3p-siRNA application in both cell types.

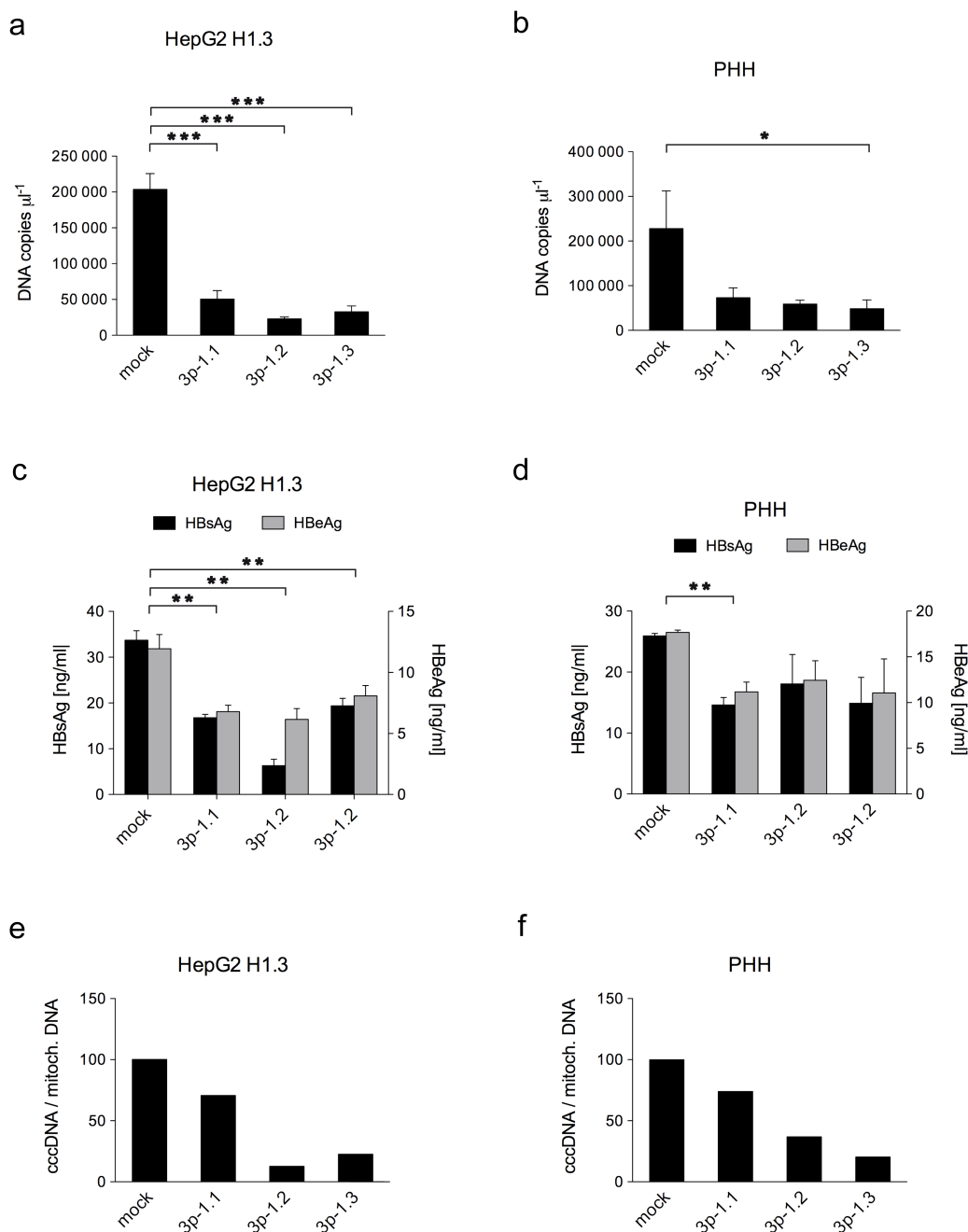


Fig. 2.15: HBV-sequence specific 3p-siRNAs suppressed HBV replication *in vitro*. HepG2 H1.3 cells and HBV infected PHHs were transfected with different 3p-siRNAs (3p-1.1, 3p-1.2 or 3p-1.3) and analyzed at day 8 p. tr.. Mock cells were treated with transfection reagent (Hiperfect). Supernatants of HepG2 H1.3 cells and PHHs were analyzed for **(a+b)** HBV-DNA levels by quantitative PCR, normalized to mock treated cells and for **(c+d)** HBeAg by enzyme immunoassay and HBsAg levels by ELISA. Data are shown as mean \pm SD, n=3 (*P<0.05,**P<0.01, ***P<0.001, t-test). Additionally, quantitative RT-PCR analysis of cccDNA levels relative to mitochondrial DNA normalized to mock treated cells was performed **(e+f)**. Data are representative of three different experiments.

As already said, PHHs were infected with genotype A HBV, secreted from stably HBV expressing HepG2 2.15 cells. To confirm the therapeutic efficiency of 3p-siRNAs on genotype A HBV, HepG2 2.15 cells were treated directly with the different 3p-siRNAs (**Fig.2.16**). At day 6 after application IFN-I dependent 2'-5'-OAS induction was determined on mRNA level by qRT-PCR (**Fig. 2.16 a**).

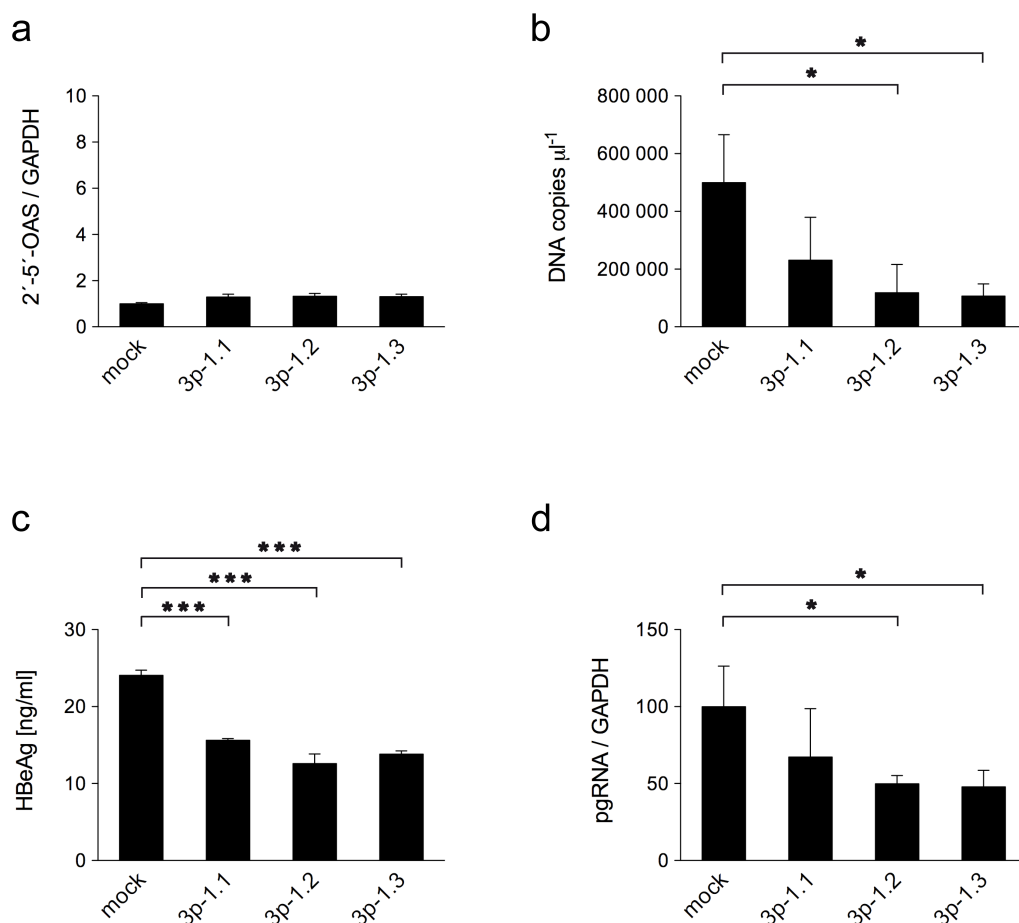


Fig. 2.16: HBV-sequence specific 3p-siRNAs suppressed genotype A HBV replication in HepG2 2.15 cells. HepG2 2.15 cells were transfected with different 3p-siRNAs (3p-1.1, 3p-1.2 or 3p-1.3) and analyzed at day 6 p. tr.. Mock cells were treated with transfection reagent (Hiperfect). **a)** 2'-5'-OAS induction was tested on mRNA level by qRT-PCR relative to GAPDH mRNA and normalized to mock treated cells. Supernatants of HepG2 2.15 cells were analyzed for **b)** progeny HBV-DNA levels by quantitative PCR and for **c)** HBeAg levels by enzyme immunoassay. **d)** pgRNA levels were determined by quantitative RT-PCR. Data are shown as mean \pm SD, n=3 (*P<0.05, ***P<0.001, t-test).

None of the transfected 3p-siRNAs revealed any, or only residual, expression of 2'-5'-OAS at day 6 after transfection in HepG2 2.15 cells, possibly due to already strongly reduced 2'-5'-OAS expression at this timepoint, but more likely through absence of IFN-I induction, which coincides to the reduced sensitivity of HepG2 2.15 cells against IFN (Guan, Lu et al. 2007). Nevertheless, apparently independent of IFN-I induction, progeny HBV-DNA levels were decreased on average around 60% (**Fig. 2.16 b**). HBeAg levels (**Fig. 2.16 c**) and pgRNA levels (**Fig. 2.16 d**) were also significantly diminished after transfection of 3p-siRNAs.

These results indicate despite lacking IFN-I response an effective suppression of HBV replication by RNAi mediated gene silencing also on genotype A HBV.

2.5.4 Comparison of 3p-RNA and 3p-siRNA treatment *in vitro*

To analyze whether immunostimulation and RNAi-mediated gene silencing acts synergistically to suppress HBV replication, the primarily used 3p-RNA was compared with the 3p-siRNAs in HepG2 H1.3 cells. Therefore, HepG2 H1.3 cells were transfected with the original RIG-I ligand 3p-RNA, the 3p-siRNAs 3p-1.1, 3p-1.2 and 3p-1.3 and si-Ctrl RNA, respectively. HepG2 H1.3 cells treated with transfection reagent Hiperfect served as mock control. The effects on HBV replication were analyzed within an expanded timeframe at day 4 and day 8 post transfection, determining intracellular HBV-DNA levels by Southern blot analysis (**Fig. 2.17 a**), episomal HBV cccDNA levels by qRT-PCR (**Fig. 2.17 b**) and HBV-protein levels by Western blot analysis (**Fig. 2.17 c**).

Indicated bands of the Southern blot analysis represented different HBV-DNA forms such as rcDNA, linear and single-stranded HBV-DNA, as well as replicative intermediates of variable size (**Fig. 2.17 a**). Detection of integrated HBV genomes served as a loading control. Intracellular HBV-DNA levels were strongly reduced at day 4 after treatment with the original 3p-RNA. Intriguingly, all three 3p-siRNAs displayed a slightly more pronounced reduction in HBV-DNA levels compared to 3p-RNA at this timepoint. Surprisingly, also si-Ctrl RNA treatment slightly reduced hepatocellular HBV-DNA levels in comparison to mock control (**Fig. 2.17 a, left**). The antiviral effect of the original 3p-RNA ligand nearly disappeared at day 8 after

treatment, whereas the effect on intracellular HBV-DNA levels by all 3p-siRNAs persisted (**Fig. 2.17 a, right**).

Accordingly, a superior antiviral effect of 3p-siRNA compared to 3p-RNA alone could be shown on HBV cccDNA levels (**Fig. 2.17 b**). The displayed quantitative PCR products of cccDNA, relative to mitochondrial DNA as loading control, indicated a potent reduction of the episomal HBV-DNA form at day 4 after treatment by both, 3p-RNA and all 3p-siRNAs in comparison to mock control. However, again si-Ctrl had some effect (**Fig. 2.17 b, left**), probably to its low, but clearly detectable immunostimulatory activity (**Fig. 2.14 a**). On day 8 3p-siRNA still decreased cccDNA levels, whereas 3p-RNA had no effect anymore (**Fig. 2.17 b, right**). This difference in antiviral activity was confirmed by Western blot analysis of the large HBV envelope protein (**Fig. 4c upper panel**). In addition, the HBV core-protein was only slightly affected by 3p-RNA at day 4, whereas all three 3p-siRNAs had a post-translational effect on core-protein expression at this timepoint. Core-protein expression was completely restored in 3p-RNA treated cells at day 8, but still decreased in cells treated with 3p-1.2 and 3p-1.3 (**Fig. 4c lower panel**).

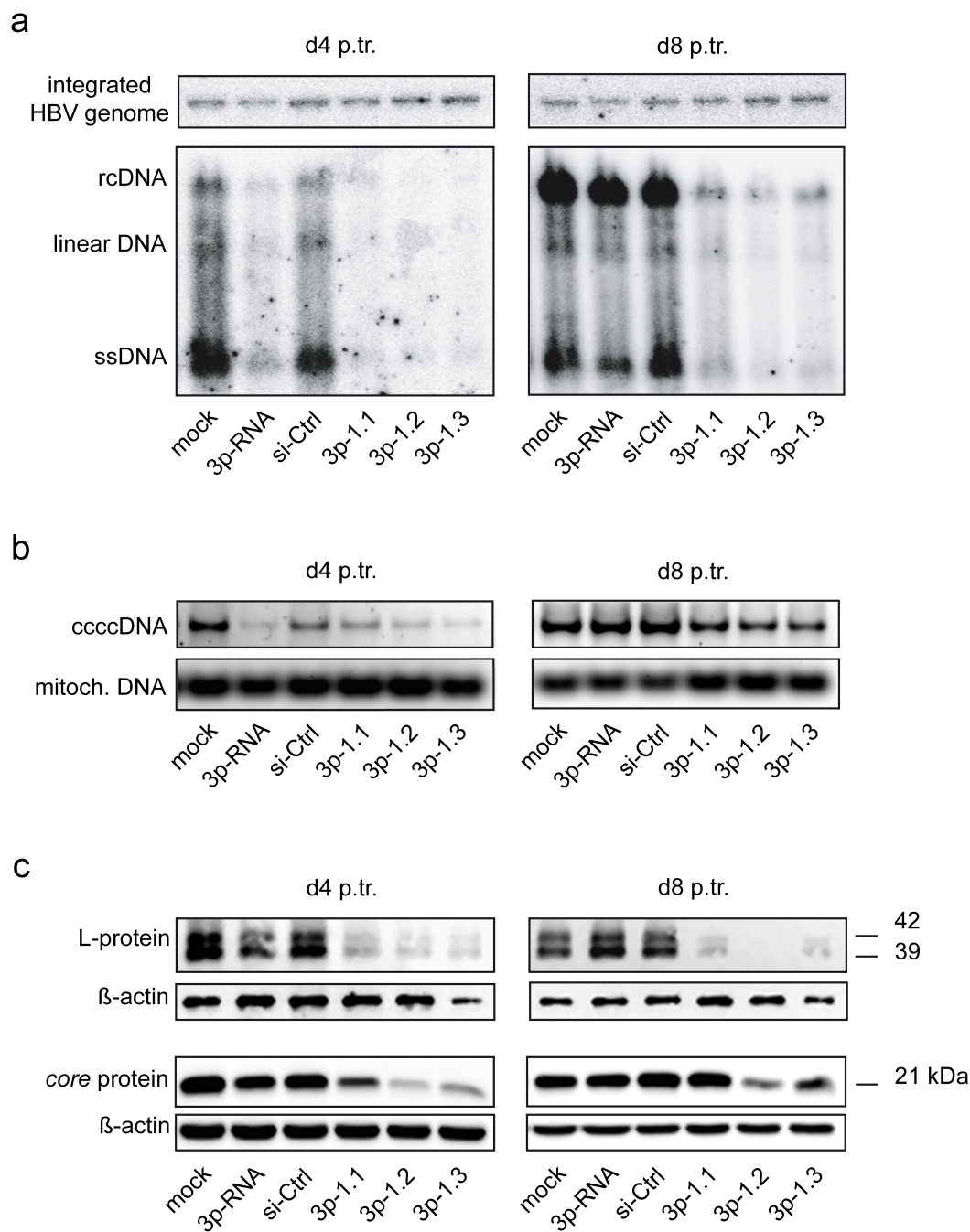


Fig. 2.17: 3p-siRNA combined RIG-I stimulation and siRNA mediated gene silencing *in vitro*.

HepG2 H1.3 cells were treated with indicated RNA-oligonucleotides and analyzed 4 days and 8 days after treatment. Mock (cells treated with transfection reagent Hiperfect), 3p-RNA (in vitro transcribed 5'-triphosphated dsRNA), si-Ctrl (HCV-sequence specific siRNA) served as negative control, 3p-1.1, 3p-1.2 and 3p-1.3 (in vitro transcribed 5'-triphosphated HBV-sequence specific siRNA). **a)** Southern blot analysis of intracellular HBV-DNA in HepG2 H1.3 cells. 20 μ g total DNA was applied per lane. **b)** Agarosegel of PCR products using cccDNA specific primers. Mitochondrial DNA PCR served as control. **c)** Western blot analysis of intracellular HBV L- and core protein expression. β -actin was detected as loading control. 15 μ g total cell lysate was applied per lane.

The results indicate comparable antiviral effects of the original RIG-I ligand 3p-RNA and the modified 3p-siRNAs on HBV replication at early time-points (day 4 after transfection) in HepG2 H1.3 cells. In contrast, an enhanced and prolonged antiviral effect of 3p-siRNAs was detected at later time-points (day 8 after transfection).

2.5.5 Long-term treatment of HBV by 3p-siRNA *in vitro*

To prove the sustained antiviral effects of 3p-siRNAs, the antiviral efficiency of 3p-RNA was compared with the most promising 3p-siRNA (3p-1.2) and its unphosphated counterpart si-1.2 over a period of 16 days in HepG2 H1.3 cells (**Fig. 2.18**). Poly (I:C) served as positive control, mock cells were treated with transfection reagent Hiperfect. Therapeutic effects were monitored in terms of progeny HBV-DNA release by quantitative PCR (**Fig. 2.18 a**) and HBeAg secretion by ELISA (**Fig. 2.18 b**). Analysis started 12 h after treatment, followed by day 4 and subsequently every second day until day 16. The medium of cells was changed every second day from day 4 onwards. The early antiviral response until day 6 was comparable between all oligonucleotides at progeny HBV-DNA and HBeAg levels. Nevertheless, both, 3p-1.2 as well as its synthetic counterpart si-1.2 controlled HBV-DNA synthesis over time. 3p-1.2 was significantly superior to si-1.2 from day 10 onwards (**Fig. 2.18 a**). HBeAg level reduction by 3p-1.2 was significantly superior to 3p-RNA or si-1.2 from day 8 onwards. Accordingly, 3p-1.2 showed a prolonged antiviral response than si-1.2 and 3p-RNA alone. Probably, IFN-I mediated reduction of HBV replication by 3p-RNA and 3p-1.2 diminished over time. Therefore, 3p-RNA and 3p-1.2, as well as poly(I:C) as IFN-I inducing positive control, were equally active at early timepoints. But 3p-RNA and poly(I:C) lost their antiviral activity at later timepoints due to the absence of gene silencing activity.

Taken together, the results indicate that the combination of immuno-stimulation and gene silencing in one single molecule displayed superior antiviral activity than each mechanism alone *in vitro*.

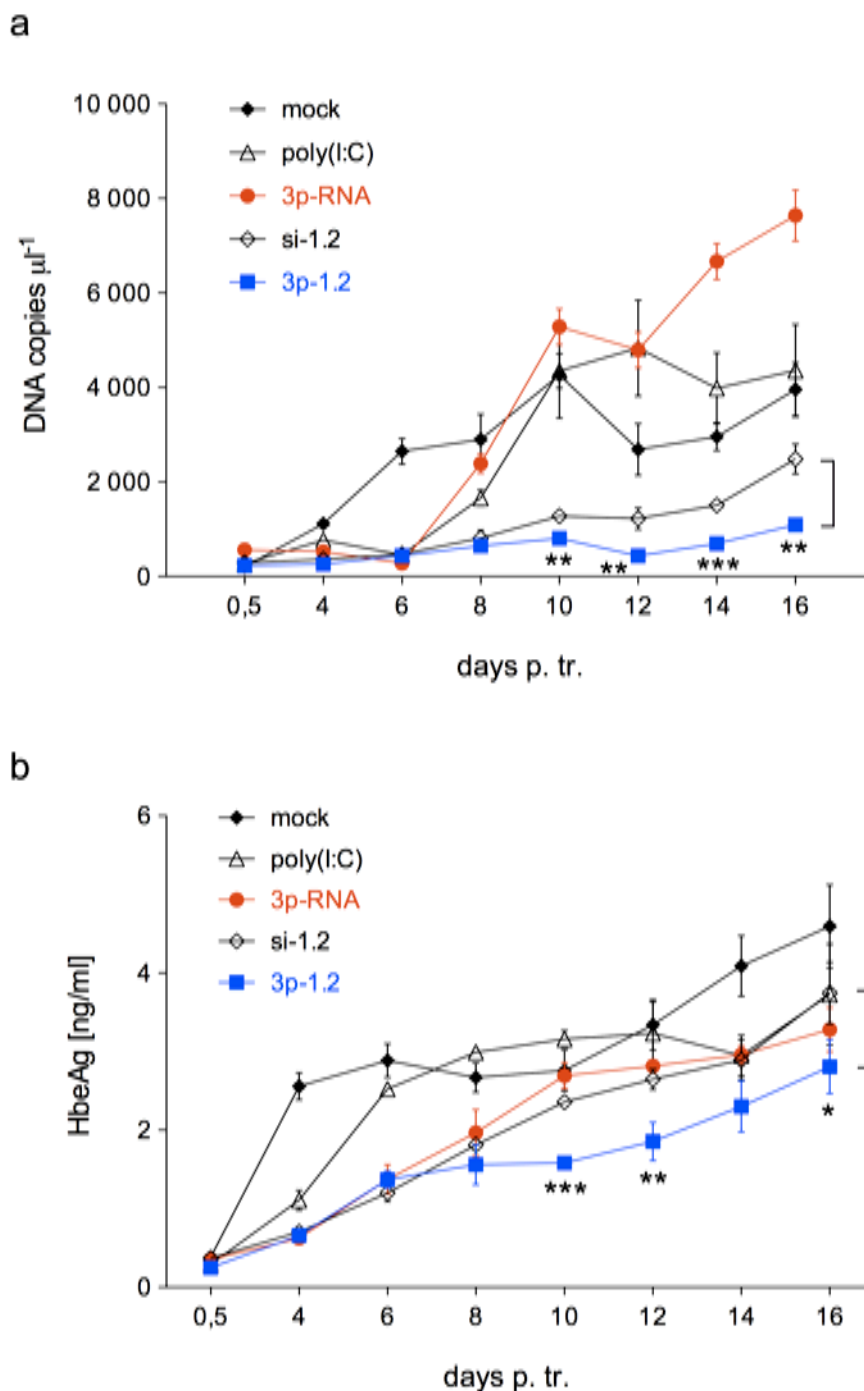


Fig. 2.18: Longterm effects of 3p-siRNA on HBV replication *in vitro*. **a)** Quantitative PCR analysis of progeny HBV-DNA and **b)** enzyme immunoassay of HBeAg levels in supernatant of HepG2 H1.3 cells until day 16 after treatment with indicated RNA-oligonucleotides; mock cells were treated only with transfection reagent Hiperfect. The experiments were performed in triplicates and results were given as mean \pm SD. Significant differences were shown between si-1.2 and 3p-1.2 treated cells (* $P < 0.05$, ** $P < 0.01$, *** $P < 0.001$, t-test).

The experiments showed a slight increase in HBV-DNA levels after treatment with 3p-1.2 or si-1.2 over more than 12 days in HepG2 H1.3 cells. Accordingly, a reduced or hampered binding of siRNA to HBV-DNA due to mutations selected by RNAi induced selection pressure was excluded. For this, the intrinsic siRNA binding site of si-1.2 was sequenced in secreted virions at day 10 and day 16 (**Fig. 2.19 b + c**). HBV-DNA sequence of mock treated cells at day 0.5 after application served as control (**Fig. 2.19 a**). The correct sequence of the control was verified by comparison with the known HBV genome sequence. None of the analyzed DNA fragments revealed any mutations inside the HBV-genome sequence targeted by si-1.2 or 3p-1.2, neither at day 10 nor at day 16 after transfection.

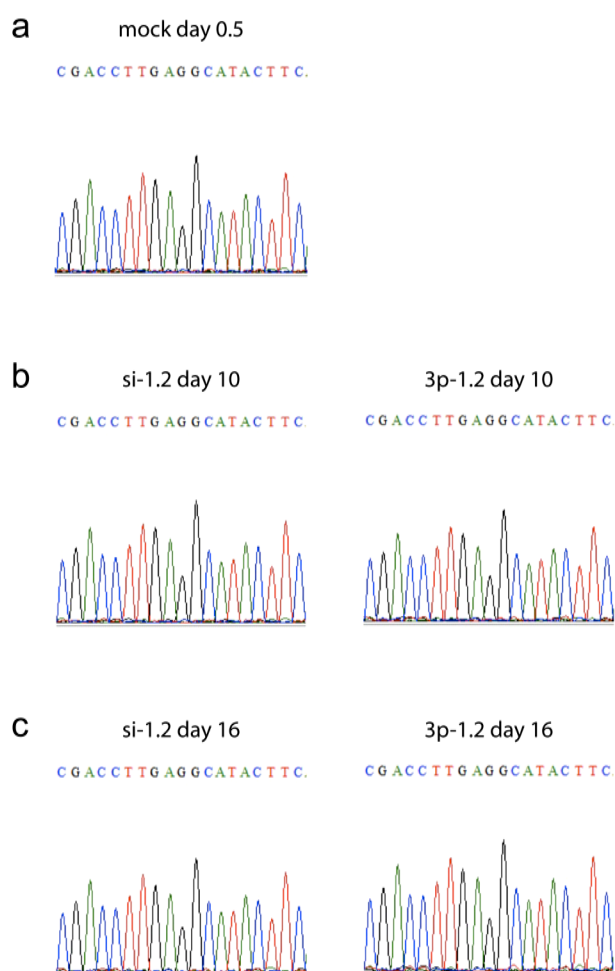


Fig. 2.19: Direct sequencing analysis of siRNA binding site within the HBV-DNA genome of secreted virions. DNA was extracted from supernatant of HepG2 H1.3 cells treated with si-1.2 or 3p-1.2 at day 10 and day 16 after transfection. Si-1.2 binding site spanning fragment of HBV-DNA was amplified by PCR and analyzed by direct sequencing.

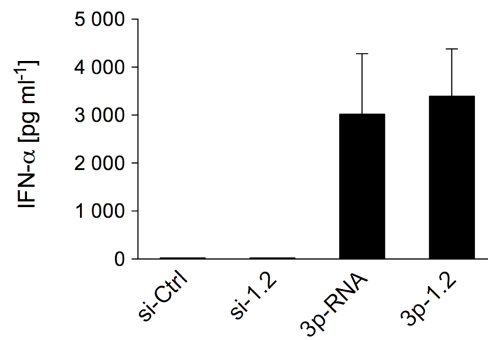
2.5.6 Antiviral effects of 3p-siRNA treatment *in vivo*

Next, the ability of 3p-1.2 and 3p-RNA to induce an antiviral IFN-I response was compared *in vivo* (**Fig. 2.20**). Therefore, 3p-1.2, 3p-RNA and si-1.2, respectively, were injected intravenously twice (day 0 and day 3) into HBV tg mice and sera of mice were tested 6 h after injection for IFN- α by ELISA assay. Mice treated with HCV-sequence specific siRNA (si-Ctrl) served as negative control (**Fig. 2.20 a**). Both ligands 3p-1.2 and 3p-RNA triggered a fast IFN- α response at comparable levels, whereas si-1.2 treated and control mice showed no response.

Next, the impact of 3p-RNA was compared with the antiviral effect of 3p-siRNAs on HBV replication in HBV tg mice. Therefore, mice were injected with 3p-RNA, 3p-1.1 and 3p-1.2, as well as their non-phosphorylated counterparts si-1.1 and si-1.2, respectively. Si-Ctrl treated mice served as negative control. HBV replication levels were determined by Southern blot analysis of pooled, intrahepatic HBV-DNA, isolated at day 6 after treatment. HBV genome integrates served as a loading control. HBV-DNA of HepG2 H1.3 cells, treated with or without the HBV-sequence single-cutter EcoRI, served as a control for different HBV-DNA forms (**Fig. 2.20 b**). Consistent with the *in vitro* data at day 6, mice treated with 3p-RNA, siRNA and 3p-siRNA showed a clear reduction on HBV-DNA replication in comparison to the control group (si-Ctrl). Nevertheless, 3p-RNA seemed to reduce HBV DNA levels superior to 3p-siRNA or siRNA at this timepoint.

The results confirm a rapid IFN-I induction by 3p-1.2 comparable to 3p-RNA *in vivo*. Moreover, mice treated with 3p-siRNA, 3p-RNA or siRNA, respectively, showed a drastic reduction of intracellular HBV-DNA levels at day 6 after treatment.

a



b

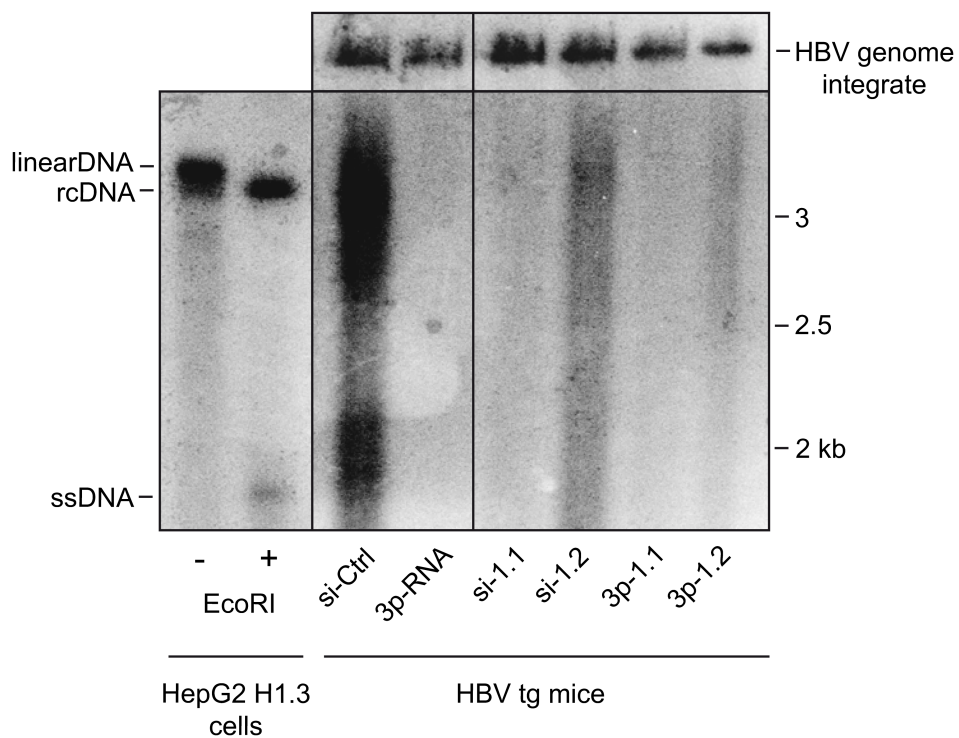


Fig. 2.20: 3p-siRNAs were functional as RIG-I ligands *in vivo*. **a)** IFN- α concentration in serum of HBV tg mice treated with indicated RNA-oligonucleotides, measured by ELISA 6 h after first injection at day 0. Data are shown as mean \pm SD, n=4. **b)** Southern blot analysis of pooled (n=5) intrahepatic HBV-DNA (75 μ g total DNA was applied per lane) of HBV tg mice 6 days after treatment with indicated RNA-oligonucleotides. HBV genome integrates in HBV tg mice served as loading control. HBV-DNA of HepG2 H1.3 cells, treated with or without the HBV-sequence single-cutter EcoRI, served as a control for different HBV-DNA forms.

2.5.7 Long-term treatment of HBV by 3p-siRNA *in vivo*

The antiviral efficiency of both RNA-oligonucleotides was compared over an extended time period of 15 days. Therefore, HBV tg mice were injected intravenously with 3p-RNA, 3p-1.2, si-1.2 or si-HCV (si-Ctrl) as negative control, respectively. Therapeutic effects against HBV were monitored at day 6, day 9 and day 15 after application by determination of hepatocellular HBV pgRNA levels and progeny HBV DNA levels in the serum of mice by qRT-PCR (**Fig. 2.21**), as well as by cytoplasmic HBV core-protein staining in liver sections (**Fig. 2.22**).

Mice treated with si-1.2 exhibited a slight decrease of pgRNA levels at day 6 and day 9. 3p-RNA or 3p-1.2 treatment, respectively, led to a significant and comparable reduction of pgRNA at day 6. However, 3p-1.2 that combines HBV-specific gene silencing and immune stimulatory properties, showed a significantly stronger effect on HBV pgRNA than 3p-RNA and si-1.2 alone at day 9. Of note, no effect on pgRNA was detectable anymore at day 15 (**Fig. 2.21 a**).

HBV DNA levels in the sera of the mice were comparable in all groups at day 0, the day of application. Mice treated with si-1.2 showed only a minor reduction of HBV viremia, and the effect had disappeared at day 9. In contrast, both, 3p-RNA more than 3p-1.2 injected mice showed a significant drop of HBV viremia at day 6 and day 9 after treatment in comparison to control group, consistent with Southern blot data (**Fig. 2.20 b**). Furthermore, HBV viremia remained reduced until day 15 in comparison to control mice. (**Fig. 2.21 b**).

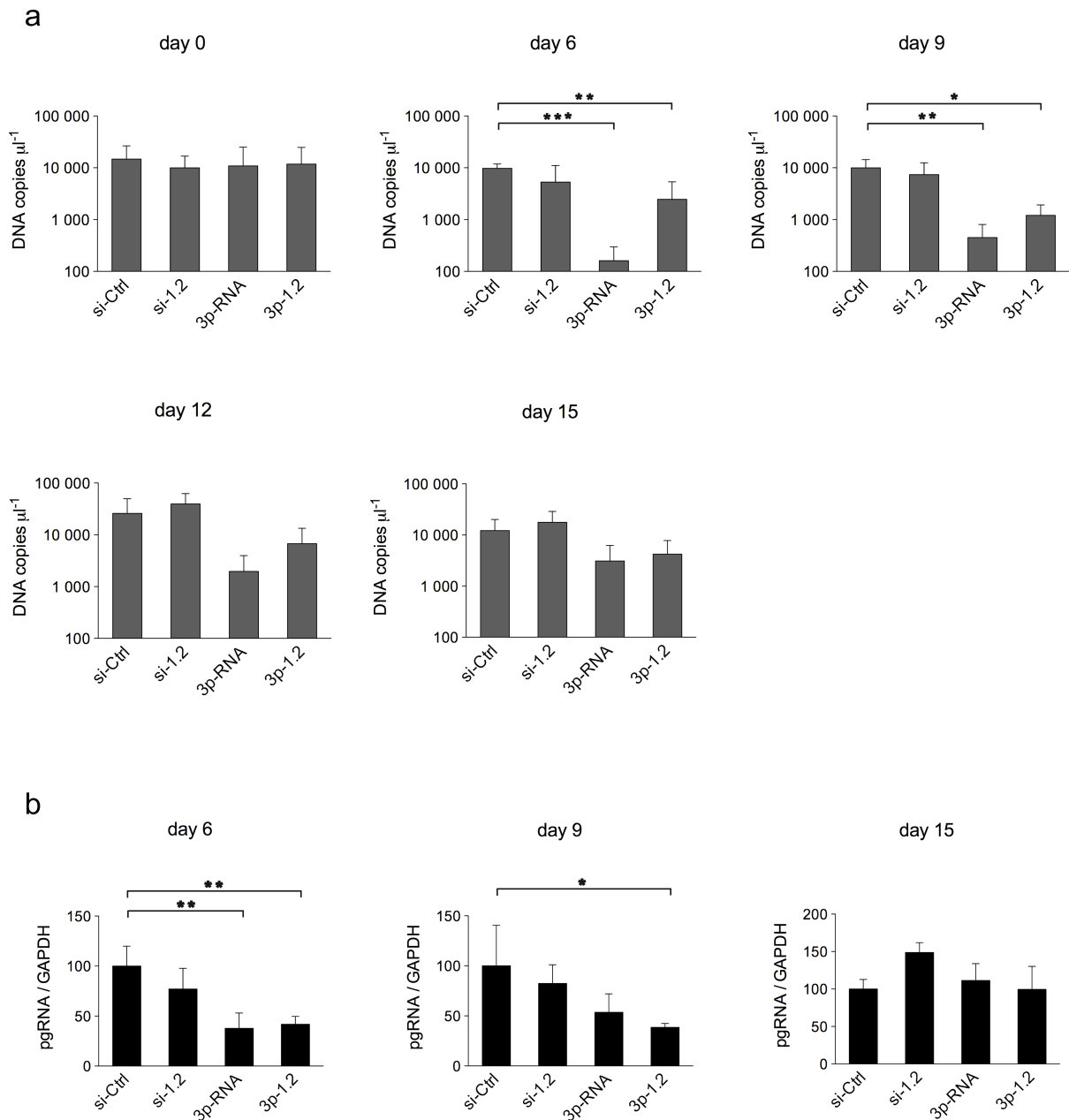


Fig. 2.21: Combined antiviral efficiency of 3p-siRNA *in vivo*. **a)** Quantitative PCR analysis of HBV DNA levels in serum of HBV tg mice at day 0, 6, 9, 12 and 15, respectively, after treatment with indicated RNA-oligonucleotides. **b)** Quantitative PCR analysis of hepatocellular pgRNA levels in HBV tg mice at day 6, 9 and 15, respectively, after treatment with indicated RNA-oligonucleotides, relative to mRNA levels GAPDH, normalized to mice treated with control siRNA. Results are shown as mean \pm SD, n=4 (*P<0.05, **P<0.01, ***P<0.001, t-test).

To investigate the antiviral effect of 3p-RNA and 3p-1.2 on protein expression, the Pathology of Helmholtz Zentrum München additionally performed a HBV core-antigen staining of the liver tissue of treated animals (**Fig. 2.22**). Two different core-antigen staining patterns were observed. First, core-protein that assembles in the nucleus of HBV positive hepatocytes by an unknown mechanism remained unaffected by treatment. This phenomenon occurs frequently in HBV mouse models and results in a nuclear core staining (N), which was observed in 90 - 95% and at comparable intensity in all samples. In addition, cytoplasmic core-staining (CP) was detected, predominantly located in the area of central veins (CV). Mice treated with si-1.2 exhibited little effect, whereas 3p-RNA treatment led to a drastic reduction of cytoplasmic core-protein at day 9. Strongly decreased levels of cytoplasmic core-protein were also observed in mice injected with 3p-1.2, even though not as drastic as in 3p-RNA treated mice (**Fig. 2.22 a**). Cytoplasmic HBV core-antigen staining at day 15 was not affected anymore in si-1.2 treated mice, but slightly diminished in both, 3p-RNA and 3p-1.2 treated mice with superior effects of 3p-1.2 (**Fig. 2.22 b**).

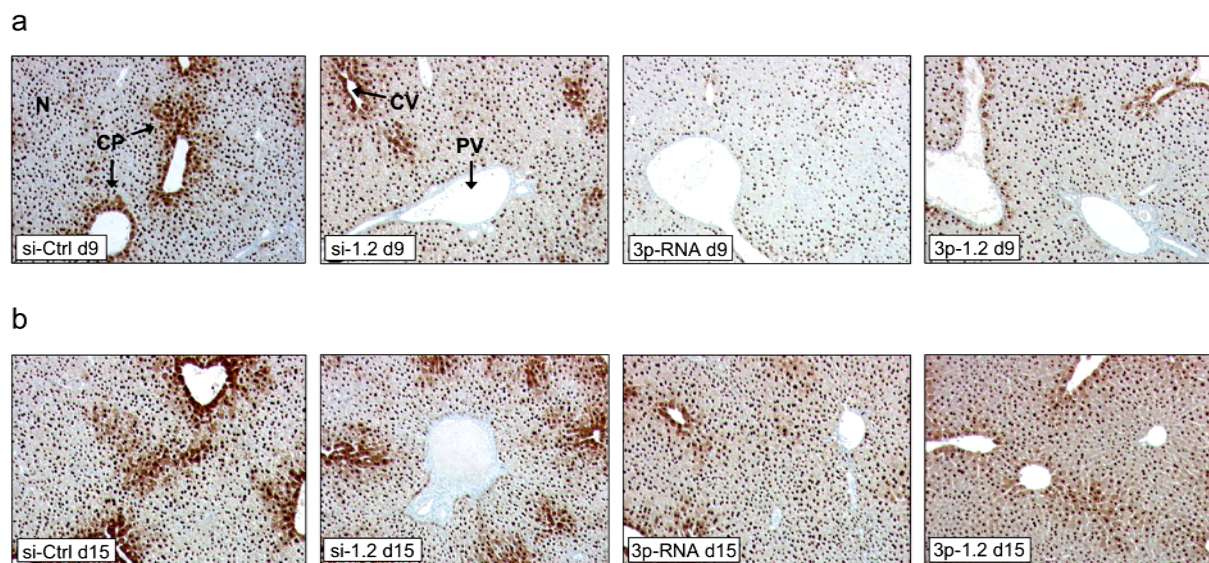


Fig. 2.22: HBV-core antigen staining in liver of RNA-oligonucleotide treated HBV tg mice. HBV tg mice were injected with indicated RNA-oligonucleotides. Liver tissue was analyzed by HBV core-antigen staining at **a)** day 9 and **b)** day 15 after treatment. N: nuclear positivity; CP: cytoplasmic positivity; CV: central vein; PV; portal vein. Results are representative for n=5 mice per group, 2 mice per group were analyzed.

The *in vivo* results confirmed that the combinatorial antiviral effect of 3p-1.2 was superior to siRNA or 3p-RNA.

2.6 Liver directed targeting of RNA-oligonucleotides *in vivo*

As already shown, HBV-sequence specific siRNAs acted on cytosolic HBV RNAs in HBV replicating hepatocytes *in vitro* and *in vivo*. For that, RNAi inducing 3p-1.2 and si-1.2 had to reach the hepatocytes. Within the *in vitro* systems efficient targeting was given by direct transfection. In the *in vivo* system, in contrast, the RNA-oligonucleotides were injected into the tail vein of HBV tg mice and had to reach the hepatocytes via bloodstream transport. In order to protect them from degradation and enhance efficient liver targeting, all RNA-oligonucleotides were complexed prior to injection with “in-vivo-jetPEI”, a reagent that protects and delivers nucleic acids to various tissues via the intravenous route, also to the liver. Nevertheless, *in vivo* experiments indicated a lower impact on HBV replication by non-phosphorylated si-1.2, indicating an insufficient delivery into hepatocytes.

2.6.1 Targeting specificity of applied RNA-oligonucleotides

To determine the delivery efficiency of RNA-oligonucleotides into the liver and to specify other targeted organs, HBV tg mice were injected intravenously with complexed si-1.2 or 3p-1.2, respectively. After isolation of liver, spleen, kidney, heart and gastric lymphatic glands 6 hours after injection, IFN- β expression was determined on mRNA levels in respective organs by qRT-PCR (**Fig. 2.23**). Interestingly, mice treated with unphosphated si-1.2 showed a strong IFN- β induction in isolated lymph nodes and in the spleen. No or minor IFN- β expression was detectable in the liver, kidney and heart, respectively, after application of si-1.2. Accordingly, 3p-1.2 injected mice revealed a potent IFN- β expression in gastric lymphatic glands and at reduced levels also in the spleen. No IFN- β induction was observed neither in the kidney nor in the heart or in the liver.

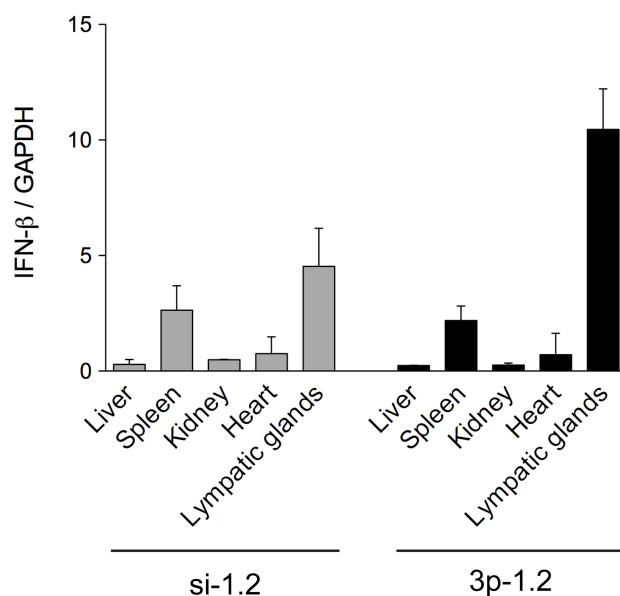


Fig. 2.23: IFN- β expression in different organs of si-1.2 and 3p-1.2 treated HBV tg mice. HBV tg mice were injected intravenously with jetPei complexed si-1.2 and 3p-1.2, respectively. 6 hours after injection IFN- β expression was determined in different isolated organs on mRNA level by qRT-PCR relative to GAPDH, normalized to IFN- β values in the liver of mice treated with si-1.2. Results are shown as mean \pm SD, n=2.

The results demonstrate that both complexed si-1.2 and 3p-1.2 were predominantly delivered into gastric lymph nodes and into the spleen after systemic administration, where they efficiently induced IFN- β , likely via TLR3 or RIG-I stimulation. No or only minor amount of injected RNA-oligonucleotides ended up in the liver.

To confirm and visualize these results, mice were injected intravenously with jetPEI complexed si-1.2, which was fluorescently labeled at the 5'-end of the plus-strand with Alexa 488 via a biotin residue. Liver, spleen, kidney and lung were isolated 6 hours after injection, thin sections of isolated organs were prepared and Alexa 488 localized by fluorescence microscopy (**Fig. 2.24**). Comparing the examined organs, only a small amount of applied fluorescently labeled si-1.2 localized to the liver, but at least partially in double-nucleated hepatocytes (solid white arrows). Most of it, however, accumulated and clotted in undefined areas of the liver (dashed white arrows), likely in LSECs or Kupffer cells. Most of the intravenously applied siRNA ended up in the spleen. Rare single fluorescence signals could also be detected in the kidney and in the lung.

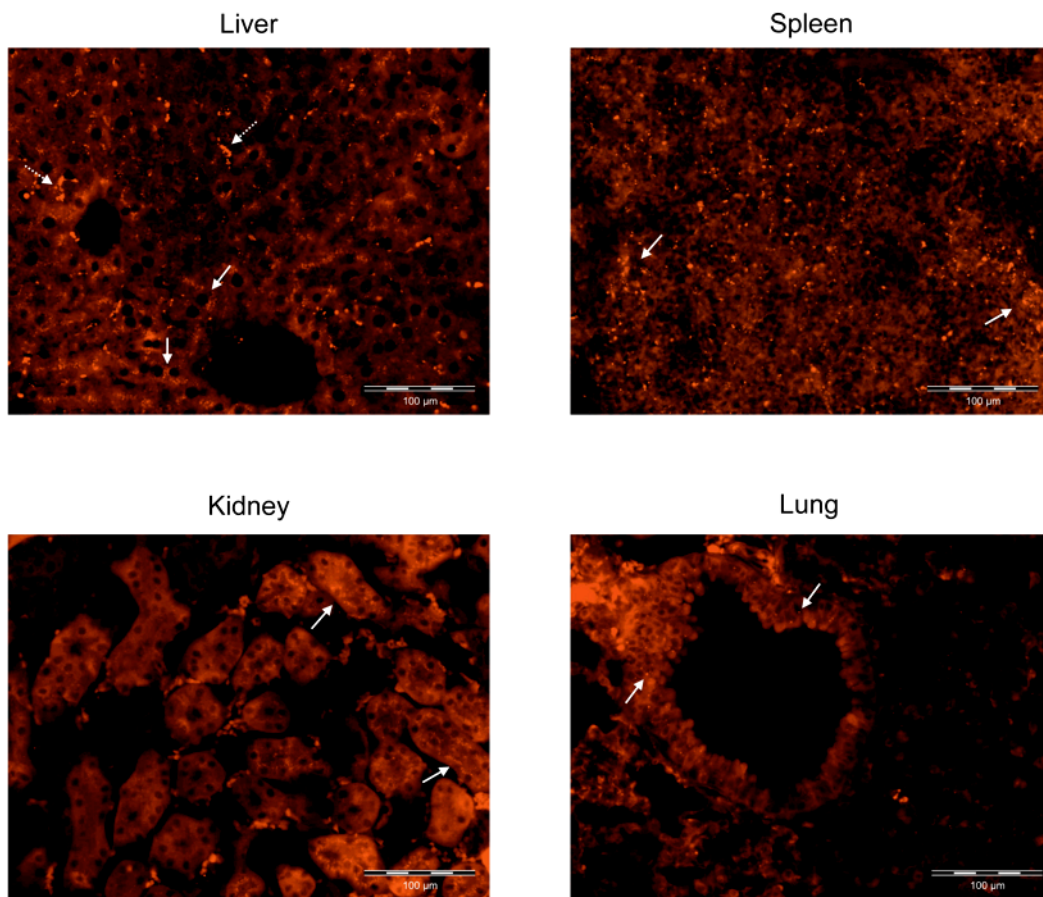


Fig. 2.24: Targeting efficiency of fluorescently labeled and complexed si-1.2 to different organs. Mice were injected intravenously with fluorescently labeled (Alexa 633) si-1.2., previously complexed with jetPEI. Organs were analyzed for siRNA distribution 6 hours p. inj., indicated by white arrows. Solid arrows point to siRNA distribution in hepatocytes, dashed arrows to aggregates in undefined structures, likely Kupffer cells or LSECs. Results are representative for n=2 / group.

The results validated that most of the complexed and intravenously injected RNA-oligonucleotides predominantly ended up in the spleen and only a low amount reached the liver.

2.6.2 Liver-specific targeting of RNA-oligonucleotides

Targeting and delivery of siRNAs into specific cell types is a major problem in RNAi treatment. To improve the RNAi-based effect of 3p-siRNA mediated combinatorial therapy of HBV, the hepatocellular uptake of siRNA had to be improved. Several possibilities for enhanced liver specific delivery were considered. A promising approach included the application of the siRNA by an alternative injection technique. The hydrodynamic injection (HDI) technique was already used to efficiently deliver nucleic acids to the liver (Klein, 2003 #668; Giladi, 2003 #1753; Morrissey, 2005 #764; Huang, 2006 #1781}. By hydrodynamic injection the siRNA is rapidly injected in a large volume under high pressure intravenously into the tail vein of the mice. To compare the efficiency of RNA-oligonucleotide delivery by classical intravenous injection and hydrodynamic injection, mice were injected by both injection techniques with naked (not complexed with jetPEI) si-1.2, which was previously fluorescently labeled at the 5'-end of the plus-strand with Alexa 488. Liver, spleen, kidney were isolated 6 hours after injection and siRNA-coupled Alexa 488 was localized in different organs by fluorescence microscopy (**Fig. 2.25**). Fluorescently labeled siRNA applied by classical intravenous injection predominantly accumulated in the spleen. A small amount of applied si-RNA reached the liver, but was primarily localized outside of the hepatocytes. Additionally, injected siRNA was detectable to a minor extent in the kidney of the mice. (**Fig. 2.25 a**). In contrast, hydrodynamic injection led to an increased targeting of the siRNA to hepatocytes, especially to hepatocytes located in an area near sinusoidal blood vessels. Less siRNA was delivered to the spleen and only minor amounts to the kidney (**Fig. 2.25 b**).

The results indicate an enhanced delivery of naked siRNA to the liver and especially into hepatocytes by hydrodynamic injection in comparison to classical intravenous injection. Nevertheless, the structure and vitality of the liver seemed to be negatively affected by hydrodynamic injection.

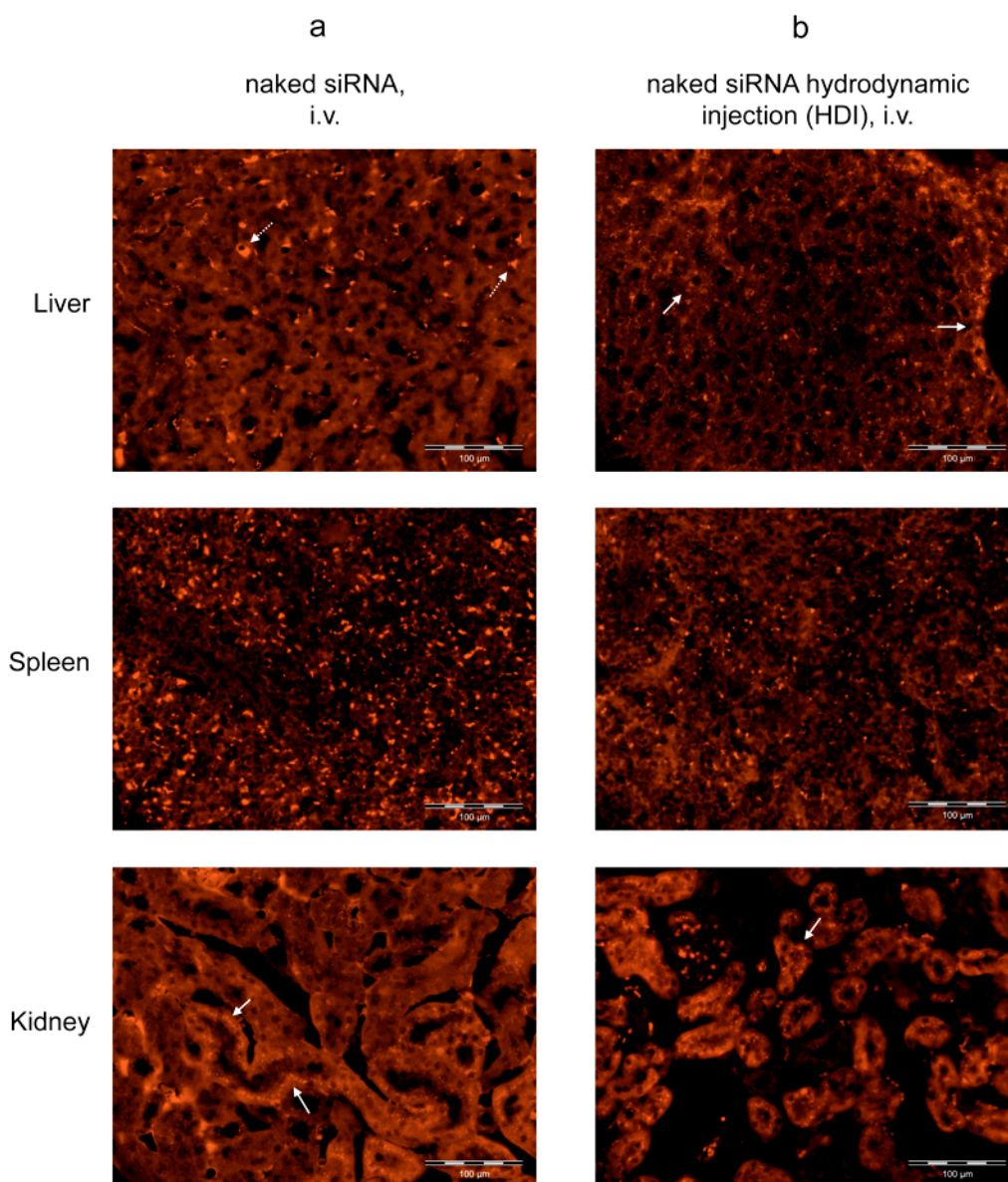


Fig. 2.25: Targeting efficiency of fluorescently labeled naked siRNA to different organs by intravenous injection and hydrodynamic injection. Mice were treated with naked (uncomplexed) fluorescently labeled (Alexa 633) si-1.2. by **a**) classical intravenous injection or **b**) hydrodynamic injection (HDI). Organs were analyzed for siRNA distribution 6 hours p. inj.. Results are representative for n=2 / group.

An alternative method to enhance the delivery efficiency of the nucleic acid to the liver is the linkage of a targeting ligand to the siRNA. Bioconjugation of the siRNA to cholesterol at the 3'-end of the plus strand via a cleavable linker (TEG, triethylene glycol) was already shown to significantly increase targeting efficiency of the modified siRNA to human liver cells (Soutschek, Akinc et al. 2004). Therefore, HBV-specific si-1.2 was coupled at the 3'-end of the plus-strand with cholesterol and labeled fluorescently at the 5'-end of the plus-strand with Alexa 488. To investigate the liver targeting of modified cholesterol-linked siRNA and additionally compare different delivery strategies, cholesterol-conjugated si-1.2 was injected by different methods and localized by fluorescent microscopy 6 hours after application (**Fig. 22.6**). First, modified siRNA was complexed before application with jetPEI and then classically injected intravenously (**Fig. 22.6 a**). Second, naked (not complexed with jetPEI) modified si-1.2 was classically injected intravenously (**Fig. 22.6 b**) and third, naked modified si-1.2 was injected by hydrodynamic injection (**Fig. 22.6 c**). All three applications led to a comparable accumulation of siRNA in the spleen, but no or only minor residues of siRNA were detected in the kidneys. Mice classically intravenously injected with complexed modified siRNA revealed an increased amount of siRNA in the liver compared to mice treated with jetPEI complexed but unmodified siRNA (**Fig. 2.24**), although a high amount accumulated outside of hepatocytes (**Fig. 22.6 a**). In contrast, naked modified siRNA, classically injected intravenously, was also efficiently delivered into the liver, but additively localized in hepatocytes (**Fig. 22.6 b**). Only little amount of naked modified siRNA injected by hydrodynamic injection ended up in the liver (**Fig. 22.6 c**).

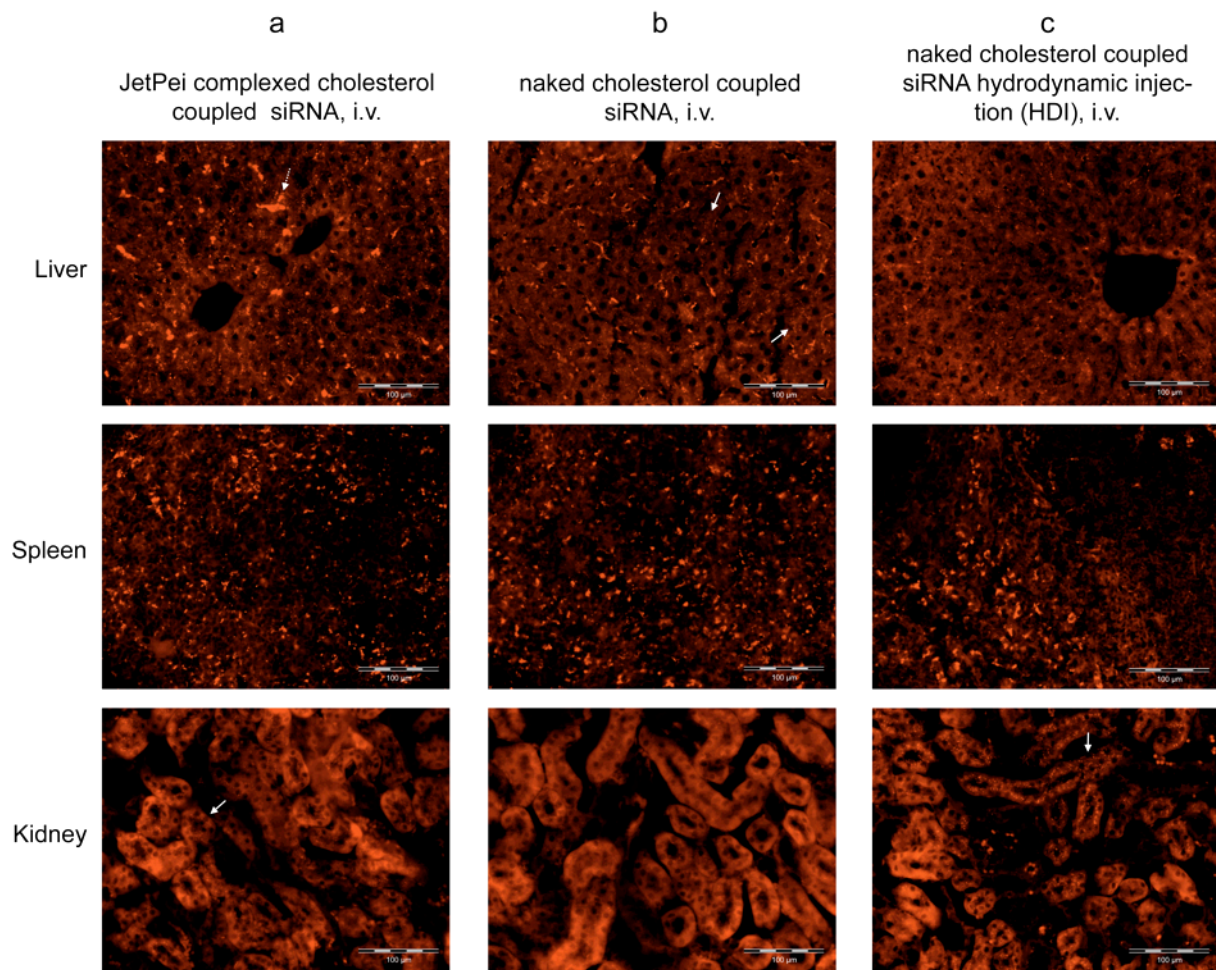


Fig. 2.26: Targeting efficiency of cholesterol coupled siRNA to different organs using different forms of applications. HBV tg mice were treated with cholesterol-coupled and fluorescently labeled (Alexa 633) si-1.2. by **a**) classical intravenous injection, previously complexed with JetPei **b**) classical intravenous injection, uncomplexed (naked) or **c**) hydrodynamic injection (HDI), uncomplexed (naked). Organs were analyzed for siRNA distribution 6 hours p. inj.. Results are representative for n=2 / group.

The results indicate that naked cholesterol-coupled siRNA, injected by classical intravenous application, efficiently reaches the liver including hepatocytes. In comparison of all investigated applications, cholesterol coupling to 5`-triphosphate RNA may represent a powerful targeting-tool. Nevertheless, the preferred method for liver directed targeting, although not optimal, was the classical intravenous injection of jetPEI-complexed nucleic acids during this study.

2.6.3 IFN- β induction by 3p-siRNA in different liver cell populations

As already stated, the liver consists beside hepatocytes also of non-parenchymal cells, such as liver sinusoidal endothelial cells (LSECs) and Kupffer cells. The previous described delivery studies revealed that injected nucleic acids partially reached the liver, but only to some extent the hepatocytes. A certain proportion apparently ended up in other liver cells, likely LSECs or Kupffer cells. To elucidate whether 3p-siRNA potentially induced an IFN-I response also in these non-parenchymal cell types, LSECs and Kupffer cells were isolated beside PHHs from fresh human liver specimen and treated with both, 3p-siRNA and si-1.2, respectively, poly(I:C) was used as positive control, si-Ctrl as negative control (**Fig. 22.7**). To mimic a potential uptake like in the *in vivo* situation, RNA-oligonucleotides were complexed with “in vivo-jetPEI” and added into the supernatant of the PHHs (**Fig. 22.7 a**), LSECs (**Fig. 22.7 b**) and Kupffer cells (**Fig. 22.7 c**), respectively. Potent IFN- β induction was shown 6 hours after application on mRNA levels by qRT-PCR in all cell types.

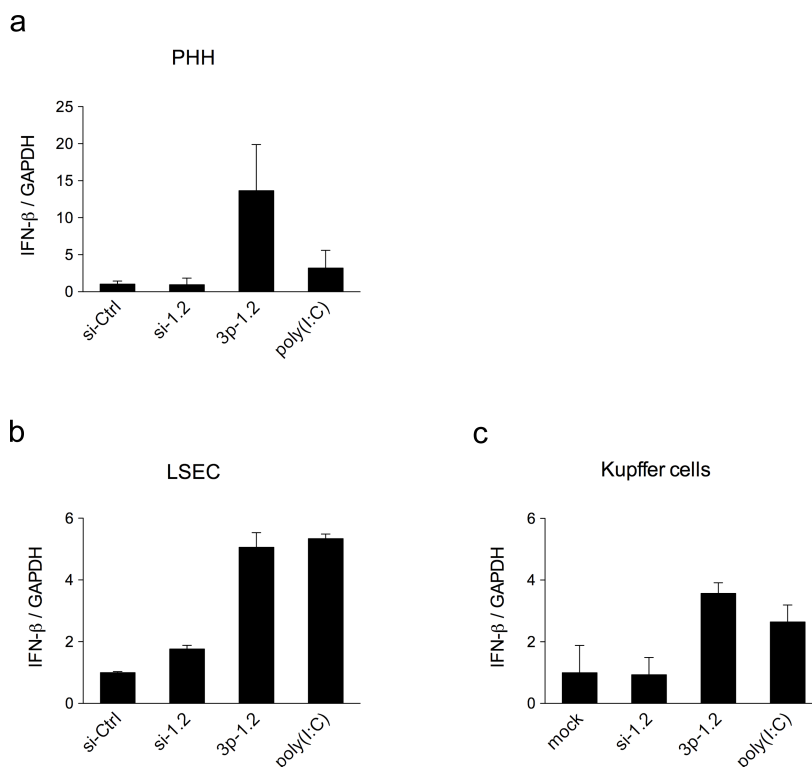


Fig. 2.27: IFN- β induction in different liver cell populations after uptake of complexed 3p-siRNA. Indicated RNA-oligonucleotides were complexed with JetPei and added to the supernatant of purified

liver cell populations. IFN- β expression was determined in **a**) Primary human hepatocytes (PHHs) **b**) liver sinusoidal endothelial cells and **c**) Kupffer cells by quantitative RT-PCR analysis 20 hours after treatment, relative to GAPDH, normalized to si-Ctrl (HCV-sequence specific siRNA) treated cells. Data represent mean values \pm SD, n=3.

2.7 Initiation of an adaptive immune response against HBV

2.7.1 3p-siRNA induced expression of proinflammatory cytokine in liver cells

It is known that poly(I:C) stimulation of TLR3 leads to a potent expression of proinflammatory cytokines like IL-6 in murine non-parenchymal liver cells, in LSECs and Kupffer cells (Wu, Lu et al. 2007). Accordingly, it was shown that stimulation of RIG-I induces the transcription of proinflammatory cytokines like IL-1, IL-6 and TNF- α via the canonical IKK pathway (Dinarello 2000). Secretion of proinflammatory cytokines like IL-6 and TNF- α lead to the recruitment of natural killer cells, natural killer T cells and T-cells. Accordingly, clearance of HBV is typically associated with multispecific CD4+ and CD8+ T cell response (Rehermann 2003).

Therefore, LSECs and Kupffer cells were stimulated with both, 3p-1.2 and si-1.2, poly(I:C) was used as positive control, si-Ctrl RNA as negative control. Based on the results of the previous experiment, RNA-oligonucleotides were complexed and applied by addition into the supernatant. Cells were tested 6 hours after application for secretion of IL-6 and TNF- α into the supernatant by ELISA assay.

Isolated LSECs and Kupffer cells showed a strong basal expression level of IL-6 (dotted red line). Nevertheless, application of 3p-1.2 and poly(I:C), respectively, led to significant additive induction of IL-6 in LSECs. In contrast, Kupffer cells revealed a lower basic induction of IL-6 and only application of 3p-1.2 induced a significant additive IL-6 expression (**Fig. 2.28 a**). Additionally, LSECs and Kupffer cells showed significant induction of TNF- α following 3p-1.2 stimulation (**Fig. 2.28 b**).

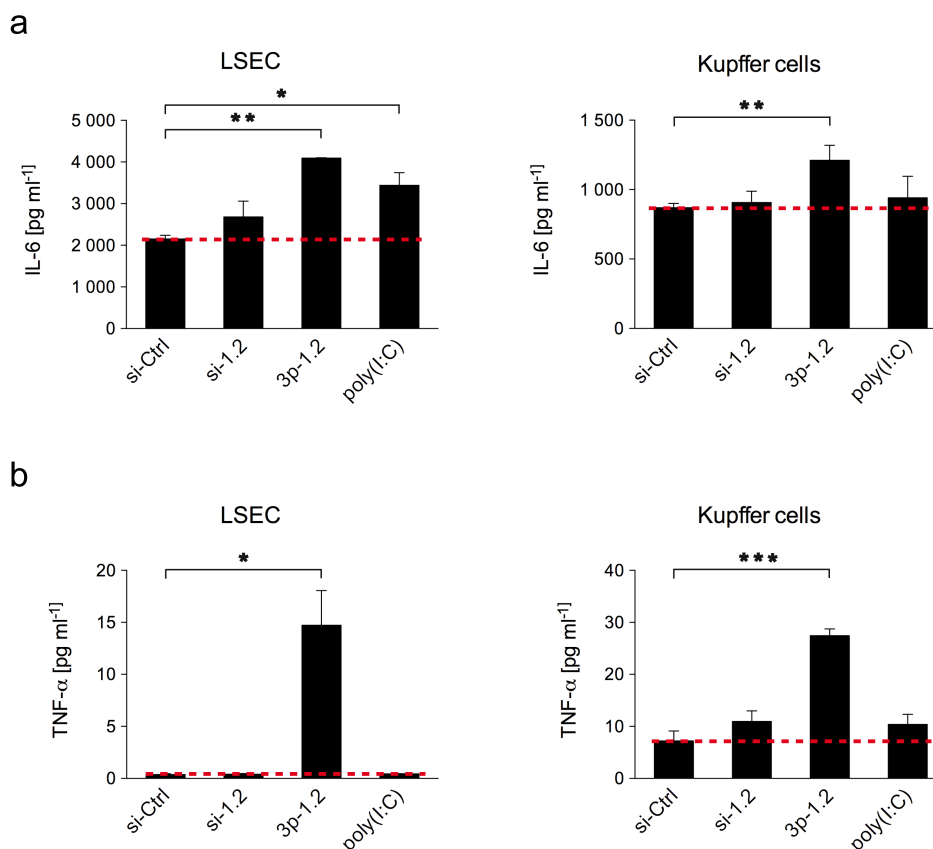


Fig. 2.28: IL-6 and TNF- α induction in purified liver cell populations after uptake of complexed 3p-siRNA. Indicated RNA-oligonucleotides were complexed with JetPei and added to the supernatant of purified liver cell populations. Liver sinusoidal endothelial cells, LSECs (**left panels**) and Kupffer cells (**right panels**) were analyzed for **a**) IL-6 and **b**) TNF- α expression by ELISA 6 hours after treatment. Basic induction indicated by dotted red line. Data represent mean values \pm SD, n=3.

The results indicate that uptake of 3p-1.2 by liver sinusoidal endothelial cells (LSECs) and Kupffer cells induced potent expression of proinflammatory cytokines such as IL-6 and TNF- α .

2.7.2 Induction of an adaptive immune response against HBV after RNA-oligonucleotide stimulation *in vivo*

It was shown that application of immune-stimulatory RNA-oligonucleotides led to a potent stimulation of an antiviral acting innate immune response against HBV. Furthermore it was presumed, due to the previous experiment, that application of 3p-

siRNA additionally led to the expression of proinflammatory cytokines and potentially could be followed by the induction of an HBV antigen specific adaptive immune response after several days. Therefore it was investigated *in vivo*, whether the mice previously treated with immune-stimulatory and antivirally active RNA-oligonucleotides revealed any induction of an adaptive immune response (**Fig. 2.29**). Accordingly, mice treated with 3p-RNA, 3p-1.2, si-1.2 and si-Ctrl as negative control, respectively, were analyzed for liver damage by determining serum alanine aminotransferase (ALT) levels at day 0, 4, 9 and 15 after injection (**Fig. 2.29 a**). In fact, nearly all treated mice showed significantly elevated ALT levels at day 9 after injection, irrelevant of the RNA-oligonucleotide, in comparison to normal ALT values at day 4. The ALT levels decreased back to normal ranges at day 15 in almost all treated mice.

Additionally, the livers of mice were analyzed at day 9 and 15 after injection for expression of CD8 (**Fig. 2.29 b**) and IFN- γ (**Fig. 2.29 c**) on mRNA level by qRT-PCR. CD8 is a surface marker of predominately cytotoxic T cells lymphocytes (CTLs). IFN- γ is a cytokine produced predominately by CD8⁺ CTLs during antigen specific adaptive immune response. The analysis revealed slightly increased overall CD8 expression in treated mice at day 9 in comparison to day 15. In particular 3p-RNA and 3p-1.2 treated mice, respectively, showed an increase in CD8 expression, indicating CD8⁺ T cell infiltration. Furthermore, overall IFN- γ expression was slightly increased at day 9 in comparison to day 15, in turn particularly in 3p-RNA and 3p-1.2 injected mice.

The results indicate induction of an HBV antigen specific adaptive immune response at day 9 after application of both, 3p-RNA and 3p-1.2, but need to be confirmed by specific T cell assays like intracellular IFN- γ staining after e.g. peptide stimulation.

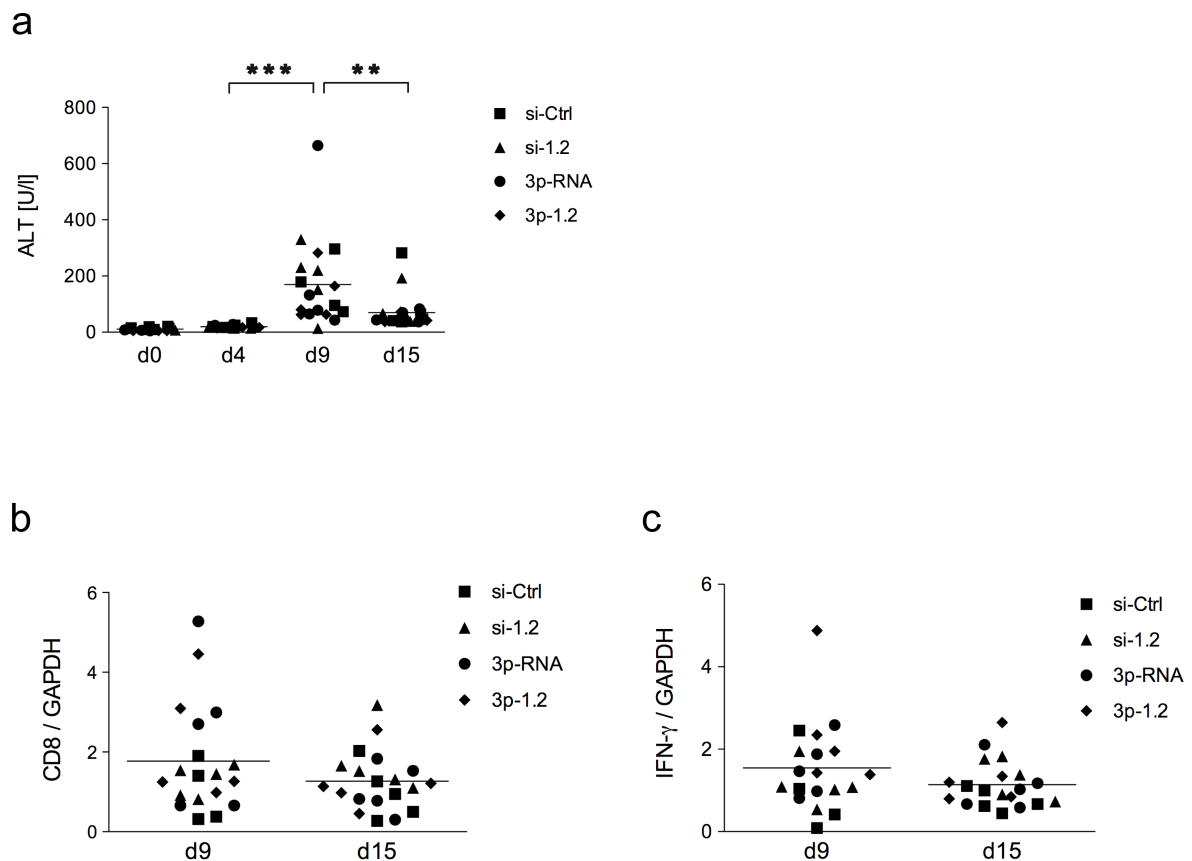


Fig. 2.29: Induction of an adaptive immune response in HBV tg mice. HBV tg mice were injected twice (day 0 and day 3) with indicate RNA-oligonucleotides. **a**) Alanine aminotransferase (ALT) levels in serum of mice at day 4, day 9 and day 15 after treatment. **b**) Quantitative RT-PCR analysis of CD8 expression and **c**) IFN- γ expression in liver of mice at day 9 and day 15 after treatment with different RNA-oligonucleotides relative to GAPDH. Data represent mean values \pm SD, n=5 (**P<0.01, t-test).

To support these results of an inflammatory immune response, the Pathology of Helmholtz Zentrum München performed histological analyses of the liver tissues of treated HBV tg mice at day 9 and day 15 after injection, respectively (**Fig. 2.30**). Histopathological alterations were classified in changes affecting the portal tracts, including liver arteries, -veins and -bile duct (e.g. inflammation, degenerative changes of the bile ducts, fibrosis), changes affecting the lobule, which are clear anatomical divisions or extensions (e.g. spotty and bridging necrosis, degenerative changes of the hepatocytes, fibrosis) and changes affecting the vessels (e.g. inflammation, fibrosis, thrombosis). Furthermore, alterations were graded as mild, moderate and severe, depending on their frequency and severity.

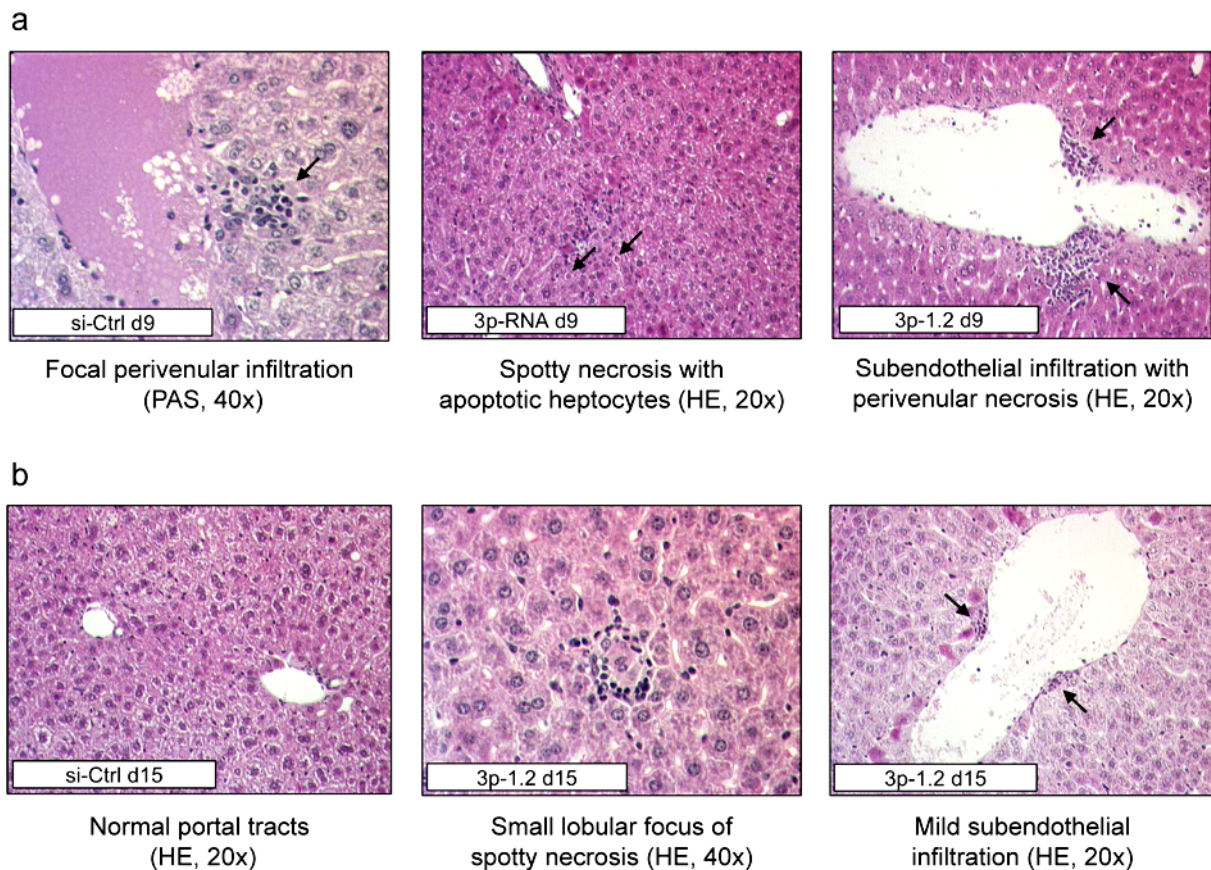


Fig. 2.30: Liver staining (HE and PAS) of RNA-oligonucleotide treated HBV tg mice. HBV tg mice were injected with indicated RNA-oligonucleotides. Liver tissue was analyzed by HE and PAS staining for alterations along with an adaptive immune response at **a**) day 9 and **b**) day 15 after treatment. One representative out of $n=5$ mice per group is shown, 2 mice per group were analyzed.

The histological analysis revealed clear symptoms of an inflammatory reaction in the liver of si-1.2, 3p-RNA and 3p-siRNA treated mice, respectively, at day 9 after injection. Foci of spotty necrosis with apoptotic hepatocytes were found in almost all cases of treated animals, except for si-Ctrl (**Fig. 2.30 a, middle and right**). Moreover, infiltration of immune cells resulting in a mild to moderate subendothelial inflammation (endothelitis) of the central and portal veins (**Fig. 2.30 a, left and right**), sometimes associated with perivenular necrosis of hepatocytes (**Fig. 2.30 a, middle**) was found only in treated animals.

Furthermore, in comparison to modest liver tissue with normal portal tracts of si-Ctrl treated animals at day 15 (**Fig. 2.30 b, left**), only small foci of spotty necrosis (**Fig. 2.20 b, middle**) and mild subendothelial infiltration of portal veins (**Fig. 2.20 b,**

middle) were found in treated animals at this timepoint. Therefore, we concluded that inflammatory changes had ceased at day 15.

The results indicate, in correlation with previous serological results (ALT values), an inflammatory reaction in the liver of si-1.2, 3p-RNA and 3p-siRNA treated animals, respectively, at day 9 after treatment and its resolution towards day 15.

3 Discussion

About two billion people worldwide (~ 30%) have been infected with HBV and about 360 million (5 - 7%) live with a chronic state of infection. Estimated 700 000 persons die each year due to the acute or chronic consequences of hepatitis B (WHO, 2008). Approved therapies of chronic hepatitis B include antiviral active IFN- α and inhibitors of viral reverse transcription. Their use leads to suppression of viral replication, but with partially limited effectiveness concerning sustained antiviral effects or even elimination of the virus. Indeed, following treatment termination, persistent cccDNA is able to initiate a new HBV replication cycle (Protzer and Schaller 2000), even after serological clearance of viral infection (Werle-Lapostolle, Bowden et al. 2004). Therefore, a lifelong therapy, accompanied by appearance of severe cytotoxic side effects and drug-resistant HBV mutants, is indispensable in most cases. This rather limited clinical success demonstrates the necessity for the development of new therapies, focused on the effective and long-lasting suppression of HBV replication, associated with enhanced physiological compatibility. Combinatorial strategies targeting simultaneously multiple steps of HBV replication represent a promising tool for the treatment of chronic hepatitis B. In this project we developed a novel immunotherapeutic approach, combining endogenous IFN-I induced antiviral activity against HBV by stimulation of the cytosolic helicase RIG-I with HBV sequence specific gene silencing by RNAi in one single molecule.

The therapeutic aspects of (1) IFN-I induction by RIG-I stimulation in (2) combination with siRNA mediated gene silencing targeting HBV replication, as well as (3) options for efficient delivery of the designed molecule *in vivo* and (4) simultaneous initiation of an HBV-specific immune response will be consecutively discussed below.

3.1 RIG-I dependent induction of IFN-I and interferon stimulated genes by 3p-RNA suppressed HBV replication *in vitro* and *in vivo*

3.1.1 3p-RNA induced IFN-I suppresses HBV replication

Hornung et al. showed in a series of elegant studies that *in vitro* transcribed 5'-triphosphated-dsRNA (3p-RNA) strongly induces endogenous IFN-I by stimulation of RIG-I (Hornung, Ellegast et al. 2006). We intended to use 3p-RNA to initiate an endogenous antivirally active IFN-I response by stimulation of RIG-I to potentially suppress HBV replication in this study.

To test the therapeutic potential of 3p-RNA against HBV in this project, we revealed the antiviral effects of transfected 3p-RNA on HBV replication in stably HBV expressing HepG2 H1.3 cells and in HBV infected PHHs. Both cell types showed a potent reduction of HBV-DNA levels after transfection with 3p-RNA, but not after treatment with control RNA. Additionally, HBeAg, HBsAg and HBV pgRNA levels were significantly diminished compared to untreated cells, indicating an antiviral activity at the level of transcription and posttranscriptionally. In addition, we examined the antiviral effect of 3p-RNA *in vivo*. HBV tg mice revealed a significant decrease of HBV-DNA levels in the blood. Furthermore, HBV antigen and intrahepatic pregenomic RNA levels were drastically reduced. These results suggest that selective engagement of RIG-I by 3p-RNA displays pronounced antiviral activity *in vitro* and *in vivo*.

RIG-I, broadly expressed in almost every cell type (Melchjorsen, Jensen et al. 2005) was proposed to detect long dsRNA (Yoneyama, Kikuchi et al. 2004) and additionally identified as a cellular key sensor of negative-strand RNA viruses (Plumet, Herschke et al. 2007; Habjan, Andersson et al. 2008; Takeuchi and Akira 2008). Furthermore, it has been demonstrated that RIG-I is essential for the production of antiviral interferons in response to RNA viruses that express a phosphorylated RNA genome (Kato, Takeuchi et al. 2006). Moreover, the presence of a triphosphate group at the 5'-end of both, ssRNA and dsRNA is an important molecular feature that is recognized by RIG-I (Kim, Longo et al. 2004; Hornung, Ellegast et al. 2006; Pichlmair, Schulz et al. 2006; Cui, Eisenacher et al. 2008; Saito, Owen et al. 2008; Takahasi, Yoneyama et al. 2008). In contrast, recent work by Kato et al. suggests

that long dsRNA of vesicular stomatitis virus (> 300 bp) can substitute for the presence of a 5'-triphosphate group (Kato, Takeuchi et al. 2008). In summary, stimulation of antivirally active IFN-I can be induced by different RNA-oligonucleotides serving as RIG-I ligands, the exact structure of the RNA remains controversial (Schlee, Hartmann et al. 2009). The antiviral effect of IFN-I on HBV replication was described extensively *in vitro* and *in vivo* (Guidotti and Chisari 1999; Rang, Gunther et al. 1999; Schultz, Summers et al. 1999; McClary, Koch et al. 2000; Wieland, Guidotti et al. 2000; Pasquetto, Wieland et al. 2002) and led to approved application of exogenous IFN- α in clinical treatment of chronic HBV infection, although still inducing severe side effects.

In search for appropriate HBV model systems we analyzed several hepatoma derived cell lines as well as isolated PHHs (Schulze-Bergkamen, Untergasser et al. 2003) for expression of RIG-I. Previous stimulation of cells with IFN-I is known to increase the expression of RIG-I (Bowie and Unterholzner 2008). We detected expression of endogenous RIG-I protein in all analyzed liver cells, which could be drastically enhanced by addition of exogenous IFN-I. It remains to be elucidated whether the expression of RIG-I can also be increased by induction of endogenous IFN-I after transfection of 3p-RNA. However, neither HuH7 cells (Nakabayashi, Taketa et al. 1982) nor its subline HuH7.5 (Blight, McKeating et al. 2002) revealed any induction of IFN- β by 3p-RNA or poly(I:C), respectively. Consistently, it has been published that Huh7 cells failed to produce IFN-I via TLR3 or RIG-I signaling pathway, explained by insufficient TLR3 expression and by an undefined defect on RIG-I receptor level, respectively (Li, Chen et al. 2005; Preiss, Thompson et al. 2008). This holds also true for HuH7.5 cells, which are highly permissive for replication of HCV RNA replicons (Blight, McKeating et al. 2002), but are also devoid of proper IFN-induction in absence of TLR3 and due to a point mutation of RIG-I within its CARD-like domain (Sumpter, Loo et al. 2005). In contrast, HepG2 cells (Hirayama, Kohgo et al. 1993) are known to be competent for IFN-I signaling via RIG-I stimulation (Preiss, Thompson et al. 2008). Moreover, the use of a stably HBV expressing cell line for *in vitro* investigations was preferred, therefore HepG2 H1.3 cells (Jost, Turelli et al. 2007; Protzer, Seyfried et al. 2007) were chosen. This cell line additionally establishes, in contrast to HepG2 2.15 cells, episomal cccDNA, helpful as an accessory replication marker and hardly to affect by antiviral therapy. PHHs were selected as an *in vitro* HBV infection model, which also express cccDNA

during HBV replication. In addition, as an *in vivo* model system, we decided to use HBV1.3 –xfs transgenic (tg) mice carrying a genotype D HBV1.3 overlength genome, with a frameshift mutation (GC) in the x-gene at position 2916/2917 (Weber, Schlemmer et al. 2002). The virus replicating in HBV1.3 –xfs mice is non-infectious *in vivo* as suggested by studies using X-mutated woodchuck HBV (WHV) in woodchucks (Chen, Kaneko et al. 1993).

A dual-luciferase assay performed in RIG-I expressing HEK 293 cells (Aiello, Guilfoyle et al. 1979) revealed clear differences in the potency to induce IFN-I via RIG-I stimulation of different 3p-RNAs derived from separate *in vitro* transcriptions. These observations could be explained as a consequence of inefficient triphosphorylation during reverse transcription by T7 RNA polymerase within diverse preparations. Another important conclusion that can be drawn from several publications is that induction of IFN-I by RIG-I stimulation strongly depends on the structure and sequence of the 3p-RNA. Interestingly, short-hairpin 3p-RNAs synthesized by T7 RNA polymerase do not induce IFN-I (Gondai, Yamaguchi et al. 2008). The 3p-RNA used in this study includes a GU-rich dsRNA sequence with an overhang of one G-nucleotide at the 5`-position of both strands and was already shown to strongly induce IFN-I (Hornung, Ellegast et al. 2006). The *guanine*-base overhang increased transcription efficiency, whereas presence of the pyrimidine base *uracil* within the dsRNA sequence was shown to be essential for double-strand formation during *in vitro* transcription by T7 RNA polymerase (Schlee, Roth et al. 2009). Controversially, it was recently suggested that fully synthetic 5`-triphosphate short blunt-end dsRNA structure without an overhang, as contained in the panhandle of negative-strand RNA genomes, confers full RIG-I ligand activity (Schlee, Roth et al. 2009). However, it remains to be elucidated whether 5`-triphosphate short blunt-end dsRNA without an overhang of one G-nucleotide at the 5`-postion on both strands would increase IFN-I induction by stimulation of RIG-I in our models.

3p-RNA has been shown to selectively induce apoptosis in melanoma cell lines by an IFN-independent antiviral signaling pathway (Poeck, Besch et al. 2008; Besch, Poeck et al. 2009). To exclude toxic effects of 3p-RNA in our cellular system, HepG2 H1.3 cells were transfected with different concentrations of 3p-RNA. Tolerance of treated cells for the 3p-RNA concentration used throughout the study (0.5 µg / ml) was confirmed by a cell viability assay determining active metabolism in mitochondria. The formed dye was quantitated in a spectrophotometer, absorbance directly

correlated with number of living cells. Vitality levels above 100% can be explained due to determination by means of linear regression analysis. Identical concentrations of Ctrl-RNA were used throughout the *in vitro* studies. Synthetic dsRNA poly(I:C), used as positive control, was transfected in lower concentrations (0.05 $\mu\text{g} / \text{ml}$), due to its known toxicity in high concentrations. Neither Ctrl-RNA, nor poly(I:C) showed any obvious cytotoxicity at applied concentrations *in vitro*, but has to be further investigated by cell viability analysis or determination of alanine aminotransferase (ALT) levels that is predominately secreted by damaged liver cells in detail.

In addition, toxicity of RNA-oligonucleotides *in vivo*, complexed with the cationic polymer polyethylenimine (PEI) before systemic distribution by intravenous injection, was examined by monitoring serum ALT levels. HBV tg mice exhibited unchanged ALT levels 6 hours after both applications of 3p-RNA (25 μg per mouse and injection, respectively), and also at day 6, comparable to mock treated mice, which demonstrated the safety of the therapy *in vivo*. Surprisingly, several mice treated with Ctrl-RNA revealed significantly elevated ALT levels. This apparent discrepancy could be explained by a possible contamination of the synthetic Ctrl-RNA by bacterial components, such as LPS, which might have elicited an inflammatory response by TLR or by complement activation in some of the animals (Zhong, Deaciuc et al. 2006; Zhang, Kimura et al. 2007).

After exclusion of cytotoxic side effects, we analyzed the potency of 3p-RNA to stimulate IFN-I expression. We found that 3p-RNA induced a potent IFN-I response *in vitro* and *in vivo*. The IFN- β response in HepG2 H1.3 cells even remained detectable until day 6 after transfection, whereas it was significantly reduced in PHHs at this timepoint. Remarkably, IFN-I expression levels in PHHs at day 1 after application were comparable with those of HepG2 H1.3 cells at day 3. This result indicated that initial IFN-I induction by 3p-RNA was significantly higher in HepG2 H1.3 cells than in PHHs, possibly as a result of reduced transfection efficiency of hardly transfectable PHHs. Since TLR3 expression is known to be diminished in HepG2 cells (Preiss, Thompson et al. 2008), its likely that the strong IFN-I induction in poly(I:C) treated HepG2 H1.3 cells appeared by stimulation of cytosolic helicase MDA-5 (Alexopoulou, Holt et al. 2001; Gitlin, Barchet et al. 2006; Kato, Takeuchi et al. 2006). However, the TLR expression pattern of PHHs is not well known and is currently characterized in our laboratory.

To obtain immunostimulatory activity of 3p-RNA *in vivo*, HBV tg mice were injected twice (day 0 and day 3), related to the experiences of our collaborators Poeck and colleagues, who observed comparable IFN-I induction after both applications, each peaking 6 hours (unpublished data). Accordingly, we detected high serum IFN- α levels 6 hours after the first injection of 3p-RNA. Interestingly, the expression of IFN- α was already markedly reduced 6 hours after the second injection at day 3 and not detectable at day 6 in an ELISA assay.

Consistent with our data, 2'-5'-oligoadenylate synthetase (OAS), which is known to be activated by IFN via dsRNA stimulation (Hovanessian and Justesen 2007; Silverman 2007), was induced by 3p-RNA application in our *in vitro* models. In the murine system studied here, only remaining levels of intrahepatic 2'-5'-OAS were detectable on mRNA level at day 6 after injection, which was unexpected considering the stunning induction of IFN- α detected in the serum of 3p-RNA treated mice 6 hours after application in comparison to mock treated mice. Reflecting this apparent discrepancy, and taking into account that the majority of 3p-RNA was taken up by non-hepatocytes, it appears more likely that IFN- α expression is also initiated by accessory cells targeted by 3p-RNA after systemic distribution. This was further investigated and results revealed that also non-parenchymal cells, such as LSECs and Kupffer cells are capable to strongly induce IFN-I.

After having confirmed IFN-I and 2'-5'-OAS induction in our HBV models, no further analysis of IFN-induced ISGs were performed in this study. Many studies aimed at defining how interferons act on HBV. Analyzing the different steps of the HBV replication cycle it became obvious, that mainly posttranscriptional steps were affected (Klocker, Schultz et al. 2000; Robek, Boyd et al. 2004), but at higher doses also transcription was controlled. Guidotti et al. showed that RNase L, an enzyme induced by 2'-5'-OAS, which is able to degrade viral RNA and cellular RNAs (Floyd-Smith, Slattery et al. 1981), does not affect HBV replication *in vivo*, demonstrated in RNase L^{-/-} knockout mice (Guidotti, Morris et al. 2002). The group showed in a similar study that the IFN induced dsRNA-dependent protein kinase (PKR) could mediate the antiviral activity against HBV (Guidotti, Morris et al. 2002). Furthermore, IFN-I upregulates the expression of GTPases Mx (Martens and Howard 2006; Haller, Staeheli et al. 2007). In addition, it was suggested that the human GTPase MxA (myxovirus resistance protein A) exhibits antiviral activity and inhibits HBV replication at posttranscriptional level in HuH7 and HepG2 cells (Melen, Keskinen et al. 2000;

Gordien, Rosmorduc et al. 2001). Furthermore, Wieland et al. revealed that gene expression of the murine GTPases IIGP is strongly upregulated by IFN stimulation and is tightly associated with inhibition of HBV replication (Wieland, Vega et al. 2003). Moreover, IFN-I induced proteins of the APOBEC3 family, which are cellular cytidine deaminases, were assumed to be involved in antiviral inhibition of HBV replication in hepatoma cell lines (Rosler, Kock et al. 2005; Baumert, Rosler et al. 2007). Bonvin et al. detected significantly elevated APOBEC3 mRNA levels in PHHs stimulated with IFN-I (Bonvin, Achermann et al. 2006). Nevertheless, it has been recently demonstrated by Tuarelli and colleagues that IFN-induced viral clearance of HBV occurs independently of APOBEC3 in HBV tg mice (Tuarelli, Liagre-Quazzola et al. 2008). It therefore remains to be further elucidated, whether IFN-I stimulated expression of antivirally active PKR and GTPases is also involved in the suppression of HBV replication in our model systems.

In addition, we investigated whether the applied RNA-oligonucleotides stimulate the induction of type-II interferon (IFN- γ). We were not able to detect hepatocellular expression of IFN- γ on mRNA level in our model systems after stimulation with 3p-RNA or poly(I:C), respectively. Moreover, we were interested whether the IFN inducible protein 10, IP-10, which is a chemoattractant for the recruitment of effector T cells, macrophages, NK cells and DCs *in vivo* (Luster, Unkeless et al. 1985; Dufour, Dziejman et al. 2002) is expressed after administration of 3p-RNA and poly(I:C) *in vitro* and *in vivo*. Despite the absence IFN- γ , both ligands induced strong expression of IP-10 via IFN-I induction *in vitro*. Remarkably, RNA-oligonucleotide treated mice showed only minor residual expression of IP-10 at hepatocellular mRNA level after treatment with Ctrl-RNA at day 6. Nevertheless, it is conceivable that high expression of IFN-I in the circulation of the murine system was followed by systemic induction of IP-10, as it has been recently described by Harkins et al. (Harkins, Szymanski et al. 2008). However, this aspect has to be further investigated.

In search for the mechanism and to further elucidate the contribution of RIG-I and interferon- α/β -receptor (IFNAR) in 3p-RNA-induced expression of IFN-I, we knocked down RIG-I and IFNAR expression, respectively, by siRNA transfection in HepG2 H1.3 cells and PHHs. We observed significantly reduced IFN- β levels in both cell types treated previously with siRNA against RIG-I, but astonishingly, only a minor reduction of IFN- β expression in cells previously treated with IFNAR specific siRNA.

Accordingly, it has been shown that hepatoma cell lines such as HuH7 and HepG2 exhibit only a minor suppression of IFN-I signal transduction after knockdown of IFNAR-I in comparison to other hepatoma derived cell lines (Damdinsuren, Nagano et al. 2007). Nevertheless, we concluded from these experiments that RIG-I is strictly required for 3pRNA-dependent induction of IFN-I. However, a feed-back loop via the IFNAR seems to play a minor role in 3p-RNA-mediated suppression of HBV replication *in vitro* and *in vivo*. For the murine system it would be helpful to cross HBV tg mice with RIG-I deficient (RIG-I^{-/-}) (Kato, Takeuchi et al. 2006) or IPS-1 deficient (IPS-1^{-/-}) mice (Kumar, Kawai et al. 2006), as well as with common IFNAR deficient (IFNAR^{-/-}) mice, respectively, to dissect this.

3.1.2 HBV escapes from antiviral activity of IFN

Detailed analysis revealed a reduced antiviral effect in PHHs in comparison to HepG2 H1.3 cells. Concurrently, we observed lower induction of 2'-5'-OAS after treatment with 3p-RNAs, which indicated a weaker antiviral IFN response due to hampered transfection efficacy. Moreover, a diminished IFN-I induction in PHHs might go along with an active counteraction of HBV against IFN-induced antiviral activity. Active HBV evasion to circumvent or even inactivate IFN-I antiviral mechanisms have been described and may be also responsible for limited IFN-I efficacy in around 30% of chronic HBV patients.

It has been shown that HBV developed various strategies to counteract IFN signaling pathways. Assumingly, HBV is able to overcome or inhibit mechanisms of antiviral effector molecules and may also inhibit IFN signaling pathway. For example it was proposed that HBV suppresses IFN- β expression at transcriptional level by direct binding of HBV-core protein to the regulatory sequence of the IFN- β gene (Twu, Lee et al. 1988; Twu and Schloemer 1989; Whitten, Quets et al. 1991). Furthermore, it had been published that expression of the IFN effector protein MxA is inhibited by direct binding of the core-protein to regulatory elements of the MxA promotor sequence in HepG2 2.15 cells (Fernandez, Quiroga et al. 2003; Guan, Lu et al. 2007), in HepG2 cells transiently transfected with a recircularized HBV genome (Fernandez, Quiroga et al. 2003) and in peripheral blood mononuclear cells (PBMC) from HBV chronically infected patients (Fernandez, Quiroga et al. 1997). Confirming

previous studies it has been suggested that encapsidation of spliced HBV RNA leads to the secretion of circulating HBV defective particles (referred to as dHBV DNA), which have been detected at higher level in patients evolving chronicity in comparison to those recovering from acute HBV infection (Rosmorduc, Petit et al. 1995; Soussan, Pol et al. 2008). The dHBV DNA may lead to cytoplasmic accumulation of the core-protein, which strongly reduced the antiviral activity of IFN- α by inhibition of MxA expression *in vitro* (Rosmorduc, Sirma et al. 1999). Besides the core-protein, other HBV proteins have been proposed to interact with the IFN pathway. For instance, it has been demonstrated that 5% of human fibroblasts transfected with the terminal protein (TP) domain of the HBV polymerase are resistant to IFN and dsRNA stimulation (Foster, Ackrill et al. 1991). Moreover, to clarify a potential clinical relevance of this inhibitory effect, expression of TP was analyzed in liver cells of patients with chronic hepatitis B. Accordingly, it was suggested that TP expression is associated with a failure of hepatocytes to respond to IFN therapy (Foster, Goldin et al. 1993). A report by Wu et al. supported these results. The authors revealed that TP inhibits expression of several interferon stimulated genes, such as ISG15 and adaptor protein MyD88 (myeloid differential primary response protein 88) by direct interference with the target promotor activity through blockage of STAT1 nuclear import (Wu, Xu et al. 2007). Moreover, it was shown that also HBV S- and X-protein are directly involved in inhibition of antiviral IFN signaling. A report by Christen et al. indicated that the S- and, or X-protein, respectively, could block nuclear import of STAT1 by upregulation of a cellular protein phosphatase named pp2A *in vitro* and in liver biopsies from chronically infected HBV patients (Christen, Duong et al. 2007). Additionally, Zhang et al. described that HBV X-protein may inhibit cellular proteasome activity, necessary for viral protein degradation, and coevally enhances viral replication (Zhang, Protzer et al. 2004). Altogether, these reports point to the fact that HBV counteracts IFN-induced suppression by interference of different HBV proteins with several actors of the IFN signaling pathway and moreover, might enhance simultaneously its own replication level. Accordingly, it was recently observed in our group that treatment of HBV replication with low concentrations of different types of IFN- α , conventionally used in antiviral therapy, led to slightly increased levels of HBV replication markers *in vitro* (Yuchen Xia, unpublished data). Higher dose of IFN, however, can clearly overcome the escape mechanisms and show antiviral activity.

There is evidence that an additionally escape mechanism of HBV is reflected in the direct interaction with PRR signaling cascades. Besides reports of HBV dependent modulation of TLR expression (Visvanathan, Skinner et al. 2007; Chen, Cheng et al. 2008), it was demonstrated that HBV suppress innate antiviral immune response elicited by TLR3 and TLR4 stimulation of both, hepatocytes and non-parenchymal cells, respectively. Accordingly, the authors found suppression of IFN- β production and decreased IFN stimulated gene expression (Wu, Meng et al. 2009). These strategies of HBV to counteract antiviral activity of IFN-I could have assisted a decreased antiviral effect in PHHs. A better understanding of these mechanisms might provide means to enhance and support antiviral treatment with IFN.

3.2 3p-siRNA combines RIG-I stimulation and siRNA mediated gene silencing and indicates a long lasting and superior anti-HBV effect

3.2.1 HBV-sequence specific siRNAs

To enhance the therapeutic efficiency against HBV we intended to combine the antiviral immune regulatory effect of RIG-I stimulation with an RNAi mediated gene-silencing effect of vulnerable cytosolic HBV-RNA. Therefore, we designed three different HBV-sequence specific siRNAs, targeting three different regions within or near the common polyadenylation signal region at the 3'-end of HBV-RNAs. The targeted regions offer the possibility of interfering with several sensitive sites due to overlapping open reading frames (ORFs). RNAi is a powerful tool to inhibit the function of HBV target genes and has already been shown to exhibit a potent antiviral effect against HBV *in vitro* (Hamasaki, Nakao et al. 2003; Konishi, Wu et al. 2003) and *in vivo* (Giladi, Ketzinel-Gilad et al. 2003; Klein, Bock et al. 2003; McCaffrey, Nakai et al. 2003). Moreover, it has been reported that the highest inhibitory effects induced by different siRNAs targeted HBcAg and HBx gene (McCaffrey, Nakai et al. 2003; Shlomai and Shaul 2003). Accordingly, we designed a siRNA named si-1.1 that targeted this preferential region of the HBV genome within the overlapping ORFs of the X-protein and the precore/core protein and therefore affected all HBV-mRNAs. The siRNA named si-1.2 target an alternative region within the X-protein ORF, but

also affected all HBV-mRNAs transcripts. Another alternative HBV-genome target region, the ORF of the polymerase, was directed by siRNA si-1.3, which affects all HBV mRNA transcripts except for the 0.7 kb transcript of the X-protein. The HBV targeting sequences of all siRNAs are conserved within the different genotypes, except the rare genotype F HBV.

Delivery of siRNA into mammalian cells is known to often induce a non-specific innate immune response. The RNA-activated protein kinase (PKR) can be stimulated by sequence unspecific double-stranded siRNA (Bridge, Pebernard et al. 2003; Sledz, Holko et al. 2003). Therefore, asymmetrical siRNA possessing a standard 3'-overhang, such as our siRNAs, have become more widely used in an attempt to improve RNAi potency (Soutschek, Akinc et al. 2004). However, it was demonstrated that blunt-ended RNA, including siRNA, can also bind to and activate RIG-I, when the RNA is released into the cytoplasm (Hornung, Guenther-Biller et al. 2005; Marques, Devosse et al. 2006). Moreover, delivered siRNA can interact with sequence-unspecific TLR3 and sequence-specific TLR7 or TLR8, respectively, as the RNA traffics through the endosomal compartment (Akashi, Miyagishi et al. 2005; Judge, Sood et al. 2005). These "off-target" effects lead to the production of IFN-I, as well as proinflammatory cytokines and induce NF κ B activation. Nevertheless, in consideration of our intention to combine siRNA mediated gene silencing of HBV with the immuno-stimulatory activity of 3p-dsRNA, endogenous IFN response is rather desired. Accordingly, we resigned any stabilizing chemical modifications of the siRNA for nuclease degradation resistance, for example substitution of the 2'-OH group in the ribose sugar backbone to a 2'-O-methyl (2'-OMe) group, as they were used for HBV siRNA treatment *in vivo* (Morrissey, Lockridge et al. 2005). It was shown that 2'-OMe modified siRNAs are recognized with high affinity by TLR7/8, but do not induce downstream signaling (Sioud, Furset et al. 2007). 2'-OMe modification of the siRNA is sufficient to abrogate siRNA-mediated interferon induction also *in vivo* (Judge, Bola et al. 2006). It has to be further investigated, whether application of unmodified siRNA had any attenuating impact on siRNA stability and efficiency *in vitro* or *in vivo*.

3.2.2 HBV-sequence specific 3p-siRNAs efficiently suppress HBV replication

5'-triphosphate groups were coupled to siRNAs during *in vitro* transcription and resulting oligonucleotides were termed 3p-1.1, 3p-1.2 and 3p-1.3. Combination of siRNA mediated gene silencing with additional antiviral approaches was already shown to exhibit greater inhibitory effects on HBV replication. For example, it was shown that combination of siRNA with lamivudine exerted a pronounced inhibition of HBV replication in HepG2 2.15 cells (Li, Xu et al. 2007). Moreover, a very recent report by Vincent et al. described the enhanced inhibitory effect by the combination of CpG-induced cytokines with lamivudine against HBV replication in HBV infected differentiated HepaRG cells (Vincent, Lucifora et al. 2009). Concerning our combinatory approach of IFN-I induction by RIG-I stimulation and siRNA mediated gene silencing, it has been lately shown by our collaborators Poeck et al. that 3p-siRNA efficiently turns gene silencing and RIG-I activation against melanoma (Poeck, Besch et al. 2008). The particular advantage using a combinatorial therapeutic strategy of immunostimulatory and siRNA over conventional monotherapy using nucleos(t)ide analogues is that the immunostimulatory 3p-component targets specifically HBV replication, whereas the siRNA gene silencing component acts independently from HBV replication and will be thus less subjected due to development of resistance. A limited half-life period and absence of cytotoxic side effects of systemically applied 3p-siRNA would prefer our combinatory molecules before other HBV treatment strategies in development, such as redirected T-cell therapy.

To demonstrate the therapeutic efficiency of our new molecules, we first showed a clear induction of IFN- β in 3p-1.2 treated HepG2 H1.3 cells, whereas cells treated with si-1.2 elicited no IFN- β expression. Next, we tested the potency of all three 3p-siRNAs to induce IFN-I. As expected, 2'-5'-OAS levels were strongly induced in both, HepG2 H1.3 cells and HBV infected PHH. Consistent with the upregulation of IFN-I and 2'-5'-OAS by all three 3p-siRNAs, we observed a significant reduction of progeny HBV DNA copies, as well as HBeAg and HBsAg levels. Similar results were obtained in HBV-infected primary cells. Remarkably, also cccDNA levels, which indicate HBV persistence and are hardly affected by any anti-HBV drug, were decreased after application of 3p-siRNAs in both *in vitro* models. Nevertheless,

comparing the antiviral effects of all three 3p-RNAs, the equally potent IFN induction did not lead to the same strong antiviral effect, suggesting a combinatorial antiviral effect of RIG-I stimulation with variable potent siRNA mediated gene silencing.

To test the efficacy against different HBV genotypes, PHHs were infected with isolated virus from stably HBV producing hepatoma cell line HepG2 2.15 several days before treatment. HepG2 2.15 cells express genotype A HBV in comparison to HepG2 H1.3 cells, which replicate genotype D HBV. Comparable reduction efficiency of HBV replication markers in HepG2 H1.3 and HBV infected PHHs indicated that the RNAi component of 3p-siRNA was also functional against genotype D HBV. To further sustain this result we tested the therapeutic efficiency of 3p-siRNAs also in HepG2 2.15 cells. Surprisingly, the transfected 3p-siRNAs revealed none or only minor residual expression of 2'-5'-OAS at day 6 after application, fitting to the reduced sensitivity of HepG2 2.15 cells against IFN (Guan, Lu et al. 2007). Nevertheless, probably independent of IFN-I induction, progeny HBV DNA-, HBeAg- and pgRNA levels, respectively, were significantly reduced. These results supported effective siRNA dependent HBV gene silencing of genotype A HBV and moreover, independent of the fact that HepG2 2.15 cells replicated HBV approximately twice as high as HepG2 H1.3 cells. It remains to be further elucidated, whether 2'-5'-OAS levels were already strongly diminished on day 6 or if RIG-I expressing HepG2 2.15 cells showed no triphosphate induced IFN-I response at all.

To analyze whether immunostimulation and RNAi-mediated gene silencing acted synergistically to suppress HBV replication, we compared the primarily used 3p-RNA with our new 3p-siRNAs in HepG2 H1.3 cells. We observed strongly reduced viremia, as well as cccDNA and HBV-protein levels, respectively, after treatment with the original 3p-RNA. Intriguingly, all three 3p-siRNAs revealed an even more pronounced reduction of HBV-DNA levels compared to 3p-RNA alone. Nevertheless, comparing all *in vitro* results, 3p-1.2 indicated the most promising antiviral effects and was used for further experiments.

To prove the sustained antiviral effects of 3p-siRNA, we compared the antiviral efficacy of 3p-RNA with 3p-1.2 over a prolonged period of 16 days in HepG2 H1.3 cells. Because HBV replication is attenuated until the cell layer is confluent, we detected only low progeny HBV-DNA and HBeAg levels at day 0.5. In correlation to increasing hepatocellular differentiation (Quasdorff, Hosel et al. 2008), HBV replication increased constantly until day 10. Application of both, 3p-1.2 and si-

1.2 decreased HBV-DNA and HBeAg levels at all timepoints. Yet, 3p-1.2 showed a significantly more prolonged antiviral response than si-1.2 or 3p-RNA alone. Thus, our data demonstrated that the early antiviral response until day 6 is comparable between all therapeutic oligonucleotides, but IFN mediated reduction of HBV replication by 3p-RNA and 3p-1.2 decreased over time. Therefore, 3p-RNA was equally active at early timepoints, but 3p-1.2 was superior over time due to its gene silencing activity. These results confirmed the superior antiviral activity by the combination of immunostimulation and HBV gene silencing in one single molecule *in vitro*. In addition, we excluded hampered siRNA binding to HBV-RNA due to appearance of mutations by RNAi selection pressure in 3p-1.2 or si-1.2 treated cells. These observations indicated a combinatory antiviral effect of IFN-I induction by RIG-I stimulation and siRNA mediated HBV gene silencing *in vitro*, superior than each mechanism alone.

In vivo, both molecules, 3p-RNA and 3p-1.2, induced comparable IFN- α levels, determined 6 hours after the first injection in the sera of mice. 3p-RNA and 3p-siRNA elicited comparable reduction of hepatocellular HBV-DNA and HBV pgRNA levels at day 6 after application. In contrary and consistent with our *in vitro* data, 3p-1.2 showed a significantly stronger effect than 3p-RNA on HBV pgRNA at day 9, pointing to an effective combinatory antiviral mechanism of 3p-1.2 *in vivo*. Remarkably, the antiviral effect of 3p-RNA and 3p-1.2 on HBV viremia remained until day 15. As previously described, HBV RNA-containing capsids are preferentially targeted by IFN-I (Schultz, Summers et al. 1999; Wieland, Guidotti et al. 2000). Consistently, 3p-RNA and 3p-siRNA induced IFN-I exhibited a strong impact on cytoplasmic core protein expression at day 9, which persisted until day 15.

Surprisingly, si-1.2 treatment alone showed only minor reduction of HBV replication markers *in vivo* over time. This observation suggested that all RNAs, including the siRNAs, were not effectively delivered to hepatocytes to fully elicit their gene silencing component after systemic administration. Nevertheless, the *in vitro* experiments confirmed that gene silencing is an important key function of 3p-1.2. Likewise, the lower antiviral response induced by si-1.2 *in vivo* highlighted the importance of inducing an innate immune response. In fact, detailed analysis revealed that even PEI complexed 3p-siRNA is systemically distributed. More than the liver, the lymphatic glands and the spleen expressed IFN-I after intravenous injection of 3p-1.2, likely via stimulation of endosomal TLRs and RIG-I in immune

cells (Applequist, Wallin et al. 2002; Heil, Hemmi et al. 2004; Hornung, Ellegast et al. 2006). In addition, fluorescently labeled si-1.2 complexed with PEI was enriched predominantly in the spleen, and to reduced extent in liver. This indicates that liver cells played only a subsidiary role in antiviral IFN-I induction by systemic 3p-siRNA application. Remarkably, the results showed that also unphosphated si-1.2 induced IFN-I in lymphatic glands and in the spleen, although to a minor extent, referred as an “off-target” effect by stimulation of TLRs or RIG-I, respectively (Akashi, Miyagishi et al. 2005; Hornung, Guenther-Biller et al. 2005; Judge, Sood et al. 2005; Marques, Devosse et al. 2006).

3.3 Liver targeting of modified siRNAs using different applications *in vivo*

Due to the poor hepatocellular uptake of siRNA and to improve the effect of 3p-siRNA based combinatory therapy we wanted to improve hepatocyte targeting. Different groups already followed up several strategies in this context, using delivery vehicles or chemical modifications and bioconjugations. The most widely used vehicles for this purpose are based on positively charged (cationic) agents that complex with, or encapsulate, the negatively charged nucleic acid. The cationic polymer PEI (polyethylenimine), used in this study for 3p-RNA application (Poeck, Besch et al. 2008), could not yield the desired hepatocyte targeting. Importantly, such delivery vehicles are typically taken up into cells by endocytosis, and are concentrated in endosomal compartments prior to releasing the nucleic acid into the cytoplasm (Robbins, Judge et al. 2009). This fact could contribute to the limited observed gene silencing efficiency of both, si-1.2 and 3p-siRNA *in vivo*. Alternatively, hydrodynamic injection (HDI) was shown to deliver nucleic acids more efficiently to the liver (Giladi, Ketzinel-Gilad et al. 2003; Klein, Bock et al. 2003; Morrissey, Blanchard et al. 2005; Huang, Wu et al. 2006). Using this injection technique we observed an increase of fluorescently labeled si-1.2 in liver cells and simultaneously a decrease in splenocytes, compared to si-1.2 after conventional intravenous administration. Nevertheless, this approach seemed rather promising, because structure and vitality of liver cells seemed to be negatively affected by HDI, due to the rapid intravenous injection of a large volume under high pressure.

In addition, chemical modifications by bioconjugation are used to increase liver directed targeting. Conjugated cholesterol to the 3'-end of the sense-strand was shown to significantly increase the levels of hepatocellular uptake (Soutschek, Akinc et al. 2004). We observed that cholesterol-conjugation to fluorescently labeled si-1.2 drastically increased the hepatocellular uptake particularly by hepatocytes after conventional injection, in comparison to unmodified si-1.2. Previous complexation with PEI even increased the targeting efficiency. Application of cholesterol-coupled si-1.2 by HDI showed no accessory targeting effect. An antagonizing attribute might be the limited stability of uncomplexed siRNA (Braasch, Jensen et al. 2003; Czauderna, Fechtner et al. 2003), which is exposed to drastic shear forces during HDI. In summary, the data showed promising prospects to further enhance hepatocellular uptake of 3p-siRNA by bioconjugation with cholesterol. Nevertheless, it remains to be investigated in more detail, whether 5'-triphosphated siRNA could be stabilized by sugar backbone modifications and moreover, modified by 3'-cholesterol coupling, or whether stoichiometric limitations might drop this approach. However, various considered alternative approaches could further enhance hepatocyte specific targeting of 3p-siRNA. Morrissey et al. incorporated chemically modified siRNAs against HBV into a specialized liposome to form a stable nucleic acid lipid particle (SNALP). After intravenous administration significant improvement of efficacy combined with a longer half-life were observed in the liver of treated animals (Morrissey, Blanchard et al. 2005; Morrissey, Lockridge et al. 2005). Furthermore, we considered the use of recombinant adeno-associated viral (rAAV) vector as a delivery vehicle. AAV-8 pseudotype shows high natural liver tropism and was already used in preclinical evaluations as a vector for hepatocyte specific delivery approaches (Gao, Alvira et al. 2002; Grimm, Zhou et al. 2003). Alternatively, antibody-mediated delivery is an effective method of targeting siRNA to liver cells. Wen et al. constructed a fusion protein containing a single chain of the human variable fragment (scFv) against HBsAg, coupled to HBV-sequence specific siRNA. The modified siRNA was specifically delivered into HBsAg-positive cells and effectively inhibited HBV gene expression *in vitro* and *in vivo* (Wen, Liu et al. 2007). Thus, efficient delivery of 3p-siRNA into hepatocytes remains the main goal of further investigations.

Previous described delivery studies revealed that injected complexed nucleic acids only partially reached the liver and only to some extent the hepatocytes. A certain proportion apparently ended up in non-parenchymal cells (NPCs) such as LSECs or

Kupffer cells. Therefore, we wanted to elucidate the contribution of these cells, beside hepatocytes, in 3p-siRNA mediated induction of IFN-I. To mimic a potential uptake like in the *in vivo* situation, PEI-complexed 3p-1.2. was added to all isolated cell types and a potent IFN- β induction could be shown in all cases. These results clearly indicated the potency of NPCs to contribute to an anti-HBV response via stimulation of endogenous IFN-I and ISGs, as it was already shown by Wu and colleagues (Wu, Lu et al. 2007). It has to be further investigated, whether other cell types are contributed to the strong IFN-I expression after systemic distribution of triphosphated RNA-oligonucleotides *in vivo*.

3.4 Application of immune-stimulatory RNA-oligonucleotides initiates an adaptive T cell response against HBV

Further investigations of LSECs and Kupffer cells revealed that both cell types additionally expressed the proinflammatory cytokines IL-6 and TNF- α , respectively, after treatment with 3p-1.2., and in contrast to PHHs. It was already shown that hepatoma cells are defective for induction of IL-6 and TNF- α after stimulation with transfected poly(I:C), acting as a TLR3 or MDA-5 ligand (Wu, Lu et al. 2007; Preiss, Thompson et al. 2008). It has to be further investigated whether this is probably also applied for RIG-I stimulation of PHHs. Nevertheless, we assumed that expression of proinflammatory cytokines might be an indicator for the induction of an HBV antigen specific adaptive immune response after several days.

A cytolytic clearance of HBV infection is dependent on adaptive T cell response by cytotoxic CD8⁺ T cells (CTLs), which inhibit viral replication and kill infected cells (Guidotti, Ishikawa et al. 1996). The elimination of cccDNA containing hepatocytes is essential for the clearance of HBV infection. HBV tg mice are immunologically tolerant to HBV antigens. Nevertheless, it was shown that the HBV tg mice used in this study are not completely xenotolerant (Quasdorff, Hosel et al. 2008). The study demonstrated that HBV envelope proteins were not expressed during the embryonic phase of development and thus probably do not induce tolerance by deletion of T cells. HBV replication only starts after birth. This enables appearance of an adaptive T cell response in HBV tg mice.

In fact, a major part of mice treated with 3p-RNA or 3p-1.2, respectively, revealed enhanced levels of IFN- γ and CD8 mRNA in the liver and significantly elevated ALT levels at day 9 after application, indicating a CD 8 T cell influx into the liver. A similar picture was observed in a very recent study during early stages of HBV infection in patients (Fisicaro, Valdatta et al. 2009). Moreover, histological analysis of liver tissue confirmed appearance of an inflammatory reaction in treated mice at this timepoint. A clear shift towards resolution of the inflammatory changes indicated by decreased ALT levels, as well as diminished expression of CD8 and IFN- γ could be observed at day 15. It is conceivable that an accessory adaptive T cell response, induced after RNA-oligonucleotide application, might additionally enhance the antiviral activity. However, this needs to be proven by the analysis of liver associated lymphocytes. It was observed that the expression of MHC I on HBV infected hepatocytes, required for effective presentation of HBV specific antigens on the cell surface to stimulate cytotoxic T-cell response, was significantly diminished (Chen, Tabaczewski et al. 2005). In contrast, it was shown that IFN-I modulates a number of immunoregulatory functions involving interactions between cells. This multiple-cell response includes the IFN-I induced expression of MHC-I antigens, (Samuel 2001), which is also increased after application of 3p-RNA or 3p-siRNA, respectively (Poeck, Besch et al. 2008). An IFN-I induced increase of antigen presentation could stimulate the direction of the adaptive immune response by priming T helper cells and cytotoxic T cells (Biron 1999), which might result in complete elimination of HBV replication. Detailed characteristics have to be examined, but it is conceivable that an optimized induction of IFN-I by RNA-oligonucleotides could even assist the cytolytic adaptive immune response against HBV.

4 Material and Methods

4.1 Biotic and abiotic material

All solutions were prepared with deionised water from the Ultra Pure Water System Easy Pure UV/UF (Werner Reinstwassersysteme, Wilhelm Werner GmbH, Leverkusen, Germany). At a resistance of 16 Mega Ohm or more obtained water is valid as desalted and is comparable to double-distilled water (ddH₂O).

4.1.1 Consumable items

Cell culture flasks	Nunc, Wiesbaden, Germany
Cell culture dishes	Nunc, Wiesbaden, Germany
Cell culture well plates	Nunc, Wiesbaden, Germany
Cell strainer	Nunc, Wiesbaden, Germany
Centrifuge vials (15 / 50ml)	Falcon, BD GmbH, Heidelberg, Germany
Chamber Slides LabTekII, RS Glass	Nunc, Wiesbaden, Germany
Cryo vials	Nunc, Wiesbaden, Germany
Cuvettes	Sarstedt, Nümbrecht, Germany
ELISA 96-well-plates	Maxisorb, Nunc, Wiesbaden, Germany
Filter paper Whatman 3MM	Biometra, Göttingen, Germany
Freezing Container	Nalgene, Nunc, Wiesbaden, Germany
Perfusion cutlery	BD Valu-Set™, Heidelberg, Germany
Pipetts, single use	Sarstedt, Nümbrecht, Germany
Hyperfilm ECL	GE Healthcare, Buckinghamshire, UK
Pipette tips	Starlab GmbH, Ahrensburg, Germany
Reaction vials	Eppendorf, Hamburg, Germany
Reflotron® ALT stripes	Roche Diagnostics, Mannheim, Germany
Saran folie	Roth, Karlsruhe, Germany
Tissue paste Histoacryl®	Braun, Melsung, Germany
Syringes	Heiland Med GmbH, Hamburg, Germany
Ultra centrifuge-tubes, polyallomer	Beraneck Laborgeräte, Weinheim, Germany
Nylon membrane, positively charged	Roche Diagnostics, Mannheim, Germany
PVDF membrane	Amersham, Buckinghamshire, UK
X-ray film	Biomax MR-Film, Kodak, Germany

4.1.2 Chemicals

Acidic acid	Roth, Karlsruhe, Germany
Acryl amide	Sigma, Deisenhofen, Germany
Agarose SeaKem LE	Cambrex Bio Science, Rockland, USA
Ammonium acetate	Merck, Darmstadt, Germany
Ammoniumpersulfate	Roth, Karlsruhe, Germany
Aqua-Phenol (pH 4,5)	Roth, Karlsruhe, Germany
Bradford Reagent	Sigma, Deisenhofen, Germany
Bromphenol blue	Merck, Darmstadt, Germany
BSA (Bovines serum albumine)	Serva, Heidelberg, Germany
Caesium chloride	Roth, Karlsruhe, Germany
Collagen	Serva, Heidelberg, Germany
1,4-Diazabicyclo[2,2,2]octane 98% (DABCO)	Sigma Aldrich Chemie GmbH, Steinheim, Germany
DEPC (Diethylpyrocarbonate)	Roth, Karlsruhe, Germany
Developer G153 A + B	Agfa Geveart NV, Mortsel, Belgium
Dimethylsulfoxide (DMSO)	Merck, Darmstadt, Germany
Ethanol	Roth, Karlsruhe, Germany
Ethylenedinitrilotetraacetic acid (EDTA)	Roth, Karlsruhe, Germany
Ethidium bromide	Merck, Darmstadt, Germany
Formaldehyde	Roth, Karlsruhe, Germany
Formamide	Roth, Karlsruhe, Germany
Glycerine (Glycerol)	Roth, Karlsruhe, Germany
Glucose	Sigma, Deisenhofen, Germany
Glutaraldehyde	Sigma, Deisenhofen, Germany
Hydrochloric acid	Roth, Karlsruhe, Germany
Isopropanol	Roth, Karlsruhe, Germany
Methanol	Roth, Karlsruhe, Germany
Milk powder	Sigma, Deisenhofen, Germany
Mowiol 4-88 reagent	Calbiochem, La Jolla, CA, USA
NP-40	Roth, Karlsruhe, Germany
Paraformaldehyde	Merck, Darmstadt, Germany

Material and methods

Polyethylenglycol (PEG) 6000	Serva Electrophoresis, Heidelberg, Germany
Ponceau S	Roth, Karlsruhe, Germany
Potassium	Roth, Karlsruhe, Germany
Potassium chloride	Merck, Darmstadt, Deutschland
Potassium acetate	Merck, Darmstadt, Germany
Potassium dihydrogenphosphate	Roth, Karlsruhe, Germany
Rapid Fixer G354	Agfa Geveart NV, Mortsel, Belgium
RNA <i>Later</i>	Quiagen, Hilden, Germany
Roti-Phenol (pH 7,5)	Roth, Karlsruhe, Germany
Saccharose	Sigma, Deisenhofen, Germany
Sodium acetate	Merck, Darmstadt, Germany
Sodium chloride	Roth, Karlsruhe, Germany
Sodium citratdihydrate	Roth, Karlsruhe, Germany
Sodium dihydrogenphosphate	Roth, Karlsruhe, Germany
Sodium hydroxid	Roth, Karlsruhe, Germany
Sodium dodecylsufate (SDS)	Merck, Darmstadt, Germany
Spermidine-HCl	Sigma, Deisenhofen, Germany
Sucrose	Sigma, Deisenhofen, Germany
Tetramethylethylendiamine (TEMED)	Sigma, Deisenhofen, Germany
Tissue-Tak® Tec	Sakura Finetec, Torrance, USA
Tris-Base	Roth, Karlsruhe, Germany
Tris-HCl	Roth, Karlsruhe, Germany
Triton X-100	Roth, Karlsruhe, Germany
Trizol reagent	Invitrogen, Karlsruhe, Germany
Tween 20	Roth, Karlsruhe, Germany
Virkon disinfectant	Tetenal AG & Co KG, Norderstedt, Germany
Yeast extract	BD Microbiology Systems, Sparks, USA

4.1.3 Kits

4.1.3.1 Cell isolation

Kupffer cells	Pierce, Rockford, IL, USA
LSECs	Miltenyi, Bergisch Gladbach, Germany

4.1.3.2 DNA labelling

Rediprime DNA Labeling System Amersham, Buckinghamshire, UK

4.1.3.3 ELISA

Human IFN- γ BD Microbiology Systems, Sparks, USA
Human IL-6 BD Microbiology Systems, Sparks, USA
Mouse IFN- α Biosource, Solingen, Germany
Murex HBsAg Version 3 Abbott, Wiesbaden, Germany

4.1.3.4 *In vitro* transcription (IVT)

Silencer siRNA construction Kit Ambion, Huntington, UK
T7 promotor primer Metabion Int. AG, Martinsried, Germany

4.1.3.5 Luciferase detection

Dual Luciferase reporter Assay Promega GmbH, Mannheim, Germany

4.1.3.6 Nucleic acid isolation

High pure RNA isolation kit Roche, Mannheim, Germany
MinElute PCR Purification Kit Qiagen, Hilden, Germany
Mini Quick Spin™ Oligo Column Roche, Mannheim, Germany
Nucleospin Tissue Kit Macherey-Nagel, Düren, Germany
Nucleospin RNA II Macherey-Nagel, Düren, Germany
PCR Purification Kit Qiagen, Hilden, Germany
QIAquick Gel Extraction Kit Qiagen, Hilden, Germany
QIAamp DNA Blood Mini Kit Qiagen, Hilden, Germany
QIAamp MinElute Virus Spin Kit Qiagen, Hilden, Germany

4.1.3.7 Plasmid preparation

QIAprep Miniprep, Maxiprep,
EndoFree Maxiprep Kit Qiagen, Hilden, Germany

4.1.3.8 PCR reaction mix

PuRetaq ready-to-go PCR Beads Amersham, Buckinghamshire, UK
PCR DNA Amplification Kit Roche Diagnostics, Mannheim, Germany

4.1.3.9 Real time PCR

DNA Amplification Kit SYBR® Green	Roche Diagnostics, Mannheim, Germany
First-strand cDNA synthesis	
qRT-PCR, Superscript III	Invitrogen, Karlsruhe, Germany
LightCycler® 1.5:	
Cycler® Capillaries (20µl)	Roche Diagnostics, Mannheim, Germany
LightCycler® 480II:	
96-microtiter plates	Roche Diagnostics, Mannheim, Germany

4.1.3.10 Transfection reagent

FuGENE 6®	Roche Diagnostics, Mannheim, Germany
Lipofectamin 2000®	Invitrogen, Karlsruhe, Germany
HiPerFect®	Qiagen, Hilden, Germany

4.1.3.11 Nucleic acid complexation

invivo-jetPEI ®	Polyplus transfection, New York, NY, USA
-----------------	--

4.1.3.12 Radioactive probes

Rediprime II Random Prime Labelling System	Amersham, Buckinghamshire, England
--	------------------------------------

4.1.3.13 Western blot

ECL Western Blotting Detection Reagents	Amersham, Buckinghamshire, UK
Enhanced Chemiluminescence	Pierce, Rockford, USA

4.1.3.14 XTT-Test

XTT - Cell Proliferation Kit II	Roche Diagnostics, Mannheim, Germany
---------------------------------	--------------------------------------

4.1.4 Cell culture

4.1.4.1 Cell lines and primary cells

HEK 293 - human embryonic kidney cell line (Aiello, Guilfoyle et al. 1979)

- HepG2 H1.3 - stably HBV producing hepatoma cell line, containing one copy of a 1.3-fold overlength HBV genome, genotype D, which establishes HBV cccDNA as additional transcription template (Jost, Turelli et al. 2007; Protzer, Seyfried et al. 2007)
- HepG2.2.15 - stably HBV producing hepatoma cell line, containing four copies of a 1.1-fold HBV genome, genotype A (Sells, Zelent et al. 1988)
- HuH7 - human hepatoma cell line (Nakabayashi, Taketa et al. 1982)
- HuH7.5 - human hepatoma cell line, point mutation in CARD-domain of RIG-I (Blight, McKeating et al. 2002)
- Kupffer cells - liver macrophages, isolated from fresh liver specimen
- LSEC - liver sinusoidal epithelial cells, isolated from fresh liver specimen
- PHH - primary human hepatocytes, isolated from fresh liver specimen (Schulze-Bergkamen, Untergasser et al. 2003)

4.1.4.2 Consumable cell culture items

Collagenase	Worthington Biochemical Corporation, Lakewood, NJ, USA
Dimethylsulfoxid (DMSO)	Merck, Darmstadt, Germany
Dulbeccos MEM	Gibco, BRL, Eggenstein, Germany
Ethyleneglycolbis (2-aminoethyl) -tetraacetic acid (EGTA)	Roth, Karlsruhe, Germany
Fetal Calf serum (FCS)	Biochrom AG, Berlin, Germany
Glutamine	Gibco, BRL, Eggenstein, Germany
HBSS	Gibco BRL, Eggenstein, Germany
HEPES	Gibco BRL, Eggenstein, Germany
Hydrocortisone	Sigma, Deisenhofen, Germany
Inosine	Serva, Darmstadt, Germany
Insulin	Serva, Darmstadt, Germany
Non essential amino acids (NEAA)	Biochrom AG, Berlin, Germany
RPMI 1640	Gibco, BRL, Eggenstein, Germany
Sodium pyruvate	Gibco BRL, Eggenstein, Germany
Trypsine	Gibco, BRL, Eggenstein, Germany
Universal type-I interferon	PBL Interferon Source, Piscataway, NJ, USA
Williams Medium E	Gibco, BRL, Eggenstein, Germany

4.1.4.3 Antibiotics

Ampicilline	Sigma, Deisenhofen, Germany
Geniticine (Neomycine) G418	Invitrogen, Karlsruhe, Germany
Gentamycine	Gibco BRL, Eggenstein, Germany
Penicilline/Streptomycine	Biochrom AG, Berlin, Germany

4.1.4.4 Cell culture media

Cell freezing medium	Dulbeccos MEM	500 ml
	FCS	20%
	DMSO	10%
HEK 293 cultivation medium	Dulbeccos MEM	500 ml
	FCS	10 %
	Glutamine, 200 mM	1.1 %
	P/S, 5000 U/ml	1.1 %
HepG2.2.15 / HepG2 H1.3 cultivation medium	Dulbeccos MEM	500 ml
	FCS	10 %
	Glutamine, 200 mM	1.1 %
	P/S, 5000 U/ml	1.1 %
	NEAA, 100 x	1.1 %
HepG2 2.15 virus production medium	PHH medium	250 ml
	Williams E medium	250 ml
	FCS	5 %
	Glutamine, 200 mM	0.5 %
	P/S, 5000 U/ml	0.5 %
	NEAA, 100 x	0.5 %
HuH7 / HuH7.5 cultivation medium	Dulbeccos MEM	500 ml
	FCS	10 %
	Glutamine, 200 mM	1.1 %
	P/S, 5000 U/ml	1.1 %
	NEAA, 100 x	1.1 %
LSECs cultivation medium	PHH medium	500 ml
	FCS	5 %

Material and methods

Kupffer cells medium	RPMI	500 ml
	FCS	5 %
Primary human hepatocytes, PHH		
- Preperfusion medium	HBSS, Ca/Mg-free	500 ml
	EGTA, 100 mM	0.5 %
	Heparine, 5000 U/ml	0.2 %
- Collagenase medium	Williams Medium E	250 ml
	CaCl ₂ , 1 M	0.36 %
	Gentamycine, 10 mg/ml	1 %
	Collagenase typeIV	200 mg
- Wash medium	Williams Med E	500 ml
	Glutamine, 200 mM	1.1 %
	Glucose, 5%	1.2 %
	Hepes, 1 M, pH 7.4	2.25 %
	P/S,5000U/ml	1.2 %
- PHH medium	Wash medium	500 ml
	Gentamycin, 10 mg/ml	1 %
	Hydrocortison	0.1 %
	Insulin	0.45 mg
	DMSO	1.75 %
	Inosine, 82.5 mg/ml	0.4 %

4.1.5 Oligonucleotides for in vitro transcription (IVT)

T7 promotor: 5' CTATAGTGAGTCG 3'

DNA-template: 5' AAGCTGACCCTGAAGTTCATCCC 3'

3p-RNA: 5'ppp GAAGCUGACCCUGAAGUUCAUCCC 3'
3' UUCGACUGGGACUUCAAGUAGGGG ppp 5'

DNA-template: 5' TTTCACCTCTGCCTAATCA 3'

3p-1.1: 5' ppp GUUUCACCUCUGCCUAAUCA 3'
3' AAAGUGGAGACGGAUUAGU ppp 5'

DNA-template: 5' CGACCTTGAGGCATACTTC 3'
3p-1.2: 5' ppp GCGACCUUGAGGCAUACUUC 3'
 3' GCUGGAACUCCGUAUGAAGG ppp 5'

DNA-template: 5' CTATTAACAGGCCTATTGA 3'
3p-1.3: 5' ppp GCUAUU AACAGGCCUAUUGA 3'
 3' GAUAAUUGUCCGGAUAACTG ppp 5'

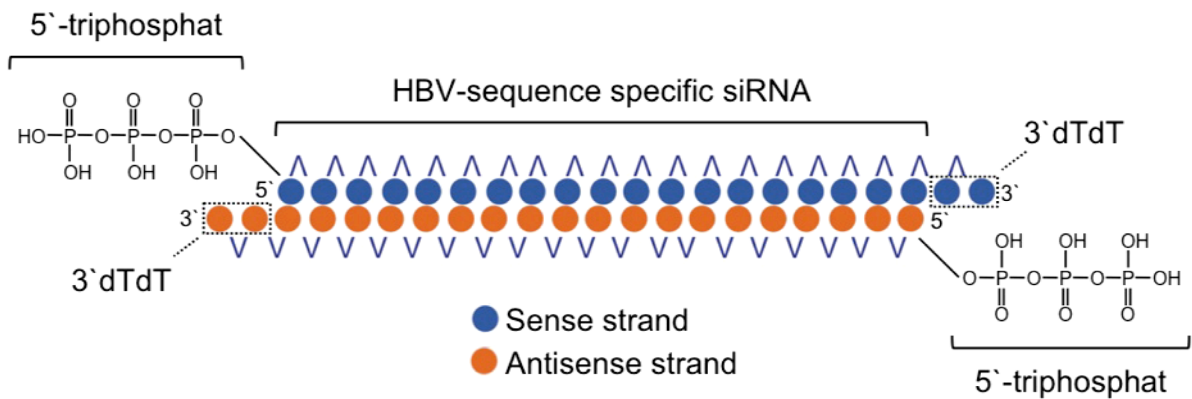


Fig. 4.1: Schematic representation of triphosphated siRNA

4.1.6 siRNAs (Eurogentec, Leiden, Belgium)

Ctrl-RNA

polyA-RNA (Polyriboadenosine) 5' AAAAAAAAAAAAAAAAAAAAAA 3'

siRNAs

si-1.1 (3105 - 3124): HBV target 5' TTTCACCTCTGCCTAATCA 3'
 sense 5' UUUCACCUCUGCCUAAUCAdTdT 3'
 antisense 3' UGAUUAGGCAGAGGUGAAAdTdT 5'

si-1.2: (2973 - 2992) HBV target 5' CGACCTTGAGGCATACTTC 3'
 sense 5' CGACCUUGAGGCAUACUUCdTdT 3'
 antisense 5' GAAGUAUGCCUCAAGGUCGdTdT 3'

si-1.3: (2241 – 2260)	HBV target	5' CTATTAACAGGCCTATTGA 3'
	sense	5' CUAUUAACAGGCCUAUUGAdTdT 3'
	antisense	5' TCAAUAGGCCUGUUAUAGdTdT 3'
si-Ctrl (HCV):	sense	5' CUGAUAGGGUGCUUGCGAGdTdT 3'
	antisense	5' CUCGCAAGCACCCUAUCAGdTdT 3'

4.1.7 PCR Primer (Invitrogen, Karlsruhe, Germany)

Amplification primer

HBV -2595- fw	5' GAGCAAACATTATCGGGACT 3'
HBV -3081- rev	5' GACCAATTTATGCCTACAGC 3'

Sequencing primer

HBV -2595- fw	5' GAGCAAACATTATCGGGACT 3'
---------------	----------------------------

4.1.8 Quantitative real time PCR primers (Invitrogen, Karlsruhe, Germany)

HBV primers

HBV rcDNA1745 fw	5' GGAGGGATACATAGAGGTTTCCTTGA 3'
HBV rcDNA1844 rev	5' GTTGCCCGTTTGTCTCTAATTC 3'
HBV pgRNA 383 fw	5' CTCCTCCAGCTTATAGACC 3'
HBV rpgRNA 705 rev	5' GTGAGTGGGCCTACAAA 3'
HBV cccDNA 92 fw	5' GCCTATTGATTGGAAAGTATGT 3'
HBV cccDNA 2251 rev	5' AGCTGAGGCGGTATCTA 3'

mitochondrial DNA primers

mitoDNA 8686 fw	5' CCCTCTCGGCCCTCCTAATAACCT 3'
mitoDNA 8796 rev	5' GCCTTCTCGTATAACATCGCGTCA 3'

Human primers

human IFN-β fw	5' GCCGCATTGACCATCT 3'
human IFN-β rev	5' AGTTTCGGAGGTAACCTG 3'
human 2`-5`-OAS fw	5' CAGTTAAATCGCCGGG 3'
human 2`-5`-OAS rev	5' AGGTTATAGCCGCCAG 3'
human IFNAR fw	5' ATTTACACCATTTTCGCAAAGC 3'

human IFNAR rev	5' CACTATTGCCTTATCTTCAGCTTCTA 3'
human GAPDH fw	5' GGTATCGTGGAAGGACT 3'
human GAPDH rev	5' GGGTGTGCTGTTGAA 3'

Mouse primers

mouse IFN- β fw	5' TTACTACTGCCTTTGCCA 3'
mouse IFN- β rev	5' GCGTAGCTGTTGTA CTTC 3'
mouse 2'-5'-OAS fw	5' CAGTGGATTGGACACTCT 3'
mouse 2'-5'-OAS rev	5' AGCACTTGAATGTTCCACC 3'
mouse CD8 fw	5' GGATTGGACTTCGCCTG 3'
mouse CD8 rev	5' CAAGTATGCTTTGTGTCAAAGA 3'
mouse IFN- γ fw	5' ATGGTGACATGAAAATCCTG 3'
mouse IFN- γ rev	5' GTGGACCACTCGGATGA 3'
mouse GAPDH fw	5' ACCAACTGCTTAGCCC 3'
mouse GAPDH rev	5' CCACGACGGACACATT 3'

4.1.9 Primers for PCR amplification of purified HBV-DNA (Invitrogen)

HBV-2595 fw	5' GAGCAAACATTATCGGGACT 3'
HBV-3081 rev	5' GACCAATTTATGCCTACAGC 3'

4.1.10 Sequencing primer of purified HBV-DNA (Invitrogen)

HBV-2595	5' GAGCAAACATTATCGGGACT 3'
----------	----------------------------

4.1.11 Enzymes

DNase I	Fermentas, St. Leon Rot, Germany
Exo-Minus Klenow DNA polymerase	Epicentre Biotechnologies, USA
Hind III restriction enzyme (hc. 10 U/ μ l)	Roche Diagnostics, Mannheim, Germany
Other restriction endonucleases	Fermentas, St. Leon Rot, Germany
RNaseA 10 mg/ml	Roche Diagnostics, Mannheim, Germany
RNase free DNase	Quiagen, Hilden, Germany
Proteinase K	Roth, Karlsruhe, Germany
Proteinase K inhibitor "Complete"	Roche Diagnostics, Mannheim, Germany
T7 RNA polymerase	Fermentas, St. Leon Rot, Germany

4.1.12 Weight- and Length standards

4.1.12.1 DNA standards

SmartLadder, 0.2-10 kb	Eurogentec, Liege, Belgium
SmartLadder, 0.1-2 kb	Eurogentec, Liege, Belgium

4.1.12.2 Protein standards

Prestained Protein ladder	Invitrogen, Karlsruhe, Germany
---------------------------	--------------------------------

4.1.13 Antibodies

4.1.13.1 Primary antibodies Western Blot

core-protein- Rabbit anti core (H800)	kindly provided by H. Schaller (ZMBH, University of Heidelberg, Germany)
L-protein - Goat anti HBsAg Antibody	Murex HBsAg ELISA, Version 3
Mouse anti RIG-I – Alme-1	Alexis biochemicals, Axxora, Lörrach, Germany
Rabbit anti -actin	Sigma, St. Louis, MO, USA

4.1.13.2 Secondary antibodies Western Blot

Goat anti rabbit, HRP-conjugated	Sigma, Deisenhofen, Germany
Goat anti mouse, HRP-conjugated	Sigma, Deisenhofen, Germany
Donkey anti goat, HRP-conjugated	Sigma, Deisenhofen, Germany

4.1.13.3 Histology

Polyclonal rabbit anti hepatitis B core antigen	Diagnostic Biosystems, CA, USA
--	--------------------------------

4.1.14 Radioactive [³²P] dCTP

Amersham, Buckinghamshire, England

4.1.15 Mouse strain

HBV transgenic mouse strain HBV1.3 -xfs was kindly provided by Prof. H. Schaller, ZMBH, University of Heidelberg, Germany. The mouse genome contains a genotype D HBV1.3 overlenght genome, with a frameshift mutation (G/C) in the x-gene at position 2916/2917 (Weber, Schlemmer et al. 2002).

4.1.16 Technical equipment

4.1.16.1 Instruments

Dot blot fraction recovery system	Beckman, München, Germany
Biocycler Thermocycler T3	Biometra, Göttingen, Germany
Blot chamber MiniProtean®3 Cell	BIO-RAD Laboratories, Hercules, USA
Dot blot apparatus Minifold I	Schleicher & Schuell, Dassel, Germany
ELISA Reader MRX Revelation	Dynex, Gaithersburg, USA
Film processor Curix 60	Agfa Geveart NV, Mortsel, Belgium
Flow cytometer FACSCanto™	BD Biosciences, Heidelberg, Germany
Gel chambers	BIO-RAD Laboratories, Hercules, USA
Heating block Thermomixer comfort	Eppendorf, Hamburg, Germany
Incubator	Heraeus Holding GmbH, Hanau, Germany
LightCycler® 1.5 and 480 II	Roche Diagnostics, Mannheim, Germany
Luminometer	Berthold Technologies, Bad Wildbad, Germany
pH-Meter	WTW, wissenschaftlich technische Werkstätten, Uniklinik Köln / MRI München
Cryostate CM 3050S	Leica Microsystems, Wetzlar, Germany
Pipetboy Swift Pet®	Abimed, Langenfeld, Germany
Phosphoimager, Molecular Imager FX	BIO-RAD Laboratories, Hercules, USA
Phosphoscreen-cassette	Amersham, Buckinghamshire, England
Photometer Smart Spec 3000	BIO-RAD Laboratories, Hercules, USA
Photometer Nanodrop	Implen, München, Germany
Photo system for agarose gels	BIO-RAD Laboratories, Hercules, USA
Gel-doc 2000	BIO-RAD Laboratories, Hercules, USA
Power Supplies Pack300	BIO-RAD Laboratories, Hercules, USA
Refrigerators and freezer	Liebherr, Lientz, Germany
Rocking platform WT12	Biometra, Göttingen, Germany
Shaker	Innova 4230, New Brunswick Scientific, USA
Sterile hood (cell cultur)	Heraeus Holding GmbH, Hanau, Germany
UV-Oven GS Gene Linker™	BIO-RAD Laboratories, Hercules, USA
ALT measurement, Reflotron®	Roche Diagnostics, Mannheim, Germany

4.1.16.2 Centrifuges

Centrifuge 5417C / 5417R	Eppendorf, Hamburg, Germany
Megafuge 1.0 / 1.0 R	Heraeus Holding GmbH, Hanau, Germany
Sorvall RC 50 Plus	Kendro, Langenselbold, Germany
XL 70	Beckman, München, Germany
Scales Kern 440-47	Sartorius AG, Göttingen, Germany

4.1.16.3 Microscopes

Fluorescence microscope IX81	Olympus, Hamburg, Germany
Confocal microscope FluoView1000	Olympus, Hamburg, Germany

4.1.16.4 Software

Autoradiography	Quantity One, 4.2.1, BIO-RAD Laboratories, Hercules, USA
Fluorescence microscopy	Cell P, AnalySIS, Soft Imaging System GmbH, Münster, Germany
Light Cycler	Probe Design Analysis and Rel Quant, Roche Diagnostics, Mannheim, Germany
Luminometer	Magellan Software, Tecan, Grödig, Austria
Data processing	Microsoft MS Office 2008 for Mac, Word and Excel 12.1.3, Microsoft, Redmont, USA Apple Macintosh OS-X, Cupertino, CA, USA
Graphic programmes	Adobe Photoshop CS3 10.0.1, Adobe Illustrator, CS3 13.0.2, Adobe, San Jose, USA Prism 5, 5.0a, for Mac OS X, Graphpad, La Jolla, CA, USA Power Point 2008 for Mac, 12.1.3, Microsoft, Redmont, USA
Statistical Analysis	Prism 5, 5.0a, for Mac OS X, Graphpad, La Jolla, CA, USA Bibliography EndNote X2, Thomson, San Francisco, CA, USA

4.2 Methods

4.2.1 Molecular biology methods

4.2.1.1 In vitro transcription (IVT)

Chemically synthesized RNA oligonucleotides were purchased from Eurogentec (Leiden, Belgium). *In vitro*-transcribed RNAs were synthesized using the Silencer siRNA construction Kit (Ambion, Huntingdon, UK) or according to the following protocol: Using partially overlapping single stranded DNA oligonucleotides, a double-stranded DNA template was constructed using Exo-Minus Klenow DNA polymerase. The obtained templates contained a T7 RNA polymerase consensus promoter sequence (5' CTATAGTGAGTCG 3'). 20 pmol of the DNA template were incubated with dNTP-Mix (2.5 mM each dATP, dCTP, dGTP and dTTP), 30 U T7-RNA polymerase, 40 U RNase inhibitor, 0.3 U yeast inorganic pyrophosphatase in a buffer containing 40 mM Tris-HCl pH 8.0, 10 mM DTT, 2 mM spermidine-HCl (Sigma) and 20 mM MgCl₂. *In vitro* transcription was carried out overnight at 37 °C. The DNA template was digested using DNase I (Fermentas) and subsequently RNAs were purified using the High pure RNA isolation kit with the following modifications: Binding buffer was 2.0 M guanidine thiocyanate in 70 % ethanol and wash buffer was substituted by 100 mM NaCl, 4.5 mM EDTA, 10 mM Tris HCl in 70 % ethanol. After elution, excess salts and NTPs were removed by passing the RNAs through a Mini Quick Spin™ Oligo Column. Size and integrity of RNAs was checked via gel electrophoresis.

4.2.1.2 Alexa 488 and cholesterol coupled siRNA

Si-1.2 was labeled at the sense-strand with 5'-Biotin or 5'-Biotin plus 3'-cholesterol, respectively (Eurogentec). Si-RNAs were incubated for 1 h at 37°C in the dark with Alexa-488 coupled streptavidin, 1 µg / µg siRNA (S21375, Invitrogen, Karlsruhe, Germany). Thereby, Alexa-488-streptavidin was linked to biotin at the 5'-end of the siRNA sense-strand. Fluorescently labeled siRNAs were precipitated (10% v/v 3M NaAc pH 5 and 400% v/v EtOH) at -20°C over night. Solution was centrifuged at 13.000 rpm for 30 min at 4°C. The siRNA pellet was washed once with 75% EtOH and solved in ddH₂O. Concentration was determined via OD measurement.

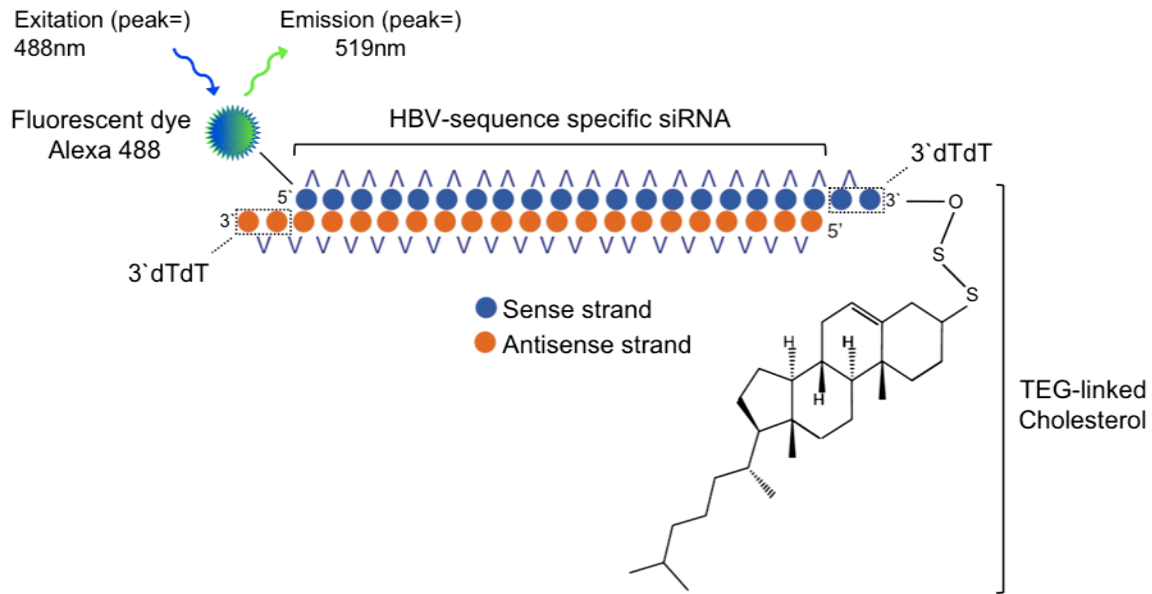


Fig. 4.2: Schematic representation of fluorescently labeled and/or cholesterol coupled si-1.2.

4.2.1.3 DNA and RNA quantification

To calculate the concentration of a DNA (or RNA) preparation, the absorption at 260 nm and 280 nm was determined with a photometer (Nanodrop). This technique relies on the characteristic of nucleic acids to absorb UV light with a wave-length of 260 nm. Absorption at 260 nm (OD_{260}) of 1 equals a DNA concentration of 50 $\mu\text{g/ml}$ (40 $\mu\text{g/ml}$). The ratio of the absorption at 260 nm and 280 nm allows estimating the purity of the DNA (or RNA) and should range between 1.8 and 2.0. The absorption was normalized to ddH_2O .

4.2.1.4 Gelelectrophoresis

DNA (or RNA) molecules are negatively charged, with the charge being proportional to the molecular weight. Therefore they can be separated according to their size in an electric field. Electrophoresis was performed in 0.8 - 2 % agarose gels. The agarose was dissolved in 1 x TAE buffer, and ethidium bromide was added to a final concentration of 0.5 $\mu\text{g/ml}$, after the agarose was cooled. Ethidium bromide intercalates into dsDNA. This results in a complex, which fluoresces when exposed to UV light (254 nm to 366 nm). Emission of 590 nm light allows the visualization of the DNA, with a detection limit of approximately 20 ng dsDNA (or RNA). The polymerized gel was covered with TAE buffer and electrophoresis was performed with a constant voltage of 30 to 120 V. The samples were mixed with 1x DNA (or RNA) sample buffer

to firstly ballast the DNA (or RNA) with glycerol, and to secondly mark the separation front with bromphenol blue. In addition to the samples a DNA (or RNA) standard with defined DNA (or RNA) sizes was loaded on the gel.

4.2.1.5 Polymerase chain reaction

PCR is a method to amplify specific DNA sequences located between 2 primers. These are complementary to the 5` and 3` ends of the sequence. The polymerase specifically amplifies the sequence in repeated amplification rounds. A master-mix was prepared with the following contents per reaction:

<u>Reagent</u>	<u>Concentration</u>
Polymerase buffer	4 µl
<i>Pfu</i> polymerase	2 µl
Primer fw	5 pmol
Primer rev	5 pmol
ddH ₂ O	12 µl

150 to 300 ng template DNA or ddH₂O were added per reaction. The Thermocycler was programmed as follows:

<u>Step</u>	<u>Temperature</u>	<u>Time</u>
1. Initial denaturation	94°C	2 min
2. Denaturation	94°C	30 sec
3. Annealing	60°C	30 sec
4. Elongation	72°C	90 sec
5. Final elongation	72°C	5 min

Steps 2 to 4 were repeated 30 times. The final elongation step is necessary to allow the complete amplification of the sequence fragments.

4.2.1.6 DNA sequencing

DNA sequencing was performed by GATC Biotech AG, Konstanz, Germany. Therefore, 30 µl of both, 10 - 50 ng / µl PCR-product and 10 pmol / µl sequencing

primer, respectively were dispatched separately. Taq-polymerase and dideoxynucleosidtriphosphates (ddNTPs) were provided by the company.

4.2.1.7 cDNA synthesis

To circumscribe RNA into cDNA the reverse transcription kit 'First-strand cDNA synthesis qRT-PCR, Superscript III' (Invitrogen) was used according to manufactures instructions.

4.2.1.8 Quantitative real time polymerase chain reaction (qRT-PCR) / Light cycler[®] PCR)

Real time PCR detection techniques make a kinetic quantification possible. PCR amplification depends mostly on the template concentration. However, reaction efficiency is also important: In high efficient reactions with low template concentrations the same plateau can be reached as in reactions with high template concentrations but low reaction efficiency. Therefore, end point quantification analyses are sometimes not accurate. The advantage of real time PCR is the measurement in the log-linear phase of constant amplification. This allows the precise quantification of the amount of starting material. For fluorescence detection the SYBR Green I Dye was used. This fluorescent dye intercalates only in dsDNA. The fluorescence intensity of this DNA-SYBR green complex is much higher than the intensity of the dye alone. Therefore, during annealing and elongation phases the fluorescent signal increases. The signal intensity is directly proportional to the DNA amount, and the highest signal is obtained at the end of the elongation phase. In the used LightCycler[®] systems 1.5 and 480 II, respectively, in which the PCR reaction takes place, a rapid thermal transfer is guaranteed. The fluorescence intensity is measured at the end of each elongation phase at a certain temperature in a single optical unit. The LightCycler PCR is very sensitive with a detection limit of 1 to 10 copies for plasmid DNA per sample. For genomic DNA the detection of a single-copy gene of 3 pg DNA is estimated. Different quantification methods are available with the LightCycler[®] System. Absolute quantification is performed with an external standard curve of known concentrations of the target DNA. The relative quantification expresses the target gene concentration in relation to a reference gene, usually a house keeping gene or mitochondrial DNA. Standard curves of both target and reference gene are used to obtain the concentrations. The template concentration is

Material and methods

determined with so-called crossing points. These points are defined as the cycle numbers, in which all amplifications exhibit the same fluorescence intensity. The identification of specific DNA products is possible using melting curve profiles. The melting temperature of dsDNA depends on length, GC content and sequence. Thus, every sequence has a specific melting curve profile. Within the PCR reaction, the melting curve is obtained by steadily increasing temperatures while the fluorescence is monitored.

This sensitive PCR technique was used to detect absolute amounts of HBV rcDNA, as well as relative amounts of HBV pgRNA, IFN- β , IFN- γ , 2'-5'-OAS, IFNAR and CD8, relativated to the housekeeping gene GAPDH, as well as HBV cccDNA relative to mitochondrial DNA. Quantification was performed relative to an internal calibrator dilution row or to an external plasmid HBV DNA standard (rcDNA) on a Light Cycler[®] instrument 1.5 or 480 II with the LightCycler FastStart DNA Masterplus SYBR Green I (Roche). This reaction mix contains the Taq-DNA-polymerase, reaction buffer, MgCl₂ and dNTPs. The following master-mix was prepared per reaction:

<u>Reagent</u>	<u>Vol.</u>
LightCycler FastStart DNA Masterplus SYBR Green I	10 μ l
Primer fw	1 μ l
Primer rev	1 μ l
ddH ₂ O	6 μ l

2 μ l template DNA or ddH₂O (negative control) were added to the mix. The light cycler instrument was basically programmed as followed:

<u>Step</u>	<u>Temperature</u>	<u>Time</u>
1. Initial denaturation	95°C	5 min
2. Denaturation	95°C	15 sec
3. Annealing	60°C	4 sec
4. Elongation	72°C	25 sec
5. Detection	88°C	2 sec

Targeting gene dependent modifications of the program were performed.

4.2.1.9 Isolation of progeny HBV-DNA from cell supernatant

HBV rcDNA was isolated from cell supernatant or mouse serum with QIAamp MinElute Virus Spin Kit (Qiagen) according to the manufacturers instructions.

4.2.1.10 Protein precipitation

Cells were washed with ice cold PBS and for whole cell protein isolation treated with SDS lysis buffer (15mM TRIS-HCl pH 6.8, 2.5% Glycerol, 0.5% SDS (10%) and 1 tablet proteinase-inhibitor `Complete`(Roche)) for 10min. Lysates were centrifuged at 11.000 rpm in table top centrifuge and supernatants were used for Western blot ananlysis.

4.2.1.11 Calculation of protein concentrations

To determine total protein concentrations the BCATM Protein Assay Kit (Pierce) was used. This assay is based on the reduction of Cu²⁺ to Cu⁺ by proteins in an alkaline medium, combined with the colorimetric detection of Cu⁺ with a reagent containing bicinchonic acid (BCA). The complex formed by the chelation of 2 BCA molecules with 1 Cu⁺ exhibits a strong absorbance at 562 nm. The absorbance is linear with increasing protein concentrations over a working range of 20 to 2000 µg / ml. The reaction was performed according to the manufacturers introductions, and an albumin protein dilution series served as protein standard.

4.2.1.12 SDS-page gel electrophoresis

Protein samples were mixed with WB sample buffer (2ml glycerol, 2ml 10% SDS, 0,25% bromphenol blue, 0.5 M TRIS-base and 1ml 10% SDS, added to 10ml with H₂O, 5 v/v β-mercaptoethanol were added freshly before use) and boiled for 10 min at 100°C. The indicated amount of protein was transferred to a 12.5 % SDS gel. (Resolving gel, 12.5%: 6.25 ml Acrylamid, 40%, 5 ml Tris, 1.5 M, pH 8.8, 8.55 ml H₂O, 230 µl SDS, 10%, 20 µl TEMED, 100 µl, APS, 10%; Stacking gel, 5%: 0.375 ml Acrylamid, 40%, 1.2 ml Tris, 0.5 M, pH 6.8, 3.325 ml H₂O, 50 µl SDS, 10%, 4 µl TEMED, 50 µl APS, 10%). As a standard for protein size a pre-stained marker (Fermentas) was added. The proteins were separated by electrophoresis in a blot chamber (MiniProtean[®]3 Cell, BIO-RAD) with constant amperage (25 mA per gel).

4.2.1.13 Western blot analysis

The proteins were transferred with transfer-buffer (25 mM TRIS, 192 mM Glycin, 20% methanol) from the SDS gel onto a methanol-activated PVDF membrane (Roche) using a semi-dry transfer cell (BIO-RAD). The amperage was calculated with the following formula: 1.2 mA/cm² of the gel for 1 h transfer. After protein transfer the membrane was blocked in blocking solution (5% w/v milk powder in PBS) for 1 h at RT or over night at 4°C and probed for 2 h at RT or over night at 4°C with the indicated antibody (H800 1:2000, goat anti HBsAg Ab and Alme-1 1:1000, anti β -actin Ab 1:5000) in antibody solution (10 mM TRIS, 5% w/v milk powder, 2% v/v BSA, 0.1 % Tween-20, pH 7.6). After 6 washing steps with PBS-Tween (0.5% v/v) 5 min each, the respective secondary HRP-conjugated antibody (1: 8000) was added in antibody solution and incubated for 1 h at RT. Blots were again washed 6 times, 5 min each with PBS-Tween (0.5% v/v). The detection was performed with the Enhanced Chemiluminescence detection kit (Amersham). If re-probing of the membrane with another antibody was necessary, the membrane was previously stripped with 0.2 M NaOH for 10 min. PDVF membranes were re-activated in methanol, and blocking and antibody incubation were performed as previously described.

4.2.1.14 ELISA assay HBsAg

The HBsAg ELISA (Murex, Abbott) detects different epitopes of the HBsAg. It was performed according to the manufacturers' instructions. The readout was in dual frequencies at 450 nm and, as a reference wavelength, 620 nm in a plate reader.

4.2.1.15 ELISA assay human IFN- γ and IL-6 and mouse IFN- α

ELISA assays were performed with undiluted cell supernatant or mouse sera 1:25 diluted according to manufacturers instructions.

4.2.1.16 Preparation of total RNA with Trizol®

Total RNA of murine liver cells was isolated out of 50 mg liver tissue by lysis in 1ml Trizol® reagent (Invitrogen). Isolation was performed according to manufacturers instructions.

4.2.1.17 Separation of total liver cell RNA and Northern blot analysis

Extracted total-RNA was separated in a vertical 1% agarosegel. 1,5 g agarose was boiled in 15 ml autoclaved 10x E-Puffer (300 mM NaH₂PO₄-2H₂O, 50 mM EDTA) and 105 ml DEPC-H₂O. After cooling down to 60°C, 30 ml formaldehyd (37%) were added. Agarose was transferred into the gel chamber. 25 µg of total-RNA were mixed on ice with 10 µl 10x E-Puffer, 15 µl formaldehyde and 40 µl formamide for denaturation. Samples were boiled 10 min at 65°C, placed on ice and 5 µl loading buffer were added to each sample. Gel electrophoresis was performed in 1 x E-Puffer at 80-100 V for 4 - 5 h at 4°C. Afterwards, the gel was washed 2x in H₂O and incubated for 4 min in 10 x SSC. Transfer onto a positively charged nylon-membrane was performed with 10 x SSC via capillary forces during 12 - 16 h. Membrane was washed for 5 min with 2 x SSC and then dried at RT for 10 min. RNA was cross-linked to the membrane under UV light at 125 mJ / cm². Membrane was stored at RT until hybridization with radioactive labeled HBV-genome specific probe.

4.2.1.18 Preparation of genomic DNA

Total DNA extraction from cultured HepG2 H1.3 cells or from liver tissue of mice, respectively, was performed by phenol / chloroform extraction. 1 x 10⁷ cells or 50 mg of homogenized liver tissue were lyzed in 1 ml proteinase K buffer (100 mM Tris pH 8,5; 5 mM EDTA; 0,2 % SDS; 200 mM NaCl) and 20 µl Proteinase K (20 mg/ml) under rotation at 37°C over night. Then, 1 ml of phenol was added, the suspension mixed and centrifuged 5 min at 5000 rpm and 4°C. Nucleic acids were solved due to their hydrophilic residues in the aqueous phase, whereas proteins accumulated in the interphase. Upper aqueous phase was transferred in a new reaction tube and 1ml of a mixture of phenol-chloroform (1:1) was added. After centrifugation for 5 min at 5000 rpm and 4°C the upper aqueous phase was again transferred to a new tube and 1 ml chloroform was added in order to remove residual phenol. After centrifugation for 5 min at 5000 rpm and 4°C the DNA containing upper aqueous phase was transferred to a new reaction tube and precipitated. Therefore, 600 µl of ice-cold isopropanol was added and incubated at 4°C for 30 min. Precipitated nucleic acids was pelleted by centrifugation at 14.000 rpm for 20 min and afterwards washed with 250 µl of 70 % ethanol. After repeated centrifugation the pellet was air-dried and resolved in 500 µl ddH₂O. Then, RNA was digested with 2,5 µl of RNase A (60mg / ml) for 2 h at 37°C.

Precipitation was repeated, DNA was resolved in 200 μ l ddH₂O and stored at -20°C until further experiments.

4.2.1.19 Separation of total liver cell DNA and Southern blot analysis

Before separation, the genomic DNA was digested with high concentrated (10 U / μ l) restriction enzyme Hind III over night at 37°C, which affected the HBV-DNA. Isolated HepG2 2.15 DNA as size control was additionally restricted with EcoR I, an HBV-genome single-cutter restriction enzyme, for 3 h at 37°C to perform linearization of the HBV-genome. DNA was separated in a vertical agarose-gel (0.8% w/v agarose in 1x TAE buffer) at 35 V for 16 h. After separation, the gel was washed with ddH₂O, incubated for 15 min with 0.4 M NaOH to denature the DNA and then incubated with 0.2 M HCl for 5 min for depurination of the DNA. Transfer onto a positively charged nylon-membrane was performed with 0.4 M NaOH via capillary forces during 12 - 16 h. for neutralization, membrane was washed for 3 min with 2 x SSC and then dried at RT for 10 min. DNA was cross-linked to the membrane under UV light at 125 mJ / cm². Membrane was stored at RT until hybridization with radioactive labeled HBV-genome specific probe.

4.2.1.20 Radioactive HBV-genome specific probes

25 ng of HBV-DNA (isolated of HBV-wt plasmid) or GAPDH-DNA, respectively, were primed with desoxy-cytosine-tri-phosphates [α 32P] dCTP] by random-priming with Rediprime II DNA Labeling System (Amersham), according to manufacturers instructions.

4.2.1.21 Hybridization with radioactive labeled probes

Northern- or southern blot membranes were incubated at 65°C for 3 h with Church-buffer (6 x SSC, 5 x Denhardt's solution; Denhardt's solution: 1% w/v Ficoll 400, 1% w/v Polyvinylpyrrolidone, 1% w/v BSA) and 50 μ l (10 μ g / ml) salmon-sperm to block unspecific binding sites. Radioactive probe was denatured at 100°C for 5 min, cooled on ice and then added to the buffer solution. Hybridization was performed over night at 65 °C. Then, membranes were washed at 65°C for 15 min each with pre-warmed washing buffer I (2 x SSC, 0.1% SDS), washing buffer II (1 x SSC, 0.1% SDS) and washing buffer III (0.5 x SSC, 0.1% SDS). Membranes were air-dried for 10 min,

radioactive signal was quantified via X-ray film or phosphoscreen after different timepoints with a phosphoimager (BIO-RAD).

4.2.2 Cell biology methods

All procedures were carried out under sterile conditions using sterile solutions and equipments. All cells were cultivated in a humidified incubator at 37°C containing 5% CO₂.

4.2.2.1 Eukaryotic cell lines

Cells were incubated at 37°C and 5% CO₂. The human hepatoma cell lines HuH7, HuH7.5 were maintained in complete DMEM medium and passaged at a ratio of 1:5 when confluent. HepG2 H1.3 and HepG2.2.15 cell were cultivated in complete DMEM or, for virus production, in a 1:1 mixture of PHH medium and complete Williams E medium. HEK 293 cells were kept in complete DMEM and passaged at a ratio of 1:5 when confluent.

4.2.2.2 Isolation of primary human hepatocytes (PHHs)

PHH were isolated from fresh surgical liver specimen from patients undergoing partial hepatectomy. The procedure was approved by the local Ethics Committee, with obtained consent of the patients. Protocol was performed as previously described (Schulze-Bergkamen, Untergasser et al. 2003). The pre-perfusion medium, perfusion medium, and the PHH medium were warmed to 37°C prior to the perfusion, and the wash medium was cooled to 4°C. The healthy liver tissue piece was placed on a kidney dish. A large branch of the port vein was canulated, and the canula was fixed with tissue paste. The two-step collagenase perfusion started with 500 ml pre-perfusion medium, with a flow rate between 20 and 40 ml/min. For a satisfactory result it is important that the whole tissue is evenly perfused. At cut surfaces with high medium passage, the large vessels were occluded with tissue paste. The medium was discarded after traversing the liver tissue. After 15 to 20 min, perfusion was continued with 250 ml perfusion medium containing freshly added collagenase type IV (Worthington). 100 ml of the collagenase perfusion medium were kept and perfusion was continued with this remaining amount of medium. Collagenase treatment was performed for 15 to 20 min, depending on liver section size. As soon

Material and methods

as the tissue softened and liver cells appeared in the medium, the liver was cut into small pieces and the tissue was scratched off with a scalpel. If collagenase digestion was incomplete, the suspension was transferred to a sterile beaker and stirred for 10 min at 37°C. The cell suspension was filtrated through double-layered gaze and a 70 µm cell strainer. After centrifugation in 50 ml Falcon tubes for 5 min at 50 x g at 10°C, the pellet was re-suspended in 40 ml wash medium. Supernatant was used for isolation of LSECs and Kupffer cells. The wash step was repeated 3 times. The cells were re-suspended in PHH medium and the cell number and viability was determined. The cells were seeded on collagenised cell culture dishes at a density of to 8×10^5 cells per ml in PHH medium supplemented with 10% FCS. After 3 h the medium was exchanged to remove non-adherent cells. One day post seeding, the cells were kept in medium containing 5% FCS. From day 2 post seeding the cells were cultivated in FCS-free medium and were usable for experiments.

4.2.2.3 Isolation of LSECs and Kupffer cells

Seperation of human Kupffer cells (KCs) and liver sinusoidal endothelial cells (LSECs) from human liver non-parenchymal cell (NPC) suspension (in 1. supernatant of PHH cell isolation described above) was performed as followed: Kupffer cells:

Suspension of cells were centrifuged with 300 rcf, 10 min, at 4°C. Pellet was washed with PBS and again centrifuged with 300 rcf, 10 min, at 4°C. Simultaneously, density-Gradient was prepared: 20 ml 9% OptiPrep diluted with PBS over 10 ml 16% OptiPrep. Pellet was resuspended in 20 ml PBS and the suspension carefully applied on the density gradient. Gradient was centrifuge with 800 rcf, 25 min, at RT, with deactivated break. NPCs were now separated into two bands: the upper band contained the ITO cells, the lower band the KCs and LSECs. The lower band was collected, cells resuspended with PBS in a 50 ml reaction tube and centrifuged with 300 rcf, 10 min, at 4°C. Then, cell pellet was resuspended in PHH medium, the volume depended on the size of the pellet. LSECs and Kupffer cells were separated as followed. Cells were counted, and dispersed (5×10^5 cells / ml) for 12-well plate range. For the adherence step of KCs, cell suspension was incubated for 20 min in humidified incubator at 37°C containing 5% CO₂ without the possibility of shaking. KCs adhered to the plastic surface. Medium was taken of and collected (contained LSECs). Each well was washed three times with warm PBS, the supernatant was collected each time. Adherent KCs were incubated with RPMI medium in a

humidified incubator at 37°C containing 5% CO₂ for further experiments. All supernatants from the washing steps were collected in a 50 ml reaction tube for isolation of LSECs:

Collected supernatants were centrifuged at 300 rcf, 5 min, at RT. Supernatant was dispersed and the pellet resuspended in an adjusted volume of LSEC medium. Cells were counted and 20 µl FcR blocking reagent (Miltenyi) per 10⁷ cells was added. Suspension was mixed gently and incubated for 5 min at 4°C. Afterwards, 20 µl CD31 magnetic beads (Miltenyi) per 10⁷ cells were added, suspension was mixed gently and incubated for 15 min at 4°C. 1 ml LSEC medium per 10⁷ cells was added and centrifuged with 300 rcf, 5 min, at RT. Pellet was resuspended in 1 ml LSEC medium. Miltenyi MS column in the magnetic field were prepared. MS column was equilibrated with 500 µl LSEC medium. Cell suspension was applied onto the column and afterwards washed 3x with LSEC medium. Then, the column was removed from the magnet and CD31 positive cells squeezed out using 1 ml LSEC medium and the stamp. Separated cells were counted and applied in collagenized wells with LSEC medium. Cells were incubated in a humidified incubator at 37°C containing 5% CO₂ for further experiments.

4.2.2.4 Transfection of cells

All cell types cell were transfected with the indicated RNA-oligonucleotides using HiPerFect® (Qiagen) according to the manufacturers protocol: Cells were plated immediately prior to transfection in fresh medium to obtain a 40 to 60% confluent monolayer at the following day. 1 µg RNA-oligonucleotide was used per 3.125 x 10⁵ cells, except poly(I:C), due to cytotoxicity, only 1/10 was used (1 µg per 3.125 x 10⁶ cells). The RNA-oligonucleotide was mixed with serum free medium and 8,75 µl HiPerFect per µg RNA-oligonucleotide. After 10 min incubation the solution was added drop wise to the cells. Inoculums were left on the cells over night. Fresh medium was applied at the next day.

4.2.2.5 Production of wild type HBV

For the production of wtHBV the HepG2.2.15 cell (genotype A) line was used. This cell line contains 1.1 fold over-lengths HBV genomes stably integrated into the cellular genome. Therefore, they permanently produce HBV, which can be harvested in the supernatant of the cells. The cells were cultivated until confluent in complete

DMEM medium. Then the medium was exchanged to 50% PHH medium and 50% complete Williams E medium. Every 2 to 3 days the virus-containing medium was collected and cell debris was removed by centrifugation at 1000 rpm for 10 min. The supernatant was transferred to centrifugal filter devices (Centricon Plus-70, Biomax 100, Millipore Corp.) The first centrifugation was performed at 3500 x g for 1 h. In this step, the virus particles are captured in a filter. Because of the exclusion limit of 100 kDa, serum proteins flow through, while proteins larger than 100 kDa are kept. In a second, invert centrifugation step, performed at 1000 x g for 3 min, the filter system was turned upside down, to elute the virus. The virus containing concentrate was filled to 1 ml with PBS and a final concentration of 10% glycerol. The virus concentrate was stored in 100 µl aliquots at -80°C until further use. The titer of the produced wtHBV was measured as enveloped, DNA-containing viral particles. A CsCl density-gradient, followed by dot blot analysis, was performed as outlined below.

4.2.2.6 Caesium chloride density gradient

In the context of a virus production different types of particles are obtained in the preparation: naked DNA, unenveloped DNA-containing capsids, and enveloped virions. Their different densities enable to separate them in a density gradient. DNA is centrifuged down to the bottom, because of the very small size. DNA-containing capsids sediment at a density of 1.3 g/l while intact virions can be found in the 1.22 g/l fraction. The CsCl density gradient ultra centrifugation was performed with the SW-60 swing bucket rotor. In SW-60 polyallomer vials (Beranek Laborgeräte) 500 µl of CsCl solutions with the following densities were carefully layered one upon the other: 1.4 g/l, 1.3 g/l and 1.15 g/l. On top of the CsCl solutions 500 µl of a 20% sucrose solution was layered, and the sample was applied. The vials were filled up with PBS and tared on micro scales. Ultra-centrifugation was performed at 55.000 rpm at 20°C for 4 h to over night. The first 12 density fractions from the bottom were collected with a Dot Blot Fraction recovery system (Beckman). Each fraction contained a volume of approximately 175 µl. The fractions were subjected to quantitative dot blot analysis.

4.2.2.7 Dot blot analysis

To quantitatively and qualitatively analyze the produced wtHBV, a DNA dot blot was performed. The DNA fractions, obtained by CsCl density centrifugation, were dotted to a nylon membrane in a dot blot aperture. A HBV DNA standard ranging from 8 pg to 1000 pg was added. Samples and standard were washed once with 200 μ l PBS and the membrane was transferred to a 3 mm Whatman paper. Following denaturation in Soak 1 (0.5 M NaOH, 1 M NaCl), renaturation in Soak 2 (0.5 M Tris, pH 7.4, 3 M NaCl) was performed. Then the DNA was cross-linked at 125 mJ / cm² to the membrane in a UV oven. The membrane hybridized with a ³²P-labelled HBV DNA probe at 65°C over night, as previously described. After wrapping the radioactive membrane in saran wrap, the DNA was quantified with a phospho-imager (BIO-RAD).

4.2.2.8 HBV-infection of PHHs

Infection of PHHs with HBV was performed in medium containing 5% PEG 8000. The cells were incubated over night with HBV at a MOI of 100 virions/cell. After over night inoculation, cells were washed 3 times with PBS. Cells were further cultivated in fresh medium, and cell culture medium was collected at indicated time points. To monitor infection, HBsAg and HBeAg were determined using commercial immuno-assays (AxSYM®, HBeAg 2.0, HBsAg V2, Abbott Laboratories, HBsAg ELISA, Abbott).

4.2.2.9 Dual-luciferase assay

First, 2×10^5 HEK 293 cells were plated per 24-well-plate and incubated over night. At day 1 cells were transfected (Fugene6, according to manufacturers instructions) with a) 100 ng/well of plasmid p125, containing ORF of *Firefly*-Luciferase under IFN- β promoter (nt-125 - nt-55) and b) 10 ng/well of plasmid pRL-TK, containing ORF of *Renilla* luciferase, used as internal control for transfection efficiency. To enhance RIG-I expression, 1000U / ml medium of universal type-I IFN (PBL) was added appropriate 8 h after transfection for 16 – 20 h (until day 2) to supernatant of cells. Therefore medium was changed previously to P/S free HEK 293 medium. At day 2 3p-RNA oligonucleotides were transfected (Lipofectamine 2000, according to manufacturers instructions) into cells. At day 3 cell lysates were prepared for luciferase detection assay. Supernatant of cells was discarded and 100 μ l of 1x

passive lysis buffer / well was added. For lysis (4.2.2.5.1) cells were incubated for 20 min at RT on a shaker platform.

Plasmids and dual luciferase kit were kindly provided by Dr. Katharina Eisenächer, AG PD Dr. med. Anne Krug, II. Medizinische Klinik und Polyklinik (Gastroenterology), MRI München.

4.2.2.10 Luciferase detection

Firefly (*Photinus pyralis*) and *Renilla* (*Renilla reniformis*) luciferase are enzymes that convert their substrate Beetle luciferin into oxyluciferin (Firefly) or coelenterazine into coelenteramide (Renilla). In this reaction light is emitted proportional to the enzyme concentration. To quantify the light emission the *Firefly*-Luciferase Assay system (Promega) was used, according to to manufacturers instructions. HEK 293 cells were lysed in 100 µl lysis buffer per well at day 3 post transfection. 80 µl LAR II buffer (luciferase assay buffer + luciferin) was added into a cuvette and 20 µl of lysate was added. After mixing by pipetting for 5 seconds the samples were transferred to a luminometer (Berthold Technologies). After 5 sec the light emission of *Firefly* luciferase expression was measured for 10 sec in a luminometer (measurement I). After quantifying the firefly luminescence 80 µl of Stop & Glow was added, which stopped the reaction and simultaneously the initiated the renilla luciferase reaction by adding its substrate (Coelenterazien). Samples were mixed by vortexing. *Renilla*-Luciferase expression was measured according to measurement of *Firefly*-Luciferase (measurement II). The luminescence (RLU) of measurement I were set as relative value to RLU of measurement II and normalised to mock transduced cells, serving as negative control. The RLU determined in these samples were defined as 1, the other values were adapted proportionally.

4.2.2.11 Cytotoxicity assays XTT

Viability of HepG2 H1.3 cells after transfection of RNA oligonucleotides in triplicate was tested with XTT - Cell Proliferation Kit II (Roche), according to manufacturers instructions at indicated timepoints from 24h up to 16 days. 25µl XTT labeling mixture was added to each well and incubated for 2 h.

The cell viability assay determining cleavage of tetrazolium salts (XTT) to formazan by the "succinate-tetrazolium reductase" system. This system belongs to the respiratory chain of mitochondria, and is only active in metabolically active cells. The

assay is based on the cleavage of the tetrazolium salt XTT in the presence of an electron-coupling reagent, producing a soluble formazan salt. This conversion only occurs in viable cells. Cells grown in a 96-well tissue culture plate are incubated with the XTT labeling mixture for approximately 2 - 20 hours. After this incubation period, the formazan dye formed is quantitated using a scanning multi-well spectrophotometer (ELISA reader). The absorbance revealed directly correlates to the cell number.

4.2.3 Mouse experiments

Animal experiments were approved by the ethics committee of the Bezirksregierung Köln and were performed in accordance with the German animal protection law. HBV tg mice used in this study were of comparable weight and age.

4.2.3.1 Bleeding of mice and serum preparation

Mice were bled retro bulbar or sacrificed, respectively. After scarification mice fixed and blood was extracted from the heart muscle with a syringe. Blood was centrifuged for 10 min at 6000 rpm and RT. Serum supernatant was added to a new reaction tube and stored at -20°C for further analysis of ALT levels or determination of viral DNA and antigen load.

4.2.3.2 Determination of ALT activity

The liver specific enzyme alanine aminotransferase (ALT) is secreted by apoptotic hepatocytes into the blood. The concentration is therefore a highly specific marker for liver damage. Determination of ALT activity in the blood was used to specify the grade of liver inflammation in mice. Analysis was performed with 32 µl of fresh mouse serum on Reflotron® stripes in Reflovet® automat.

4.2.3.3 Classical and hydrodynamic intravenous injection

All mouse studies were conducted at animal facility of IMMIH in Köln under S2 conditions and animal care guidelines (authorized by Regierung von Köln). RNA oligonucleotides (25g/mice/injection) were intravenously injected after complexation with *in vivo-JetPEI* (Polyplus) in a total volume of 200 µl (5% glucose), according to

manufacturers instructions. Injection was repeated after 3 days and antiviral effects were analyzed 6 to 15 days after first injection.

Alternatively, mice were injected by hydrodynamic injection (HDI). By HDI the nucleic acid is intravenously injected in a high volume of buffer (8% of body weight) during 5 – 10 seconds under high pressure into the tail vein of the mice. By an averaged bodyweight of 20 g per mouse the siRNA is diluted in 1,6 ml of PBS, which reflects ~50% of the blood volume.

4.2.3.4 Organ perfusion

Mice were sacrificed and perfused with 50 ml buffered paraformaldehyd (PFA, 4%) via left ventricle, vena portae or the vena cava, respectively. Fixed organs were removed and stored in buffered PFA (4%) over night. To remove H₂O, organs were then stored in 25% sucrose solution at 4°C over night. For tissue-slices organs were completely embedded in Tissue-Tak® Tec. After freezing at -80°C over night organ slices of 8µm were cut in a cyrostate (Leica) and embedded on object-slides. Organ-slices were mounted with Mowiol/Dabco. A cover slip was sealed on the slide with nail polish. The slides were stored at 4°C and analyzed by fluorescence microscopy.

4.2.3.5 Fluorescence microscopy

Examination was performed on an Olympus IX81 microscope or on an Olympus FluoView1000 confocal microscope.

4.2.3.6 Histology

Mice were sacrificed and organs were removed. Organ samples were treated with formalin. Pathology Helmholtz-Center Munich embedded the pieces in paraffin for blinded histological examination. Two-µm-thick sections were cut and stained with a) haematoxylin and eosin (H&E) and periodic acid-Schiff (PAS) or b) polyclonal rabbit anti hepatitis B core antigen antibody. The histopathological alterations were classified for a) in: -changes affecting the portal tracts (e.g. inflammation, degenerative changes of the bile ducts, fibrosis); - changes affecting the lobule (e.g. spotty and bridging necrosis, degenerative changes of the hepatocytes, fibrosis); - changes affecting the vessels (e.g. inflammation, fibrosis, thrombosis). The histopathological alterations were graded as mild, moderate and severe depending on their frequency and severity. Focal lesions (e.g. spotty necrosis) were counted

through the whole tissue specimen. The histopathological core-staining was classified in: nuclear positivity; the intensity was comparable in all samples, the localization was always diffuse. As well as in cytoplasmic positivity; the localization, intensity and distribution (diffuse: around most central venules; multifocal: around multiple central venules; focal) were determined.

4.2.4 Statistical analysis

For statistical analysis, the data were subjected to unpaired, two-tailed Student's *t*-test and statistical significance was determined confidence intervals of 95%.

4.2.5 HBV sequence

Read from ASCII file hpb ayw.gbo; HBV -3182 nt- (ayw)-Galibert; AccNo. J02203; ori set to core ATG.

Targeting sequences of siRNAs si-1.1, si-1.2 and si-1.3 are marked

```
ATGGACATCGACCCTTATAAAGAATTTGGAGCTACTGTGGAGTTACTCTCGTTTTTGCCTTC
TGA CTTCTTTCCCTTCAGTACGAGATCTTCTAGATAACCGCCTCAGCTCTGTATCGGGAAGCCT
TAGAGTCTCCTGAGCATTGTTACCTCACCATACTGCACTCAGGCAAGCAATTCCTTGCTGG
GGGGA ACTAATGACTCTAGCTACCTGGGTGGGTGTTAATTTGGAAGATCCAGCGTCTAGAGA
CCTAGTAGTCAGTTATGTCAACACTAATATGGGCCTAAAGTTCAGGCAACTCTTGTGGTTTC
ACATTTCTTGTCTCACTTTTGGGAAGAGAAACAGTTATAGAGTATTTGGTGTCTTTCGGAGTG
TGGATTTCGCACTCCTCCAGCTTATAGACCACCAAATGCCCTATCCTATCAACACTTCCGGA
GACTACTGTTGTTAGACGACGAGGCAGGTCCCCTAGAAGAAGAACTCCCTCGCCTCGCAGAC
GAAGGTCTCAATCGCCGCGTCGCAGAAGATCTCAATCTCGGGAATCTCAATGTTAGTATTC
TTGGACTCATAAGGTGGGGAAC TTTACTGGGCTTTATTCTTCTACTGTACCTGTCTTTAATC
CTCATTGGAAAACACCATCTTTTCCTAATATACATTTACACCAAGACATTATCAAAAAATGT
GAACAGTTTGTAGGCCACTCACAGTTAATGAGAAAAGAAGATTGCAATTGATTATGCCTGC
CAGGTTTTATCCAAAGGTTACCAAATATTTACCATTGGATAAGGGTATTAACCTTATTATC
CAGAACATCTAGTTAATCATTACTTCCAAACTAGACACTATTTACACACTCTATGGAAGGCG
GGTATATTTATATAAGAGAGAAACAACACATAGCGCCTCATTTTGTGGGTCACCATATTCTTG
GGAACAAGATCTACAGCATGGGGCAGAATCTTTCCACCAGCAATCCTCTGGGATTCTTTCCC
GACCACCAGTTGGATCCAGCCTTCAGAGCAAACACCGCAAATCCAGATTGGGACTTCAATCC
CAACAAGGACACCTGGCCAGACGCCAACAAGGTAGGAGCTGGAGCATTCCGGGCTGGGTTTCA
CCCCACCGCACGGAGGCCTTTTGGGGTGGAGCCCTCAGGCTCAGGGCATACTACAAACTTTG
CCAGCAAATCCGCCTCCTGCCTCCACCAATCGCCAGTCAGGAAGGCAGCCTACCCCGCTGTC
TCCACCTTTGAGAAACACTCATCCTCAGGCCATGCAGTGGAATTCACAACCTTCCACCAA
CTCTGCAAGATCCCAGAGTGAGAGGCCTGTATTTCCCTGCTGGTGGCTCCAGTTCAGGAACA
GTAAACCCTGTTCTGACTACTGCCTCTCCCTTATCGTCAATCTTCTCGAGGATTGGGGACC
TGCGCTGAACATGGAGAACATCACATCAGGATTCCTAGGACCCCTTCTCGTGTACAGGCGG
GGTTTTTCTTGTGACAAGAATCCTCACAATACCGCAGAGTCTAGACTCGTGGTGGACTTCT
CTCAATTTTCTAGGGGGA ACTACCGTGTGTCTTGGCCAAAATTCGCAGTCCCCAACCTCAA
TCACTACCAAACCTCTTGTCTCCA ACTTGTCTGGTTATCGCTGGATGTGTCTGCGGCGTT
```

TTATCATCTTCCTCTTCATCCTGCTGCTATGCCTCATCTTCTTGTGGTTCTTCTGGACTAT
CAAGGTATGTTGCCCGTTTGTCTCTAATTCAGGATCCTCAACAACCAGCACGGGACCATG
CCGGACCTGCATGACTACTGCTCAAGGAACCTCTATGTATCCCTCCTGTTGCTGTACCAAAC
CTTCGGACGGAAATTGCACCTGTATTCCCATCCCATCATCCTGGGCTTTCGGAAAATTCCTA
TGGGAGTGGGCCTCAGCCCCTTTCCTGGCTCAGTTTACTAGTGCCATTTGTTTCAAGTGGT
CGTAGGGCTTTCCTCCACTGTTTGGCTTTCAGTTATATGGATGATGTGGTATTGGGGCCAA
GTCTGTACAGCATCTTGAGTCCCTTTTACCCTGTTACCAATTTTCTTTTGTCTTTGGGTA
TACATTTAAACCCTAACAAAACAAAGAGATGGGGTACTCTCTAAATTTTATGGGTTATGTC
ATTGGATGTTATGGGTCCTTGCCACAAGAACACATCATACAAAAAATCAAAGAATGTTTTAG
AAAACCTC**CTATTAACAGGCCTATTGA**ATTGGAAAGTATGTCAACGAATTGTGGGTCTTTTGG
GTTTTGCTGCCCTTTTACACAATGTGGTTATCCTGCGTTGATGCCTTTGTATGCATGTATT
CAATCTAAGCAGGCTTTCACTTTCGCAACTTACAAGGCCTTTCCTGTGTAAACAATACCT
GAACCTTTACCCCGTTGCCCGCAACGGCCAGGTCTGTGCCAAGTGTGGCTGACGCAACCC
CCACTGGCTGGGGCTTGGTCATGGGCCATCAGCGCATGCGTGGAACCTTTTCGGCTCCTCTG
CCGATCCATACTGCGGAACCTTAGCCGCTTGTTTTGGCTCGCAGCAGGTCTGGAGCAAACAT
TATCGGGACTGATAACTCTGTTGTCTATCCCGCAAATATACATCGTTTCCATGGCTGCTAG
GCTGTGCTGCCAACTGGATCCTGCGCGGGACGTCCTTTGTTTACGTCCCGTCGGCGCTGAAT
CCTGCGGACGACCCTTCTCGGGGTCGCTTGGGACTCTCTCGTCCCCTTCTCCGTCTGCCGTT
CCGACCGACCACGGGGCGCACCTCTCTTTACGCGGACTCCCCGTCTGTGCCTTCTCATCTGC
CGGACCGTGTGCACTTCGCTTACCTCTGCACGTCGCATGGAGACCACCGTGAACGCCACC
AAATATTGCCCAAGGTCTTACATAAGAGGACTCTTGGACTCTCAGCAATGTCAACGAC**CGAC**
CTTGAGGCATACTTCAAAGACTGTTTGTTTAAAGACTGGGAGGAGTTGGGGGAGGAGATTAG
GTTAAAGGTCTTGTACTAGGAGGCTGTAGGCATAAATTGGTCTGCGCACCAGCACCATGCA
ACTT**TTTACCTCTGCCTAATCA**TCTCTTGTTCATGTCTACTGTTCAAGCCTCCAAGCTGT
GCCTTGGGTGGCTTTGGGGC

6 List of abbreviations

2`-5`-OAS	2`-5`-oligoadenylate synthetase
3p	5`-Triphosphated
A	Adenine
aa	Amino acid
ALT	Alanine aminotransferase
Ab	Antibody
APS	Ammonium persulphate
bp	Base pair
C	Cytosine
cccDNA	Covalently closed circular DNA form of HBV
cDNA	CopyDNA, to mRNA complementary DNA
C-terminal	Carboxy-terminal
Ctrl	Control
d	Day
ddH ₂ O	Double distilled water
DNA	Desoxyribonucleic acid
ds	Double-stranded
EDTA	Ethylenedinitrilotetraacetic acid
e.g.	exempli gratia
EIA	Enzyme immuno-assay
ELISA	Enzyme linked immunoabsorbent assay
Enh	Enhancer
EtBr	Ethidiumbromide
FCS	Fetal calf serum
G	Guanine
GAPDH	Glyceraldehyde 3-phosphate dehydrogenase
h	Hour
HBeAg	HBV e-antigen
HBsAg	HBV s-antigen
HBV	Hepatitis B virus
HCC	Hepatocellular carcinoma

Abbreviations

HRP	Horse radish peroxidase
IFNAR	Interferon α/β receptor
Ig	Immunoglobulin
IL-6	Interleucin-6
IFN	Interferon
IP-10	Interferon-inducible protein 10
IVT	<i>In vitro</i> transcription
kb	Kilo base
kDa	Kilo Dalton
l	Liter
L-protein	Large surface protein of HBV envelope
LPS	Lipopolysaccharide
mA	Milli-ampere
MDA-5	Melanoma differentiation associated gene-5
μg	Microgram
mg	Milligram
MHC	Major histocompatibility complex
Min	Minute
μl	Microliter
ml	Milliliter
μM	Micromolar
mM	Millimolar
MOI	Multiplicity of infection; infection ratio in number of virus per cell
M-protein	Middle surface protein of HBV envelope
mRNA	Messenger RNA
n	Number
ng	Nanogram
nM	Nanomolar
N-terminal	Amino-terminal
nt	Nucleotide
OD	Optical density
ori	Origin of replication
ORF	Open reading frame
P	P-value

Abbreviations

PAGE	Polyacrylamide gel electrophoresis
PCR	Polymerase chain reaction
pgRNA	Pregenomic RNA template of HBV
PHH	Primary human hepatocytes
PolyA	Polyriboadenosine
Poly(I:C)	Polyinosinic-polycytidylic acid
preS1	C-terminal domain of HBV L-protein
preS2	C-terminal domain of HBV M-protein
p.inf.	After infection
p.inj.	After injection
p.tr.	After transfection
qRT-PCR	Quantitative real-time polymerase chain reaction
rcDNA	Relaxed circular DNA: partial double-stranded HBV-genome
RIG-I	Retinoic acid inducible gene I
RLU	Relative light units
RNA	Ribonucleic acid
Rpm	Rounds per minute
RT	Room temperature
scFv	Single chain fragment of the variable region
SD	Standard deviation
sgRNA	Subgenomic RNA template of HBV
S-protein	Small surface protein of HBV envelope
ss	Single-stranded
SVP	Subviral particle
T	Thymine
TAE	Tris-acetate-EDTA buffer
TBS	Tris buffered saline
Tg	Transgenic
TLR	Toll-like receptor
TNF α	Tumor necrosis factor α
U	Uracil
U	Units
v/v	volume per volume
w/v	weight per volume

6 Bibliography

- Aiello, L., R. Guilfoyle, et al. (1979). "Adenovirus 5 DNA sequences present and RNA sequences transcribed in transformed human embryo kidney cells (HEK-Ad-5 or 293)." *Virology* **94**(2): 460-9.
- Akashi, H., M. Miyagishi, et al. (2005). "Escape from the interferon response associated with RNA interference using vectors that encode long modified hairpin-RNA." *Mol Biosyst* **1**(5-6): 382-90.
- Akira, S. and K. Takeda (2004). "Toll-like receptor signalling." *Nat Rev Immunol* **4**(7): 499-511.
- Akira, S., S. Uematsu, et al. (2006). "Pathogen recognition and innate immunity." *Cell* **124**(4): 783-801.
- Alexopoulou, L., A. C. Holt, et al. (2001). "Recognition of double-stranded RNA and activation of NF-kappaB by Toll-like receptor 3." *Nature* **413**(6857): 732-8.
- Almeida, R. and R. C. Allshire (2005). "RNA silencing and genome regulation." *Trends Cell Biol* **15**(5): 251-8.
- Andreyev, H. J., A. R. Norman, et al. (2001). "Kirsten ras mutations in patients with colorectal cancer: the 'RASCAL II' study." *Br J Cancer* **85**(5): 692-6.
- Applequist, S. E., R. P. Wallin, et al. (2002). "Variable expression of Toll-like receptor in murine innate and adaptive immune cell lines." *Int Immunol* **14**(9): 1065-74.
- Banchereau, J., F. Briere, et al. (2000). "Immunobiology of dendritic cells." *Annu Rev Immunol* **18**: 767-811.
- Banchereau, J., F. Briere, et al. (1994). "Molecular control of B lymphocyte growth and differentiation." *Stem Cells* **12**(3): 278-88.
- Barnard, D. L. (2001). "Pegasys (Hoffmann-La Roche)." *Curr Opin Investig Drugs* **2**(11): 1530-8.
- Bartenschlager, R. and H. Schaller (1992). "Hepadnaviral assembly is initiated by polymerase binding to the encapsidation signal in the viral RNA genome." *EMBO J* **11**(9): 3413-20.
- Barton, G. M. (2007). "Viral recognition by Toll-like receptors." *Semin Immunol* **19**(1): 33-40.
- Baumert, T. F., C. Rosler, et al. (2007). "Hepatitis B virus DNA is subject to extensive editing by the human deaminase APOBEC3C." *Hepatology* **46**(3): 682-9.
- Bchini, R., F. Capel, et al. (1990). "In vitro infection of human hepatoma (HepG2) cells with hepatitis B virus." *J Virol* **64**(6): 3025-32.
- Beasley, R. P., L. Y. Hwang, et al. (1981). "Hepatocellular carcinoma and hepatitis B virus. A prospective study of 22 707 men in Taiwan." *Lancet* **2**(8256): 1129-33.
- Beck, J. and M. Nassal (2007). "Hepatitis B virus replication." *World J Gastroenterol* **13**(1): 48-64.
- Berting, A., J. Hahnen, et al. (1995). "Computer-aided studies on the spatial structure of the small hepatitis B surface protein." *Intervirology* **38**(1-2): 8-15.
- Bertoletti, A., C. Ferrari, et al. (1991). "HLA class I-restricted human cytotoxic T cells recognize endogenously synthesized hepatitis B virus nucleocapsid antigen." *Proc Natl Acad Sci U S A* **88**(23): 10445-9.
- Besch, R., H. Poeck, et al. (2009). "Proapoptotic signaling induced by RIG-I and MDA-5 results in type I interferon-independent apoptosis in human melanoma cells." *J Clin Invest* **119**(8): 2399-411.

- Bevan, M. J. (1976). "Cross-priming for a secondary cytotoxic response to minor H antigens with H-2 congenic cells which do not cross-react in the cytotoxic assay." J Exp Med **143**(5): 1283-8.
- Biron, C. A. (1999). "Initial and innate responses to viral infections--pattern setting in immunity or disease." Curr Opin Microbiol **2**(4): 374-81.
- Blight, K. J., J. A. McKeating, et al. (2002). "Highly permissive cell lines for subgenomic and genomic hepatitis C virus RNA replication." J Virol **76**(24): 13001-14.
- Block, T. M., H. Guo, et al. (2007). "Molecular virology of hepatitis B virus for clinicians." Clin Liver Dis **11**(4): 685-706, vii.
- Block, T. M. and R. Jordan (2001). "Iminosugars as possible broad spectrum anti hepatitis virus agents: the glucovirs and alkovirs." Antivir Chem Chemother **12**(6): 317-25.
- Blumberg, B. S., L. Melartin, et al. (1966). "Family studies of a human serum isoantigen system (Australia antigen)." Am J Hum Genet **18**(6): 594-608.
- Blumberg, B. S., A. I. Sutnick, et al. (1969). "Australia antigen and hepatitis." JAMA **207**(10): 1895-6.
- Bohne, F., M. Chmielewski, et al. (2008). "T cells redirected against hepatitis B virus surface proteins eliminate infected hepatocytes." Gastroenterology **134**(1): 239-47.
- Bonvin, M., F. Achermann, et al. (2006). "Interferon-inducible expression of APOBEC3 editing enzymes in human hepatocytes and inhibition of hepatitis B virus replication." Hepatology **43**(6): 1364-74.
- Bouchard, M. J. and R. J. Schneider (2004). "The enigmatic X gene of hepatitis B virus." J Virol **78**(23): 12725-34.
- Bowie, A. G. and L. Unterholzner (2008). "Viral evasion and subversion of pattern-recognition receptor signalling." Nat Rev Immunol **8**(12): 911-22.
- Braasch, D. A., S. Jensen, et al. (2003). "RNA interference in mammalian cells by chemically-modified RNA." Biochemistry **42**(26): 7967-75.
- Bridge, A. J., S. Pebernard, et al. (2003). "Induction of an interferon response by RNAi vectors in mammalian cells." Nat Genet **34**(3): 263-4.
- Brode, S. and P. A. Macary (2004). "Cross-presentation: dendritic cells and macrophages bite off more than they can chew!" Immunology **112**(3): 345-51.
- Cao, T., U. Lazdina, et al. (2001). "Hepatitis B virus core antigen binds and activates naive human B cells in vivo: studies with a human PBL-NOD/SCID mouse model." J Virol **75**(14): 6359-66.
- Cattaneo, R., H. Will, et al. (1984). "Hepatitis B virus transcription in the infected liver." EMBO J **3**(9): 2191-6.
- Chaudhuri, N., S. K. Dower, et al. (2005). "Toll-like receptors and chronic lung disease." Clin Sci (Lond) **109**(2): 125-33.
- Chen, H. S., S. Kaneko, et al. (1993). "The woodchuck hepatitis virus X gene is important for establishment of virus infection in woodchucks." J Virol **67**(3): 1218-26.
- Chen, M., P. Tabaczewski, et al. (2005). "Hepatocytes express abundant surface class I MHC and efficiently use transporter associated with antigen processing, tapasin, and low molecular weight polypeptide proteasome subunit components of antigen processing and presentation pathway." J Immunol **175**(2): 1047-55.

- Chen, Z., Y. Cheng, et al. (2008). "Expression profiles and function of Toll-like receptors 2 and 4 in peripheral blood mononuclear cells of chronic hepatitis B patients." Clin Immunol **128**(3): 400-8.
- Chisari, F. V. and C. Ferrari (1995). "Hepatitis B virus immunopathogenesis." Annu Rev Immunol **13**: 29-60.
- Chisari, F. V. and C. Ferrari (1995). "Hepatitis B virus immunopathology." Springer Semin Immunopathol **17**(2-3): 261-81.
- Chisari, F. V., C. A. Pinkert, et al. (1985). "A transgenic mouse model of the chronic hepatitis B surface antigen carrier state." Science **230**(4730): 1157-60.
- Christen, V., F. Duong, et al. (2007). "Inhibition of alpha interferon signaling by hepatitis B virus." J Virol **81**(1): 159-65.
- Crowther, R. A., N. A. Kiselev, et al. (1994). "Three-dimensional structure of hepatitis B virus core particles determined by electron cryomicroscopy." Cell **77**(6): 943-50.
- Cui, S., K. Eisenacher, et al. (2008). "The C-terminal regulatory domain is the RNA 5'-triphosphate sensor of RIG-I." Mol Cell **29**(2): 169-79.
- Czaderna, F., M. Fechtner, et al. (2003). "Structural variations and stabilising modifications of synthetic siRNAs in mammalian cells." Nucleic Acids Res **31**(11): 2705-16.
- Damdinsuren, B., H. Nagano, et al. (2007). "Interferon alpha receptors are important for antiproliferative effect of interferon-alpha against human hepatocellular carcinoma cells." Hepatol Res **37**(1): 77-83.
- Dandri, M., M. R. Burda, et al. (2005). "Chronic infection with hepatitis B viruses and antiviral drug evaluation in uPA mice after liver repopulation with tupaia hepatocytes." J Hepatol **42**(1): 54-60.
- Dane, D. S., C. H. Cameron, et al. (1970). "Virus-like particles in serum of patients with Australia-antigen-associated hepatitis." Lancet **1**(7649): 695-8.
- Darnell, J. E., Jr., I. M. Kerr, et al. (1994). "Jak-STAT pathways and transcriptional activation in response to IFNs and other extracellular signaling proteins." Science **264**(5164): 1415-21.
- Delaney, W. E. t., R. Edwards, et al. (2002). "Phenylpropenamide derivatives AT-61 and AT-130 inhibit replication of wild-type and lamivudine-resistant strains of hepatitis B virus in vitro." Antimicrob Agents Chemother **46**(9): 3057-60.
- Der, S. D., A. Zhou, et al. (1998). "Identification of genes differentially regulated by interferon alpha, beta, or gamma using oligonucleotide arrays." Proc Natl Acad Sci U S A **95**(26): 15623-8.
- Deres, K., C. H. Schroder, et al. (2003). "Inhibition of hepatitis B virus replication by drug-induced depletion of nucleocapsids." Science **299**(5608): 893-6.
- Dienstag, J. L. (2009). "Benefits and risks of nucleoside analog therapy for hepatitis B." Hepatology **49**(5 Suppl): S112-21.
- Dinarello, C. A. (2000). "Proinflammatory cytokines." Chest **118**(2): 503-8.
- Dufour, J. H., M. Dziejman, et al. (2002). "IFN-gamma-inducible protein 10 (IP-10; CXCL10)-deficient mice reveal a role for IP-10 in effector T cell generation and trafficking." J Immunol **168**(7): 3195-204.
- Epidemiologisches 2004, Bulletin Robert Koch Institut.
- Fernandes-Alnemri, T., J. W. Yu, et al. (2009). "AIM2 activates the inflammasome and cell death in response to cytoplasmic DNA." Nature **458**(7237): 509-13.
- Fernandez, M., J. A. Quiroga, et al. (2003). "Hepatitis B virus downregulates the human interferon-inducible MxA promoter through direct interaction of precore/core proteins." J Gen Virol **84**(Pt 8): 2073-82.

- Fernandez, M., J. A. Quiroga, et al. (1997). "Impaired interferon induction of human MxA protein in chronic hepatitis B virus infection." J Med Virol **51**(4): 332-7.
- Ferrari, C., A. Penna, et al. (1990). "Cellular immune response to hepatitis B virus-encoded antigens in acute and chronic hepatitis B virus infection." J Immunol **145**(10): 3442-9.
- Fisicaro, P., C. Valdatta, et al. (2009). "Early kinetics of innate and adaptive immune responses during hepatitis B virus infection." Gut **58**(7): 974-82.
- Fitzgerald, K. A., S. M. McWhirter, et al. (2003). "IKKepsilon and TBK1 are essential components of the IRF3 signaling pathway." Nat Immunol **4**(5): 491-6.
- Floyd-Smith, G., E. Slattery, et al. (1981). "Interferon action: RNA cleavage pattern of a (2'-5')oligoadenylate--dependent endonuclease." Science **212**(4498): 1030-2.
- Foster, G. R., A. M. Ackrill, et al. (1991). "Expression of the terminal protein region of hepatitis B virus inhibits cellular responses to interferons alpha and gamma and double-stranded RNA." Proc Natl Acad Sci U S A **88**(7): 2888-92.
- Foster, G. R., R. D. Goldin, et al. (1993). "Expression of the terminal protein of hepatitis B virus is associated with failure to respond to interferon therapy." Hepatology **17**(5): 757-62.
- Funk, A., M. Mhamdi, et al. (2004). "Itinerary of hepatitis B viruses: delineation of restriction points critical for infectious entry." J Virol **78**(15): 8289-300.
- Gaboriaud, C., G. Uze, et al. (1990). "Hydrophobic cluster analysis reveals duplication in the external structure of human alpha-interferon receptor and homology with gamma-interferon receptor external domain." FEBS Lett **269**(1): 1-3.
- Gack, M. U., Y. C. Shin, et al. (2007). "TRIM25 RING-finger E3 ubiquitin ligase is essential for RIG-I-mediated antiviral activity." Nature **446**(7138): 916-920.
- Galibert, F., E. Mandart, et al. (1979). "Nucleotide sequence of the hepatitis B virus genome (subtype ayw) cloned in E. coli." Nature **281**(5733): 646-50.
- Ganem, D. (1982). "Persistent infection of humans with hepatitis B virus: mechanisms and consequences." Rev Infect Dis **4**(5): 1026-47.
- Ganem, D. and A. M. Prince (2004). "Hepatitis B virus infection--natural history and clinical consequences." N Engl J Med **350**(11): 1118-29.
- Ganem, D., and Schneider, R. (2001). Hepadnaviridae: The viruses and their replication. In Field's Virology (Philadelphia, Lipincott-Raven).
- Gao, G. P., M. R. Alvira, et al. (2002). "Novel adeno-associated viruses from rhesus monkeys as vectors for human gene therapy." Proc Natl Acad Sci U S A **99**(18): 11854-9.
- Gerlich, W. H. and Kann, M. (2005). Hepatitis B. In Topley & Wilson's Microbiology and Microbial Infections. 9th edition., (eds L. Collier A. Balows and M. Sussman), pp. 1226-1269. London, U.K.: Edward Arnold Ltd.
- Giladi, H., M. Ketzinel-Gilad, et al. (2003). "Small interfering RNA inhibits hepatitis B virus replication in mice." Mol Ther **8**(5): 769-76.
- Gilbert, R. J., L. Beales, et al. (2005). "Hepatitis B small surface antigen particles are octahedral." Proc Natl Acad Sci U S A **102**(41): 14783-8.
- Gitlin, L., W. Barchet, et al. (2006). "Essential role of mda-5 in type I IFN responses to polyriboinosinic:polyribocytidylic acid and encephalomyocarditis picornavirus." Proc Natl Acad Sci U S A **103**(22): 8459-64.
- Glebe, D. and S. Urban (2007). "Viral and cellular determinants involved in hepadnaviral entry." World J Gastroenterol **13**(1): 22-38.

- Glebe, D., S. Urban, et al. (2005). "Mapping of the hepatitis B virus attachment site by use of infection-inhibiting preS1 lipopeptides and tupaia hepatocytes." Gastroenterology **129**(1): 234-45.
- Gondai, T., K. Yamaguchi, et al. (2008). "Short-hairpin RNAs synthesized by T7 phage polymerase do not induce interferon." Nucleic Acids Res **36**(3): e18.
- Gordien, E., O. Rosmorduc, et al. (2001). "Inhibition of hepatitis B virus replication by the interferon-inducible MxA protein." J Virol **75**(6): 2684-91.
- Grethe, S., J. O. Heckel, et al. (2000). "Molecular epidemiology of hepatitis B virus variants in nonhuman primates." J Virol **74**(11): 5377-81.
- Grimm, D., S. Zhou, et al. (2003). "Preclinical in vivo evaluation of pseudotyped adeno-associated virus vectors for liver gene therapy." Blood **102**(7): 2412-9.
- Gripon, P., S. Rumin, et al. (2002). "Infection of a human hepatoma cell line by hepatitis B virus." Proc Natl Acad Sci U S A **99**(24): 15655-60.
- Guan, R. (2000). "Interferon monotherapy in chronic hepatitis B." J Gastroenterol Hepatol **15 Suppl**: E34-40.
- Guan, S. H., M. Lu, et al. (2007). "Interferon-alpha response in chronic hepatitis B-transfected HepG2.2.15 cells is partially restored by lamivudine treatment." World J Gastroenterol **13**(2): 228-35.
- Guidotti, L. G. and F. V. Chisari (1999). "Cytokine-induced viral purging--role in viral pathogenesis." Curr Opin Microbiol **2**(4): 388-91.
- Guidotti, L. G., T. Ishikawa, et al. (1996). "Intracellular inactivation of the hepatitis B virus by cytotoxic T lymphocytes." Immunity **4**(1): 25-36.
- Guidotti, L. G., B. Matzke, et al. (1995). "High-level hepatitis B virus replication in transgenic mice." J Virol **69**(10): 6158-69.
- Guidotti, L. G., A. Morris, et al. (2002). "Interferon-regulated pathways that control hepatitis B virus replication in transgenic mice." J Virol **76**(6): 2617-21.
- Guo, H., D. Jiang, et al. (2009). "Activation of pattern recognition receptor-mediated innate immunity inhibits the replication of hepatitis B virus in human hepatocyte-derived cells." J Virol **83**(2): 847-58.
- Gust, I. D., C. J. Burrell, et al. (1986). "Taxonomic classification of human hepatitis B virus." Intervirology **25**(1): 14-29.
- Habjan, M., I. Andersson, et al. (2008). "Processing of genome 5' termini as a strategy of negative-strand RNA viruses to avoid RIG-I-dependent interferon induction." PLoS One **3**(4): e2032.
- Haller, O., P. Staeheli, et al. (2007). "Interferon-induced Mx proteins in antiviral host defense." Biochimie **89**(6-7): 812-8.
- Hamasaki, K., K. Nakao, et al. (2003). "Short interfering RNA-directed inhibition of hepatitis B virus replication." FEBS Lett **543**(1-3): 51-4.
- Harkins, R. N., P. Szymanski, et al. (2008). "Regulated expression of the interferon-beta gene in mice." Gene Ther **15**(1): 1-11.
- Harris, R. S. and M. T. Liddament (2004). "Retroviral restriction by APOBEC proteins." Nat Rev Immunol **4**(11): 868-77.
- Hashimoto, C., K. L. Hudson, et al. (1988). "The Toll gene of Drosophila, required for dorsal-ventral embryonic polarity, appears to encode a transmembrane protein." Cell **52**(2): 269-79.
- Hassel, B. A., A. Zhou, et al. (1993). "A dominant negative mutant of 2-5A-dependent RNase suppresses antiproliferative and antiviral effects of interferon." EMBO J **12**(8): 3297-304.

- Hatton, T., S. Zhou, et al. (1992). "RNA- and DNA-binding activities in hepatitis B virus capsid protein: a model for their roles in viral replication." J Virol **66**(9): 5232-41.
- Heil, F., H. Hemmi, et al. (2004). "Species-specific recognition of single-stranded RNA via toll-like receptor 7 and 8." Science **303**(5663): 1526-9.
- Helenius, A. (1994). "How N-linked oligosaccharides affect glycoprotein folding in the endoplasmic reticulum." Mol Biol Cell **5**(3): 253-65.
- Hirayama, M., Y. Kohgo, et al. (1993). "Regulation of iron metabolism in HepG2 cells: a possible role for cytokines in the hepatic deposition of iron." Hepatology **18**(4): 874-80.
- Hösel, M., 2009, in press, Hepatology
- Hon, H., A. Oran, et al. (2005). "B lymphocytes participate in cross-presentation of antigen following gene gun vaccination." J Immunol **174**(9): 5233-42.
- Hoofnagle, J. H. (1981). "Serologic markers of hepatitis B virus infection." Annu Rev Med **32**: 1-11.
- Hornung, V., A. Ablasser, et al. (2009). "AIM2 recognizes cytosolic dsDNA and forms a caspase-1-activating inflammasome with ASC." Nature **458**(7237): 514-8.
- Hornung, V., J. Ellegast, et al. (2006). "5'-Triphosphate RNA is the ligand for RIG-I." Science **314**(5801): 994-7.
- Hornung, V., M. Guenther-Biller, et al. (2005). "Sequence-specific potent induction of IFN-alpha by short interfering RNA in plasmacytoid dendritic cells through TLR7." Nat Med **11**(3): 263-70.
- Hovanessian, A. G. (1991). "Interferon-induced and double-stranded RNA-activated enzymes: a specific protein kinase and 2',5'-oligoadenylate synthetases." J Interferon Res **11**(4): 199-205.
- Hovanessian, A. G. and J. Justesen (2007). "The human 2'-5'oligoadenylate synthetase family: unique interferon-inducible enzymes catalyzing 2'-5' instead of 3'-5' phosphodiester bond formation." Biochimie **89**(6-7): 779-88.
- Hu, J., D. O. Toft, et al. (1997). "Hepadnavirus assembly and reverse transcription require a multi-component chaperone complex which is incorporated into nucleocapsids." EMBO J **16**(1): 59-68.
- Hu, K. Q. and A. Siddiqui (1991). "Regulation of the hepatitis B virus gene expression by the enhancer element I." Virology **181**(2): 721-6.
- Huang, J. and T. J. Liang (1993). "A novel hepatitis B virus (HBV) genetic element with Rev response element-like properties that is essential for expression of HBV gene products." Mol Cell Biol **13**(12): 7476-86.
- Huang, L. R., H. L. Wu, et al. (2006). "An immunocompetent mouse model for the tolerance of human chronic hepatitis B virus infection." Proc Natl Acad Sci U S A **103**(47): 17862-7.
- Huovila, A. P., A. M. Eder, et al. (1992). "Hepatitis B surface antigen assembles in a post-ER, pre-Golgi compartment." J Cell Biol **118**(6): 1305-20.
- Inohara, Chamailard, et al. (2005). "NOD-LRR proteins: role in host-microbial interactions and inflammatory disease." Annu Rev Biochem **74**: 355-83.
- Isaacs, A. and J. Lindenmann (1957). "Virus interference. I. The interferon." Proc R Soc Lond B Biol Sci **147**(927): 258-67.
- Ishii, K. J., C. Coban, et al. (2006). "A Toll-like receptor-independent antiviral response induced by double-stranded B-form DNA." Nat Immunol **7**(1): 40-8.
- Ishii, K. J., T. Kawagoe, et al. (2008). "TANK-binding kinase-1 delineates innate and adaptive immune responses to DNA vaccines." Nature **451**(7179): 725-9.

- Isogawa, M., K. Kakimi, et al. (2005). "Differential dynamics of the peripheral and intrahepatic cytotoxic T lymphocyte response to hepatitis B surface antigen." *Virology* **333**(2): 293-300.
- Isogawa, M., M. D. Robek, et al. (2005). "Toll-like receptor signaling inhibits hepatitis B virus replication in vivo." *J Virol* **79**(11): 7269-72.
- Janeway, C. A., Jr. and R. Medzhitov (2002). "Innate immune recognition." *Annu Rev Immunol* **20**: 197-216.
- Janeway, A.J., Travers, P., Walport, M., and Shlomchik, M. (2007). *Immunobiology. The Immune System in Health and Disease*, 7th edn (New York, Garland Publishing).
- Janssen, E. M., E. E. Lemmens, et al. (2003). "CD4+ T cells are required for secondary expansion and memory in CD8+ T lymphocytes." *Nature* **421**(6925): 852-6.
- Jost, S., P. Turelli, et al. (2007). "Induction of antiviral cytidine deaminases does not explain the inhibition of hepatitis B virus replication by interferons." *J Virol* **81**(19): 10588-96.
- Judge, A. D., G. Bola, et al. (2006). "Design of noninflammatory synthetic siRNA mediating potent gene silencing in vivo." *Mol Ther* **13**(3): 494-505.
- Judge, A. D., V. Sood, et al. (2005). "Sequence-dependent stimulation of the mammalian innate immune response by synthetic siRNA." *Nat Biotechnol* **23**(4): 457-62.
- Kajino, K., A. R. Jilbert, et al. (1994). "Woodchuck hepatitis virus infections: very rapid recovery after a prolonged viremia and infection of virtually every hepatocyte." *J Virol* **68**(9): 5792-803.
- Kalinina, T., A. Iwanski, et al. (2003). "Deficiency in virion secretion and decreased stability of the hepatitis B virus immune escape mutant G145R." *Hepatology* **38**(5): 1274-81.
- Kann, M., A. Schmitz, et al. (2007). "Intracellular transport of hepatitis B virus." *World J Gastroenterol* **13**(1): 39-47.
- Kann, M., B. Sodeik, et al. (1999). "Phosphorylation-dependent binding of hepatitis B virus core particles to the nuclear pore complex." *J Cell Biol* **145**(1): 45-55.
- Kao, J. H., N. H. Wu, et al. (2000). "Hepatitis B genotypes and the response to interferon therapy." *J Hepatol* **33**(6): 998-1002.
- Karin, M. and Y. Ben-Neriah (2000). "Phosphorylation meets ubiquitination: the control of NF- κ B activity." *Annu Rev Immunol* **18**: 621-63.
- Kato, H., O. Takeuchi, et al. (2008). "Length-dependent recognition of double-stranded ribonucleic acids by retinoic acid-inducible gene-I and melanoma differentiation-associated gene 5." *J Exp Med* **205**(7): 1601-10.
- Kato, H., O. Takeuchi, et al. (2006). "Differential roles of MDA5 and RIG-I helicases in the recognition of RNA viruses." *Nature* **441**(7089): 101-5.
- Kawai, T., K. Takahashi, et al. (2005). "IPS-1, an adaptor triggering RIG-I- and Mda5-mediated type I interferon induction." *Nat Immunol* **6**(10): 981-8.
- Kessler, D. S., S. A. Veals, et al. (1990). "Interferon-alpha regulates nuclear translocation and DNA-binding affinity of ISGF3, a multimeric transcriptional activator." *Genes Dev* **4**(10): 1753-65.
- Kim, D. H., M. Longo, et al. (2004). "Interferon induction by siRNAs and ssRNAs synthesized by phage polymerase." *Nat Biotechnol* **22**(3): 321-5.
- Klein, C., C. T. Bock, et al. (2003). "Inhibition of hepatitis B virus replication in vivo by nucleoside analogues and siRNA." *Gastroenterology* **125**(1): 9-18.

- Klein, J. (1986). "Antigen-major histocompatibility complex-T cell receptors: inquiries into the immunological menage a trois." Immunol Res **5**(3): 173-90.
- Klocker, U., U. Schultz, et al. (2000). "Endotoxin stimulates liver macrophages to release mediators that inhibit an early step in hepadnavirus replication." J Virol **74**(12): 5525-33.
- Kock, J. and H. J. Schlicht (1993). "Analysis of the earliest steps of hepadnavirus replication: genome repair after infectious entry into hepatocytes does not depend on viral polymerase activity." J Virol **67**(8): 4867-74.
- Konishi, M., C. H. Wu, et al. (2003). "Inhibition of HBV replication by siRNA in a stable HBV-producing cell line." Hepatology **38**(4): 842-50.
- Korn, T., M. Oukka, et al. (2007). "Th17 cells: effector T cells with inflammatory properties." Semin Immunol **19**(6): 362-71.
- Kramvis, A., M. Kew, et al. (2005). "Hepatitis B virus genotypes." Vaccine **23**(19): 2409-23.
- Kuby J., Goldsby, R., Kindt, T.J., Osborne, B.A. (2000). Immunology, 4th edition (W.H. Freeman & Company)
- Kulka, M., L. Alexopoulou, et al. (2004). "Activation of mast cells by double-stranded RNA: evidence for activation through Toll-like receptor 3." J Allergy Clin Immunol **114**(1): 174-82.
- Kumar, H., T. Kawai, et al. (2006). "Essential role of IPS-1 in innate immune responses against RNA viruses." J Exp Med **203**(7): 1795-803.
- Lanford, R. E., D. Chavez, et al. (1998). "Isolation of a hepadnavirus from the woolly monkey, a New World primate." Proc Natl Acad Sci U S A **95**(10): 5757-61.
- Lanzavecchia, A. and F. Sallusto (2001). "Regulation of T cell immunity by dendritic cells." Cell **106**(3): 263-6.
- Lau, G. K., T. Piratvisuth, et al. (2005). "Peginterferon Alfa-2a, lamivudine, and the combination for HBeAg-positive chronic hepatitis B." N Engl J Med **352**(26): 2682-95.
- Lemaitre, B., E. Nicolas, et al. (1996). "The dorsoventral regulatory gene cassette spatzle/Toll/cactus controls the potent antifungal response in Drosophila adults." Cell **86**(6): 973-83.
- Li, G. Q., W. Z. Xu, et al. (2007). "Combination of small interfering RNA and lamivudine on inhibition of human B virus replication in HepG2.2.15 cells." World J Gastroenterol **13**(16): 2324-7.
- Li, K., Z. Chen, et al. (2005). "Distinct poly(I-C) and virus-activated signaling pathways leading to interferon-beta production in hepatocytes." J Biol Chem **280**(17): 16739-47.
- Liang, T. J. (2009). "Hepatitis B: the virus and disease." Hepatology **49**(5 Suppl): S13-21.
- Liaw, Y. F., J. J. Sung, et al. (2004). "Lamivudine for patients with chronic hepatitis B and advanced liver disease." N Engl J Med **351**(15): 1521-31.
- Lien, J. M., C. E. Aldrich, et al. (1986). "Evidence that a capped oligoribonucleotide is the primer for duck hepatitis B virus plus-strand DNA synthesis." J Virol **57**(1): 229-36.
- Lien, J. M., D. J. Petcu, et al. (1987). "Initiation and termination of duck hepatitis B virus DNA synthesis during virus maturation." J Virol **61**(12): 3832-40.
- Limmer, A., J. Ohl, et al. (2000). "Efficient presentation of exogenous antigen by liver endothelial cells to CD8+ T cells results in antigen-specific T-cell tolerance." Nat Med **6**(12): 1348-54.

- Lindh, M., A. S. Andersson, et al. (1997). "Genotypes, nt 1858 variants, and geographic origin of hepatitis B virus--large-scale analysis using a new genotyping method." J Infect Dis **175**(6): 1285-93.
- Liu, Y. J., J. Zhang, et al. (1991). "Sites of specific B cell activation in primary and secondary responses to T cell-dependent and T cell-independent antigens." Eur J Immunol **21**(12): 2951-62.
- Lu, X., T. M. Block, et al. (1996). "Protease-induced infectivity of hepatitis B virus for a human hepatoblastoma cell line." J Virol **70**(4): 2277-85.
- Luster, A. D., J. C. Unkeless, et al. (1985). "Gamma-interferon transcriptionally regulates an early-response gene containing homology to platelet proteins." Nature **315**(6021): 672-6.
- Lustgarten, J., T. Waks, et al. (1991). "CD4 and CD8 accessory molecules function through interactions with major histocompatibility complex molecules which are not directly associated with the T cell receptor-antigen complex." Eur J Immunol **21**(10): 2507-15.
- Magnius, L. O. and H. Norder (1995). "Subtypes, genotypes and molecular epidemiology of the hepatitis B virus as reflected by sequence variability of the S-gene." Intervirology **38**(1-2): 24-34.
- Mahato, R. I., K. Cheng, et al. (2005). "Modulation of gene expression by antisense and antigene oligodeoxynucleotides and small interfering RNA." Expert Opin Drug Deliv **2**(1): 3-28.
- Mangeat, B., P. Turelli, et al. (2003). "Broad antiretroviral defence by human APOBEC3G through lethal editing of nascent reverse transcripts." Nature **424**(6944): 99-103.
- Mangold, C. M. and R. E. Streeck (1993). "Mutational analysis of the cysteine residues in the hepatitis B virus small envelope protein." J Virol **67**(8): 4588-97.
- Marcellin, P., G. K. Lau, et al. (2004). "Peginterferon alfa-2a alone, lamivudine alone, and the two in combination in patients with HBeAg-negative chronic hepatitis B." N Engl J Med **351**(12): 1206-17.
- Marion, P. L., L. S. Oshiro, et al. (1980). "A virus in Beechey ground squirrels that is related to hepatitis B virus of humans." Proc Natl Acad Sci U S A **77**(5): 2941-5.
- Marques, J. T., T. Devosse, et al. (2006). "A structural basis for discriminating between self and nonself double-stranded RNAs in mammalian cells." Nat Biotechnol **24**(5): 559-65.
- Martens, S. and J. Howard (2006). "The interferon-inducible GTPases." Annu Rev Cell Dev Biol **22**: 559-89.
- Martinon, F., O. Gaide, et al. (2007). "NALP inflammasomes: a central role in innate immunity." Semin Immunopathol **29**(3): 213-29.
- Mason, W. S., G. Seal, et al. (1980). "Virus of Pekin ducks with structural and biological relatedness to human hepatitis B virus." J Virol **36**(3): 829-36.
- McCaffrey, A. P., H. Nakai, et al. (2003). "Inhibition of hepatitis B virus in mice by RNA interference." Nat Biotechnol **21**(6): 639-44.
- McClary, H., R. Koch, et al. (2000). "Relative sensitivity of hepatitis B virus and other hepatotropic viruses to the antiviral effects of cytokines." J Virol **74**(5): 2255-64.
- McMahon, B. J., W. L. Alward, et al. (1985). "Acute hepatitis B virus infection: relation of age to the clinical expression of disease and subsequent development of the carrier state." J Infect Dis **151**(4): 599-603.

- Medzhitov, R. (2001). "Toll-like receptors and innate immunity." Nat Rev Immunol **1**(2): 135-45.
- Meister, G., M. Landthaler, et al. (2004). "Human Argonaute2 mediates RNA cleavage targeted by miRNAs and siRNAs." Mol Cell **15**(2): 185-97.
- Melchjorsen, J., S. B. Jensen, et al. (2005). "Activation of innate defense against a paramyxovirus is mediated by RIG-I and TLR7 and TLR8 in a cell-type-specific manner." J Virol **79**(20): 12944-51.
- Melen, K., P. Keskinen, et al. (2000). "Interferon-induced gene expression and signaling in human hepatoma cell lines." J Hepatol **33**(5): 764-72.
- Michallet, M. C., E. Meylan, et al. (2008). "TRADD protein is an essential component of the RIG-like helicase antiviral pathway." Immunity **28**(5): 651-61.
- Milich, D. and T. J. Liang (2003). "Exploring the biological basis of hepatitis B e antigen in hepatitis B virus infection." Hepatology **38**(5): 1075-86.
- Moore, C. B., D. T. Bergstralh, et al. (2008). "NLRX1 is a regulator of mitochondrial antiviral immunity." Nature **451**(7178): 573-7.
- Morrissey, D. V., K. Blanchard, et al. (2005). "Activity of stabilized short interfering RNA in a mouse model of hepatitis B virus replication." Hepatology **41**(6): 1349-56.
- Morrissey, D. V., J. A. Lockridge, et al. (2005). "Potent and persistent in vivo anti-HBV activity of chemically modified siRNAs." Nat Biotechnol **23**(8): 1002-7.
- Moser, M. and K. M. Murphy (2000). "Dendritic cell regulation of TH1-TH2 development." Nat Immunol **1**(3): 199-205.
- Nakabayashi, H., K. Taketa, et al. (1982). "Growth of human hepatoma cells lines with differentiated functions in chemically defined medium." Cancer Res **42**(9): 3858-63.
- Nassal, M. (1992). "The arginine-rich domain of the hepatitis B virus core protein is required for pregenome encapsidation and productive viral positive-strand DNA synthesis but not for virus assembly." J Virol **66**(7): 4107-16.
- Neurath, A. R., S. B. Kent, et al. (1985). "Hepatitis B virus contains pre-S gene-encoded domains." Nature **315**(6015): 154-6.
- Norder, H., A. M. Courouce, et al. (1992). "Molecular basis of hepatitis B virus serotype variations within the four major subtypes." J Gen Virol **73** (Pt 12): 3141-5.
- Norder, H., J. W. Ebert, et al. (1996). "Complete sequencing of a gibbon hepatitis B virus genome reveals a unique genotype distantly related to the chimpanzee hepatitis B virus." Virology **218**(1): 214-23.
- Norder, H., B. Hammas, et al. (1993). "Genetic relatedness of hepatitis B viral strains of diverse geographical origin and natural variations in the primary structure of the surface antigen." J Gen Virol **74** (Pt 7): 1341-8.
- Oganesyan, G., S. K. Saha, et al. (2006). "Critical role of TRAF3 in the Toll-like receptor-dependent and -independent antiviral response." Nature **439**(7073): 208-11.
- Palsson-McDermott, E. M. and L. A. O'Neill (2007). "Building an immune system from nine domains." Biochem Soc Trans **35**(Pt 6): 1437-44.
- Pasquetto, V., S. F. Wieland, et al. (2002). "Cytokine-sensitive replication of hepatitis B virus in immortalized mouse hepatocyte cultures." J Virol **76**(11): 5646-53.
- Peng, G., S. Li, et al. (2008). "Circulating CD4+ CD25+ regulatory T cells correlate with chronic hepatitis B infection." Immunology **123**(1): 57-65.

- Peng, J., Y. Zhao, et al. (2005). "Inhibition of hepatitis B virus replication by various RNAi constructs and their pharmacodynamic properties." J Gen Virol **86**(Pt 12): 3227-34.
- Penna, A., F. V. Chisari, et al. (1991). "Cytotoxic T lymphocytes recognize an HLA-A2-restricted epitope within the hepatitis B virus nucleocapsid antigen." J Exp Med **174**(6): 1565-70.
- Pichlmair, A., O. Schulz, et al. (2006). "RIG-I-mediated antiviral responses to single-stranded RNA bearing 5'-phosphates." Science **314**(5801): 997-1001.
- Plumet, S., F. Herschke, et al. (2007). "Cytosolic 5'-triphosphate ended viral leader transcript of measles virus as activator of the RIG I-mediated interferon response." PLoS One **2**(3): e279.
- Poeck, H., R. Besch, et al. (2008). "5'-Triphosphate-siRNA: turning gene silencing and Rig-I activation against melanoma." Nat Med **14**(11): 1256-63.
- Pollack, J. R. and D. Ganem (1994). "Site-specific RNA binding by a hepatitis B virus reverse transcriptase initiates two distinct reactions: RNA packaging and DNA synthesis." J Virol **68**(9): 5579-87.
- Preiss, S., A. Thompson, et al. (2008). "Characterization of the innate immune signalling pathways in hepatocyte cell lines." J Viral Hepat **15**(12): 888-900.
- Protzer, U. and H. Schaller (2000). "Immune escape by hepatitis B viruses." Virus Genes **21**(1-2): 27-37.
- Protzer, U., S. Seyfried, et al. (2007). "Antiviral activity and hepatoprotection by heme oxygenase-1 in hepatitis B virus infection." Gastroenterology **133**(4): 1156-65.
- Protzer-Knolle, U., U. Naumann, et al. (1998). "Hepatitis B virus with antigenically altered hepatitis B surface antigen is selected by high-dose hepatitis B immune globulin after liver transplantation." Hepatology **27**(1): 254-63.
- Pungpapong, S., W. R. Kim, et al. (2007). "Natural history of hepatitis B virus infection: an update for clinicians." Mayo Clin Proc **82**(8): 967-75.
- Quasdorff, M., M. Hosel, et al. (2008). "A concerted action of HNF4alpha and HNF1alpha links hepatitis B virus replication to hepatocyte differentiation." Cell Microbiol **10**(7): 1478-90.
- Randall, R. E. and S. Goodbourn (2008). "Interferons and viruses: an interplay between induction, signalling, antiviral responses and virus countermeasures." J Gen Virol **89**(Pt 1): 1-47.
- Rang, A., S. Gunther, et al. (1999). "Effect of interferon alpha on hepatitis B virus replication and gene expression in transiently transfected human hepatoma cells." J Hepatol **31**(5): 791-9.
- Rapicetta, M., E. D'Ugo, et al. (2009). "New perspectives for hepatitis B vaccines and immunization." Vaccine **27**(25-26): 3271-5.
- Rebouillat, D. and A. G. Hovanessian (1999). "The human 2',5'-oligoadenylate synthetase family: interferon-induced proteins with unique enzymatic properties." J Interferon Cytokine Res **19**(4): 295-308.
- Rehermann, B. (2003). "Immune responses in hepatitis B virus infection." Semin Liver Dis **23**(1): 21-38.
- Rehermann, B. and M. Nascimbeni (2005). "Immunology of hepatitis B virus and hepatitis C virus infection." Nat Rev Immunol **5**(3): 215-29.
- Rehermann, B., C. Pasquinelli, et al. (1995). "Hepatitis B virus (HBV) sequence variation of cytotoxic T lymphocyte epitopes is not common in patients with chronic HBV infection." J Clin Invest **96**(3): 1527-34.
- Ren, S. and M. Nassal (2001). "Hepatitis B virus (HBV) virion and covalently closed circular DNA formation in primary tupaia hepatocytes and human hepatoma

- cell lines upon HBV genome transduction with replication-defective adenovirus vectors." J Virol **75**(3): 1104-16.
- Ribeiro, R. M., A. Lo, et al. (2002). "Dynamics of hepatitis B virus infection." Microbes Infect **4**(8): 829-35.
- Ridge, J. P., F. Di Rosa, et al. (1998). "A conditioned dendritic cell can be a temporal bridge between a CD4+ T-helper and a T-killer cell." Nature **393**(6684): 474-8.
- Robaczewska, M., R. Narayan, et al. (2005). "Sequence-specific inhibition of duck hepatitis B virus reverse transcription by peptide nucleic acids (PNA)." J Hepatol **42**(2): 180-7.
- Robbins, M., A. Judge, et al. (2009). "siRNA and innate immunity." Oligonucleotides **19**(2): 89-102.
- Robek, M. D., B. S. Boyd, et al. (2004). "Signal transduction pathways that inhibit hepatitis B virus replication." Proc Natl Acad Sci U S A **101**(6): 1743-7.
- Robek, M. D., S. F. Wieland, et al. (2002). "Inhibition of hepatitis B virus replication by interferon requires proteasome activity." J Virol **76**(7): 3570-4.
- Roberts, R. M., L. Liu, et al. (1998). "The evolution of the type I interferons." J Interferon Cytokine Res **18**(10): 805-16.
- Robinson, W. S. (1996). Biology of human hepatitis viruses. In, D. Zakim, and T. D. Boyer, eds. (Philadelphia, W.B. Saunders Company), pp. 1171-1174.
- Rosler, C., J. Kock, et al. (2005). "APOBEC-mediated interference with hepadnavirus production." Hepatology **42**(2): 301-9.
- Rosmorduc, O., M. A. Petit, et al. (1995). "In vivo and in vitro expression of defective hepatitis B virus particles generated by spliced hepatitis B virus RNA." Hepatology **22**(1): 10-9.
- Rosmorduc, O., H. Sirma, et al. (1999). "Inhibition of interferon-inducible MxA protein expression by hepatitis B virus capsid protein." J Gen Virol **80** (Pt 5): 1253-62.
- Rothenfusser, S., N. Goutagny, et al. (2005). "The RNA helicase Lgp2 inhibits TLR-independent sensing of viral replication by retinoic acid-inducible gene-I." J Immunol **175**(8): 5260-8.
- Saito, T., R. Hirai, et al. (2007). "Regulation of innate antiviral defenses through a shared repressor domain in RIG-I and LGP2." Proc Natl Acad Sci U S A **104**(2): 582-7.
- Saito, T., D. M. Owen, et al. (2008). "Innate immunity induced by composition-dependent RIG-I recognition of hepatitis C virus RNA." Nature **454**(7203): 523-7.
- Samuel, C. E. (2001). "Antiviral actions of interferons." Clin Microbiol Rev **14**(4): 778-809, table of contents.
- Sasai, M., M. Shingai, et al. (2006). "NAK-associated protein 1 participates in both the TLR3 and the cytoplasmic pathways in type I IFN induction." J Immunol **177**(12): 8676-83.
- Sato, M., H. Suemori, et al. (2000). "Distinct and essential roles of transcription factors IRF-3 and IRF-7 in response to viruses for IFN-alpha/beta gene induction." Immunity **13**(4): 539-48.
- Satoh, O., H. Imai, et al. (2000). "Membrane structure of the hepatitis B virus surface antigen particle." J Biochem **127**(4): 543-50.
- Scheiffele, P., A. Rietveld, et al. (1999). "Influenza viruses select ordered lipid domains during budding from the plasma membrane." J Biol Chem **274**(4): 2038-44.

- Schettler, C. H. (1971). "Goose virus hepatitis in the Canada Goose and Snow Goose." J Wildl Dis **7**(3): 147-8.
- Schlee, M., E. Hartmann, et al. (2009). "Approaching the RNA ligand for RIG-I?" Immunol Rev **227**(1): 66-74.
- Schlee, M., A. Roth, et al. (2009). "Recognition of 5' triphosphate by RIG-I helicase requires short blunt double-stranded RNA as contained in panhandle of negative-strand virus." Immunity **31**(1): 25-34.
- Schlicht, H. J. and H. Schaller (1989). "Analysis of hepatitis B virus gene functions in tissue culture and in vivo." Curr Top Microbiol Immunol **144**: 253-63.
- Schmitt, S., D. Glebe, et al. (1999). "Analysis of the pre-S2 N- and O-linked glycans of the M surface protein from human hepatitis B virus." J Biol Chem **274**(17): 11945-57.
- Schultz, U., J. Summers, et al. (1999). "Elimination of duck hepatitis B virus RNA-containing capsids in duck interferon-alpha-treated hepatocytes." J Virol **73**(7): 5459-65.
- Schulze-Bergkamen, H., A. Untergasser, et al. (2003). "Primary human hepatocytes-- a valuable tool for investigation of apoptosis and hepatitis B virus infection." J Hepatol **38**(6): 736-44.
- Seeger, C., D. Ganem, et al. (1986). "Biochemical and genetic evidence for the hepatitis B virus replication strategy." Science **232**(4749): 477-84.
- Sells, M. A., M. L. Chen, et al. (1987). "Production of hepatitis B virus particles in Hep G2 cells transfected with cloned hepatitis B virus DNA." Proc Natl Acad Sci U S A **84**(4): 1005-9.
- Sells, M. A., A. Z. Zelent, et al. (1988). "Replicative intermediates of hepatitis B virus in HepG2 cells that produce infectious virions." J Virol **62**(8): 2836-44.
- Sharma, S., B. R. tenOever, et al. (2003). "Triggering the interferon antiviral response through an IKK-related pathway." Science **300**(5622): 1148-51.
- Shlomai, A. and Y. Shaul (2003). "Inhibition of hepatitis B virus expression and replication by RNA interference." Hepatology **37**(4): 764-70.
- Sigal, L. J., S. Crotty, et al. (1999). "Cytotoxic T-cell immunity to virus-infected non-haematopoietic cells requires presentation of exogenous antigen." Nature **398**(6722): 77-80.
- Silverman, R. H. (2007). "Viral encounters with 2',5'-oligoadenylate synthetase and RNase L during the interferon antiviral response." J Virol **81**(23): 12720-9.
- Sioud, M., G. Furset, et al. (2007). "Suppression of immunostimulatory siRNA-driven innate immune activation by 2'-modified RNAs." Biochem Biophys Res Commun **361**(1): 122-6.
- Sledz, C. A., M. Holko, et al. (2003). "Activation of the interferon system by short-interfering RNAs." Nat Cell Biol **5**(9): 834-9.
- Soussan, P., J. Pol, et al. (2008). "Expression of defective hepatitis B virus particles derived from singly spliced RNA is related to liver disease." J Infect Dis **198**(2): 218-25.
- Soutschek, J., A. Akinc, et al. (2004). "Therapeutic silencing of an endogenous gene by systemic administration of modified siRNAs." Nature **432**(7014): 173-8.
- Sprengel, R., E. F. Kaleta, et al. (1988). "Isolation and characterization of a hepatitis B virus endemic in herons." J Virol **62**(10): 3832-9.
- Sprinzi, M. F., H. Oberwinkler, et al. (2001). "Transfer of hepatitis B virus genome by adenovirus vectors into cultured cells and mice: crossing the species barrier." J Virol **75**(11): 5108-18.

- Stoop, J. N., R. G. van der Molen, et al. (2005). "Regulatory T cells contribute to the impaired immune response in patients with chronic hepatitis B virus infection." Hepatology **41**(4): 771-8.
- Summers, J., J. M. Smolec, et al. (1978). "A virus similar to human hepatitis B virus associated with hepatitis and hepatoma in woodchucks." Proc Natl Acad Sci U S A **75**(9): 4533-7.
- Sumpter, R., Jr., Y. M. Loo, et al. (2005). "Regulating intracellular antiviral defense and permissiveness to hepatitis C virus RNA replication through a cellular RNA helicase, RIG-I." J Virol **79**(5): 2689-99.
- Sun, Q., L. Sun, et al. (2006). "The specific and essential role of MAVS in antiviral innate immune responses." Immunity **24**(5): 633-42.
- Suvas, S., A. K. Azkur, et al. (2004). "CD4+CD25+ regulatory T cells control the severity of viral immunoinflammatory lesions." J Immunol **172**(7): 4123-32.
- Tai, P. C., F. M. Suk, et al. (2002). "Hypermethylation and immune escape of an internally deleted middle-envelope (M) protein of frequent and predominant hepatitis B virus variants." Virology **292**(1): 44-58.
- Takahashi, K., T. Kawai, et al. (2006). "Roles of caspase-8 and caspase-10 in innate immune responses to double-stranded RNA." J Immunol **176**(8): 4520-4.
- Takahashi, K., M. Yoneyama, et al. (2008). "Nonself RNA-sensing mechanism of RIG-I helicase and activation of antiviral immune responses." Mol Cell **29**(4): 428-40.
- Takaoka, A., Z. Wang, et al. (2007). "DAI (DLM-1/ZBP1) is a cytosolic DNA sensor and an activator of innate immune response." Nature **448**(7152): 501-5.
- Takeuchi, O. and S. Akira (2008). "MDA5/RIG-I and virus recognition." Curr Opin Immunol **20**(1): 17-22.
- Tang, G. (2005). "siRNA and miRNA: an insight into RISCs." Trends Biochem Sci **30**(2): 106-14.
- Thimme, R., S. Wieland, et al. (2003). "CD8(+) T cells mediate viral clearance and disease pathogenesis during acute hepatitis B virus infection." J Virol **77**(1): 68-76.
- Thomis, D. C., J. P. Doohan, et al. (1992). "Mechanism of interferon action: cDNA structure, expression, and regulation of the interferon-induced, RNA-dependent P1/eIF-2 alpha protein kinase from human cells." Virology **188**(1): 33-46.
- Thompson, A. J. and S. A. Locarnini (2007). "Toll-like receptors, RIG-I-like RNA helicases and the antiviral innate immune response." Immunol Cell Biol **85**(6): 435-45.
- Todo, S., A. J. Demetris, et al. (1991). "Orthotopic liver transplantation for patients with hepatitis B virus-related liver disease." Hepatology **13**(4): 619-26.
- Trifari, S., C. D. Kaplan, et al. (2009). "Identification of a human helper T cell population that has abundant production of interleukin 22 and is distinct from T(H)-17, T(H)1 and T(H)2 cells." Nat Immunol **10**(8): 864-71.
- Turelli, P., A. Liagre-Quazzola, et al. (2008). "APOBEC3-independent interferon-induced viral clearance in hepatitis B virus transgenic mice." J Virol **82**(13): 6585-90.
- Tuttleman, J. S., C. Pourcel, et al. (1986). "Formation of the pool of covalently closed circular viral DNA in hepadnavirus-infected cells." Cell **47**(3): 451-60.
- Twu, J. S., C. H. Lee, et al. (1988). "Hepatitis B virus suppresses expression of human beta-interferon." Proc Natl Acad Sci U S A **85**(1): 252-6.

- Twu, J. S. and R. H. Schloemer (1989). "Transcription of the human beta interferon gene is inhibited by hepatitis B virus." J Virol **63**(7): 3065-71.
- Vaudin, M., A. J. Wolstenholme, et al. (1988). "The complete nucleotide sequence of the genome of a hepatitis B virus isolated from a naturally infected chimpanzee." J Gen Virol **69 (Pt 6)**: 1383-9.
- Vieth, S., C. Manegold, et al. (2002). "Sequence and phylogenetic analysis of hepatitis B virus genotype G isolated in Germany." Virus Genes **24**(2): 153-6.
- Vincent, I. E., J. Lucifora, et al. (2009). "Inhibitory effect of the combination of CpG-induced cytokines with lamivudine against hepatitis B virus replication in vitro." Antivir Ther **14**(1): 131-5.
- Visvanathan, K., N. A. Skinner, et al. (2007). "Regulation of Toll-like receptor-2 expression in chronic hepatitis B by the precore protein." Hepatology **45**(1): 102-10.
- von Weizsacker, F., S. Wieland, et al. (1997). "Gene therapy for chronic viral hepatitis: ribozymes, antisense oligonucleotides, and dominant negative mutants." Hepatology **26**(2): 251-5.
- Walter, E., R. Keist, et al. (1996). "Hepatitis B virus infection of tupaia hepatocytes in vitro and in vivo." Hepatology **24**(1): 1-5.
- Walton, C. M., C. H. Wu, et al. (2001). "A ribonuclease H-oligo DNA conjugate that specifically cleaves hepatitis B viral messenger RNA." Bioconjug Chem **12**(5): 770-5.
- Wang, G. H. and C. Seeger (1992). "The reverse transcriptase of hepatitis B virus acts as a protein primer for viral DNA synthesis." Cell **71**(4): 663-70.
- Weber, O., K. H. Schlemmer, et al. (2002). "Inhibition of human hepatitis B virus (HBV) by a novel non-nucleosidic compound in a transgenic mouse model." Antiviral Res **54**(2): 69-78.
- Webster, G. J., S. Reignat, et al. (2004). "Longitudinal analysis of CD8+ T cells specific for structural and nonstructural hepatitis B virus proteins in patients with chronic hepatitis B: implications for immunotherapy." J Virol **78**(11): 5707-19.
- Wen, W. H., J. Y. Liu, et al. (2007). "Targeted inhibition of HBV gene expression by single-chain antibody mediated small interfering RNA delivery." Hepatology **46**(1): 84-94.
- Werle-Lapostolle, B., S. Bowden, et al. (2004). "Persistence of cccDNA during the natural history of chronic hepatitis B and decline during adefovir dipivoxil therapy." Gastroenterology **126**(7): 1750-8.
- Whalley, S. A., D. Brown, et al. (2004). "Evolution of hepatitis B virus during primary infection in humans: transient generation of cytotoxic T-cell mutants." Gastroenterology **127**(4): 1131-8.
- Whitten, T. M., A. T. Quets, et al. (1991). "Identification of the hepatitis B virus factor that inhibits expression of the beta interferon gene." J Virol **65**(9): 4699-704.
- WHO, World Health Organization (2008). "www.who.int/nuvi/hepb/en/"
- Wieland, S., R. Thimme, et al. (2004). "Genomic analysis of the host response to hepatitis B virus infection." Proc Natl Acad Sci U S A **101**(17): 6669-74.
- Wieland, S. F., L. G. Guidotti, et al. (2000). "Intrahepatic induction of alpha/beta interferon eliminates viral RNA-containing capsids in hepatitis B virus transgenic mice." J Virol **74**(9): 4165-73.
- Wieland, S. F., R. G. Vega, et al. (2003). "Searching for interferon-induced genes that inhibit hepatitis B virus replication in transgenic mouse hepatocytes." J Virol **77**(2): 1227-36.

- Willment, J. A. and G. D. Brown (2008). "C-type lectin receptors in antifungal immunity." Trends Microbiol **16**(1): 27-32.
- Wolfrum, C., S. Shi, et al. (2007). "Mechanisms and optimization of in vivo delivery of lipophilic siRNAs." Nat Biotechnol **25**(10): 1149-57.
- Wu, J., M. Lu, et al. (2007). "Toll-like receptor-mediated control of HBV replication by nonparenchymal liver cells in mice." Hepatology **46**(6): 1769-78.
- Wu, J., Z. Meng, et al. (2009). "Hepatitis B virus suppresses toll-like receptor-mediated innate immune responses in murine parenchymal and nonparenchymal liver cells." Hepatology **49**(4): 1132-40.
- Wu, M., Y. Xu, et al. (2007). "Hepatitis B virus polymerase inhibits the interferon-inducible MyD88 promoter by blocking nuclear translocation of Stat1." J Gen Virol **88**(Pt 12): 3260-9.
- Wu, T. T., L. Coates, et al. (1990). "In hepatocytes infected with duck hepatitis B virus, the template for viral RNA synthesis is amplified by an intracellular pathway." Virology **175**(1): 255-61.
- Xie, Q., H. C. Shen, et al. (2009). "Patients with chronic hepatitis B infection display deficiency of plasmacytoid dendritic cells with reduced expression of TLR9." Microbes Infect **11**(4): 515-23.
- Xu, L. G., Y. Y. Wang, et al. (2005). "VISA is an adapter protein required for virus-triggered IFN-beta signaling." Mol Cell **19**(6): 727-40.
- Yan, R. Q., J. J. Su, et al. (1996). "Human hepatitis B virus and hepatocellular carcinoma. I. Experimental infection of tree shrews with hepatitis B virus." J Cancer Res Clin Oncol **122**(5): 283-8.
- Yang, W. and J. Summers (1995). "Illegitimate replication of linear hepadnavirus DNA through nonhomologous recombination." J Virol **69**(7): 4029-36.
- Yim, H. J. and A. S. Lok (2006). "Natural history of chronic hepatitis B virus infection: what we knew in 1981 and what we know in 2005." Hepatology **43**(2 Suppl 1): S173-81.
- Yoneyama, M. and T. Fujita (2008). "Structural mechanism of RNA recognition by the RIG-I-like receptors." Immunity **29**(2): 178-81.
- Yoneyama, M. and T. Fujita (2009). "RNA recognition and signal transduction by RIG-I-like receptors." Immunol Rev **227**(1): 54-65.
- Yoneyama, M., M. Kikuchi, et al. (2005). "Shared and unique functions of the DExD/H-box helicases RIG-I, MDA5, and LGP2 in antiviral innate immunity." J Immunol **175**(5): 2851-8.
- Yoneyama, M., M. Kikuchi, et al. (2004). "The RNA helicase RIG-I has an essential function in double-stranded RNA-induced innate antiviral responses." Nat Immunol **5**(7): 730-7.
- Zeng, Y. and B. R. Cullen (2002). "RNA interference in human cells is restricted to the cytoplasm." RNA **8**(7): 855-60.
- Zhang, H., F. A. Kolb, et al. (2004). "Single processing center models for human Dicer and bacterial RNase III." Cell **118**(1): 57-68.
- Zhang, X., Y. Kimura, et al. (2007). "Regulation of Toll-like receptor-mediated inflammatory response by complement in vivo." Blood **110**(1): 228-36.
- Zhang, Y., W. Jiang, et al. (2008). "Engineering enhancement of the immune response to HBV DNA vaccine in mice by the use of LIGHT gene adjuvant." J Virol Methods **153**(2): 142-8.
- Zhang, Z., U. Protzer, et al. (2004). "Inhibition of cellular proteasome activities enhances hepadnavirus replication in an HBX-dependent manner." J Virol **78**(9): 4566-72.

Bibliography

- Zhao, T., L. Yang, et al. (2007). "The NEMO adaptor bridges the nuclear factor-kappaB and interferon regulatory factor signaling pathways." Nat Immunol **8**(6): 592-600.
- Zhong, B., Y. Yang, et al. (2008). "The adaptor protein MITA links virus-sensing receptors to IRF3 transcription factor activation." Immunity **29**(4): 538-50.
- Zhong, J., I. V. Deaciuc, et al. (2006). "Lipopolysaccharide-induced liver apoptosis is increased in interleukin-10 knockout mice." Biochim Biophys Acta **1762**(4): 468-77.
- Zhou, S. and D. N. Strating (1992). "Hepatitis B virus capsid particles are assembled from core-protein dimer precursors." Proc Natl Acad Sci U S A **89**(21): 10046-50.
- Zoulim, F. (2004). "Mechanism of viral persistence and resistance to nucleoside and nucleotide analogs in chronic hepatitis B virus infection." Antiviral Res **64**(1): 1-15.
- Zoulim, F. and Lucifora, J. (2006). "Hepatitis B virus drug resistance: mechanism and clinical implications for the prevention of treatment failure." Future Virol **1**(3):361-376

Erklärung

Ich versichere, dass ich die von mir vorgelegte Dissertation selbständig angefertigt, die benutzten Quellen und Hilfsmittel vollständig angegeben und die Stellen der Arbeit -einschließlich Tabellen, Karten und Abbildungen -, die anderen Werken im Wortlaut oder dem Sinn nach entnommen sind, in jedem Einzelfall als Entlehnung kenntlich gemacht habe; dass diese Dissertation noch keiner anderen Fakultät oder Universität zur Prüfung vorgelegen hat; dass sie noch nicht veröffentlicht worden ist sowie, dass ich eine solche Veröffentlichung vor Abschluß des Promotionsverfahrens nicht vornehmen werde. Die Bestimmungen dieser Promotionsordnung sind mir bekannt. Die von mir vorgelegte Dissertation ist von Prof. Dr. Thomas Langer betreut worden.

Köln, den 10. September 2009

Gregor Ebert

Publications

Papers

Gastroenterology. 2008 Jan;134(1):239-47. Epub 2007 Nov 4

Bohne F, Chmielewski M, Ebert G, Wiegmann K, Kürschner T, Schulze A, Urban S, Krönke M, Abken H, Protzer U.

“T cells redirected against hepatitis B virus surface proteins eliminate infected hepatocytes”